GEOLOGICAL SURVEY OF CANADA
OPEN FILE 7200

Indicator mineral signatures of magmatic Ni-Cu deposits, Thompson Nickel Belt, Manitoba: Part 2 — till data

M.B. McClenaghan, I.M. Kjarsgaard, S.A. Averill, D. Layton-Matthews, D. Crabtree, G. Matile, I. McMartin, and M. Pyne

2013

Natural Resources Canada | Ressources naturelles Canada

Canada

GEOLOGICAL SURVEY OF CANADA
OPEN FILE 7200

Indicator mineral signatures of magmatic Ni-Cu deposits, Thompson Nickel Belt, Manitoba: Part 2 — till data

M.B. McClenaghan[1], I.M. Kjarsgaard[2], S.A. Averill[3], D. Layton-Matthews[4], D. Crabtree[5], G. Matile[6], I. McMartin[1], and M. Pyne[1]

[1]Geological Survey of Canada, 601 Booth Street, Ottawa, ON K1A 0E8
[2]Consulting Mineralogist/Petrolgist, 15 Scotia Place, Ottawa, ON K1S 0W2
[3]Overburden Drilling Management Ltd., 15 Capella Court, Unit 17, Ottawa, ON K2E 7X1
[4]Department of Geological Sciences and Geological Engineering, Queen's University, Kingston, ON K7L 3N6
[5]Geoscience Laboratories, 933 Ramsey Road, Sudbury, ON P3E 6B5
[6]Manitoba Geological Survey, 360-1395 Ellice Avenue, Winnipeg, MB R3G 3P2

©Her Majesty the Queen in Right of Canada 2013

doi:10.4095/292543

This publication is available for free download through GEOSCAN (http://geoscan.ess.nrcan.gc.ca/).

Recommended citation
McClenaghan, M.B., Kjarsgaard, I.M., Averill, S.A., Layton-Matthews, D., Crabtree, D., Matile, G., McMartin, I., and Pyne, M., 2013. Indicator mineral signatures of magmatic Ni-Cu deposits, Thompson Nickel Belt, Manitoba: Part 2 – till data; Geological Survey of Canada, Open File 7200. doi:10.4095/292543

Publications in this series have not been edited; they are released as submitted by the author.

Contribution to the Targeted Geoscience Initiative (TGI-3) 2005-2010

TABLE OF CONTENTS

Figures

Tables

INDICATOR MINERAL SIGNATURES OF MAGMATITE Ni-Cu DEPOSITS, THOMPSON NICKEL BELT, MANITOBA: PART 2 — TILL DATA

M.B. McClenaghan[1], I.M. Kjarsgaard[2], S.A. Averill[3], D. Layton-Matthews[4], D. Crabtree[5], G. Matile[6], I. McMartin, and M. Pyne[2]

[1]Geological Survey of Canada, 601 Booth Street, Ottawa, Ontario K1A 0E8
[2]Consulting Mineralogist/Petrologist, 15 Scotia Place, Ottawa, Ontario K1S 0W2
[3]Overburden Drilling Management Ltd., 15 Capella Court, Unit 107, Ottawa, ON K2E 7X1
[4]Department of Geological Sciences and Geological Engineering, Queen's University, Kingston, Ontario K7L 3N6
[5]Geoscience Laboratories, 933 Ramsey Lake Road, Sudbury, Ontario P3E 6B4
[6]Manitoba Geological Survey, 360-1395 Ellice Avenue, Winnipeg, Manitoba R3G 3P2

ABSTRACT

The Geological Survey of Canada (GSC) conducted an indicator mineral study around the komatiite-associated Ni-Cu deposits in the northern Thompson Nickel Belt, northern Manitoba, to document the indicator mineral signatures of the Ni-Cu deposits. Samples used in this study include archived till heavy mineral concentrates from 1996, till and bedrock samples collected in 2005 and 2006, and till samples collected in 2007 as part of another GSC study. The Laurentide Ice Sheet flowed across the Thompson Nickel Belt southwestward, and subsequently westward, and striations from both ice-flow events are readily apparent on outcrops along the Belt. Till samples were collected to evaluate glacial dispersal along both ice-flow trends. Till and bedrock samples were processed to recover heavy (specific gravity>3.2) mineral concentrates. Potential indicator minerals picked from heavy mineral concentrates included Cr-diopside, olivine, chromite, spinel, gahnite, rutile, pink corundum, and sapphirine, as well as metallic minerals such as pyrrhotite, pentlandite, chalcopyrite, pyrite, arsenopyrite, gold, and sperrylite.

Elevated chromite abundances combined with the presence of Ni-Cu sulphide minerals are strong indicators of potential magmatic Ni-Cu mineralization in till down ice of the Ni-Cu deposits in the Belt. Chalcopyrite and sperrylite are the most useful metallic indicator minerals as they are the most likely to survive glacial transport and postglacial weathering. Elevated Zn content (>2 wt.% ZnO) in chromite is only found in strongly mineralized rocks and is the strongest indicator for mineralization other than the actual ore minerals. The Zn content in chromite from Ni-deposits might be considerabley lower in regions with lower metamorphic grade and thus this feature does not have universal application. The distribution of Cr-diopside, olivine, enstatite, and chromite are similar and are most abundant just east of the Thompson Nickel Belt, at the Thompson deposit and south of the Pipe deposit. Their mafic Cr- or Ni-rich compositions reflect the abundance of ultramafic rocks in the area. Chemical variations in Cr-diopside (higher Cr, Na) and olivine (variable Ni) and the occurrence of high-grade metamorphic minerals, such as corundum, sapphirine, rutile, and spinel, reflect the higher metamorphic grades in certain areas, rather than presence or absence of mineralization. Exploration along the Thompson Nickel Belt and in the surrounding terranes should consider both the older southwest and younger westward ice-flow events when interpreting and following up till indicator mineral results.

INTRODUCTION

Numerous case studies have been published that document the till geochemical and indicator mineral signatures for a broad range of mineral deposit types (e.g. Coker and DiLabio, 1989; McClenaghan et al., 2000; McClenaghan 2005), however, only a few have been published for magmatic Ni-Cu-PGE deposits (Coker et al. 1991; Tiainen et al. 1991; Cook and Fletcher 1992; Barnett, 2007) and few that document the indicator mineral signatures of this deposit type (Bajc, 2000; Bajc and Hall, 2000; Searcy, 2001; Barnett and Averill, 2010). To address this knowledge gap, the Geological Survey of Canada (GSC), through its Targeted Geoscience Initiative 3 Program (2005-2010) and the Canadian Mining Industry Research Organization (CAMIRO) through Project 04E01, collected and analyzed a suite of till and bedrock samples from around the ultramafic hosted Ni-Cu sulphide deposits in the northern part of the Thompson Nickel Belt (TNB), northern Manitoba (Fig. 1). The TNB was chosen as one of the five CAMIRO international test sites for Ni-Cu-PGE indicator mineral studies, with the others being 1) Jinchuan, China; 2) Noril'sk, Russia; 3) Nebo-Babel, West Musgraves, Australia; and 4) Eagle, Michigan, USA.

The Thompson site was chosen because it contains world-class magmatic Ni-Cu deposits, is till-covered and easily accessible, and displays a suspected Ni-Cu indicator mineral signature, as suggested in Table 1, in till up to 300 km down-ice to the southwest as defined by the Cr-diopside content of till (>2 grains per sample) (Matile and Thorleifson, 1997). The indicator mineral signature in till, as reported by Matile and Thorleifson (1997), is broadest and best developed for

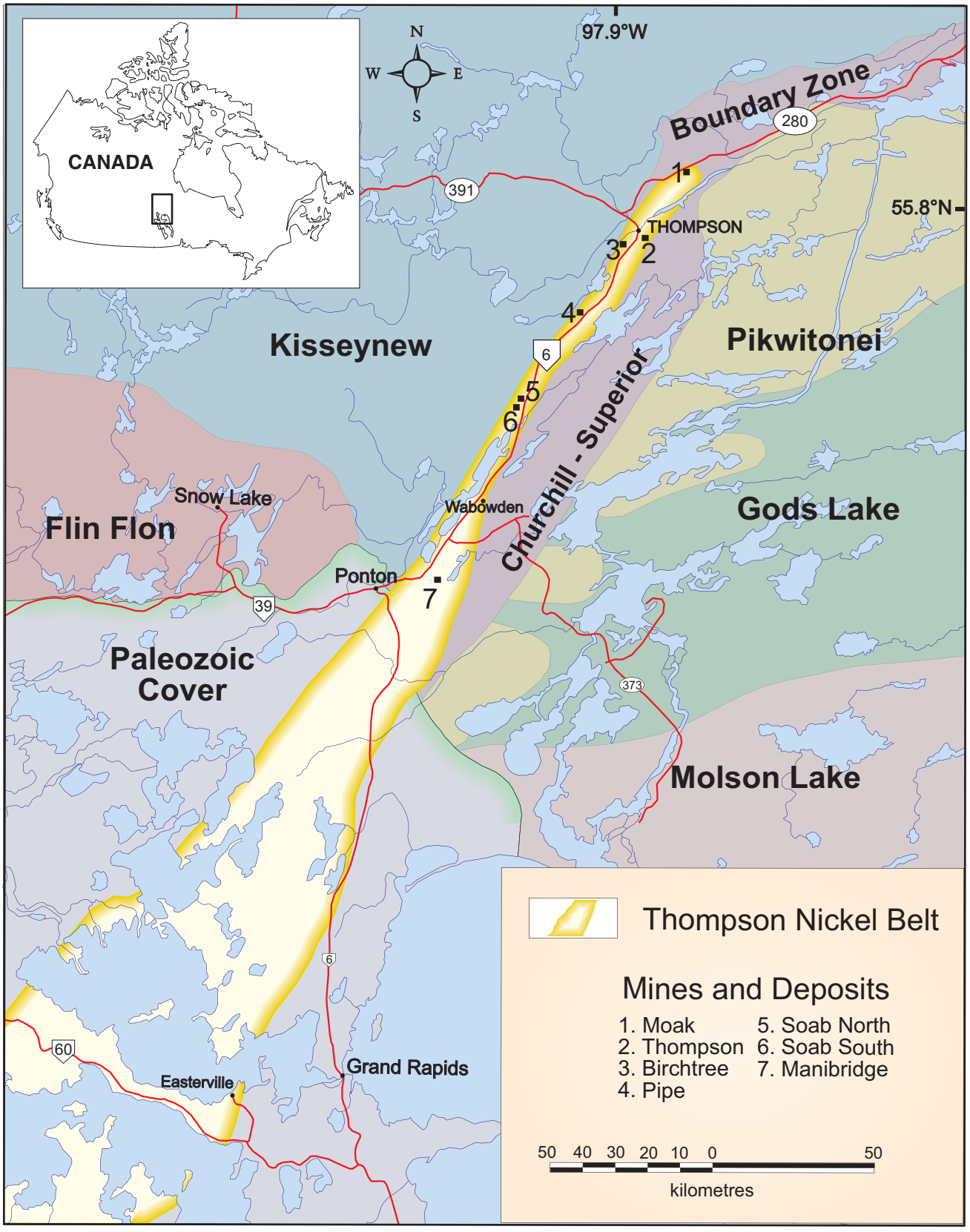

Figure 1. Location of the Thompson Nickel Belt in northern Manitoba (modified from Layton-Matthews et al., 2007) and location of the Thompson, Birchtree, Pipe, and Soab mines and deposits.

Table 1. Summary of ore mineralogy for the Thompson, Pipe, Birchtree, and Soab deposits (summarized from Arnold and Malik, 1974; Cabri, 1981; Cabri and Laflamme, 1981; Chen et al., 1993; Burnham et al., 2009).

Minerals in Ore	Formula
Major and minor minerals	
pentlandite	$(Fe,Ni,Co)_9S_8$
pyrrhotite	Fe(1-x)S
pyrite	FeS_2
millerite	NiS
Minor to rare minerals	
chalcopyrite	$CuFeS_2$
magnetite	Fe_3O_4
ferrochromite	$FeO\text{-}Cr_2O_3$
sphalerite	(Zn,Fe,Cd)S
violarite	$Fe^{2+}Ni2S_4$
cubanite	$CuFe_2S_3$
galena	PbS
marcasite	FeS_2
Te-bearing minerals	
melonite	$NiTe_2$
hessite	Ag_2Te
wehrlite	BiTe
Bi-tellurides	
As-bearing minerals	
niccolite	NiAs
gersdorffite	NiAsS
maucherite	$Ni_{11}As_8$
arsenopyrite	FeAsS
cobaltite	CoAsS
loellingite	$FeAs_2$
Precious metal minerals (Ag, Au)	
native silver	Ag
native gold	Au
electrum	$Au_{68\text{-}78}Ag_{22\text{-}32}$
Platinum Group minerals (Pd, Pt)	
merenskyite	$(Pd)(Te,Bi)_2$
michenerite	PdBiTe
sperrylite	$PtAs_2$
kotulskite	PdTe
irarsite	(Ir,Ru,Rh,Pt)AsS
sudburyite	(Pd,Ni)Sb
unnamed PGM	$(Pd, Ni)_{0.44}(Te, Sb)_{0.56}$
majakite	PdNiAs
froodite	$PdBi_2$

Cr-diopside (Fig. 2) but also includes chalcopyrite, hercynite, chromite, Cr-rutile, and loellingite in till closer to the deposits. In this previous reconnaissance-scale survey, the presence of these indicator minerals were merely noted and were not traced to source. A further advantage to selecting the TNB as a test site is that the heavy mineral concentrates from Matile and Thorleifson's (1997) regional survey were archived at the GSC and were available for re-examination as part of this study. In addition, the geology, stratigraphy, petrology, metamorphic and deformation history, age relationships, and petrogenesis of the TNB rocks were well documented by a recent CAMIRO project (Burnham et al. (2009) summarized in Layton-Matthews et al., 2007, 2010)).

The specific objectives of this TNB study are 1) to determine the indicator minerals and their trace element signatures that are indicative of the magmatic Ni-Cu deposits; and 2) to establish practical methods for their recovery from glacial sediments and their identification that can be routinely applied in Ni-Cu-PGE exploration in glaciated terrain. Both bedrock and till samples were collected for this study to establish a clear link between indicator minerals in till and their bedrock source.

This report documents the indicator mineral species, abundances, and compositions in the heavy mineral fraction of till within the TNB and up-ice (north and east) of the belt. Indicator mineral data for bedrock samples have been published in GSC Open File 6766 (McClenaghan et al., 2012). Till geochemical data for the <0.063 mm fraction of the till samples have been published in GSC Open File 6005 (McClenaghan et al., 2009a) and reported by McClenaghan et al. (2009b, 2011).

GEOLOGY

Bedrock Geology

The bedrock geology of the TNB region is summarized below from and Zwanzig et al. (2007), Layton-Matthews et al. (2007, 2010), and Burnham et al. (2009). The belt is 10 to 35 km wide (Fig. 1) and consists of variably reworked Archean basement gneiss and Early Proterozoic cover rocks along the northwestern margin of the Superior Craton (Bleeker and Macek, 1996). The TNB hosts several past- and currently producing world-class magmatic Ni-Cu deposits that have been strongly structurally and metamorphically modified. Metamorphic grades reached granulite facies (700-850ºC and 5 to 7 kbar) in the Pikwitonei domain east of the TNB (Paktunç and Baer, 1986). While this area east of the belt retained granulite-facies assemblages, the TNB was overprinted by a later upper amphibolite-facies event (Paktunç and Baer, 1986; Bleeker, 1990). Nickel sulphide mineralization is associated almost exclusively with, or localized within, ultramafic bodies within the lower part of the Proterozoic Ospwagan Group, in particular the Pipe Formation, along either one of two sulphide-facies iron formations (Bleeker and Macek, 1988, 1996). The Ospwagan Group is interpreted to have been deposited near a passively rifted margin on a continental platform that experienced a subsequent period of active rifting and ultramafic to mafic magmatism, as represented by the boudinaged mineralized and non-mineralized ultramafic sills (bodies). The Ospwagan Group sits uncon-

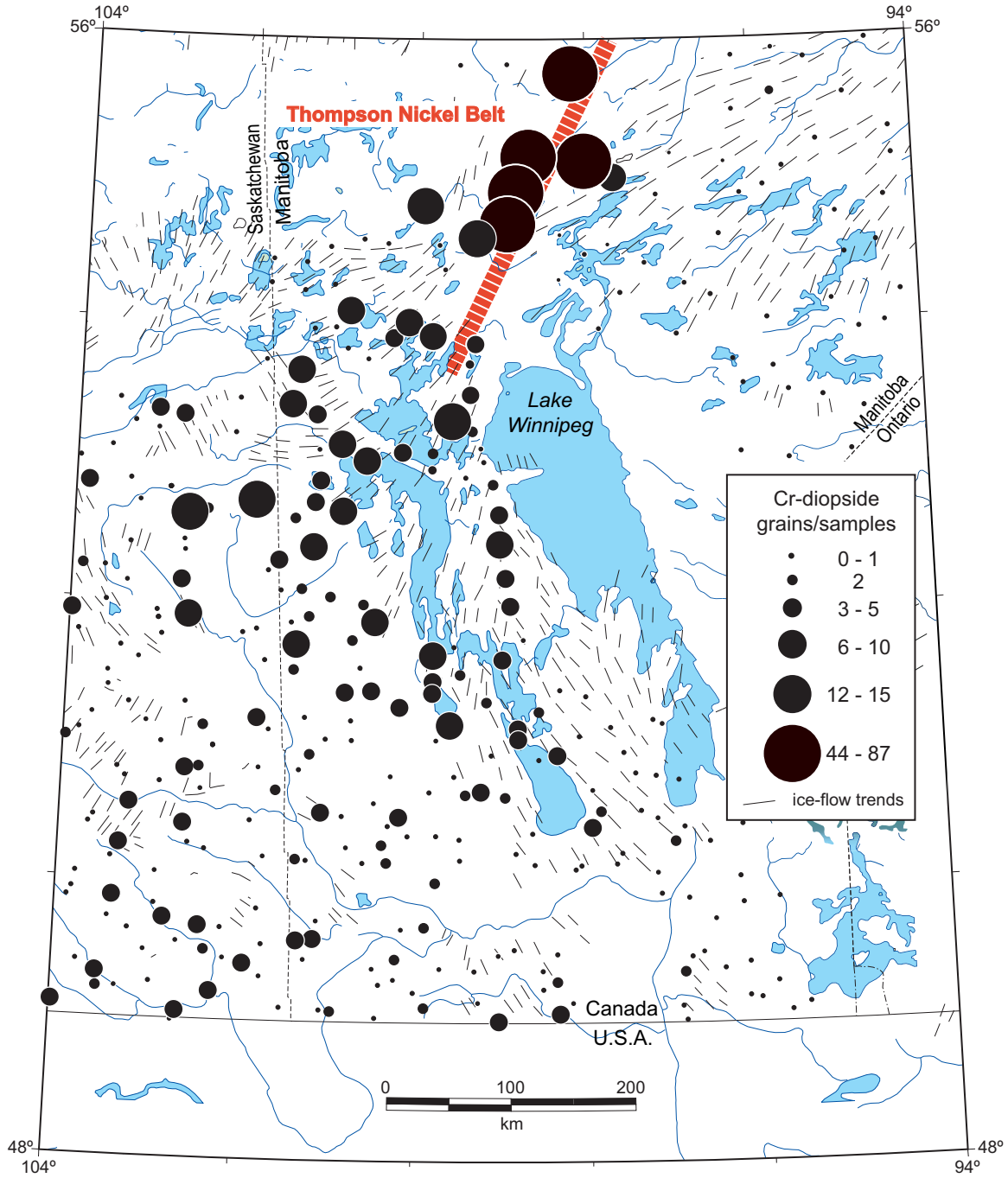

Figure 2. Abundance of Cr-diopside in till samples across central and southern Manitoba. Location of the Thompson Nickel Belt is highlighted by the thick dashed line. Data plotted on the map are from Thorleifson and Garrett (1993) and Matile and Thorleifson (1997).

formably on Archean basement and consists of four sedimentary formations, from oldest to youngest (Bleeker and Macek, 1988): basal conglomerate and quartzite of the Manasan Formation; impure calc-silicate of the Thompson Formation; semipelite, sulphidic sediments, and iron formation of the Pipe Formation; and interlayered quartzite and semipelite of the Setting Formation. The Setting Formation is overlain by mafic-ultramafic metavolcanic rocks and/or a younger suite of clastic metasedimentary rocks (Grass River Group: Zwanzig and McRitchie, 1997). The ultramafic bodies have been classified into three main lithologies: metadunite, metaperidotite (including harzburgite and rare wehrlite), and metapyroxenite (both orthopyroxenite and clinopyroxenite). Massive sulphide ores are of two types: 1) magmatic sulphide ore, formed by assimilation of sulphide-rich country rocks; and 2) Ni-enriched sedimentary sulphide ore, formed by extensive redistribution of Ni and other metals during high-grade metamorphism, from high-grade magmatic sulphides to

previously barren sedimentary sulphides in the immediate country rock (Bleeker and Macek, 1996). Primary (i.e. non-supergene) ores are dominated by pyrrhotite, pentlandite, pyrite, and millerite assemblages (Bleeker, 1990; Liwanag, 2001). Chalcopyrite, magnetite, and ferrochromite are ubiquitous minor phases.

The Thompson deposit is stratabound and occurs within pelitic schist of the Pipe Formation. The Thompson Mine site consists of the currently operating T1 and T3 underground mines, as well as the mined-out South, B, and C open pits (Fig. 3). The Birchtree and Pipe deposits are hosted in discontinuous ultramafic bodies that occur within graphitic sulphide-facies iron formation of the Pipe Formation. The Birchtree deposit is currently being mined underground. The Pipe deposit was explored and mined from the Pipe 1 and 2 underground mines as well as the Pipe open pit (Fig. 4). The major and minor ore minerals present in the Thompson and Pipe deposits are summarized in Table 1. Metamorphic grades within the TNB were highest at the Thompson deposit area (~740-780ºC), slightly lower at the Birchtree deposit and in the East Kisseynew domain (~680-735ºC) and lower still (~530-635ºC) in the Ospwagan Lake and Pipe deposit areas at pressures of ~5 to 7 kbar (Bleeker, 1990). However, granulite-facies relicts exists within the TNB (Paktunç, 1984).

The TNB (and part of the Churchill-Superior Boundary Zone) borders to the east on the Pikwitonei region orthogneisseand granite-greenstone domains that were metamorphosed to granulite-facies assemblages during or after the 2.7 Ga cratonization event (http://www.gov.mb.ca/stem/mrd/geo/exp-sup/mbgeology.html). Bedrock types in the Pikwitonei domain close to the TNB include biotite gneiss, metamorphosed granite-granodiorite and tonalite bodies, migmatite, metagabbro, mafic to ultramafic amphibolite, orthopyroxene-gneiss, and, further to the east, vast areas of enderbite (hypersthene tonalite). The high-grade metamorphic terrain is cut by a series of parallel north-northeast- to south-southwest-trending mafic to ultramafic dykes, called Molson dykes, of which the Cuthbert Lake dyke is the most prominent dyke close to the TNB. It runs through the Cuthbert Lake trending ~30º north-northeast (subparallel to the TNB) and can be traced using aeromagnetic data for almost 100 km. Several ultramafic (meta-peridotite) lenses are embedded in amphibolite and pyroxene-plagioclase-hornblende-garnet-quartz gneiss just to the west of the Cuthbert Lake dyke and east of the Thompson deposit. Metagabbro bodies occur further southwest in biotite gneiss around Paint Lake. The metamorphic grade changes from upper amphibolite facies within the TNB and just to the east, to granulite facies in the Pikwitonei domain with temperatures as high as 880ºC and pressures up to 11 kbar (Paktunç and Baer, 1986). Metamorphic conditions for sapphirine-bearing granulite at Sipiwesk Lake (southeast of the TNB) were determined by Arima and Barnett (1984) to have been 780-880ºC and 9 kbar.

Surficial Geology

Northern Manitoba has been affected by repeated patterns of southward and westward ice flow during the Quaternary. The most recent glaciation, during the Wisconsin, resulted in ice that first flowed south from an ice centre in Keewatin and then westward from ice centered in Hudson Bay (Dredge et al., 1986; Klassen, 1986; Kaszycki 1989; Dredge and Nixon, 1992; McMartin et al., 1996, 2010a,b, 2012) (Fig. 5). Striation data collected across the TNB as part of this study in 2005 and 2006 support earlier observations of these two phases of Wisconsin ice flow. Sculpted and streamlined bedrock landforms and striationsrepresent both ice-flow events on the exposed shoulders of the open pits at the Thompson and Pipe mines (Figs. 3b, 4) and throughout the area (McClenaghan et al., 2009a,b, 2011). Striation data and photos of selected striation sites are included in McClenaghan et al. (2009a). Based on striations observed at the Thompson and Pipe mine sites, the authors conclude that both Wisconsin ice-flow events eroded and transported metal-rich debris from the TNB deposits. Till exposed on the flanks of bedrock outcrops and in open pits is likely the net product of both phases of ice flow; i.e., till might be composed of debris first transported to the south and then to the west.

In the region, a single till unit overlies bedrock and it is likely the net product of both ice-flow phases. This unit is thin (<0.5 to 3 m thick), has a silty sand matrix (~50% sand) and contains about 10 to 30% clasts (McClenaghan et al., 2009a). The pebble fraction is dominated by local Precambrian lithologies, although it also includes minor Paleozoic carbonate clasts derived from the Hudson Bay Platform 200 km to the east. As the Laurentide Ice Sheet melted back 7800 years BP (Thorleifson 1996; Dyke et al. 2003; Dyke 2004), the region was inundated by glacial Lake Agassiz for approximately 100 years. Within glacial Lake Agassiz, rhythmically bedded clay and silt were draped over bedrock and till, in places up to 40 m thick. As a result, the region is a typical clay plain comprising a relatively low-relief, poorly drained landscape dominated by organic deposits with few bedrock outcrops. Glacial Lake Agassiz drained 7700 years BP, exposing the surficial sediments to postglacial weathering processes (Dyke et al., 2003; Dyke, 2004).

The TNB is the source of a well developed indicator mineral dispersal train best defined by Cr-diopside content in till, with more than 2 grains per till sample

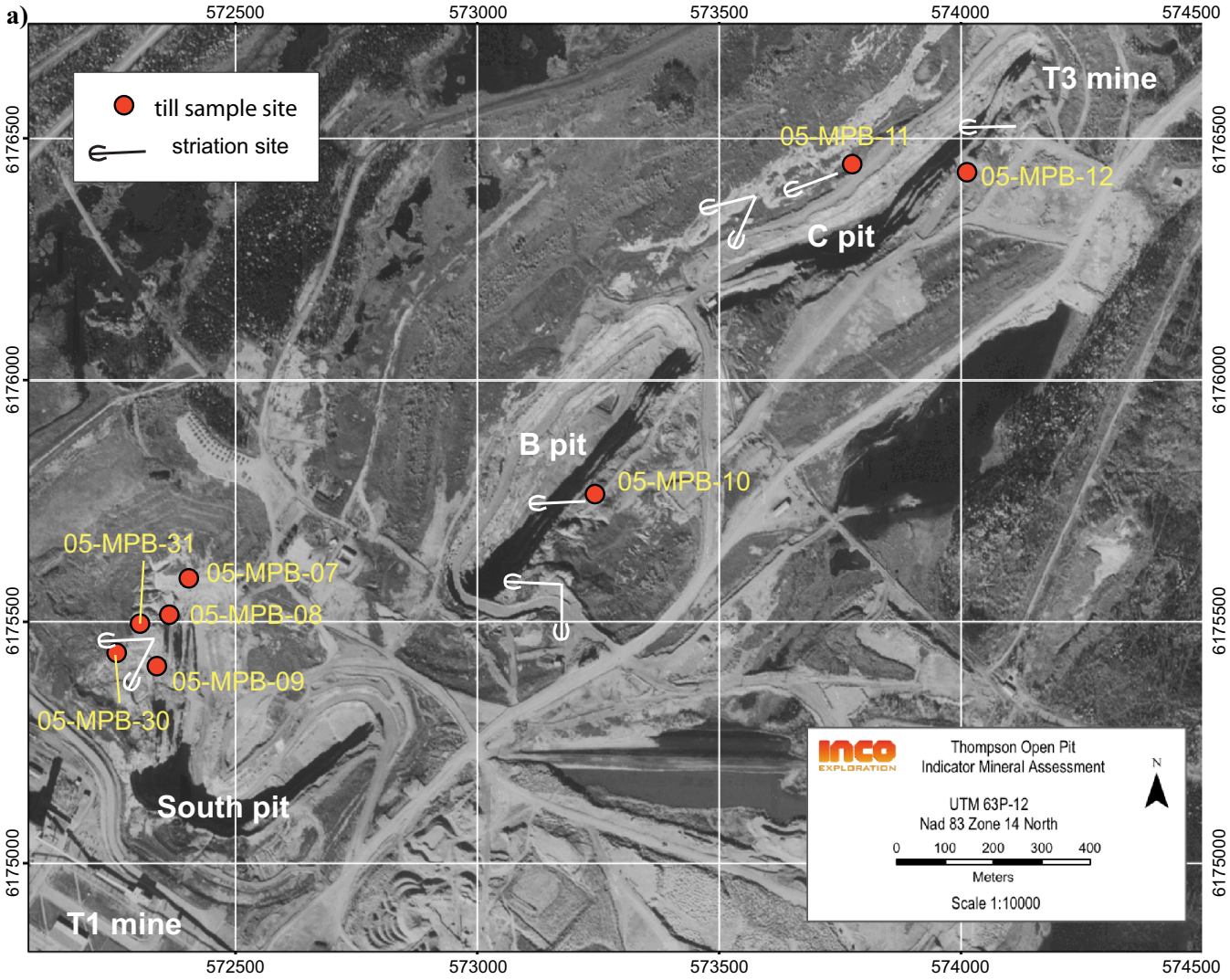

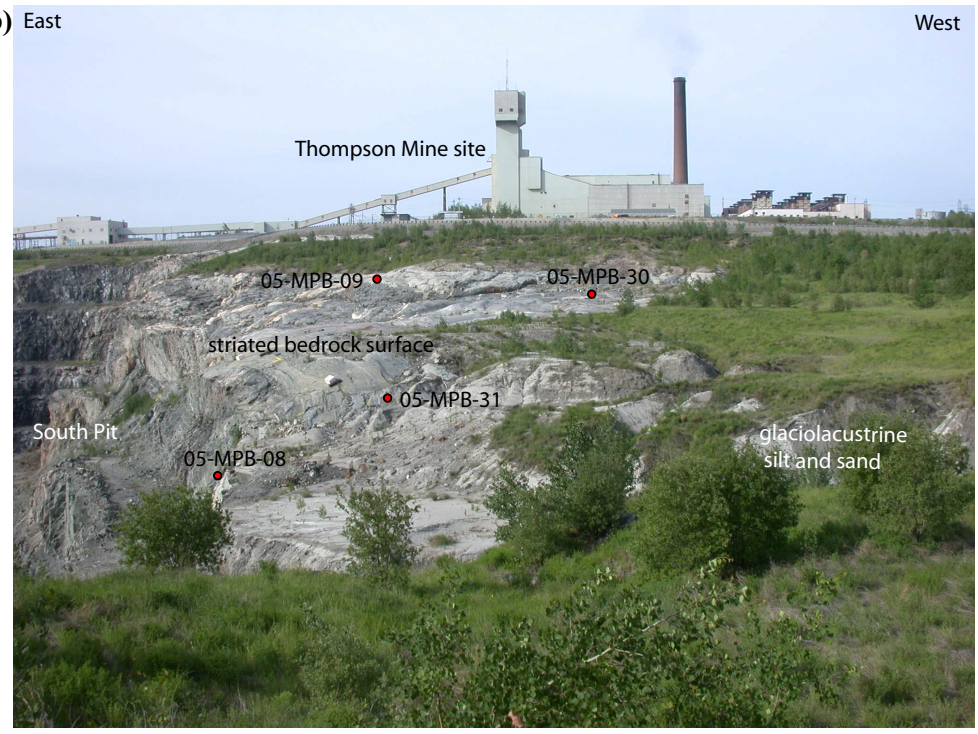

Figure 3. a) Airphoto showing the location of till samples collected around the Thompson Mine open pits (photo from Vale). **b)** Oblique photo looking south at selected till sample locations (red dots) and striated bedrock outcrop on the west side of the South Pit, Thompson Mine. Striations at this site trend southwest (older) and west (younger).

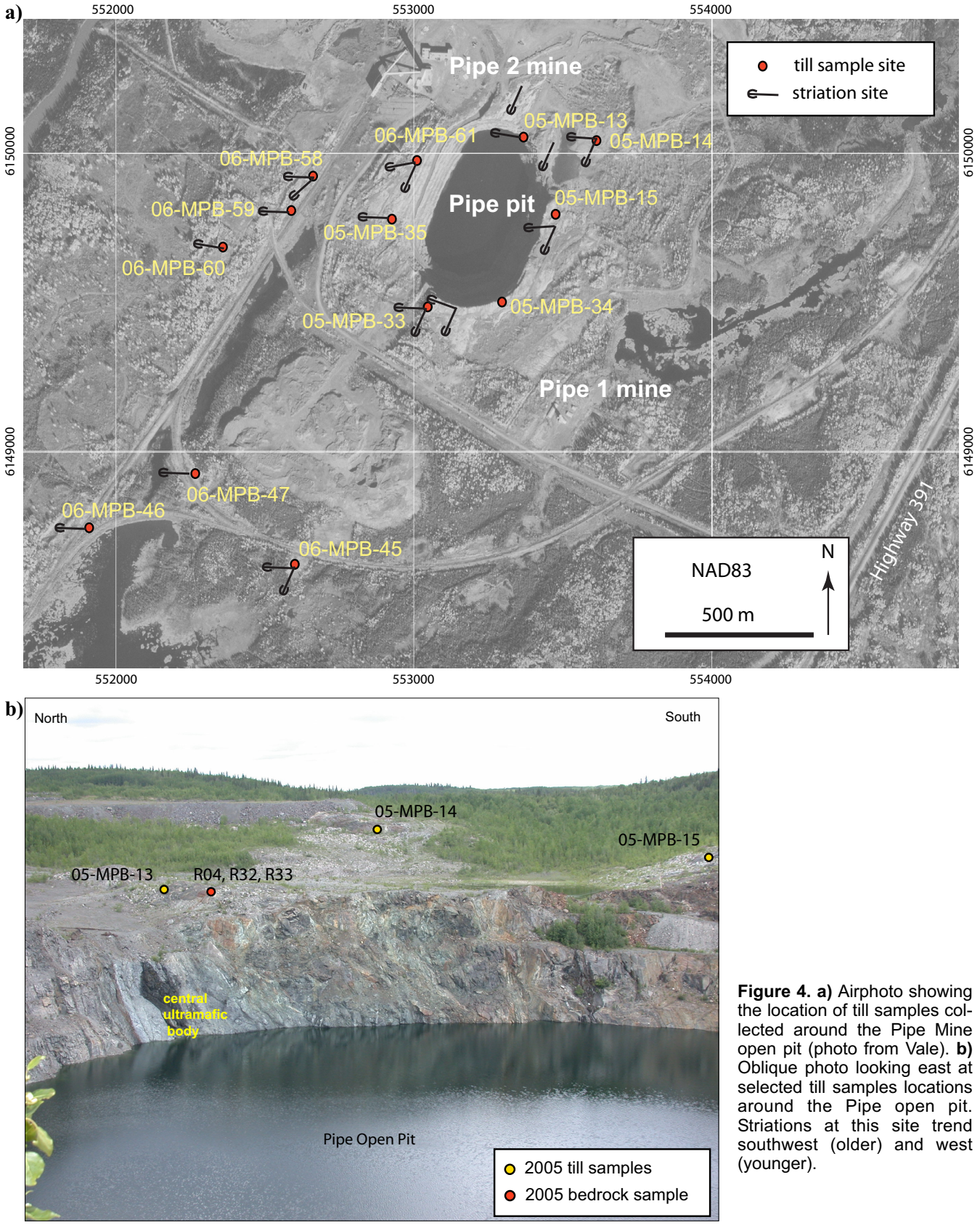

Figure 4. a) Airphoto showing the location of till samples collected around the Pipe Mine open pit (photo from Vale). **b)** Oblique photo looking east at selected till samples locations around the Pipe open pit. Striations at this site trend southwest (older) and west (younger).

occurring up to 300 km down ice (southwest) of the Belt (Fig. 2) (Matile and Thorleifson,1997). The elevated Cr-diopside abundances in till overlying the TNB are accompanied by local occurrences of chalcopyrite, hercynite, chromite, Cr-rutile, and loellingite in till closer to the Ni-Cu deposits.

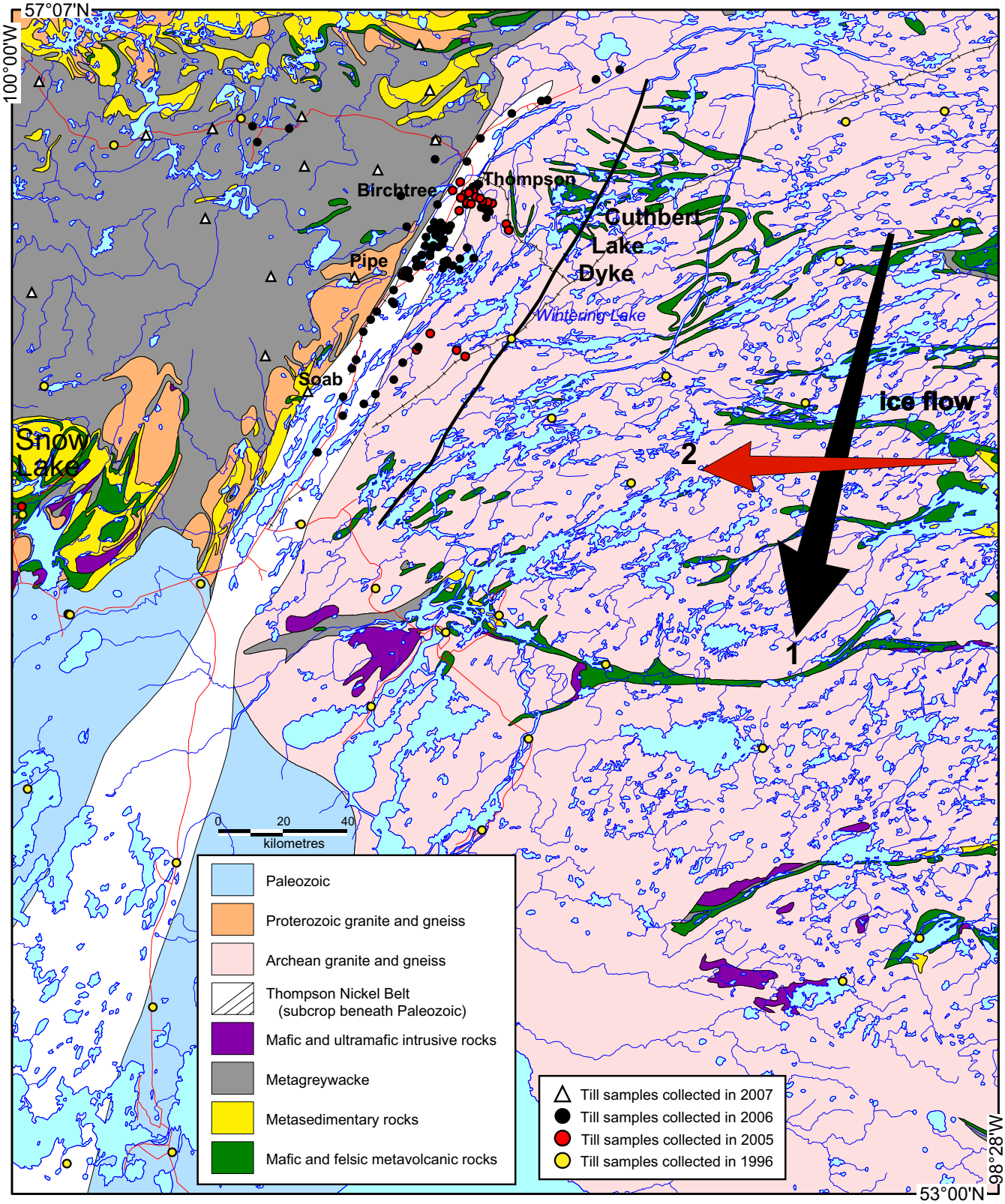

Figure 5. Location of the 2005 till samples (red dots), 2006 till samples (black dots), GSC archived (1996-TCA series) till samples (yellow dots), and 2007 (MOB series; white triangles) collected from across the region. Wisconsin regional ice-flow patterns for northern Manitoba are also shown: 1) black arrow represents the trend of older flow to the southwest; 2) red arrow represents the trend of younger flow to the west.

Thompson Mine Surficial Geology and Ice-Flow Features

The Thompson Mine complex includes three open pits, the South, B, and C pits (Fig. 3, Appendix A), where bedrock surfaces have been stripped of the overlying till and glaciolacustrine sediments. Most till sampling and striation measurements at the Thompson Mine were carried out on the west shoulder of the South pit because of its large (250 m^2) expanse of polished, flat-lying outcrop and exposed till sections. Evidence of both phases of ice flow is well represented on this outcrop, known informally as the West outcrop. However, striations from each flow were never found crosscutting one another. The West outcrop is well striated and sculpted, and displays moderate- to large-sized roche moutonnées oriented westward (younger ice flow). In some areas on the outcrop, the bedrock surface is striated and moderately sculpted by the older, southwestward ice flow in protected lee-side facets on the bedrock surface (McClenaghan et al., 2009a).

At the northwest corner of the South pit, a ~20 m section exposes well stratified glacio-lacustrine silt and sand overlying till. From this location, the bedrock surface dips down towards the centre of the pit where the ore zone subcropped prior to mining. Some till remains on the surface of the West outcrop and some of this till was sampled in this study (Fig. 3). When initially stripped for open-pit mining, the subcropping ore zone in the South pit was observed to be well striated (Vale staff, pers comm., 2005). Thus, the ore zone was eroded by the glacier and metal-rich till should be found down ice of the Thompson deposit. Till on the west side of the South pit contains numerous mineralized cobbles and boulders. Also, clasts of Paleozoic limestone/dolostone and Omarolluk Formation greywacke containing calcareous concretions, derived from rocks from the eastern part of the Hudson Bay region (Prest et al., 2000), were observed in the till exposed at the South pit. Till was poorly exposed in the B and C pits, which limited till sampling. Previous reverse circulation drilling around the T3 mine site at the north end of the C pit, which was carried out by Inco, revealed that the area around the C pit is overlain by 10 to 30 m of clay, which in turn overlies 1 to 3 m of till on bedrock (Webster, 1973).

Pipe Mine Surficial Geology

Surficial sediments overlying bedrock around the Pipe open pit consist of thin till (1-2 m) overlain by glaciolacustrine clay and silt. Large expanses of stripped bedrock on the east side of the pit (Fig. 4) are well striated and sculpted by both the older southward and younger westward ice flows. The peridotite outcrop on the northeast shoulder of the open pit has been glacially sculpted into west-trending roche moutonnées. Elsewhere on the east side of the pit, Pipe Formation iron formation has been sculpted and striated by both the older southward and younger westward flows, although the younger set was never seen to crosscut the older set (McClenaghan et al., 2009).

Thompson Nickel Belt Exploration History

Inco was first attracted to the Thompson region in 1946 because of known nickel occurrences at Ospwagan Lake and elsewhere (Peredery et al., 1982). Inco's first discovery of Ni mineralization in the TNB was in 1955, which was quickly followed by the discovery of the Thompson orebody in 1956 (Peredery et al., 1982; Fraser, 1985; Layton Matthews et al., 2010). Subsequently, additional deposits were discovered and Inco brought the Thompson, Pipe, Soab, and Birchtree mines into production between 1961 and 1971 (Fig. 1). Exploration in the belt over the past 50 years has relied exclusively on geophysical and bedrock mapping methods. Indicator mineral methods have never been used as an exploration tool for Ni-Cu mineralization in this region.

METHODS

Field Sampling

In 2005 and 2006, till samples were collected for indicator mineral analysis from the north part of the TNB, including areas west and east of the belt (Fig. 5; Appendix A). Sample sites included mine properties, road cuts, borrow pits, river sections, and backhoe trenches, at varying distances up- and down-ice of the Ni-Cu deposits at the Thompson, Pipe, and Birchtree mines. The objective of the till sampling was not to define dispersal trains from each deposit but rather to characterize the mineralogical signature of Ni-Cu mineralization at the deposit- and camp-scale at varying distances down-ice. As is typical of most glacial lake basin-dominated glaciated terrains of the Canadian Shield, 1 to 2 m of till was accessible for sampling on the flanks of bedrock outcrops or where road cuts had exposed till underlying glaciolacustrine sediments.

In 2005, 49 till samples were collected from the northern part of the TNB; their locations are reported in Appendix A1 and plotted on a large map in Appendix A2. Eight till samples were collected from the exposed bedrock shoulders of the three open pits on the Thompson Mine property (Fig. 3, Appendix A3): samples 05-MPB-007, -008, -009, -030, -031 from the South pit, 05-MPB-010 from the B pit, and 05-MPB-011 and -012 from the C pit. Six till samples were collected from around the edges of the Pipe Mine open pit: samples 05-MPB-013, -014, -015, -033, -034, and -035 (Fig. 4, Appendix A4). Sample 05-MPB-032 was collected from exposed bedrock on the south shoulder of the Manasan Quarry, 10 km southwest of the

Thompson Mine. The other 34 till samples were collected from the flanks of bedrock outcrops, road-cut exposures, or borrow pits at various locations within and outside of the TNB to provide a regional context to interpret the metal-rich till from around the deposits. Samples 05-MPB-001 to -006 and -016 to -019 were collected west and east of the north end of the TNB to determine backgrounds concentrations outside the TNB.

In 2006, 70 till samples were collected to augment the 2005 till-sample coverage (Appendix A1, A2) from areas proximal to the Thompson, Birchtree, and Pipe mines that were difficult to sample in 2005 because of the thick cover of glaciolacustrine clay. Sample locations are listed in Appendix A2. A wheeled backhoe excavator was used to collect several of the samples on the Thompson and Pipe mine properties. A total of 22 till samples were collected from 1 to 10 km southeast to southwest of the Thompson Mine site (samples 06-MPB-40 to -44, -53, -56, -57, -63 to -69, -89 to -95). Eight till samples were collected immediately south and west of the Pipe open pit (06-MPB-45 to -47, -58 to -62). Two samples (06-MPB-54, -55) were collected 3 km west of the Birchtree and Thompson mines from natural shoreline exposures along the Burntwood and Manasan rivers. Four samples were collected further west of the Birchtree mine, west of the TNB (06-MPB-118, -120 to 122). Five samples were collected along a forest access road, south of Paint Lake, to augment coverage in background areas southeast of the TNB (06-MPB-48 to -52). Two samples (06-MPB-70, -71) were collected 200 km southwest of the TNB, in the Snow Lake area, to augment regional-scale coverage west of the Belt. Field duplicates were collected at sites 05-MPB-48 and 06-MPB-72; 06-MPB-065 and -093; and 06-MPB-066 and -092 to document field variability. Samples 06-MPB-96 to -104 were collected around the shores of Paint Lake. Samples 06-MPB-85 to -88, 06-MPB-105 to -117, and 06-MPB-119 were collected around the shoreline of Ospwagan Lake and Upper Ospwagan Lake. All 2005 and 2006 till sample locations, field descriptions, and site photos are included in McClenaghan et al. (2009a). Field duplicates were collected at three sites: 06-MPB-72 is a duplicate of 05-MPB-48, 06-MPB-093 is a duplicate of 06-MPB-065, and 06-MPB-092 is a duplicate of 06-MPB-066.

In addition to the 2005 and 2006 till samples, 32 archived heavy mineral concentrates of till samples (96-TCA-01 to -12, -15 to -17, -19 to -27, -30 to -32, -35, -37, -39, -40, -44), which were collected in 1996 by the Manitoba Geological Survey (MGS) and GSC (Appendix A.1) during a reconnaissance-scale survey of the region (Matile and Thorleifson, 1997), were re-examined. Most samples are from 150 km east and west of the TNB and provide the regional context for interpretation of the more closely spaced samples from the TNB. Sample locations for the 1996 till samples are listed in Appendix A1 and detailed sample descriptions are provided in Matile and Thorleifson (1997). Mineral chemistry data for selected 96-TCA samples published by Matile and Thorleifson (1997) were also used in this study for comparison with the 2005 and 2006 till samples.

Mineral abundance and chemistry data for till samples (07MOB- series, Appendix A2), which were collected by the GSC in 2007 from the west side of the study area as part of the Flin Flon TGI3 project (McMartin et al., 2012), have been plotted with data from this study on maps and discrimination diagrams in this report.

In additional to till sampling, bedrock striations were measured in 2005 and 2006 to record the direction of glacial transport. Striation data and striation site photos are included in McClenaghan et al. (2009a).

Sample Processing and Indicator Mineral Picking

Till samples were shipped to Overburden Drilling Management Ltd. (ODM) in Ottawa for processing, production of heavy mineral concentrates, and indicator mineral picking. The raw data files reported by ODM are listed in Appendix B and formatted data listings are reported in Appendix C for ease of viewing. The <2.0 mm material was processed to produce a nonferromagnetic heavy mineral concentrate for selection of indicator minerals as outlined in Figure 6; weights for all fractions produced are reported in Appendix C1. First, the <2.0 mm material was passed over a shaking table and the heavy table concentrate recovered was micropanned to recover gold, sulphide, and platinum group minerals (PGM). The minerals in the panned concentrates were counted, their size and shape characteristics recorded (Appendix C2-C4), and then returned to the sample. Concentrates were then sieved at 0.25 mm. The 0.25 to 2.0 mm pre-concentrate was then further refined using heavy liquid separation in methylene iodide diluted to a specific gravity of 3.2. After panning and heavy liquid separation, the ferromagnetic fraction, including magnetite and pyrrhotite, was then removed and the nonferromagnetic heavy mineral fraction was sieved into four size fractions: <0.25, 0.25-0.5, 0.5-1.0, 1.0-2.0 mm. Ten samples collected in 2005 and 2006 and two samples collected by McMartin (MOB series) generated large concentrates weighing up to 150 g, thus only 10%, 25%, or 50% of these nonferromagnetic concentrates were sieved and picked for indicator minerals. The percentage sieved and picked is highlighted in red for these samples in Appendix C1. The indicator mineral counts for subsets of these 12 samples were normalized to reflect the total indicator mineral count in the entire sample (Appendix C5 and C6). For exam-

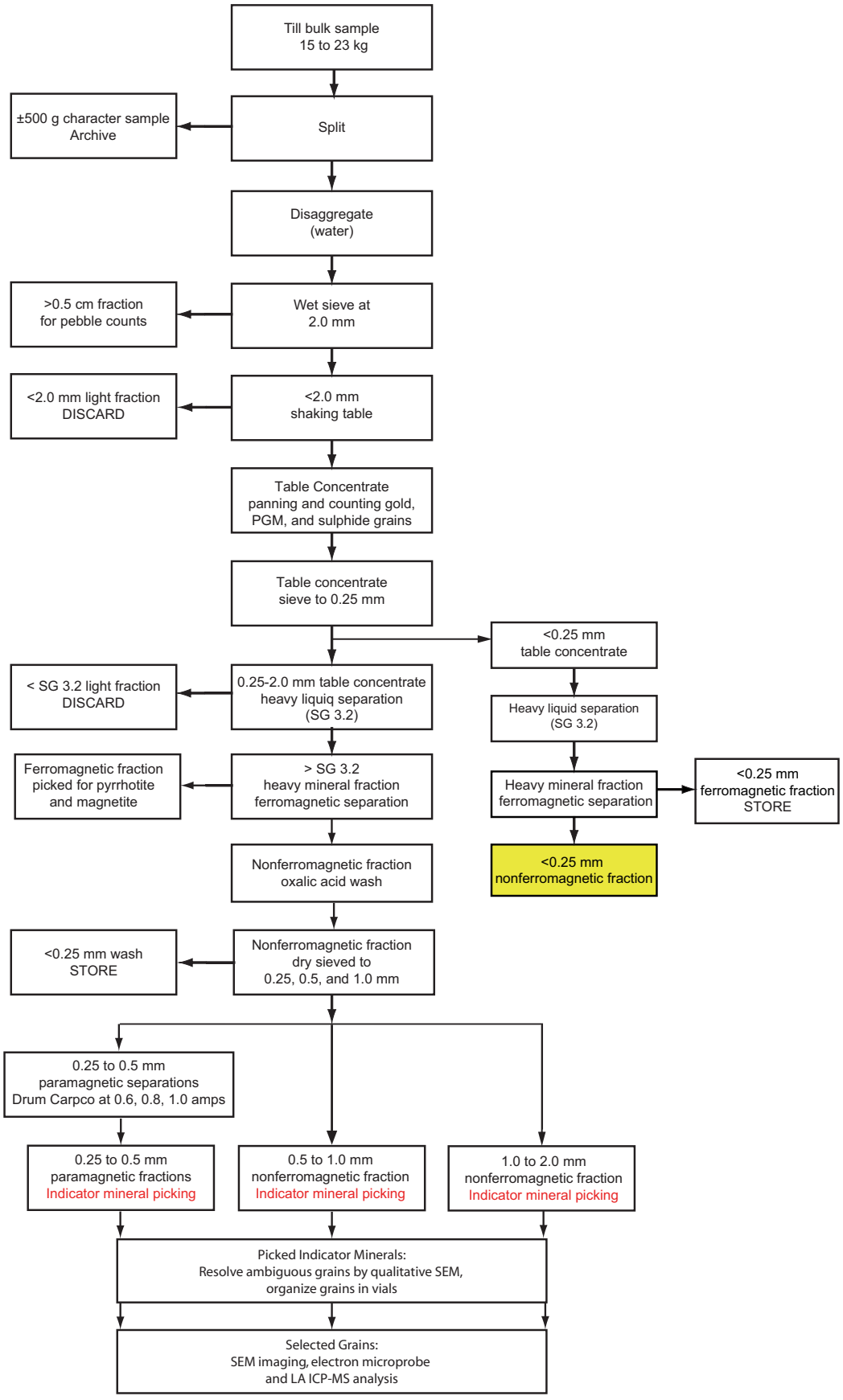

Figure 6. Flowsheet outlining the sample processing and picking procedures used for the till samples at Overburden Drilling Management Ltd.

Table 2. Predicted Ni-Cu-PGE indicator minerals based on observations of surficial sediment heavy mineral concentrates by Overburden Drilling Management Ltd. The cumulus indicators are identical to the melt fertility indicators but occur in higher, more localized concentrations in bedrock and produce stronger, more constricted dispersal anomalies (from Averill, 2009).

Melt Fertility Indicators		Cumulus Indicators		Hybrid Indicators		Indicators of Mineralization	
Mineral	Compostion	Mineral	Compostion	Mineral	Compostion	Mineral	Compostion
Enstatite	$(Mg,Fe)_2Si_2O_6$	Enstatite	$(Mg,Fe)_2Si2O_6$	Ruby corundum	$(Al,Cr)_2O_3$	Chalcopyrite	$CuFeS_2$
Forsterite	$(Mg,Fe)SiO_4$	Forsterite	$(Mg,Fe)SiO_4$	Hercynite	$FeAl_2O_4$	Isoferroplatinum	Pt_3Fe
Low-Cr diopside	$Ca(Mg,Cr)Si_2O_6$	Low-Cr diopside	$Ca(Mg,Cr)Si_2O_6$	Cr-andradite	$Ca_3(Fe,Cr)_2(SiO_4)_3$	Native palladium	Pd
Chromite	$(Fe,Mg)(Cr,Al)_2O_4$	Chromite	$(Fe,Mg)(Cr,Al)_2O_4$	Cr-grossular	$Ca_3(Al,Cr)_2(SiO_4)_3$	Native gold	Au
				Uvarovite	$Ca_3Cr_2(SiO4)_3$	Sperrylite	$PtAs_2$
						Stillwaterite	Pd_8As_3
						Loellingite	$(Fe,Ni)As_2$
						Stibiopalladinite	Pd_5Sb_2

ple, if 50% of the heavy mineral fraction was picked, then the number of indicator mineral grains reported by ODM was multiplied by 2.

The <0.25 mm heavy mineral fraction of all till samples was archived and the 0.25-0.5 mm fraction was further subjected to paramagnetic separations using a Carpo® magnetic separator to produce <0.6 amp (strongly paramagnetic), 0.6 to 0.8 amp (moderately paramagnetic), 0.8 to 1.0 amp (weakly paramagnetic), and >1.0 amp (nonparamagnetic fractions) to assist counting and picking indicator minerals in this very fine-grained fraction. The 0.25-0.5 mm fraction was cleaned with oxalic acid to remove oxidation stains (tarnish) from the grains and restore their natural colour, which is important for the sulphide minerals.

The 0.25-0.5, 0.5-1.0, and 1.0-2.0 mm nonferromagnetic fractions were examined by personnel at ODM; indicator minerals counted/selected included gold and PGM grains (Appendix C2-C4), kimberlite indicator minerals (Appendix C5), and metamorphosed massive sulphide indicator minerals including minerals indicative of magmatic Ni-Cu-PGE deposits (Appendix C6). The magmatic Ni-Cu-PGE indicator mineral suite (Table 2) was first identified by Averill (2001). A selection of apatite was also picked because of its presence in pegmatite related to the Thompson and Pipe deposits. The concentrates were scanned for kimberlite indicator minerals (Appendix C5), three of which (chromite, Cr-diopside, and forsterite) are common to both kimberlite and Ni-Cu-PGE deposits (Averill, 2011). The visual identification of several mineral grains was verified by personnel at ODM using a scanning electron microscope (SEM). A selection of picked grains was analyzed using an electron microprobe (EMP) to determine their elemental composition.

The digital data files reported by ODM (Appendix B) consist of several worksheets for each of the three batches of samples processed: (1) 2005 till samples (Appendix B1), (2) 2006 till samples 06-MPB-40 to -72 (Appendix B2), and (3) 2006 till samples 06-MPB-84 to 122 (Appendix B3). The weights of the fractions produced during sample processing are reported in four worksheets: "Tabling Data", "Weights", "Paramag" (weights for the paramagnetic fractions), and "TC weight" (<0.25 mm table concentrate weights). For bedrock samples, the weights of the fractions produced during sample processing are reported in four worksheets: "Tabling data", "KIM data", "Paramag" (weights for the paramagnetic fractions), and "TC weight" (<0.25 mm table concentrate and heavy liquid weights). Gold grain data are reported in two worksheets: "Gold summary" and "Detailed VG", which describe the abundance, size, and shape of the visible gold, sulphide, and PGM grains observed during panning. PGM abundances are listed in the "PGMs" worksheet. Indicator minerals (0.25-2.0 mm in size) of massive sulphide deposits are listed in worksheet "MMSIM". Kimberlite indicator mineral abundances are reported in the worksheet "KIM data". The abundance of pyrrhotite in the <2.0 mm ferromagnetic fraction of 2005 till and 2006 till samples 06-MPB-040 to -72 are reported in worksheet "Pyrrhotite" (Appendix B4).

The 0.25-0.5 mm fraction of 32 of the archived 96-TCA (1996) heavy mineral concentrates were re-examined in two batches and indicator minerals counted to augment sample coverage in distal areas both east and west of the TNB (Appendix A2 map). These till samples were processed by ODM in 1996 using heavy mineral concentrating procedures similar to those used for the current study; these are described in Matile and Thorleifson (1997). All grains picked in 1996 were analyzed using EMP and the mineral chemistry results are reported in Matile and Thorleifson (1997). The original 1996 picking data and the 2006 re-picking results are listed for the two batches in Appendix B5 and B6; these data were combined in Appendix C7 for data plotting and interpretation. Digital data files in Appendix B5 include the original weight data reported by ODM in 1996 as the "HMC Weights worksheet and indicator mineral counts are listed in the "MMSIM" worksheet. For the second batch of repicked samples

listed in Appendix B6, kimberlite indicator mineral count data are listed in the "KIM" worksheet and other indicator mineral counts are listed in the "MMSIM" worksheet.

Pebble Llithology Examination

The 0.5 to 2.5 cm (pebble) fraction of the 2005 and 2006 till samples that was recovered during processing at ODM was sent to Consorminex Inc., Gatineau, Quebec, for examination and classification of the bedrock lithologies present. Such pebble lithology information may assist in determining the distance and direction of glacial transport of the till. Classification categories included the major rocks types identified in the samples and adjacent to the TNB. Pebble data listings, including raw counts and frequency percent, as well as high-resolution photographs of the classified pebbles in each sample are included in Appendix D.

Data Plotting

Because till sample weights of the <2.0 mm fraction that was processed to recover the heavy mineral fraction varied between 5.0 to 14.6 kg, visual indicator mineral counts for the 0.25 to 0.5 mm fraction of 2005, 2006, 2007, and 1996 till samples were normalized to 10 kg of <2 mm (table feed) material (Appendix C8). These normalized abundances of selected indicator minerals were plotted with MapInfo® v 7.8, using proportional dots, both at a regional scale and at a local scale, in the vicinity of the Thompson and Pipe deposits (Appendix E) and are discussed below.

Electron Microprobe Analyses

A subset of the indicator mineral grains picked (Cr-diopside, olivine, chromite, spinel, gahnite, corundum, sapphirine, rutile) from selected samples were analyzed at Geoscience Laboratories, Sudbury, Ontario using a Cameca SX-100 Electron Probe Micro Analyzer (EPMA) to confirm their visual identification and characterize their compositions. The probe routines described in Appendix F illustrate the choice of standards, together with the analyzing crystals (XTAL's), counting times, operating voltage, beam current, limits of detection (L.O.D.s using the 3 sigma definition), and limits of quantification (L.O.Q.s using the 10 sigma definition). Major elements were analyzed under normal operating conditions (20 kV and 20nA), whereas minor/trace element analyses were carried out using a higher beam current (20kV and 200nA) and — where possible — large surface area crystals (LLIF and LPET) were employed to improve the L.O.D.s. operating conditions are listed in Appendix F.

A random selection of 10 to 20 pyrrhotite grains from the <2.0 mm ferromagnetic fraction of till samples 05-MPB-09, -12, (Thompson deposit) and 05-MPB13, -14, 06-MPB-058 (Pipe deposit) were analyzed at the Earth Sciences Department, Carleton University, Ottawa, using an automated 4 spectrometer Cameca MBX electron microprobe by wavelength dispersive x-ray analysis method (WDX). Raw data were processed using the PAP overlap correction procedure. Operating conditions are listed in Appendix F.

Published EMP data for selected 96-TCA series till samples reported by Matile and Thorliefson (1997) and 07MOB series samples reported by McMartin et al. (2012) were used in this study for comparison with EMP results for the 2005 and 2006 till samples (Table 3).

RESULTS

Raw ODM weight and mineral grain abundance data are reported in Appendix B. Unless otherwise noted, the grain counts discussed below refer to counts in the 0.25-0.5 mm fraction normalized (Appendix B.9) to 10 kg sample weight of <2.0 mm fraction (table feed) listed in Appendix B.2. Note, results are not reported here for till sample 05-MPB-022, collected on the north side of the road into Paint Lake Provincial Park, as the sample was found to contain slag grains (27, 20) in the 0.5-1.0 mm and 0.25-0.5 mm fractions, respectively. Also, the sample contained pentlandite, chalcopyrite, and malachite. Such significant numbers of slag grains combined with the unstable sulphide minerals would only be expected in a mixture of unweathered till proximal to mineralization and anthropogenic material. It is likely that the material sampled at site 05-MPB-022 was reworked till combined with road fill brought in from the Thompson Mine site.

Results for field duplicate pairs are compared at the bottom of the data listing in Appendix C6. Mineral abundances for duplicate pairs are similar except for the number of grains of forsterite and low Cr-diopside and percentage of orthopyroxene and apatite. The significant variations between duplicate pairs for these minerals are a function of both field site variability and variations related to mineral grain abundance estimating/counting in the lab.

General Mineralogy of Concentrates

Most till samples yielded large (30 to 70 g) heavy mineral concentrates due to the overall highly metamorphosed condition that resulted in high concentrations of heavy minerals in the regional bedrock. The principal exception is at the northeast extremity of the Thompson Belt, beyond the Thompson Mine (Fig. 5, Appendix A2), where samples 05-MPB-001 to -006 yielded smaller (3 to 30 g) concentrates. Epidote is a major mineral in these small till concentrates, suggesting that the main source rocks for these samples are granitoid plutons, which typically are heavy mineral deficient. The most common major background miner-

Table 3. Geographic groupings of till samples used for plotting and interpreting mineral chemical data.

Till Groups		GSC 2005 Samples	n	GSC 2006 Samples	n	Matile & Thorleifson (1997)	n	McMartin et al. (2012)	n
1	background northeast	05-MPB-001- to -006	6						
2	background west of TNB	05-MPB-016- to -019	4	06-MPB-118, -120 to -122	4	96-TCA-001, -002, -007, -008, -012	5	07MOB-22 to -27 -29 to -34,-37	15
3	Thompson Mine site	05-MPB-007- to -012, -30, -31	8						
4	Pipe Mine site	05-MPB-013 to -15, -33 to -35	6	06-MPB-45 to -47, -58 to -62	8				
5	Ospwagan Lake	05-MPB-021,-025, -026, -32	4	06-MPB-84 to -88, -105 to -117, -119	19				
6	South of Pipe	05-MPB-027 to -029,-036 to -039	7			96-TCA-013	1		
7	South of Soab, TNB south	05-MPB-040 to -042, -049	3			96-TCA-006, -009, -014 to -015	4	07-MOB-28	1
8	southeast of Pipe, east of Soab	05-MPB-043- to -048	7	06-MPB-48 to -52, -72	6				
9	north of Thompson, within TNB	05-MPB-020	1			96-TCA-018	1		
10	east and east-south-east of Thompson	05-MPB-023, -24	2	06-MPB-40 to -42, -63 to-68, -90 to -95	15				
11	south+southwest of Thompson			06-MPB-43, -44, -53 -56, -57, -69, -89	7				
12	west of Birchtree/ Thompson			06-MPB-54, -55	2				
13	east of TNB			06-MPB-96 to -104	9	96-TCA-10, -11, -16, -20 to -44	21		
14	south of Snow Lake			06-MPB-70	1	96-TCA-003 to -005	3		
15	Snow Lake belt			06-MPB-71	1				
16	Cuthbert Lake Dyke					96-TCA-019	1		

als in the larger concentrates are paramagnetic hornblende, almandine garnet and orthopyroxene, and non-paramagnetic diopside. The four samples (05-MPB-016 to -019) overlying the Kisseynew paragneiss west of the TNB yielded negligible orthopyroxene and significant sillimanite.

Hornblende and almandine in the TNB till samples are not diagnostic of a specific bedrock source as they occur in many of the rock formations throughout the region. Most diopside in till is dark green and Fe-bearing, which is typical of two-pyroxene granulite terranes such as Pikwitonei rather than the pure, pale green-white variety of the TNB calc-silicate. Furthermore, most of the orthopyroxene in till is dark brown hypersthene, which is characteristic of granulite, rather than pale brown enstatite, which is typical of the Mg-rich TNB peridotite and pyroxenite. Hypersthene is the dominant mineral in all six samples (05-MPB-043 to -048) collected on a traverse across the Superior Boundary Zone. The overall distribution of both clinopyroxene and orthopyroxene suggests significant glacial transport by late westward ice flow from the Pikwitonei terrane onto the TNB wtih minor transport further westward onto the Kisseynew terrane. Consequently, earlier south-southwest ice flow subparallel to the Thompson Ni Belt would be expected to be reflected in the Ni-Cu-PGE indicator minerals.

The abundance and distribution of minerals in till that may be derived from the Ni-Cu mineralization, as well as minerals indicative of other base metal deposit types (e.g. gahnite) are reported below. Unless otherwise stated, grain abundances in the 0.25-0.5 mm fraction are described.

Sulphide and Arsenide Minerals

Pentlandite

Pentlandite was identified in the heavy mineral concentrates by its pyrrhotite-like bronze colour (Fig. 7a) in combination with its nonmagnetic character. It is most abundant in the 0.25-0.5 mm fraction and background concentration in till across the region is zero grains (Appendix E1, map 1). Pentlandite was only found in unweathered till samples 05-MPB-007 to -

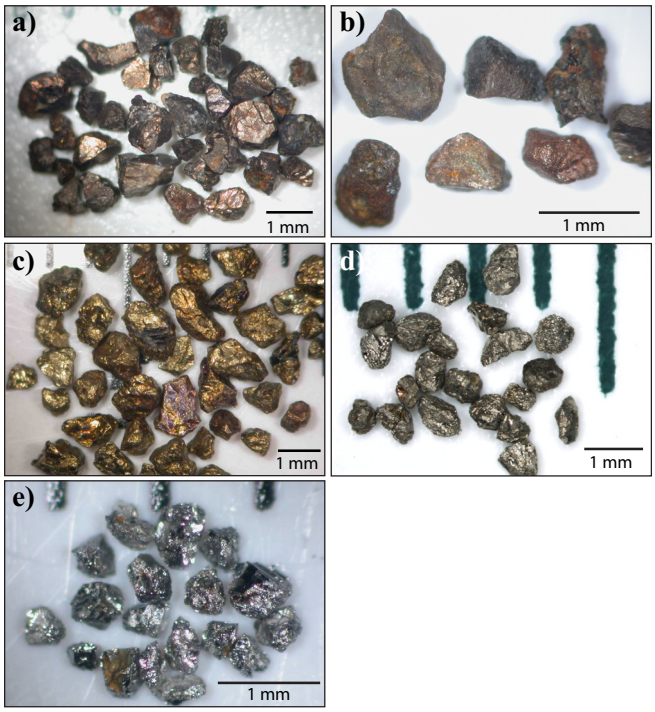

Figure 7. Colour photographs of sulphide and arsenide indicator mineral grains from till samples: **a)** pentlandite grains from the 0.5-1.0 mm fraction of sample 05-MPB-10 from the Thompson deposit; b) pyrrhotite grains from the 1.0-2.0 mm fraction of sample 05-MPB-14 from the Pipe deposit; **c)** chalcopyrite grains from the 0.5-1.0 mm fraction of sample 05MPB-09 from the Thompson deposit; **d)** pyrite grains from the 0.25-0.5 mm fraction of sample 05-MPB-08 from the Thompson deposit; and **e)** arsenopyrite grains from the 0.25-0.5 mm fraction of sample 05-MPB-14 from the Pipe deposit.

012, -030, and -031 at the Thompson deposit (Appendix E2, map 16) and these samples contained 2 grains to ~41,000 grains. No pentlandite grains were found in till at the Pipe deposit. A few coarser grains (0.5-1.0, 1.0-2.0 mm) were also recovered from till samples 05-MPB-007 to -010, -030, and -031 at the Thompson deposit (Table 4). Pentlandite was also recovered from the coarser 0.5-1.0 mm and 1.0-2.0 mm fractions. Samples 05-MPB-007- 0010, -012, -030, and -031 from the South pit at the Thompson deposit contain between 1 and 1500 grains in these coarser fractions (Table 4).

Pyrrhotite

Pyrrhotite was identified by its bronze colour, crystal habit (Fig. 7b) and strong magnetic character. Its abundance in the <2.0 mm ferromagnetic fraction of the heavy mineral concentrate was determined for all of the 2005 till samples and a selection of the 2006 samples (06-MPB-40 to -72), and is reported in Appendix B4. Background concentration in till is zero grains. Ten samples contained pyrrhotite in the ferromagnetic fraction, with concentrations ranging from 14 grains in sample 05-MPB-013 to >41,000 grains in sample 05-MPB-009 (Appendix E1, map 2). All till samples found to contain pyrrhotite are from the shoulders of the Thompson or Pipe open pits, i.e., within 500 m of mineralization (Appendix E2, map 17 and Appendix E3, map 29).

Chalcopyrite

Chalcopyrite was identified by its metallic brass yellow colour, i.e., more yellow than pyrite (Fig. 7c). It is most abundant in till in the 0.25-0.5 mm fraction and varies in abundance from 0 to ~2100 grains (Appendix B.9). Trace (background) amounts (1 to 10 grains) are found in till samples all along the TNB (Appendix E.3, map 3). The highest abundances (100s to 1000s of grains) are in unweathered till at the Thompson deposit (05-MPB-08 to -10, -30). Moderate abundances (11 to 99 grains) are contained in till samples from the Thompson deposit (05-MPB-007, -011, -012, -031), Pipe deposit (05-MPB-013 to -015), 800 m west of the Soab North deposit (sample site 05-MPB-041), near Snow Lake (site 96-TCA-03), on the shore of Upper Ospwagan Lake (site 06-MPB-84), and southwest of the Birchtree deposit (site 06-MPB-118). Till samples around the Thompson deposit contain a maximum of 2083 grains (Appendix E2, map 18) in contrast to much lower abundances (maximum 33 grains) in till proximal to the Pipe deposit (Appendix E3, map 30). The highest grain counts at the Pipe deposit are located east of the central ultramafic body and the open pit, overlying iron formation (Pipe Formation).

Chalcopyrite was also recovered from the coarser 0.5-1.0 mm and 1.0-2.0 mm fractions (Table 4). Samples 05-MPB-008, -009, -010, and -030, from the South pit at the Thompson deposit, contain >14 grains each in the 0.5-1.0 mm fraction. Other samples that contain coarse chalcopyrite include 05-MPB-013 to -015, 06-MPB-59, -61 from the Pipe deposit, samples 05-MPB-21, 06-MPB-84, and -85 from Upper Ospwagan Lake, and samples 06-MPB-087, -111, -112, -115 from the north shore of Ospwagan Lake. Very coarse (1.0-2.0 mm) grains were recovered from samples 05-MPB-008, -009, -011, -030 from the Thompson deposit, samples 05-MPB -013 to -015 from the Pipe deposit, site 05-MPB-041 just west of the Soab North deposit, and site 06-MPB-85 on the shore of Upper Ospwagan Lake (Table 4).

Pyrite

Pyrite was identified by its metallic pale brass yellow colour (Fig. 7d). Its abundance in till samples varies between 0 and ~13,000 grains (Appendix B.9), with background concentrations ranging from 1 to 5 grains (Appendix E.1, map 4). Counts are highest (1000s of grains) in unweathered till samples at the Thompson pits (samples 05-MPB-007 to -012, -030, -031)

Table 4. Comparison of abundances of pentlandite, chalcopyrite, and pyrite in four size fractions of till heavy mineral concentrates: pan concentrate (<0.25 mm), 0.25-0.5 mm, 0.5-1.0 mm, and 1.0-2.0 mm fractions.

Sample	Pentlandite				Chalcopyrite				Pyrite			
	No. grains pan concentrate	No. grains 0.25-0.5 mm	No. grains 0.5-1.0 mm	No. grains 1.0-2.0 mm	No. grains pan concentrate	No. grains 0.25-0.5 mm	No. grains 0.5-1.0 mm	No. grains 1.0-2.0 mm	No. grains pan concentrate	No. grains 0.25-0.5 mm	No. grains 0.5-1.0mm	No. grains 1.0-2.0 mm
05-MPB-001		0				2				0		
05-MPB-002		0				6				0		
05-MPB-003		0				0				2		
05-MPB-004		0				0				0		
05-MPB-005		0				3			5	1200		
05-MPB-006		0				0				3		
05-MPB-007	1	19	6			19	1			1200		
05-MPB-008		400	82			100	15	1	400	12000		
05-MPB-009		50,000	1500	35		2500	200	9	2000	15000		
05-MPB-010		350	40	4		700	22		2000	7000		
05-MPB-011		2				23	1	1	2000	6000		
05-MPB-012		7	1			9				2200		
05-MPB-013		0				30	8	3	300	10000		
05-MPB-014		0				32	3	1	500	13000		
05-MPB-015		0				20	5	2	500	16000	1	
05-MPB-016		0				4	4	1		0		
05-MPB-017		0				10				10		
05-MPB-018		0				4				15		
05-MPB-019		0				1				3		
05-MPB-020		0				0				3		
05-MPB-021		0				4	1			2		
05-MPB-023		0				6				30		
05-MPB-024		0				3				30		
05-MPB-025		0				1				0		
05-MPB-026		0				2				0		
05-MPB-027		0				0				10		
05-MPB-028		0				6		1		3		
05-MPB-029		0				2				2		
05-MPB-030		40	19	1		350	75	4	1000	10000		1
05-MPB-031		40	11	1		16	2			3000		
05-MPB-032		0				1				8		
05-MPB-033		0				11	1			0		
05-MPB-034		0				0				1		
05-MPB-035		0				3				10		
05-MPB-036		0				2			25	15		
05-MPB-037		0				2			50	5		
05-MPB-038		0				2			20	5		
05-MPB-039		0				2				3		
05-MPB-040		0				1	1		5	0		
05-MPB-041		0				41	1	2		95		
05-MPB-042		0				2				0		

Table 4 continued.

Sample	Pentlandite				Chalcopyrite				Pyrite			
	No. grains pan concentrate	No. grains 0.25-0.5 mm	No. grains 0.5-1.0 mm	No. grains 1.0-2.0 mm	No. grains pan concentrate	No. grains 0.25-0.5 mm	No. grains 0.5-1.0 mm	No. grains 1.0-2.0 mm	No. grains pan concentrate	No. grains 0.25-0.5 mm	No. grains 0.5-1.0mm	No. grains 1.0-2.0 mm
05-MPB-043		0				0				1		
05-MPB-044		0				1				0		
05-MPB-045		0				3				0		
05-MPB-046		0				3				0		
05-MPB-047		0				2			5	0		
05-MPB-048		0				2				0		
05-MPB-049		0				0				5		
06MPB-040		0				3				1		
06MPB-041		0				3				10		
06MPB-042		0				0				2		
06MPB-043		0				2				0		
06MPB-044		0				2				0		
06MPB-045		0				0				2		
06MPB-046		0				0				0		
06MPB-047		0				0				1		
06MPB-048		0				1				3		
06MPB-049		0				0				2		
06MPB-050		0				1				1		
06MPB-051		0				4				1		
06MPB-052		0				1				5		
06MPB-053		0				3				0		
06MPB-054		0				0				15		
06MPB-055		0				2				0		
06MPB-056		0				2	2			2		
06MPB-057		0				2				3		
06MPB-058		0				2				20		
06MPB-059		0				2	2			30		
06MPB-060		0				1				1		
06MPB-061		0				13	3			0		
06MPB-062		0				7				5		
06MPB-063		0				0				0		
06MPB-064		0				0				0		
06MPB-065		0				1				2		
06MPB-066		0				0				0		
06MPB-067		0				1				5		
06MPB-068		0				3				0		
06MPB-069		0				4				1		
06MPB-070		0				0				0		
06MPB-071		0				0				2500		
06MPB-072		0				0				0		
06-MPB-84		0				40	5	2		6		
06-MPB-85		0				9	1			8		

Table 4 continued.

Sample	Pentlandite				Chalcopyrite				Pyrite			
	No. grains pan concentrate	No. grains 0.25-0.5 mm	No. grains 0.5-1.0 mm	No. grains 1.0-2.0 mm	No. grains pan concentrate	No. grains 0.25-0.5 mm	No. grains 0.5-1.0 mm	No. grains 1.0-2.0 mm	No. grains pan concentrate	No. grains 0.25-0.5 mm	No. grains 0.5-1.0mm	No. grains 1.0-2.0 mm
06-MPB-86		0				4				2		
06-MPB-87		0				5	1		1	5		
06-MPB-88		0				0				7		
06-MPB-89		0				3				1		
06-MPB-90		0				0				3		
06-MPB-91		0				2				4		
06-MPB-92		0				0				0		
06-MPB-93		0				0				15		
06-MPB-94		0				2				0		
06-MPB-95		0				2				1		
06-MPB-96		0				1				4		
06-MPB-97		0				1				2		
06-MPB-98		0				0				0		
06-MPB-99		0				0				4		
06-MPB-100		0				0				0		
06-MPB-101		0				8				0		
06-MPB-102		0				2				0		
06-MPB-103		0				0				4		1
06-MPB-104		0				0				0		
06-MPB-105		0				2			5	100		
06-MPB-106		0				0				30		
06-MPB-107		0				0				2		
06-MPB-108		0				2				10		
06-MPB-109		0				4				35		
06-MPB-110		0				0			2	0		
06-MPB-111		0				13	2		10	100		
06-MPB-112		0				7	4		20	20		
06-MPB-113		0				0			5	30		
06-MPB-114		0				0				200		
06-MPB-115		0				3	1			15		
06-MPB-116		0				0				2		
06-MPB-117		0				2			10	20		
06-MPB-118		0				11			20	10		
06-MPB-119		0				0			10	3		
06-MPB-120		0				0				0		
06-MPB-121		0				0			25	80		
06-MPB-122		0				0				0		

* Calculated PPB Au based on assumed nonmagnetic HMC weight equivalent to 1/250th of the table feed.

(Appendix E2, map 19) and the Pipe pit (samples 05-MPB-013 to -015) (Appendix E3, map 31). Not unexpectedly, sample 06-MPB-71 from the Snow Lake volcanogenic massive sulphide camp to the west contains ~1900 grains. Till sample 05-MPB-005, from east of the north end of the TNB, contains ~1100 grains. Samples containing 100s of grains include 06-MPB-114 from the west side of Ospwagan Lake, sample 06-MPB-121 from 15 km west of the Birchtree mine, and site 96-TCA-11 located west of Lake Winnipeg. Till samples containing 10s of pyrite grains may also be noteworthy because they are proximal to Ni-Cu deposits (e.g. samples 06-MPB-58 and -59 from just west of the Pipe open pit; site 05-MPB-041 located 800 m west of the Soab North deposit). Sites 05-MPB-23 and -24, 5 km southeast of the Thompson deposit on the Jonas Forest access road, also contain 10s of pyrite grains.

Pyrite was also found in the <0.25 mm panned concentrates of some samples (Appendix B4, B5; Table 4). Samples at the Thompson and Pipe open pits and site 96-TCA-20, southeast of the TNB, contain 100s to 1000s of grains in this fraction. Tens of grains were panned from samples, from southwest of the Pipe deposit (samples 05-MPB-036 to -038), along the north shore of Ospwagan Lake (samples 06-MPB-110 to -112,-117), and west and southwest of the Birchtree deposit (samples 06-MPB-118, -121).

Arsenopyrite

Arsenopyrite (FeAsS) was distinguished from pyrite in the heavy mineral concentrates by its metallic white colour (Fig. 7e); however, some grains resembled loellingite ($FeAs_2$) to such a degree that their identity had to be confirmed by SEM analysis. Aresenopyrite content in till is low compared to that of pentlandite, pyrite, and chalcopyrite, and it was only found in nine till samples. Background concentration in till across the region is zero grains (Appendix E, map 5). Anomalous counts (1 to 27 grains) in till are restricted to unweathered till samples at the Thompson (samples 05-MPB-007, -010, -030, -031) and Pipe deposits (samples 05-MPB-013 to -015, -033), and weakly oxidized till at the Pipe deposit (sample 06-MPB-058) (Appendix E3). At the Thompson deposit, till samples contain a maximum of one grain (Appendix E2). In contrast, , till samples from the Pipe deposit contain up to 27 grains, with the most grains recovered from till samples that overlie iron formation (Pipe Formation) east of the open pit. One to three grains were recovered from pan concentrates of only three samples: 05-MPB-002, 06-MPB-108, and 06-MPB-115 (Appendix B5).

Sperrylite

Sperrylite ($PtAs_2$) was identified visually by its tin white colour and small size, and by using SEM analysis. Sperrylite counts for the pan concentrates and the 0.25 to 0.5 mm fraction were combined into a 'total' sperrylite count for each sample, and then normalized to a 10 kg sample weight (Appendix B5). The normalized values are discussed here and plotted in Appendix E (map 7). Background sperrylite concentration in till across the region is zero grains. Only 13 of the 152 till samples were found to contain sperrylite, and most of these contained 1 grain. Sperrylite was recovered from samples from the Thompson deposit (samples (05-MPB-08, -09, -10, -30, -31), and from a sample approximately 2 km southeast of the deposit (sample 06-MPB-69) (Appendix E2, map 22). At the Pipe deposit, sperrylite was recovered from samples 05-MPB-35, 06-MPB-58, -60, and -61 collected on south and west sides of the open pit (Appendix E3, map34). Sample 05-MPB-35 contained 14 grains of sperrylite, the largest number of grains recovered from a till sample collected in the TNB study area.

Platinum and Pd concentrations in the <0.063 mm fraction of the same till samples (McClenaghan et al., 2009a) were used to predict which heavy mineral concentrates might contain visible sperrylite grains. Two grains were recovered from the 0.25-0.5 mm fraction of samples 05-MPB-10 and -31, but additional grains (15 to 200 µm in size) were recovered by panning the <0.25 mm fraction (Appendix B7). Elevated Pd and Pt values were reported for three till samples that did not contain sperrylite. As a result, the <0.25 mm fractions of heavy mineral concentrates for samples 05-MPB-008, -030, and -035 were repanned and up to 15 sperrylite grains were found (Table 5).

Gold

Most till samples contain 0 to 5 gold grains, which is considered to be background concentrations. Sample 05-MPB-12, from the C pit at the Thompson deposit, contained 24 grains/10 kg, the most gold grains of any till sample in this study. Gold grains in till ranged in size from 15x15 µm to 125x250 µm, with most grains <50x50 µm; most grains shapes have been classified as 'reshaped', indicating a distal bedrock source (Appendix C2, C3).

Other Metallic Minerals

Loellingite ($FeAs_2$), which is optically similar to arsenopyrite, was identified by its silver-grey colour. All samples were systematically inspected for loellingite and when found its identity was confirmed by SEM. It was found in 15 till samples from 5 locatilities (Appendix B5): 1) samples 05-MPB-13, -15, and 06-MPB-62 from the Pipe deposit; 2) samples 05-MPB-16

Table 5. Comparison of sperrylite abundance and Pt and Pd concentrations in selected till samples.

Sample	Location	Distance (m) from Ore Zone	Direction from Ore Zone	Pt (ppb)	Pd (ppb)
05-MPB-007	Thompson-South pit	50	northwest	0.8	1.4
05-MPB-008	Thompson-South pit	50	west	2.8	12.3
05-MPB-009	Thompson-South pit	100	west	10.3	97.9
05-MPB-010	Thompson-B pit	0	over	3.2	54.6
05-MPB-011	Thompson-C pit	200	east	0.2	<.5
05-MPB-012	Thompson-C pit	200	west	0.8	1.8
05-MPB-013	Pipe-east side	0	over	3.5	1.7
05-MPB-014	Pipe-east side	250	east	1.9	1.5
05-MPB-015	Pipe-east side	200	east	1.3	1.1
05-MPB-030	Thompson	150	west	7.3	23.7
05-MPB-031	Thompson	50	west	1.4	2.4
05-MPB-033	Pipe- south side	100	southwest	2.4	3.3
05-MPB-034	Pipe- south side	200	south	2.4	2.4
05-MPB-035	Pipe-west side	400	west	13.1	19.8
06-MPB-058	Pipe-west side	500	west	0.9	0.7
06-MPB-059	Pipe-west side	500	west	1.9	2.5
06-MPB-060	Pipe-west side	750	west	3.6	4.3
06-MPB-061	Pipe-west side	300	west	2.1	6.6
06-MPB-062	Pipe- south side	500	south	2.0	1.9
06-MPB-069	Thompson Mine area	2000	southwest	1.1	1.2

and 96-TCA-12 from the same location 10 km west of the north end of the belt; 3) samples 05-MPB-18, 96-TCA-07, and 07MOB-034, -07MOB-0038 from 100 km west of the Thompson deposit and south of Osik Lake; 4) samples 06-MPB-118 and 05-MPB-55 from west and southwest of the Thompson and Birchtree deposits; and 5) samples 06-MPB-084 and -111 from Ospwagan Lake (Appendix E1, map 7).

One grain of millerite (NiS) was found in the 1.0-2.0 mm fraction of unweathered till (sample 05-MPB-08) from the Thompson deposit. It was picked because it resembled pentlandite and was identified by SEM analysis. Note that millerite was not systematically picked as an indicator mineral from the till samples. Two grains of cinnabar (HgS) (Appendix B5) were recovered from sample 06-MPB-109, from an island in Ospwagan Lake.

Silicate, Oxide, and Carbonate Minerals

Diopside

Two visually distinct sub-populations of Cr-diopside were identified in the till samples by ODM and were counted separately: 1) a dominant, pale emerald green (Fig. 8a), low-Cr variety (~0.5 to ~1.25 wt.% Cr_2O_3) and 2) less commonly, an intense emerald green Cr-rich diopside (Fig. 8b) containing >1.25 wt.% Cr_2O_3; these are reported with other kimberlite indicator minerals in Appendix B6. It should be noted, however, that the visual distinction between low Cr- and high Cr-diopside does not reliably discriminate between medium and high Cr content. Therefore actual proportions of low, medium, and high Cr-diopside, as confirmed by EMPA, are listed in Appendix B4.

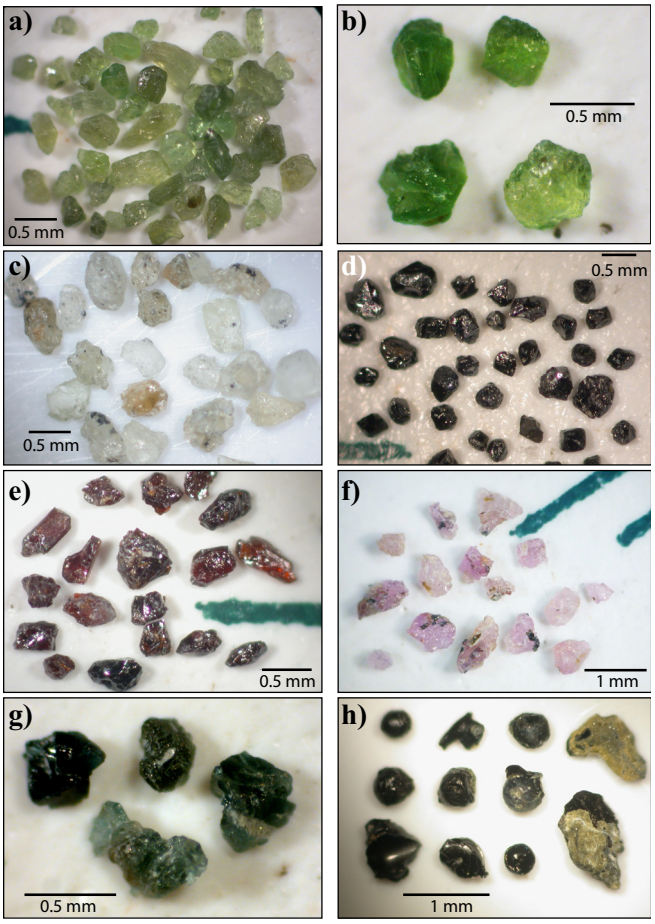

Figure 8. Colour photographs of mineral grains from till samples: **a)** low Cr-diopside grains from the 0.25-0.5 mm fraction of sample 05-MPB-013 from the Pipe deposit; **b)** high Cr-diopside grains from the 0.25-0.5 mm fraction of sample 05-MPB-013 from the Pipe deposit; **c)** olivine grains from the 0.25-0.5 mm fraction of sample 05-MPB-14 from the Pipe deposit; **d)** chromite grains from the 0.25-0.5 mm fraction of sample 05-MPB-013 from the Pipe deposit; **e)** red rutile grains from the 0.25-0.5 mm fraction of sample 05-MPB-45 from the forest access road, south of Paint Lake and east of the TNB; **f)** pink corundum grains from the 0.25-0.5 mm fraction of sample 05-MPB-44 from the forest access road, south of Paint Lake and east of the TNB; **g)** gahnite grains from the 0.25-0.5 mm fraction of sample 05-MPB-14 from the Pipe deposit; **h)** slag grains from the 0.5-1.0 mm fraction of sample 05-MPB-007 from the Thompson deposit.

Both low and high Cr varieties are often intergrown with enstatite, suggesting that they have a common source within a variably Cr-enriched two-pyroxene rock, presumably either lherzolitic peridotite or websteritic pyroxenite. Both Cr-diopside varieties were picked from the TNB till samples to confirm the presence of the Cr-diopside dispersal train first identified in southern Manitoba by Thorleifson and Garrett (1993) and further investigated by Matile and Thorleifson (1997). Cr-rich diopside is well known as a kimberlite indicator mineral (e.g. Fipke et al. 1995; Nimis and Taylor, 2000; McClenaghan and Kjarsgaard, 2007). Low Cr-diopside was picked from till samples because

Averill (2001) suggested that it could be a useful indicator mineral for Ni-Cu sulphide deposits based on his observations of till samples from around other magmatic Ni-Cu deposits. The visual counts for low Cr- and Cr-diopside grains in both 2005 and 2006 till samples were combined for each sample and plotted as one value on the mineral distribution maps in Appendix E (maps 8, 23, 35) and are referred to collectively as total Cr-diopside.

Cr-diopside was the second most abundant indicator mineral in the heavy mineral concentrates after olivine (excluding orthopyroxene). Cr-diopside content in till ranges from 0 to 393 grains across the study area. It is present in most till samples but is most abundant within the TNB and just to the east of the TNB. Samples from the Thompson Mine site (Appendix E2, map 23) contained up to 139 grains, and samples from around the Pipe deposit contained up to 127 grains (Appendix E3, map 35). Counts were highest in till samples from just south of the Pipe deposit, southeast of Paint Lake on the forest access road, and also from southeast of the Thompson deposit along the Jonas Forest access road.

Orthopyroxene

Members of the orthopyroxene series found to occur in till samples from this study include enstatite and hypersthene. Enstatite in heavy mineral concentrates was identified by its distinct 88º cleavage and pale brown colour, whereas hypersthene is darker brown. Orthopyroxene was sufficiently abundant in many samples to qualify as a major mineral but appears to be mainly hypersthene derived from the (granulitic) gneiss outside the TNB rather than enstatite derived from the ultramafic rocks within the TNB. The abundance of orthopyroxene, reported as a percentage of the total 0.25-0.5 mm non-ferromagnetic heavy mineral concentrate, is plotted in Appendix E1 (map 9). Abundance in till varied from 0 to 60%. The greatest abundances in till was from samples east of, and overlying, the TNB.

Olivine

Forsteritic olivine was identified visually by its pale yellow-green colour and lack of cleavage (Fig. 8c). Many of the olivine grains are impure, containing microscopic magnetite or Cr-magnetite inclusions. The distribution of olivine in till is shown in Appendix E1 (map 10). Olivine is by far the most abundant indicator mineral in the heavy mineral concentrates of the till samples and was found in virtually every till sample collected within the TNB at concentrations of between 1 and 1000 grains per 10 kg sample. The highest olivine concentrations, however, were found east to east-southeast of Thompson and at the Thompson Mine site (Appendix E2, map 25). Background till samples from northwest of the TNB contained 0 to 2 olivine grains and samples from northeast of the belt contained 2 to 10 grains. Till samples from around the Thompson deposit (Appendix E2) can be subdivided into three groups based on their olivine abundance: 1) samples from north of the T1 deposit contained very few olivine grains (29-39 grains/10kg), which is most likely related to the low olivine content of the local bedrock (Thompson and Mansan formations); 2) samples from southwest of the T3 Mine contained up to 620 grains/10 kg of olivine , and 3) samples from sites southeast of the deposits, collected on the tailings pond access road, have the highest olivine abundances. In this last group, olivine content decreases westward from 625 grains in sample 06-MPB-41 to 5 grains in sample 06-MPB-43, which is from just south of the T1 deposit. This westward decrease suggests there is a bedrock source containing fresh olivine just to the east of the TNB. Till samples from the Pipe deposit (Appendix E3, map 37) contain up to 273 olivine grains, with the highest counts in till samples being from east of the open pit and overlying the Pipe Formation.

Fayalite

Fayalite is a cloudy, yellow-brown mineral that is darker in colour than forsteritic olivine. Its abundance was reported by ODM in the MMSIM worksheet (Appendix B1) as a percentage of the 0.25-0.5 mm total nonferromagnetic heavy mineral concentrate. It is virtually absent in the till from across the entire Thompson Belt; it was found only in trace amounts (a few grains) in two till samples, 06-MPB-063 and -092 collected east of the Thompson deposit and the TNB, along the Jonas Forest access road.

Chromite and Cr-Spinel

Chromite grains are identified by their glassy black colour, octahedral crystal form, and dark brown streak (Fig. 8d). The regional distribution of chromite in the 0.25-0.5 mm fraction of till is shown in Appendix E1 (map 11). Background concentrations in till are between 0 and 5 grains. Two clusters of chromite-rich till are evident within the TNB: one centred on the Pipe deposit and the other around the Thompson deposit (Appendix E.1). On closer inspection of the Thompson anomaly (Appendix E2, map 26), samples can be subdivided into three groups based on abundance: 1) samples collected at the T1 and T3 mines; 2) samples from one site 5 km southwest of the mines; and 3) samples from sites southeast of the mines on the tailings pond access road. Chromite content in the third group decreases westward from 40 to 65 grains, and then to background levels (1-5 grains) just south of the mines. This pattern suggests westward transport of glacial

debris from an ultramafic source to the east of the tailings pond. Most till samples from around the Pipe Mine (Appendix E3, map 38) contain elevated numbers of grains (>20 grains). The highest contents are in till samples both west and southwest of the pit. This distribution suggests westward and southwestward dispersal of chromite from the ultramafic rocks at Pipe. Chromite counts are also elevated at sites 07MOB-033 and -034 in the East Kisseynew domain, west of the TNB, and less so at site 96-TCA-04, which is southeast of the Snow Lake Belt that also hosts ultramafic rocks.

Red Rutile

Red rutile grains were identified by their deep red to red-black colour (Fig. 8e) and were picked because they may contain significant Cr, and hence may provide a vector to ultramafic rocks and their mineralization. The distribution of red rutile in the 0.25-0.5 mm fraction of till is shown in Appendix E (map 12). Background concentrations are 0 to 5 grains across the study area (Appendix E.1). Red rutile is particularly abundant (1-49 grains) in till samples 05-MPB-043 to -049 collected along the forest access road, south of Paint Lake (southeast of the TNB), as well as in sample 05-MPB-020 collected 5 km northwest of the Thompson deposit, and samples 06-MPB-63 and -64 collected on the Jonas Forest access road. Till samples from the Thompson (Appendix E2, map27) and Pipe mine sites (Appendix E3, map 39) contain only a few grains of rutile. The high abundances in samples from east of the TNB suggest that the bedrock source of red rutile is likely metamorphic rocks east and/or northeast of the TNB.

Pink Corundum

Pink corundum grains were identified by their distinctive ruby-pink to pink-purple colour (Fig. 8f) and by striated cleavage faces, which are absent from similarly coloured Cr-pyrope garnet. The pink colour is due to trace amounts of Cr, which — like Cr-bearing rutile — would indicate the presence of ultramafic rocks in the vicinity. The regional distribution of pink corundum in the 0.25-0.5 mm fraction of till is shown in Appendix E1 (map 13). Background concentrations of pink corundum are very low (0 to 1 grain). The highest counts are in till east of the TNB, along the forest access road south of Paint Lake (1 to 17 grains), and south of the Soab deposit (up to 15 grains), which is similar to the distribution of red rutile. Around Ospwagan Lake, up to 7 grains of corundum was found in till samples, while till from the Thompson open pits contained up to 3 grains and from the Pipe deposit, up to 5 grains.

Spinels (ss) and Gahnite

Gahnite grains were identified by their distinctive dark blue-green colour (Fig. 8g) and octahedral crystal habit but required SEM confirmation to distinguish it from common spinel, which looks very similar. There are also compositional gradations between these two members of the spinel group. Most till samples did not contain gahnite. Those that did (maximum of 2 grains of gahnite) were randomly distributed across the study area, suggesting its distribution is not related to mineralized rocks of the TNB.

Other coloured spinel grains occur in till samples from the Thompson and Pipe mine sites, with a few grains per sample. However, much higher concentrations of spinel can be found in select background samples from west of the TNB (up to 34 grains) and slightly elevated spinel counts (3-7 grains) occur in samples 06-MPB-63 and -64 from the Jonas Forest access road and southeast of Pipe.

Sapphirine

Sapphirine grains were identified by their uneven grey-blue to pale blue colour. Similar to spinel and sapphire (corundum) in composition and appearance, sapphirine [$(Mg,Al)_8(Al,Si)_6O_{20}$] is a mineral characteristic of highly metamorphosed Mg-rich, Si-poor, and/or Al-rich rocks. Twenty-five grains were picked from 2005 till samples as sapphirine, however, upon analysis, eight turned out to be spinel or corundum. Ten of the seventeen grains analyzed as sapphirine were in till from southeast of the TNB, three in local till north of Thompson, and one grain in each of a till sample from the Thompson deposit, from south of the Thompson deposit, and from south of the Pipe deposit, as well as in a background sample from north-northeast of the TNB (Appendix E1, map 14). This distribution appears to be random and unrelated to the presence of mineralized and/or ultramafic rocks in the TNB.

Kimberlite Indicator Minerals

Cr-diopside, chromite, and forsteritic olivine are not only indicators for crustal ultramafic rocks, such as komatiite, pyroxenite, and peridotite, but are also part of the kimberlite indicator mineral suite, indicating they are derived from mantle xenocrysts and xenoliths or kimberlite phenocrysts (Averill, 2011). Their compositions overlap widely and can therefore not be used to discriminate between being of crustal or of mantle origin. However, physical properties of the grains recovered in this study indicate that few if any of them are kimberlitic. Non-kimberlitic forsterite is colourless to very pale yellow, often contains Cr-magnetite inclusions that render the grains paramagnetic, and is rarely >0.5 mm in size. In contrast, kimberlitic forsterite is pale green, nonparamagnetic, and more commonly

occurs at size s of >0.5 mm (Averill, 2011). Non-kimberlitic chromite is similarly small (rarely>0.5 mm) and the crystals are angular to rough textured. In contrast, chromite xenocrysts from kimberlite are smooth and rounded, reflecting crystal resorption.

In till containing kimberlite debris, Cr-diopside, chromite, and olivine are usually accompanied by more definitive kimberlite indicator mineral species, such as Cr-pyrope and Mg-ilmenite (McClenaghan and Kjarsgaard, 2007). These two minerals were absent in the till samples collected and/or examined for this study. A few Cr-pyrope and Mg-ilmenite grains were found by Matile and Thorleifson (1997) in samples from east of the TNB and by McMartin (unpublished) in samples from west of the TNB (sample 07MOB-34, -35 and -37) and are probably derived from very distal kimberlitic sources.

Siderite

Three till samples (05-MPB-007, -009, and -030), collected on the shoulders of the Thompson South pit, contain siderite. Siderite was found only as a result of SEM checks for other mineral species, and was not systematically picked as an indicator mineral.

Anthropogenic Grains

Twelve samples were found to contain grains of slag (Fig. 8h), a product of the smelting process at the Thompson Mine and smelter site (T1 Mine). Most grains are in the 0.25-0.5 mm fraction but occasionally occur in the coarser fractions as well. For samples sites within 3 km of the smelter (Appendix E1, map 15), slag grains likely were introduced to till samples by wind during sampling and from shovels not cleaned sufficiently after digging for sampling near the smelter. Sample sites further from the mine site that contain slag grains have likely been contaminated by unclean sampling equipment.

Lead and Zn-metal grains found in sample 06-MPB-89 and 06-MPB103 (Appendix B3) were likely introduced to the samples in the field, when the samples were sieved through a metal sieve to remove pebbles.

Pebble Counts

The distribution of major rock lithologies in till samples from across the Belt are listed in Appendix D. Most till samples contain 1 to 3% ultramafic rocks, which is considered to be the background range of values for till in the region. Samples 06-MPB-58 to -61, from 250 to 500 m west of the central ultramafic body at the Pipe open pit, contained the greatest concentration of ultramafic rock fragments (10-30%). Paleozoic carbonate pebble abundance in till varies from 0 to 81%. Not unexpectedly, sample 06-MPB-70, overlying Paleozoic carbonate rocks west of the TNB and south of Snow Lake, contained the highest amount (81%). Till samples from the east side of the TNB and further east, ie., southeast of the Thompson Mine and south and southeast of Paint Lake, contained 10 to 44% Paleozoic carbonate pebbles, with the eastern most sample (06-MPB-063) containing the greatest amount of carbonate,with the exception of sample 06-MPB-70. Most other till samples collected from further west, and thus further from Paleozoic bedrock in the Hudson Bay Lowland, contained much lower percentages of carbonate pebbles (0 to 9%). Till samples from the Pipe deposit contained less carbonate clasts than till samples from the Thompson Mine, which is not unexpected as the Pipe deposit is 20 km farther west than the Thompson deposit.

Till samples 05-MPB-009, -010, and -030 from the Thompson deposit and sample 05-MPB-015 from the east side of the Pipe open pit contained pebble-sized fragments of massive sulphide. Fragments of iron formation were identified in the pebble fraction of 11 till samples, including six samples from the Pipe deposit and two samples (05-MPB-040 and -041) from around the Soab deposit.

INDICATOR MINERAL COMPOSITIONS

In order to assess compositional changes in indicator minerals by geographic distribution, the mineral data were plotted on a map and subdivided into 15 different groups based on sample location (Table 3, Appendix A2 map). Indicator mineral EMP compositional data are listed in 11 worksheets in Appendix F1 and EMP grain mount maps are included in Appendix F2.

Sulphides

A random selection of 20 to 25 grains of pyrrhotite grains from each of five metal-rich till samples from around the Thompson and Pipe deposits were analyzed by EMP (Appendix F1, sulphides). Many of the grains were strongly altered and yielded insufficient totals due to loss of sulphur and/or iron during the alteration process. Some grains were altered to Fe-(hydr-)oxides. Analyses with acceptable totals and stoichiometry are plotted in Figure 9 and show that pyrrhotite grains in samples from the Thompson deposit had significantly higher Ni concentrations (0.4-1.13 wt.% Ni) than the few fresh grains recovered from Pipe samples (0.03-0.3 wt.% Ni). Cobalt concentrations, however, were similar in samples from both deposits (0.02-0.11 wt.%, with one outlier at 0.15 wt.%), with the pyrrhotite from Pipe samples averaging slightly higher than the bulk of the pyrrhotite from Thompsonsamples.

Ni concentrations in pyrite (Appendix F1, sulphides), which was accidentally analyzed because it was picked as pyrrhotite, and pyrrhotite from Pipe sampleswere similar, with two exceptions where the pyrite

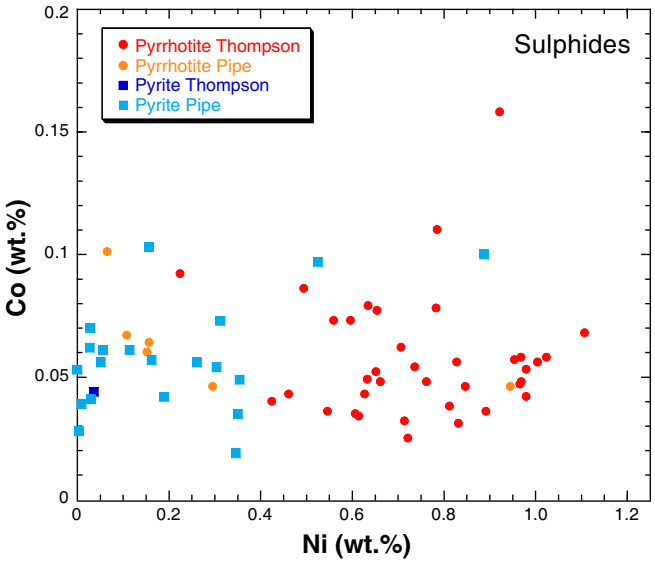

Figure 9. Ni versus Co concentration for pyrrhotite and pyrite from till samples around the Thompson and Pipe deposits.

had higher Ni concentrations more in the range of Thompson pyrrhotite (Fig. 9). Only one grain of pyrite from Thompson was analyzed and it had very low Ni concentrations (<0.01 wt.% Ni). No other sulphide mineral compositions were determined.

Cr-Diopside

The composition of the 2086 Cr-diopside till grains that were analyzed (Appendix F1, Diopside) varied from Mg-# 70 to 95, from 0.0 to 2.25 wt.% Cr_2O_3, from 0.2 to 4.78 wt.% Al_2O_3, from 0 to 0.46 wt.% TiO_2, and from 0.1 to 2.21 wt.% Na_2O with a few outliers at higher or lower values (Figs. 10, 11). The data have been subdivided by geographic distribution (Appendix A2 map) for plotting in Figures 10 and 11. Compositional variations of diopside in background till from northeast of the TNB (Fig. 10a) is similar to that from north of the Thompson Mine (Fig. 10c) with both a limited range of Mg-#s and Cr_2O_3 <1.3 wt.%. Diopside from west of the TNB (Fig.10b) and south of Soab deposit (i.e. southern TNB) (Fig. 10c) are similar in that they have a limited range of Cr_2O_3 concnetra-

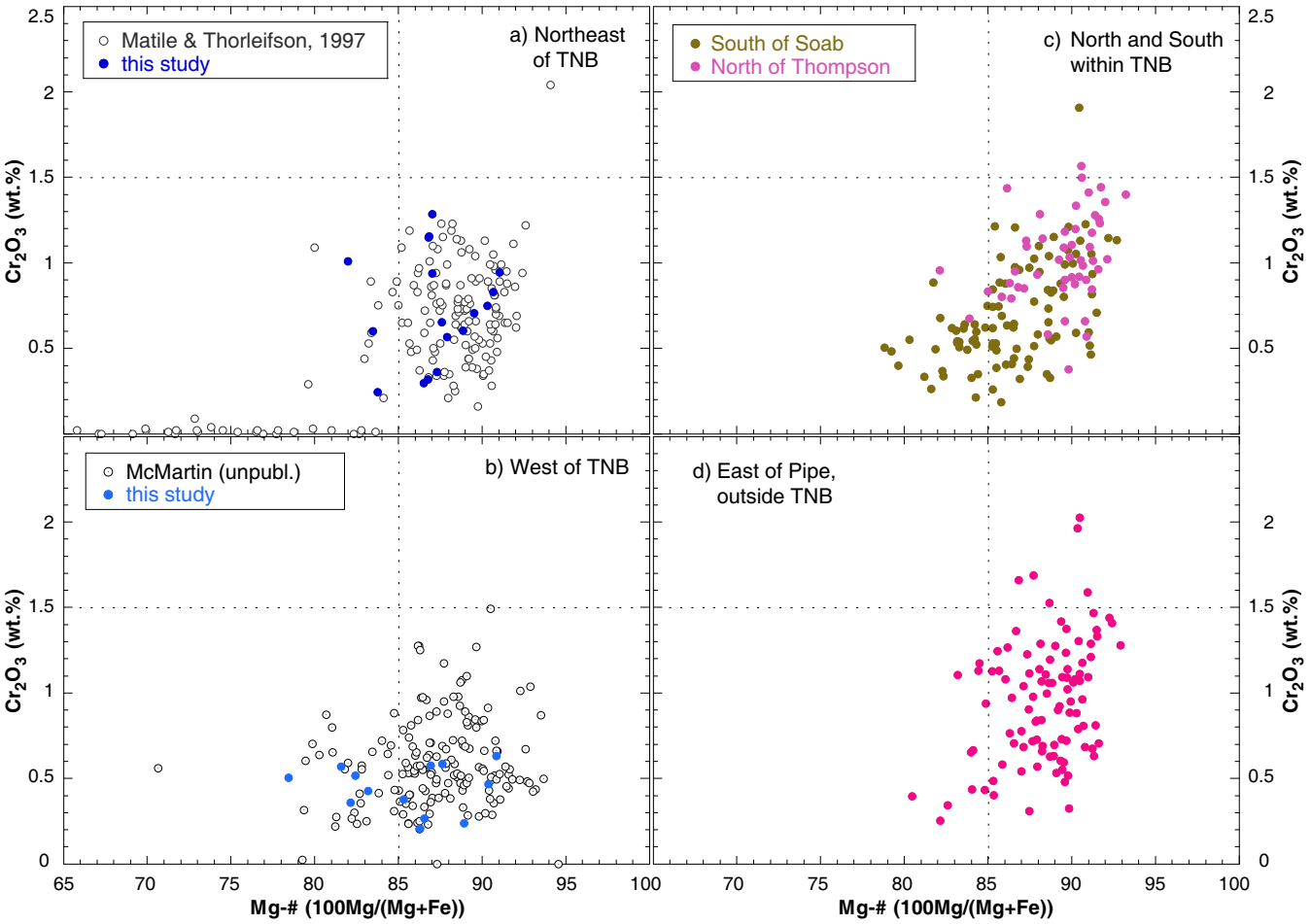

Figure 10. Cr_2O_3 versus Mg-# (100*Mg/(Mg+Fe)) for diopside from till samples. Dashed lines are guides for better comparison: **a)** regional samples (background) from outside the TNB including data from Matile and Thorleifson (1997); **b)** regional samples from north of the Thompson deposit within the TNB; **c)** regional samples (background) from west of the TNB including samples from I. McMartin (unpublished data); **d)** samples from south of the Soab deposit, southern TNB.

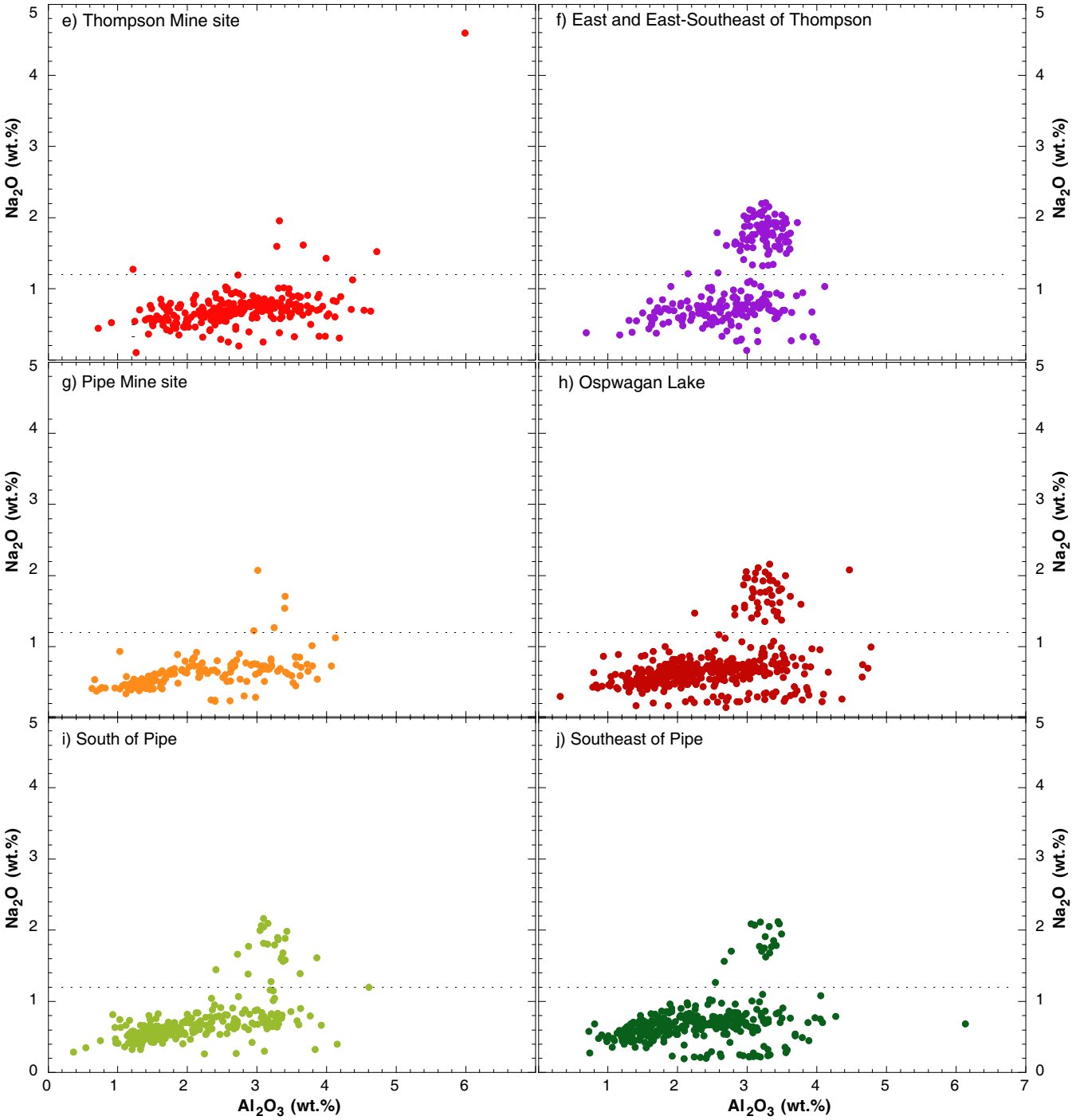

Figure 10 continued. Cr_2O_3 versus Mg-# (100*Mg/(Mg+Fe)) for diopside from till samples. Dashed lines are guides for better comparison: **e)** Thompson Mine site; **f)** east to east-southeast of the Thompson deposit along forest access roads (outside the TNB); **g)** Pipe Mine site; **h)** around Ospwagan Lake (between Birchtree and Pipe Mines); **i)** south of Pipe; and **j)** south-south-east of the Pipe deposit, mostly outside the TNB.

tions (<1.3 wt.%) and a wider range of Mg-#s (78 to 94.5). Diopside immediately east of the TNB (east of Pipe) has clearly a larger range of Cr_2O_3 concentrations (Fig.10d) than other background samples. Diopside in till at the Thompson Mine site (Fig. 10e), till east of the Thompson Mine (Fig. 10f), around Ospwagan Lake (Fig. 10h), and south-southeast of Pipe or east of Soab (Fig. 10j) have a comparatively narrow range of Mg-#s (~83 to ~93) but a wide spread in Cr_2O_3 concentrations (<2.25 wt.%). Diopside grains in till from the Pipe Mine site (Fig.10g) and further south (Fig. 10i) show a wide spread of Mg-#s due to a large population of low Mg-#s (80 to 87) and Cr_2O_3 concentrations (<0.7 wt.%), which are not found at Thompson, east of Thompson, or east of Soab. These grains are probably derived from mafic volcanic rocks

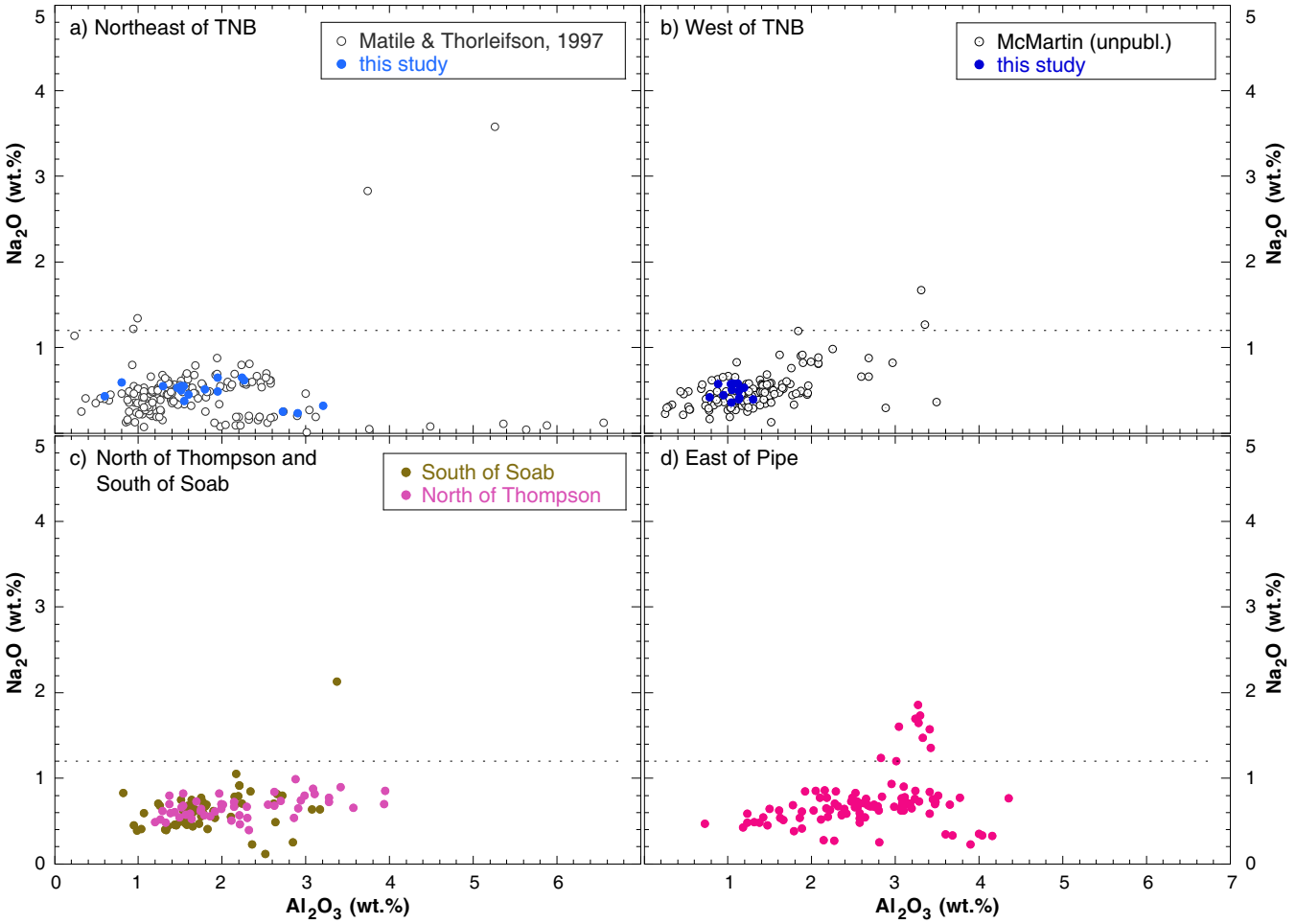

Figure 11. Na_2O versus Al_2O_3 content for diopside from till samples. Dashed lines are guides for better comparison: **a)** regional samples (background) from outside the TNB including data from Matile and Thorleifson (1997); **b)** regional samples from north of the Thompson deposit, within the TNB; **c)** regional samples (background) from west of the TNB including samples from I. McMartin (unpublished data); **d)** samples from south of the Soab deposit within the TNB.

of the Bah Lake Formation that crops out in the central TNB (Layton-Mathews et al., 2007). The most Cr-rich diopside grains, those containing >1.5 wt.% Cr_2O_3, occur predominantly in till east of Thompson (Fig. 10f), around Ospwagan Lake (Fig. 10h), south and southeast of Pipe (Fig. 10i ,j), indicating a local source of Cr-rich ultramafic rocks not present at the Pipe and Thompson mine sites. Very Cr-poor diopside grains, containing <0.1 wt.% Cr_2O_3, occur in background samples collected by Matile and Thorleifson (1997) but not in samples collected during this study (probably because only pale green to green diopside was picked for this study). These diopside grains are probably from calc-silicate rocks and marble.

Plots of Na_2O versus Al_2O_3 (Fig. 11) show a continuous range of Al_2O_3 values, which is smallest in diopside in till from outside the TNB (Fig. 11a,b) and larger (towards higher Al_2O_3) in diopside from within the TNB (Fig. 11c-j). Na_2O values, however, reveal different diopside populations: 1) a main trend at 0.3 to 1.1 wt.% Na_2O, 2) a low Na-trend (< 0.3 wt.%), and 3) a high Na_2O population, which is most pronounced in till east of Thompson (Fig. 11f) and around Ospwagan Lake (Fig. 11h), but also occurs in till south and south-southeast of Pipe (Fig. 11i,j) and in a few grains in till from the Thompson and Pipe mine sites (Fig. 11e, g).

Figure 12 compares the compositional range of diopside in till to that of the few available analyses of bedrock diopside, and shows the much larger range of Cr_2O_3 concentrations in till diopside, which is not matched by the scarce grains in bedrock. The red box in Figure 12 outlines the compositional range of high-Cr diopside.

Orthopyroxene/Pigeonite

Orthopyroxene was not systematically picked or analyzed. Twenty-one orthopyroxene and low-Ca clinopyroxene grains were accidentally analyzed because they looked like olivine or diopside. Their compositional data are compiled in Appendix F1 (worksheet 2OPX). Their compositions range from enstatite to pigeonite (or mixtures of clinopyroxene and orthopyroxene, due

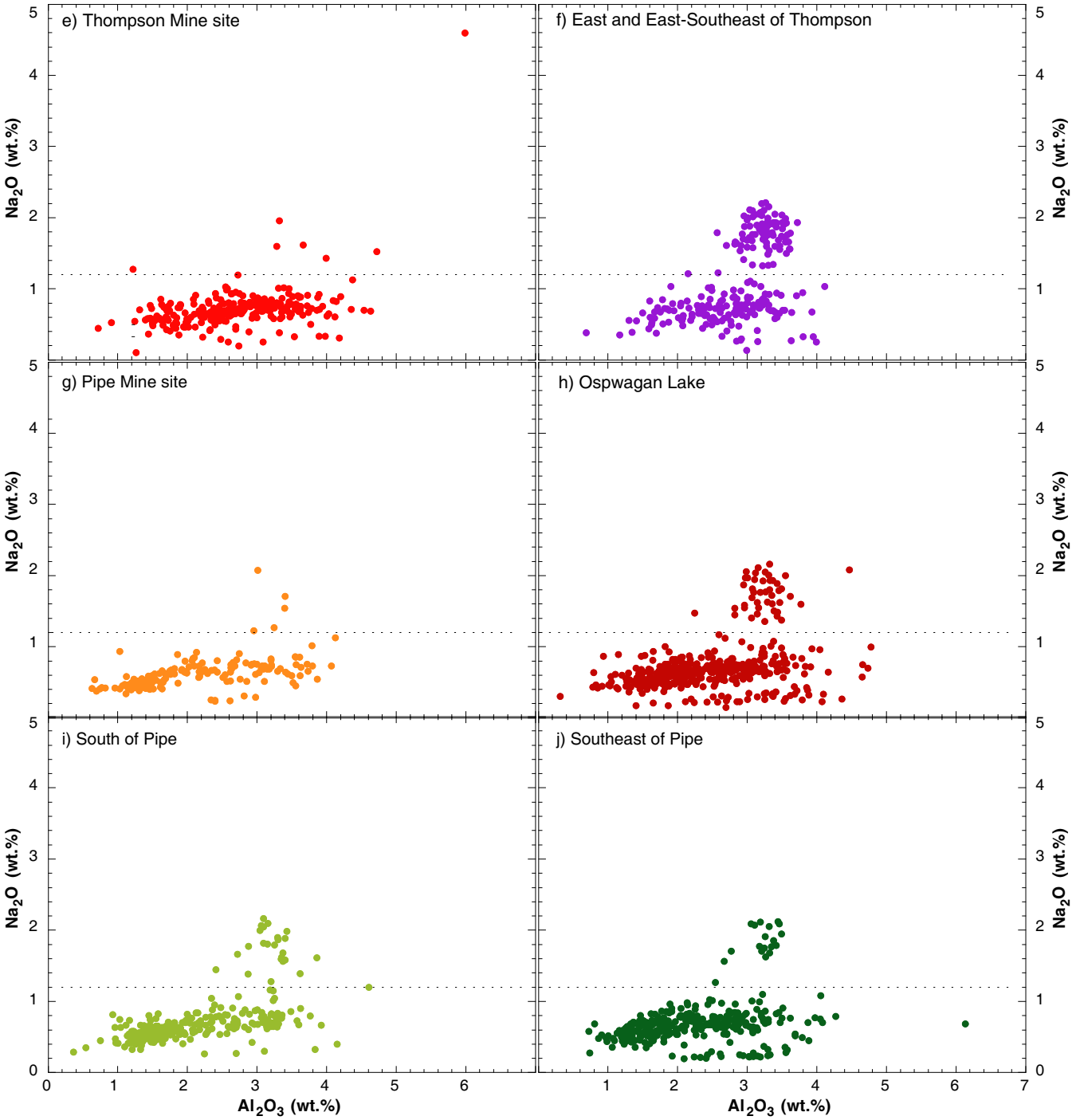

Figure 11 continued. Na_2O versus Al_2O_3 content for diopside from till samples. Dashed lines are guides for better comparison: **e)** Thompson Mine site; **f)** east to east-southeast of the Thompson deposit, along forest access roads (mostly east of the TNB); **g)** Pipe Mine site; **h)** around Ospwagan Lake (between Birchtree and Pipe); **i)** south of Pipe; and **j)** south-southeast of the Pipe deposit and east of the Soab deposit, mostly outside the TNB.

to orthopyroxene exsolving clinopyroxene or vice versa) with En70 to En88.

Olivine

A selection of 628 olivine grains from 30 till samples were analyzed (Appendix B.5, 7) to determine their compositional variation; the data are listed in Appendix F1 (worksheet 8olivine).Olivine grains in till have a very wide compositional range from Fo55 to Fo93, with NiO concentrations ranging from 0.01 to 0.79 wt.% (0 to 6208 ppm Ni; Fig. 13) and MnO concentrations from to 0.02 to 0.69 wt.%; there are three outliers at 0.85, 2.83, and 3.09 wt.% MnO. Most grains plot in a tight cluster between Fo80 and Fo90 and 1500 to 4000 ppm Ni, which is characteristic of igneous ultramafic source rocks. However, a large number of olivine

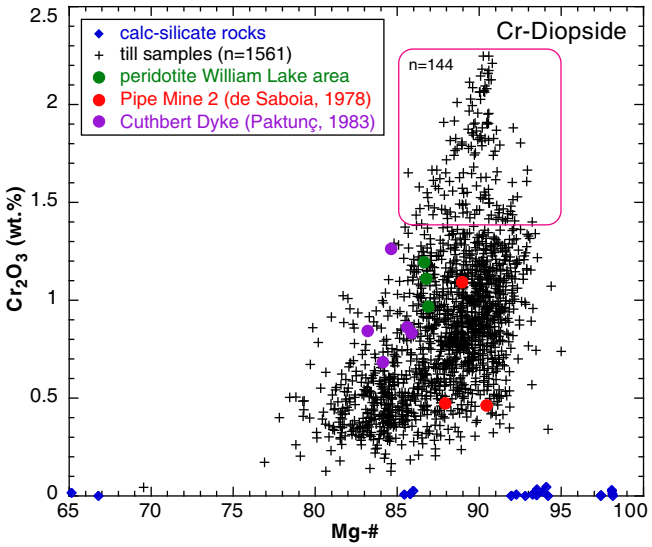

Figure 12. Cr_2O_3 versus Mg-# for diopside from till samples (crosses) compared to diopside from bedrock, with data from de Saboia (1978) (red dots), Paktunç (1983) (purple dots), and this study (calc-silicate rocks (blue diamonds) and Williams Lake peridotite (green dots)). Red box outlines the field of high Cr-diopside (>1.4 wt.% Cr_2O_3).

grains have high Ni concentrations (>4500 ppm) of Fo80 to Fo87, in till from both east of and within the TNB (Fig.13a-c), but are absent in the olivine-poor background samples north and west of the TNB (Fig. 13d). No strong regional variation in olivine composition exists, with the exception of several low-Fo/low-Ni grains from Ospwagan Lake and the Pipe Mine site, which are distinctly lower in Fo and Ni than the bulk of the olivine grains. These low-Fo/low-Ni compositions indicate a mafic rather than ultramafic source rock, probably the mafic volcanics of the Bah Lake Formation that outcrop in the area (Layton-Matthews et al., 2007).

Figure 14a compares olivine data from till samples in this study with those from non-mineralized to weakly mineralized ultramafic TNB rocks analyzed by Burnham et al. (2009) and Figure 14b compares ultramafic rocks from the Thompson Mine (Paktunç, 1983, 1984) and from the Cuthbert Ddyke (Paktunç, 1983) . These plots show that, although there is a general overlap, many of the till grains exceed the Ni concentrations of the bedrock olivine, whereas the bedrock data

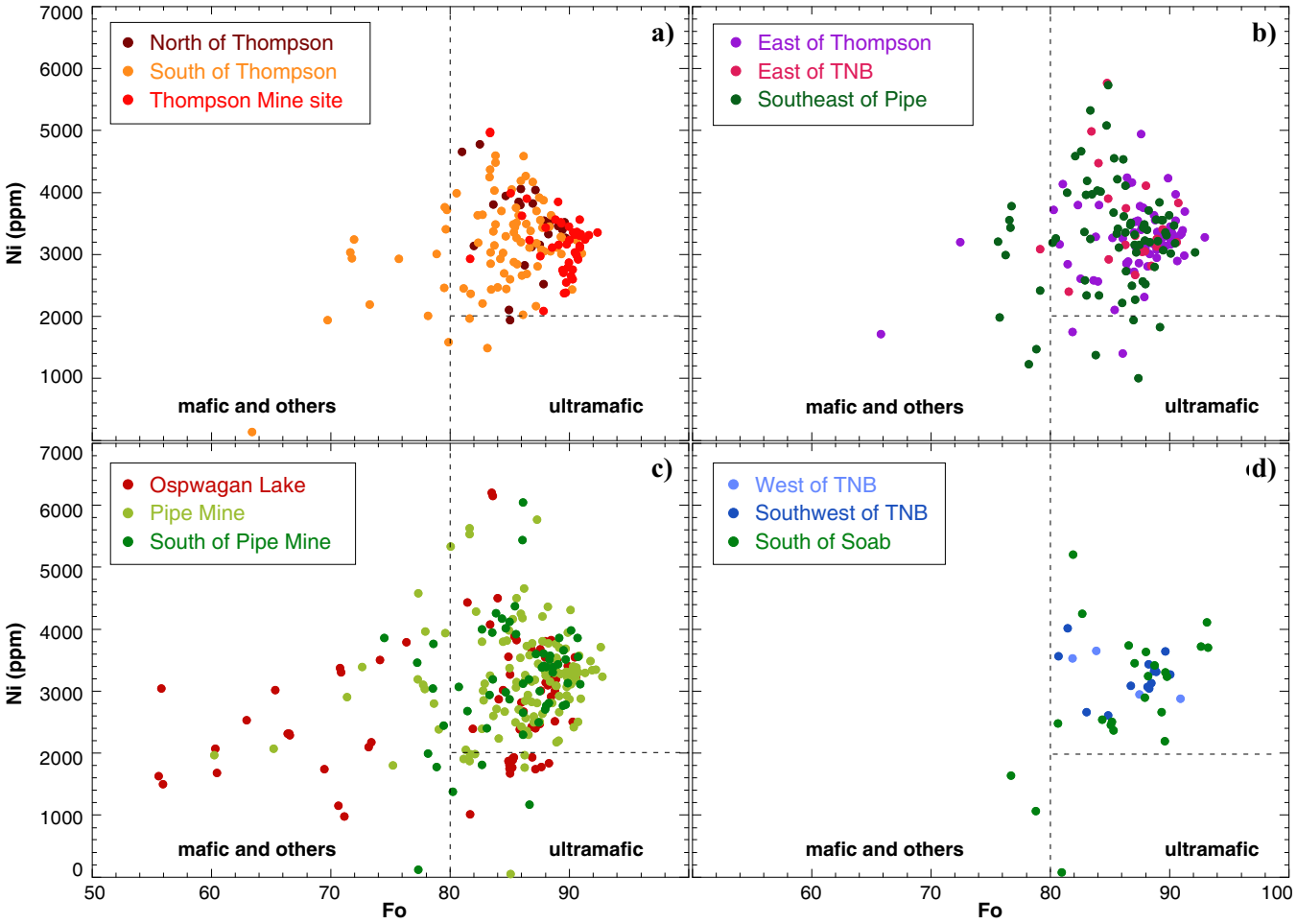

Figure 13. Ni versus Fo (100*Mg/(Mg+Fe)) for olivine in till samples subdivided by sample location: **a)** samples from the Thompson deposit and immediate surroundings; **b)** samples from east and southeast of the Thompson deposit, along the forest access roads (outside TNB); **c)** samples from around Ospwagan Lake, Pipe Mine site, and south of Pipe; and **d)** background samples from west and southwest of the TNB and south of the Soab deposit within the TNB.

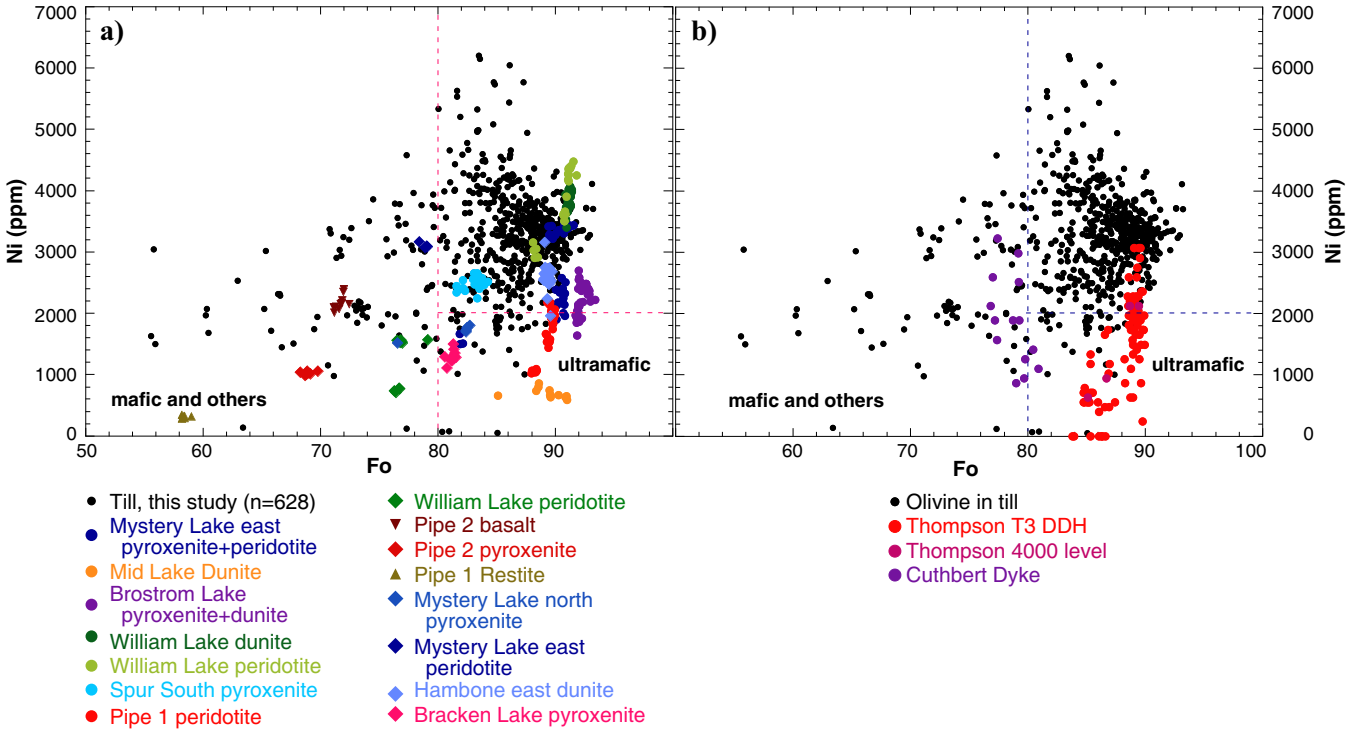

Figure 14. Ni content versus Fo (100*Mg/(Mg+Fe)) for olivine in till samples versus bedrock samples: **a)** olivine from non-mineralized to moderately mineralized ultramafic rocks (data from Burnham et al., 2009); round symbols indicate igneous olivine and diamond symbols indicate metamorphic olivine according to Burnham et al. (2009); and **b)** olivine from mineralized ultramafics from the Thompson Mine (Paktunç, 1983, 1984) as well as from the mafic to ultramafic Cuthbert dyke (Paktunç, 1983).

show many compositions with high Fo and very low Ni that have no match in the till.

Chromite, Cr-Spinel, and Cr-Magnetite

A total of 1104 chromite and chromian spinel grains were analyzed from till samples, mostly from the 0.25 to 0.5 mm fraction. The data are listed in Appendix F1(worksheet chromite). The compositional spectrum of this mineral group ranges from chromite ($(Fe,Mg)(Cr,Al)_2O_4$) with >60 wt.% Cr_2O_3 and 3 to 10 wt.% MgO, through chromian spinel (picotite) to spinel *sensu stricto* ($MgAl_2O_4$) due to substitution of Al_2O_3 for Cr_2O_3 and MgO for FeO. Another trend ranges from MgO-poor ferro-ferrichromite ($FeCr_2O_4$) with >60 wt.% Cr_2O_3 and <2 wt.% MgO through ferro-ferrichromite to Cr-rich magnetite ($Fe(Fe,Cr)_2O_4$) with >10 wt.% Cr_2O_3 (Fig. 15a, c). These two trends can easily be distinguished in a Cr_2O_3 versus MgO diagram (Fig. 15a, c), where the magnetite trend is characterized by compositions of <2 wt.% MgO and the spinel trend by compositions of >2 wt.% MgO. Approximately 75% of the chromite in till from the Thompson Mine site (Fig. 15a) follows the magnetite trend, whereas all other locations (including 38 grains from the Thompson Mine site) show chromite compositions that follow the spinel trend (Fig. 15c, e, g). The Cr-magnetite grains from Thompson show increasing ZnO with decreasing Cr_2O_3 extending even further the trend seen in the crushed bedrock samples from Thompson (Fig. 16). Similar compositions are only found in till immediately south of Thompson (Fig. 15c, d) and for three samples south of Pipe (Fig. 15f). The chromite compositions from till samples collected at the Pipe Mine, Ospwagan Lake, and Thompson fall into two population: one with concentration of ~50 wt.% Cr_2O_3 and between 3 and 10 wt.% MgO and a second with a smaller population with higher Cr_2O_3 concentrations (around 60 wt.%), which is most evident at Pipe (Fig. 15a). Till from east and east-southeast of Thompson, in contrast, shows a strong trend towards Cr-spinel. Interestingly, till from west, southwest, and northeast of the TNB show more Cr_2O_3-rich chromite compositions than most chromite from within the belt (Fig. 15g, h).

Spinel (ss) and Gahnite

A total of 89 blue-green spinel and 24 gahnite grains from the 2005 till samples were analyzed and are listed in Appendix F1 (worksheets Gahnite and Spinel). Neither mineral was found in any of the 43 bedrock samples collected as reference samples for this study. Spinel compositions in till range from 17.7 to 27.5 wt.% MgO (approaching the end-member spinel value of 28.33 wt.% MgO) (Fig. 17). The main substitution for MgO is FeO (1.38 to 17.4 wt.% FeO_{tot}), as well as minor MnO (up to 1.69 wt.%), and in some grains substantial ZnO (up to 10.6 wt.%). Zn-poor spinels are particularly numerous at the Pipe mine site, north of Thompson, and

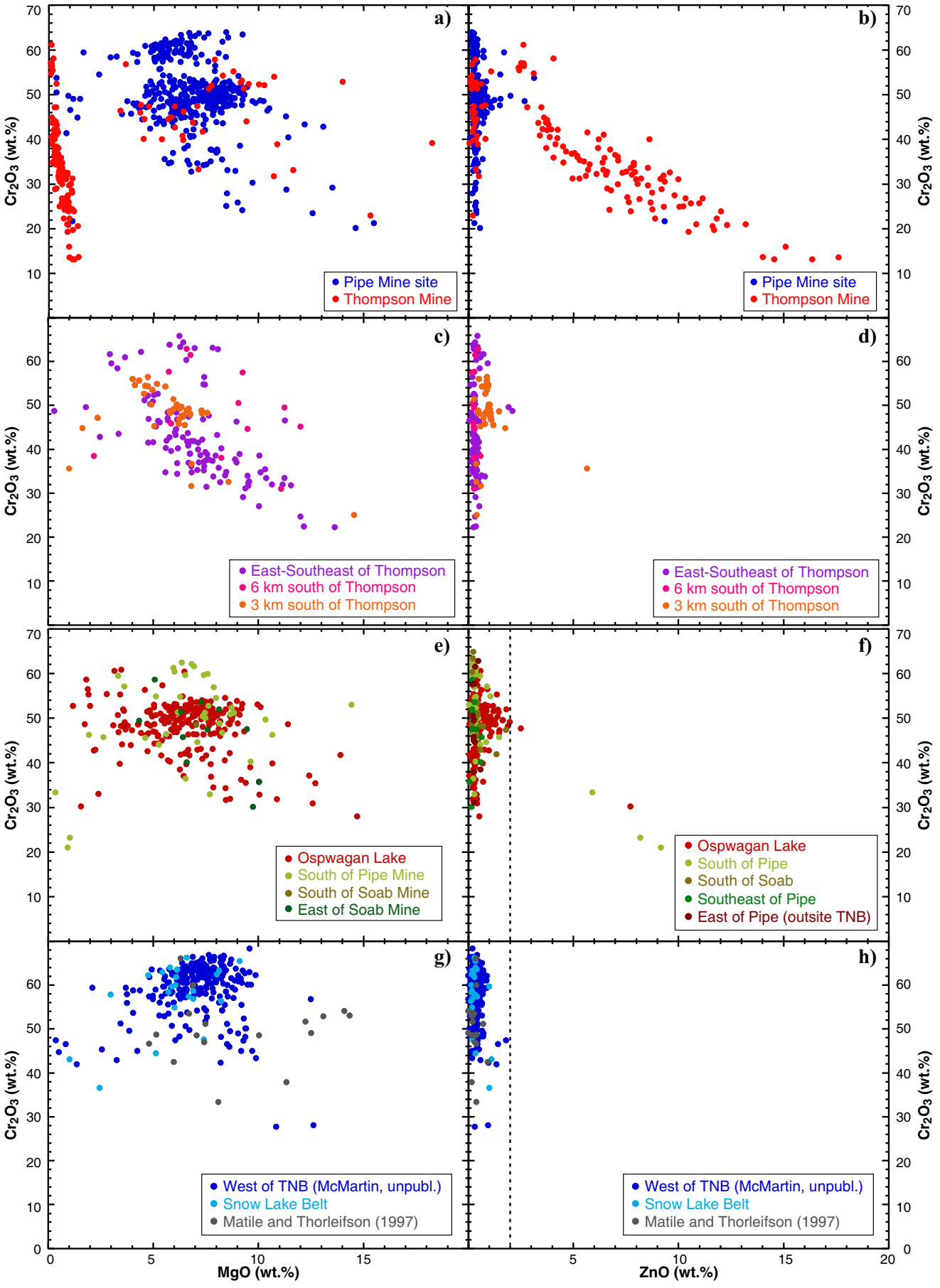
a)
b)
c)
d)
e)
f)
g)
h)
Cr2O3 (wt.%)
MgO (wt.%)
ZnO (wt.%)
Pipe Mine site
Thompson Mine
East-Southeast of Thompson
6 km south of Thompson
3 km south of Thompson
Ospwagan Lake
South of Pipe Mine
South of Soab Mine
East of Soab Mine
South of Pipe
South of Soab
Southeast of Pipe
East of Pipe (outsite TNB)
West of TNB (McMartin, unpubl.)
Snow Lake Belt
Matile and Thorleifson (1997)

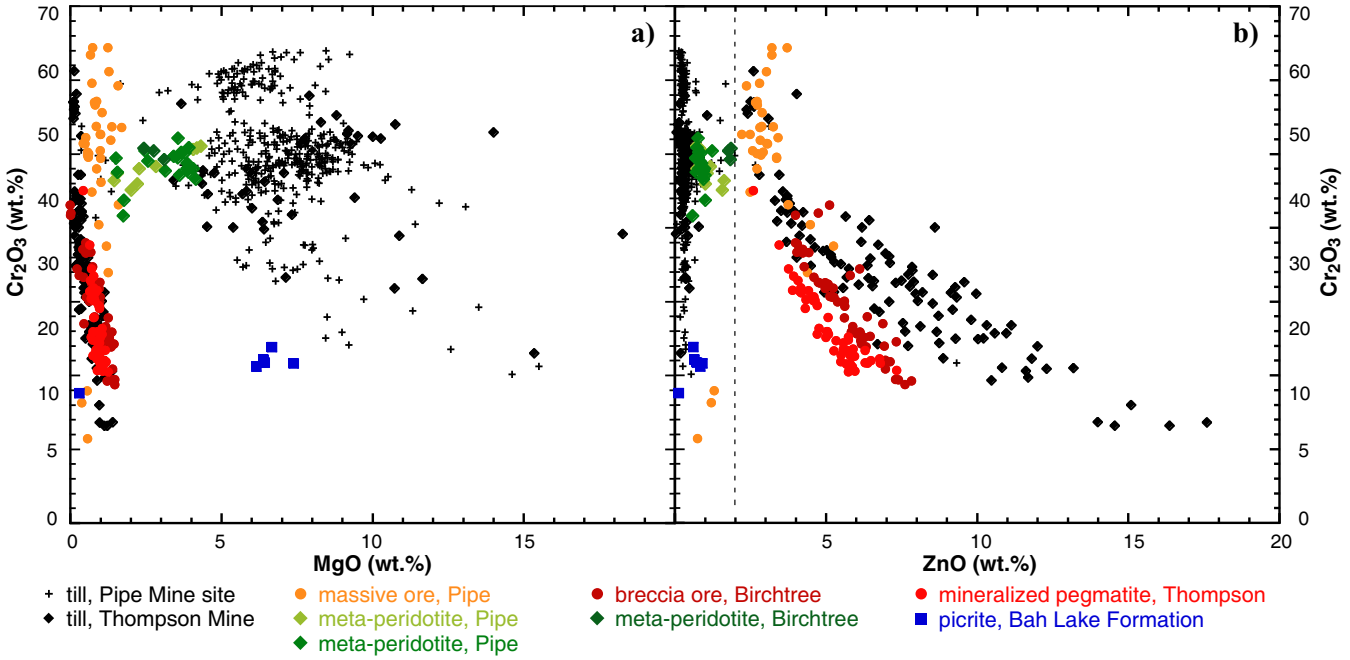

Figure 16. a) Cr_2O_3 versus MgO and **b)** Cr_2O_3 versus ZnO in chromian spinels from bedrock samples and till samples from the Pipe and Thompson mine sites. The legend is the same for both figures.

east-southeast of the TNB (Fig. 17). Compositions intermediate between spinel ($MgAl_2O_4$) and gahnite ($ZnAl_2O_4$) occur in samples from the Thompson and Pipe mines, as well as in background samples from west and north-northeast of the TNB (Matile and Thorleifson, 1997; I. McMartin, unpublished data), which tend to be more Fe-rich and deviate stronger from the spinel (ss) – gahnite mixing line. In contrast to the Zn-rich chromite and chromian spinel discussed above, these spinels are Cr-poor (<0.6 wt.% Cr_2O_3).

Ilmenite

Ilmenite was not systematically picked from till samples. However, a number of grains were analyzed because they looked like chromite and the analytical data are listed in Appendix F1 (worksheet 1Ilmenite) and are plotted with ilmenite from bedrock samples in Figure 18. Most analyzed ilmenite grains in till are MgO-poor with concentrations of <1 wt.% MgO.Only illmenite grains from Ospwagan Lake samples and one grain from a Thompson Mine sample had concentrations of >1 wt.% MgO, with a maximum concentration of 2.5 wt.% MgO. The MgO-poor ilmenite grains are moderately MnO-rich, with values up to 2.5 wt.%; only one grain from the Thompson Mine had a concentration of > 4 wt.% MnO (Fig. 18a). The compositions of bedrock ilmenite grains (from polished thin sections), which were plotted for comparison, indicate that the

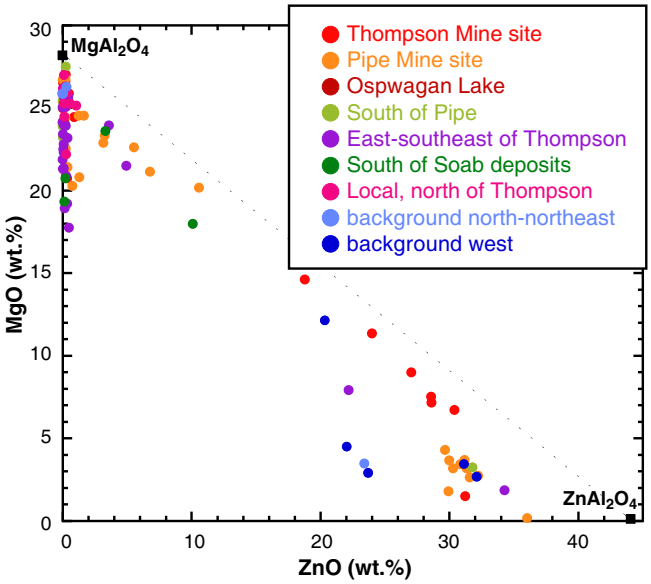

Figure 17. MgO versus ZnO in spinel and gahnite grains from till samples (this study) showing: **a)** regional compositional range of spinel and gahnite grains in till.

MgO-rich illmenite grains are in till probably derived from Bah Lake Formation volcanics (picrite 05-MPB-R23), whereas the MgO-poor variably MnO-bearing grains in till are from various metasedimentary rocks, including Archean gneiss. None of the till ilmenite grains (sample 05-MPB-R33) are surfficiently MgO-

Figure 15 opposite. Cr_2O_3 versus MgO and ZnO in chromite in till samples from: **a and b)** Thompson and Pipe mine sites; **c and d)** regional till samples from south-southwest of the Thompson deposit, and east and east-southeast of the Thompson deposit; **e and f)** regional till samples from around Ospwagan Lake, south of the Pipe Mine and south of the Soab deposit; **g and h)** background samples west and northeast of the TNB, including data from Matile and Thorleifson (1997) and unpublished data from I. McMartin.

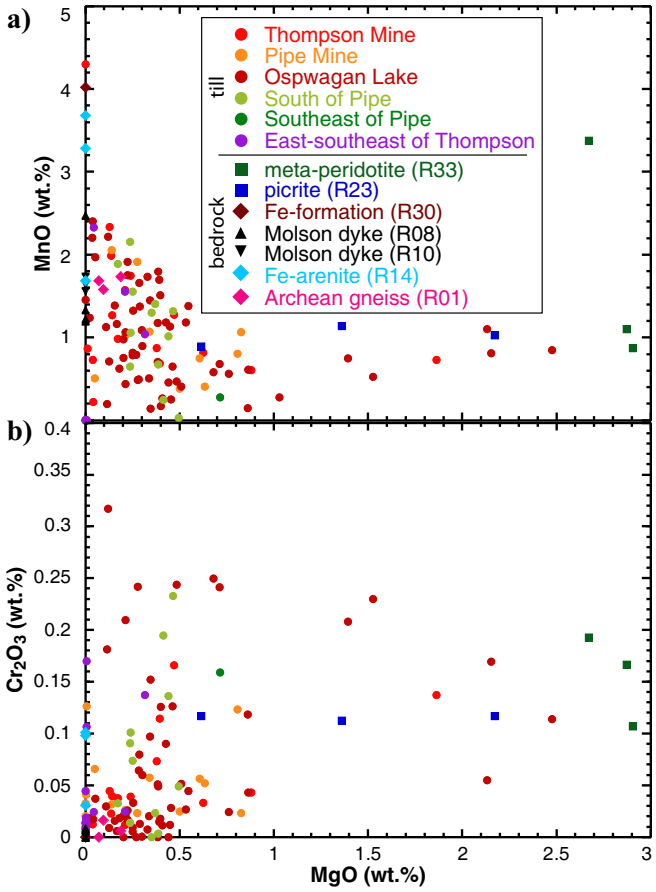

Figure 18. a) MnO versus MgO; and **b)** Cr_2O_3 versus MgO for ilmenite grains in till accidentally analyzed as chromite compared to ilmenite in polished thin sections of local Thompson Nickel Belt bedrock samples from this study.

rich to resemble metaperidotite ilmenite compositions. The Cr content of the ilmenite grains does not correlated with MgO content (as is usually the case) and the highest values (0.31 wt.% Cr_2O_3) are found in almost MgO-free ilmenite from Ospwagan Lake (Fig. 18b).

Red Rutile

A total of 238 red rutile grains from the 2005 till samples were analyzed to document their compositional range (Appendix F1, worksheet Rutile). Red rutile occurs predominantly in till samples southeast of Pipe, southeast of the TNB (n=129 grains), south of Pipe (n=40), south of Soab (n=31), and north of Thompson (n=21), whereas red rutile grain counts at the Thompson and Pipe mine sites are comparatively low (n=6 and n=5, respectively). The most dominant substitutions for Ti^{4+} are Cr^{3+}, V^{3+}, Nb^{5+}, and Fe^{3+}. Fe content is fairly low with < 1 wt.% FeO_{tot} — probably because only red rutile was picked (higher concentrations of Fe would make the rutile appear black).

Cr_2O_3 content in red rutile from the study area reach a maximum of 1.01 wt.% (Fig. 19) and Nb_2O_5 concentrations of up to 1.28 wt.% (Fig. 19c,d). The few red rutile grains found in till from around the Thompson and Pipe deposits are both Cr- and Nb-poor (<0.34 wt.% Cr_2O_3 and <0.02 wt.% Nb_2O_5) but slightly Fe-rich (Fig. 19a,b), whereas rutile grains from southeast of Pipe, south of Soab, and north of Thompson are generally more Cr-rich than rutile at the deposits and in background samples (Fig. 19a,c). It should be noted that red rutile compositions from till directly overlying the Cuthbert dyke, the largest of the Molson dykes (as reported by Matile and Thorleifson, 1997) is identical in composition to rutile found further southwest, just east of and within the TNB. Trace elements Sn (up to 0.047 wt.%) and Ta (up to 0.09 wt.%) show no significant regional differences in concentration. No red rutile was found in bedrock samples in this study and thus no bedrock compositional data are available for comparisons to till data.

Pink Corundum

Ninety-eight pink corundum grains were analyzed from the 2005 till samples and compositions (Appendix F1, worksheet Corundum) are similar to corundum analyses reported for the 1996 regional till samples by Matile and Thorleifson (1997) (Fig. 20). The Cr_2O_3 content varies between 0.07 and 1.33 wt.%. This compositional range is similar to that for pink corundum from metamorphic rocks in general (<0.77 wt.% Cr_2O_3; Hutchinson et al., 2004) and much lower than strongly coloured rubies and pink corundum reported from kimberlite (e.g. Sage, 2000; Hood and McCandless, 2004), which contain 3 to 7 wt.% Cr_2O_3. Corundum compositions from this study plot as two clusters in Figure 20: one cluster is Fe-poor (<0.45 wt.% FeO_{tot}) with variable to high Cr_2O_3 concentrations (up to 1.33 wt.%) and the second cluster is Fe-rich (>0.45 wt.% FeO_{tot}) and comparatively Cr-poor (<0.4 wt.% Cr_2O_3). Corundum grains from the Thompson and Pipe deposits, as well as south of Thompson, are predominantly Cr-poor with FeO_{tot} from 0.1 to 0.7 wt.%, whereas corundum grains in till southeast of the TNB span the entire compositional spectrum.

Sapphirine

A total of 36 potential sapphirine grains were picked from the 2005 and 2006 till samples by ODM and 25 grains from the 2005 till samples were mounted for analysis by EMP (Appendix F1, worksheet Sapphirine). Eight of the twenty-five grains were spinel or blue corundum, and were picked as sapphirine because they look very similar. Ten of the 17 sapphirines analyzed from the 2005 till samples occur in till southeast of the TNB, three in local till north of Thompson and west of the TNB, and one each in till from the Thompson Mine site, Ospwagan Lake, south of the Pipe Mine, as well as in background samples north-northeast of the TNB (Fig. 21). Additional sap-

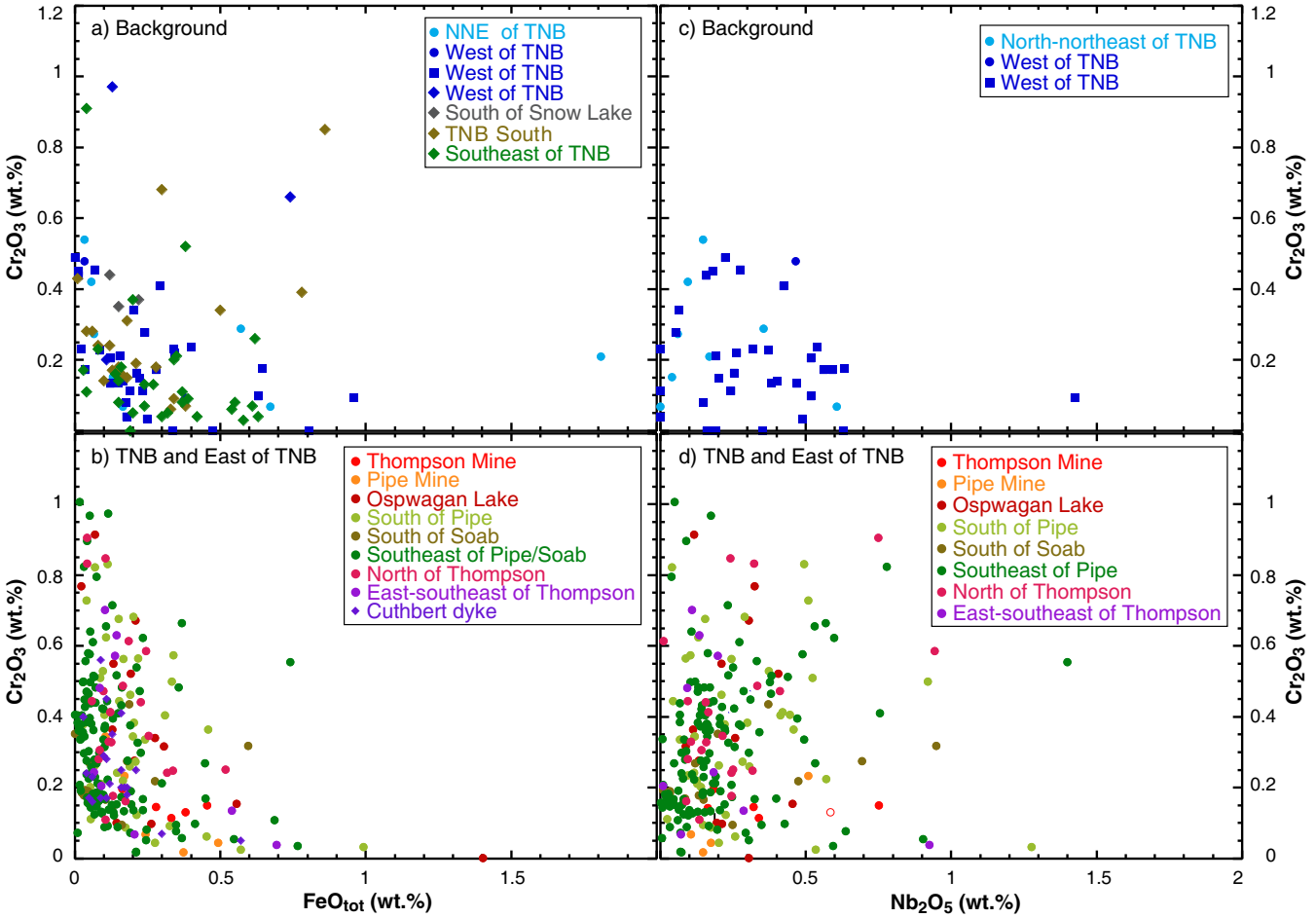

Figure 19. a and b) Cr_2O_3 versus FeO_{tot}; and **c and d)** Cr_2O_3 versus Nb_2O_5 in rutile from (a, c) back-ground till samples; and (b, d) till samples from within and east of the TNB. Filled circles represent data from this study, squares are data from the East Kisseynew till study (McMartin et al., 2012), and diamonds are from the regional survey by Matile and Thorleifson (1997).

phirine compositional data from the Pikwitonei granulite terrain at Sipiwesk Lake were reported by Arima and Barnett (1984) and show low Fe content and variable Al_2O_3 content in sapphirine from highly magnesian orpthopyroxene-cordierite granulite, where sapphirine forms coronas around cordierite and spinel (hence the strong variation in Al_2O_3), as well as more Fe-rich sapphirine from more felsic plagioclase-sillimanite granulite (Fig. 21). The compositions reported by Arima and Barnett (1984) bracket the FeO range of sapphirine grains analyzed for this study and suggest that the less Fe-rich sapphirine grains (e.g. from Thompson, north-northeast of the TNB, and north of Thompson) are derived from ultramafic rocks, whereas the more FeO-rich sapphirine grains (e.g. from south of Pipe, south of Soab, and southeast of the TNB) are derived from host rock with mafic to intermediate compositions.

A few sapphirine grains have slightly elevated Ni contents but the values do not appear to be related to location or proximity to Ni-Cu mineralization; the highest value (0.11 wt.% NiO) was found in the most Fe-poor grain from southwest of the TNB.

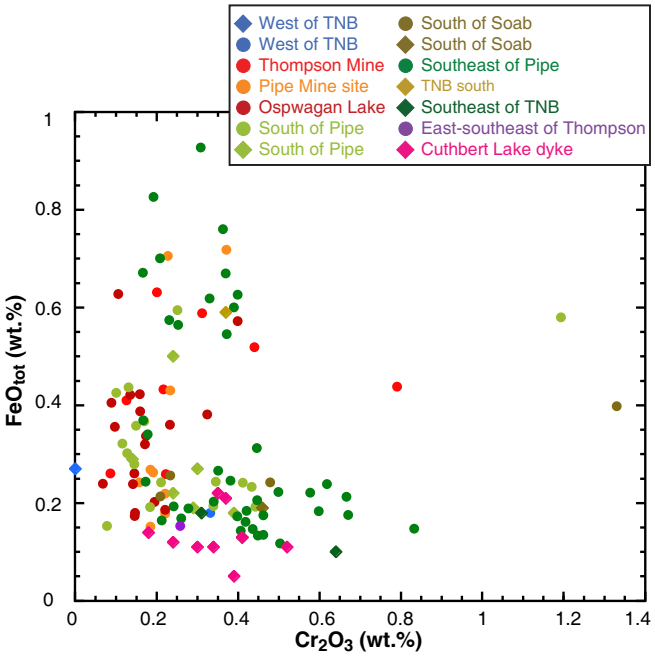

Figure 20. FeO_{tot} versus Cr_2O_3 content in corundum grains found in 2005 till samples from this study (circles) and in regional till reported by Matile and Thorleifson(1997) (diamonds).

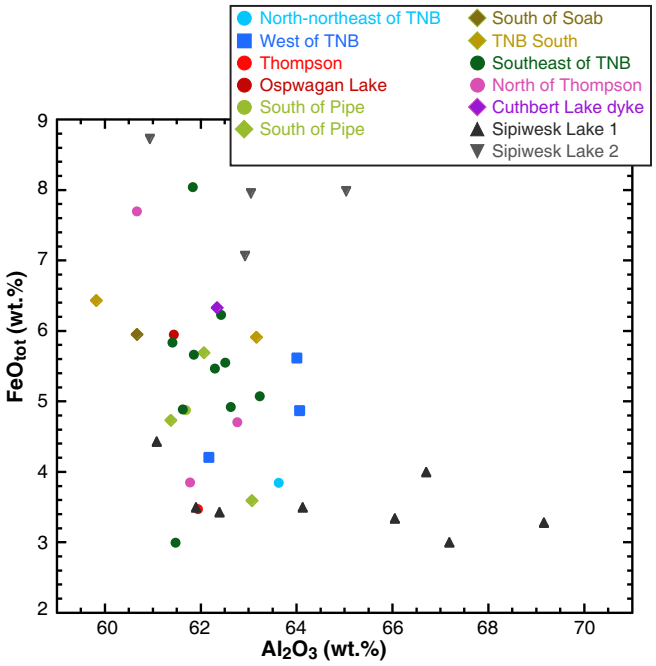

Figure 21. FeO_{tot} versus Al_2O_3 content in sapphirine from 2005 till samples (solid circles) compared to data from Matile and Thorleifson (1997; diamonds), McMartin et al. (2012; squares), and Arima and Barnett (1984; triangles). The latter are divided into sapphirine from orthopyroxene-cordierite-granulite (Sipiwesk Lake 1) and feldspar-sillimanite granulite (Sipiwesk Lake 2) from Sipiwesk Lake in the Pikwitonei, south-southeast of the TNB.

DISCUSSION

Pentlandite

Pentlandite is abundant (100,000s grains/kg) in mineralized rocks from the deposits studied and in trace amounts a few other local TNB rocks. Pentlandite was only found in unweathered till samples and <500 m down ice of the Thompson deposit. These samples contained up to ~41,000 grains/10 kg. In samples containing hundreds to thousands of pentlandite grains, pentlandite abundance typically exceeds chalcopyrite, reflecting the 12:1 pentlandite:chalcopyrite ratio of the Thompson ore. No pentlandite grains were found in till at the Pipe deposit. Grains in bedrock and till range in size from <0.25 mm to 1.0-2.0 mm, but are most abundant in the 0.25-0.5 mm pan concentrates.

Pyrrhotite

Pyrrhotite is the most abundant sulphide mineral in the mineralized rocks studied (up to 65 modal %). Up to 10% of pyrrhotite occurs in silicate-facies iron formation and trace amounts occur in the metasedimentary units of the Manasan, Thompson, and Pipe formations (McClenaghan et al., 2012). Pyrrhotite is absent in the Archean basement rocks and the non-mineralized ultramafic rocks studied (McClenaghan et al. 2012). Background concentration in till is zero grains. Ten till samples contained pyrrhotite in the ferromagnetic fraction, with concentrations ranging up to >41,000 grains. All till samples found to contain pyrrhotite are unweathered till samples from the shoulders of the Thompson or Pipe open pits, i.e., within 500 m of mineralization. Pyrrhotite abundance was determined only for the 0.25-0.5 mm fraction, therefore no conclusions can be made about its size distribution in till or bedrock. Pyrrhotite from the Thompson deposit has significantly higher Ni concentrations (0.4 to 1.13 wt.% Ni) than the few grains recovered from Pipe (0.03 to 0.3 wt.% Ni). The range in Ni concentration for the Thompson pyrrhotite is comparable to pyrrhotite from other Ni-Cu-deposits (e.g. such as Sudbury – GSC unpublished data), while the values at Pipe seem low for a magmatic Ni-Cu deposit, possibly indicating metamorphic recrystallization of the pyrrhotite.

Chalcopyrite

Chalcopyrite is present in mineralized rocks from the deposits studied (100s to 1000s grains per 1 kg) and in trace amounts in metasedimentary rocks along the TNB (McClenaghan et al. 2012) In till, chalcopyrite is most abundant just down ice of the Ni-Cu deposits (100 to 1000s grains/10kg). Trace (background) amounts (1 to 10 grains) are found in till samples all along the TNB. Its presence in both fresh and weathered till both proximal and distal to deposits indicates that chalcopyrite survives in a surface-weathering environment and that the known Ni-Cu deposits are not the only bedrock source of chalcopyrite in the region. Grains in bedrock and till range in size from <0.25 mm to 1.0-2.0 mm, but are most abundant in the 0.25-0.5 mm size range.

Pyrite

Significant amounts (1000s of grains/kg) of pyrite were recovered from most bedrock lithologies, including mineralized and unmineralized rocks. Its abundance in till samples varies between 0 and ~13,000 grains/10 kg with background concentrations ranging from 1 to 5 grains. Counts are highest (1000s of grains) in unweathered till samples at the Thompson and Pipe deposits. Grains in bedrock and till range in size from <0.25 mm to 1.0-2.0 mm, but are most abundant in the <0.25 mm pan concentrates.

Arsenopyrite

A few grains of arsenopyrite were found in only two bedrock samples in this study: Archean biotite gneiss and pegmatite from the Thompson deposit. Not unexpectedly, arsenopyrite content in till is also low (0 to a few grains/10 kg). It was found in only nine till samples and these are at the Thompson and Pipe deposits. It is most abundant in till directly overlying iron for-

mation east of the Pipe open pit and likely reflects the local derivation from these rocks.

Mineral Abundance, Distribution, Composition, and Provenance

Sulphides and Arsenides

Till samples from the Thompson and Pipe open pit shoulders are ideal for detailed mineralogical study of ore dispersal because they are <500 m down-ice from ore zones and were collected below the zone of surface oxidation and thus are fresh to only very weakly oxidized. As a result of their proximity and freshness, their sulphide mineral assemblages and abundances likely reflect the abundances in the mineralized zones that were eroded by the glacier. Pentlandite, pyrrhotite, pyrite, and millerite are the main ore minerals in the Thompson Ni-Cu deposits and these are the dominant ore minerals in these local till samples. The samples contain 1000s of grains of pyrrhotite, pentlandite, pyrite, and chalcopyrite, as well as a few grains of sperrylite, loellingite, and millerite. The most metal-rich sample (05-MPB-09) is from the South pit of the Thompson deposit. It contains ~50,000 pentlandite, ~2500 chalcopyrite grains, and ~15,000 pyrite grains in the 0.25-0.50 mm fraction normalized to 10 kg (Appendix C6), as well as 2 grains of <0.25 mm sperrylite (Appendix C4).

Till samples from the Pipe deposit are characterized by elevated counts of arsenopyrite, chalcopyrite, pyrite, and sperrylite, but do not contain pentlandite and only a few grains of pyrrhotite. On the east (up-ice) side of the open pit overlying sulphide-bearing iron formation (Pipe Formation), till samples contain elevated amounts of pyrite, chalcopyrite, and arsenopyrite. These sulphide minerals in till east (up-ice) of the ore zone are likely indicators of the presence of sulphide-bearing iron formation. In contrast, sperrylite-bearing till samples (05-MPB-035, 06-MPB-58, -60,-61) are found only west (down-ice) of the open pit and known mineralization, and thus sperrylite is an ideal indicator of Ni-Cu mineralization in the TNB.

Only eight till samples contained pentlandite, the most important Ni-ore mineral in the TNB deposits, and all eight samples are within 500 m of mineralization at the Thompson deposit. The absence of pentlandite in till farther down ice likely reflects the mineral's low durability during glacial erosion and transport (well developed cleavage and a low hardness of 3.5-4) as well as its instability in weathering till that was sampled farther down ice. Consequently, pentlandite remains a potential local indicator of buried Ni-Cu mineralization and might provide valuable information about the proximity of the mineralized source. Pentlandite abundance in till is similar to pyrrhotite abundance in the till ferromagnetic fraction.

Table 6. Relative stability of Fe-sulphide and Ni-Cu-PGE ore minerals weathered under temperate to humid, tropical climatic conditions, including the surficial weathering environment of Canada (from Averill, 2011).

Mineral	stability in surface weathering environment
pentlandite	very unstable
millerite	very unstable
PGE sulphides	very unstable
PGE tellurides	very unstable
pyrrhotite	very unstable
pyrite	unstable
chalcopyrite	marginally stable
FeNi and PGE arsenides	stable
PGE antimonides	stable
native Au and PGE	very stable

In the metal-rich till samples containing 100s to 1000s of pentlandite grains (05-MPB- 008, -009, -010), the abundance of pentlandite typically exceeds that of chalcopyrite, reflecting the 12:1 pentlandite:chalcopyrite ratio of Thompson ore. In till samples where pentlandite is less abundant (10s of grains), chalcopyrite is generally more abundant that pentandite. This relative abundance has been noted by Averill (2009, 2011) for surface till samples in the glaciated terrain of Canada. This reversal of the pentlandite/chalcopyrite ratio probably reflects the higher resistance to weathering of chalcopyrite compared to pentlandite or pyrite in a surface environment (Averill, 2011). Based on the abundance of these minerals in till, chalcopyrite is more resistant to glacial comminution and postglacial weathering compared to other sulphides, such as pyrite and pendlandite (Table 6). This pattern is seen in many of the till samples collected from shallow surface pits rather than open pit shoulders (e.g. samples 05-MPB-002, -021, -028), and even from the Pipe open pit (sample 05-MPB-033), where the surviving chalcopyrite population typically numbers <10 grains but often exceeds the pyrite population. However, chalcopyrite is also found in background samples to the east and west of the TNB, where minor Ni-sulphide mineralization occurs in the Molson dykes and volcanogenic massive sulphide (VMS) mineralization style in the Snow Lake area. Since chalcopyrite is common in many different types of sulphide mineralization, including VMS, sedimentary exhalative (SEDEX), iron oxide-copper-gold (IOCG), and stratabound Cu, its presence alone is not necessarily indicative of Ni-Cu mineralization.

The same is true for pyrite. It is abundant in till (100s to 1000s grains) not only within the TNB, and especially at the Thompson and Pipe deposits, but also occurs in high concentrations (100s grains) northeast of

the TNB and in the Snow Lake area, where there are known VMS deposits. Pyrite is also present (1 to 5 grains) in most background till samples. In the fresh metal-rich till samples from the TNB, pyrite is 2 to 800 times more abundant than chalcopyrite. Averill (2007) observed that this ratio is reversed in weathered metal-rich tills. The high pyrite:chalcopyrite ratios (2-800) in fresh till and the very low ratios observed by Averill for weathered till suggest that pyrite succumbs to chemical weathering more readily than chalcopyrite.

A few grains of arsenopyrite were found in till at the Thompson and Pipe deposits, but more so at Pipe. It is a rare to minor mineral in magmatic Ni-Cu deposits, and more common in VMS deposits. Its presence in the till at Pipe likely reflects the presence of sulphide-bearing iron formation on the east side of the ore zone. Loellingite is compositionally and optically very similar to arsenopyrite and often found intergrown with it. The presence of a few grains of loellingite in till proximal to the Thompson and Pipe deposits, as well as in a cluster west of the TNB, may reflect magmatic Ni-Cu mineralization.

Although platinum group minerals (PGM) are not significantly enriched in the TNB ores compared to other Ni-Cu deposits, a variety do occur in the ores of the Thompson and Pipe mines (e.g. Cabri and Laflamme, 1981; Chen et al., 1993; Burnham et al., 2009). Two sperrylite grains were picked from the >0.25 mm fraction of two till samples from the Thompson Mine site. The presence of these two large grains is significant, as PGM grains typically are silt sized. This case study is one of the first reports of coarse-grained PGM recovered from till. Smaller, silt-sized grains (<200 μm) were recovered during panning from 13 metal-rich till samples. The number and size of the sperrylite grains recovered here are remarkable and suggest that it presense the <0.25 mm heavy mineral fraction may be a useful indicator of proximity to magmatic Ni-Cu mineralization.

This case study is one of the first to systematically examine and count the number of pyrrhotite grains in the ferromagnetic fraction of till. Pyrrhotite abundance was determined because it is a major sulphide mineral in the TNB deposits. As part of this study, its usefulness as an indicator mineral for massive sulphide deposits was evaluated. The presence of pyrrhotite grains in till proximal to the deposits suggests that it is indeed a useful indicator mineral.

Silicates and Oxides

Cr-Diopside Distribution

Matile and Thorleifson (1997) identified a significant, >300 km long, Cr-diopside dispersal fan extending southwest from the TNB into Saskatchewan that is clearly a product of early southwest and later westward ice flow. The westward extent of Matile and Thorleifson's dispersal fan is undocumented, as they did not collect samples directly west of the TNB. Our study area includes the up-ice source area of the large fan and many of the till samples in this study contain 100s of Cr-diopside grains. The highest proportion of Cr-diopside grains was found in till to the east of the TNB (along the forest access roads) and around the Thompson, Birchtree, and Pipe deposits. One aim of this study was to identify the bedrock source of the Cr-diopside fan. In fact, Averill (2001) suggested that low-Cr diopside is an indicator mineral for Ni-Cu massive sulphide deposits, in part based on his empirical observations of the dispersal fan from the TNB.

However, none of the peridotite and pyroxenite bedrock samples examined as part of this study (McClenaghan et al., 2012) contain Cr-diopside. Examination of approximately 700 thin sections of mafic to ultramafic rocks from the TNB from an earlier CAMIRO project on the TNB (Burnham et al., 2009) also yielded extremely few samples that contained fresh Cr-diopside, one of which was analyzed for this study (Fig. 11). Most of the TNB ultramafic rocks sampled were severely altered and metamorphosed and contained only serpentinized olivine and orthopyroxene and no clinopyroxene, or, if clinopyroxene was present, it had been replaced by tremolite + carbonate ± chlorite. Published literature on Thompson rocks contains few analyses of Cr-diopside. In 1978, an Inco researcher (de Saboia) identified and analyzed Cr-diopside grains occurring with enstatite in pyroxenite at the Pipe deposit (Fig. 11). This dearth of bedrock Cr-diopside data makes it difficult to link Cr-diopside abundance and composition in till to that from mineralized or unmineralized rocks in the TNB. In light of the high abundance of Cr-diopside in till overlying the TNB, the scarcity of Cr-diopside in bedrock is baffling. The bedrock source of the abundantt Cr-diopside grains in till has not been clearly identified yet. One possible explanation is that at the time of glacial erosion, ultramafics exposed at the surface were either less altered and/or less metamorphosed and/or contained more fresh Cr-diopside than the rocks exposed now and that have sampled for this and previous studies.

Cr-Diopside Compositions and Provenance

The Cr-rich and Mg-rich compositions of the Cr-diopside in till clearly indicate that most of these grains are likely derived from ultramafic rocks, such as pyroxenite and peridotite. Slightly lower Mg-#s and Cr values in the area around Pipe and south thereof indicate contribution from the mafic (picritic) volcanic rocks of the Bah Lake Formation.

A striking feature are the high Cr_2O_3 concentrations (>1.4 wt.%) found in 11% of the 2085 Cr-diopside

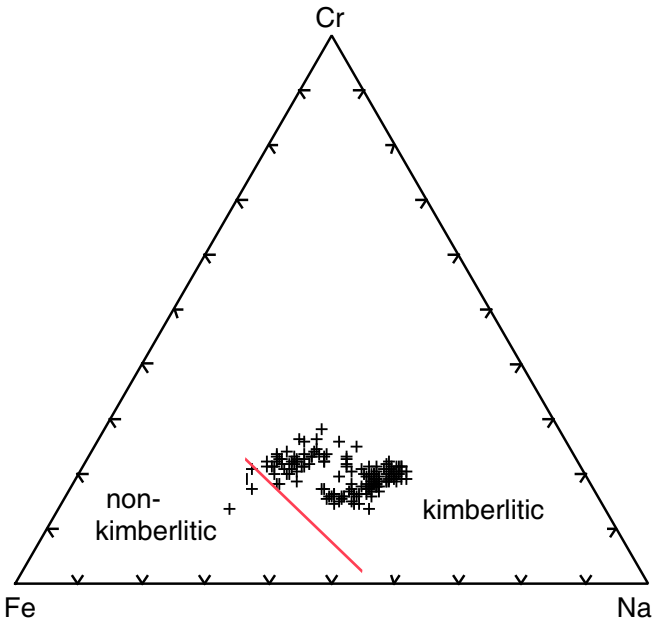

Figure 22. High Cr-diopside (>1.4 wt. $Cr_2O_{3)}$ compositions plotted in a Al-Cr-Na ternary diagram (molar proportions) with discrimination line separating kimberlitic versus non-kimberlitic Cr-diopside from Quirt (2004).

grains that were analyzed. These grains with high Cr_2O_3 values occur predominantly east of Thompson (Fig. 10f), around Ospwagan Lake (Fig. 10h), south of Pipe and east of Soab (Fig. 10j). These compositions have no match in analyzed bedrock samples, which have a maximum Cr_2O_3 concentration of 1.3 wt.% (Fig. 12). The dissimilar compostions between bedrock and till may be partially due to the lack of Cr-diopside data from ultramafic bedrock samples. Note that diopside with >1.5 wt.% Cr_2O_3 is extremely rare in crustal igneous rocks and is typically only found in mantle peridotite brought up as xenoliths by kimberlite eruptions (see Deer et al., 1978). The majority of the high-Cr-diopside grains (>1.4 wt.% Cr_2O_3) in till from this study are also Na-rich (Fig. 22), indicating a higher jadeite ($NaAlSi_2O_6$) or kosmochlor ($NaCrSi_2O_6$) component, which is indicative of either high-pressure formation in the mantle or very high-grade metamorphic conditions, such as experienced, for example, in blueschist or eclogite-facies terranes. When plotted in a discrimination triangle devised by Quirt (2004) for distinguishing crustal Cr-diopside from mantle-derived Cr-diopside contained in kimberlite, most of the till Cr-rich diopside (>1.4 wt.% Cr_2O_3) from this study plot in the kimberlite field (Fig. 22). However the discrimination diagram does not take into account the possibility of high-grade metamorphic Cr-diopisde.

Till concentrate samples that contained high-Cr diopside grains were examined for other kimberlite indicator minerals (e.g. Cr-pyrope, Mg-ilmenite) but none were found. The absence of these kimberlite indicator minerals in the till suggests that the high-Cr-diopside grains are likely derived from high-grade ultramafic metamorphic rocks rather than from mantle-derived rocks. There are a few examples of Cr-rich diopside from high-pressure/high-grade metamorphic ultramafic rocks from China, Russia, and Japan reported in the literature (Sobolev et al., 1975; Liu et al., 1998; Tsujimori and Liou, 2004) with Cr_2O_3 values similar or even higher than those reported here. According to Paktunç and Baer (1986), the Pikwitonei domain east of the TNB experienced metamorphic temperatures up to 850ºC at 5 to 7 kbar (granulite facies), which might be sufficient to explain the significant abundance of Cr- and Na-rich diopside grains in till east of the TNB. The high Cr-diopside found in till within the TNB (Ospwagan Lake and south thereof) might have been glacially transported from host rocks located immediately east of the TNB by the younger westerly ice-flow. Alternatively, the amphibolite-facies overprint in the central TNB did not affect all rock types equally, leaving domains of granulite-facies rocks that may have contained high-Cr diopside. Especially dry (water-free) ultramafic rocks, which are least affected by metamorphic reequilibration due to the absence of hydrous phases and the high pT stability of their major minerals (pyroxene, olivine), may have retained granulite-facies mineralogy and compositions.

Olivine

Olivine is more abundant than Cr-diopside and chromite, with maximum values of over 800 grains/10 kg (sample 05-MPB-011 from the Thompson South pit) compared to 700 grains for Cr-diopside (sample 05-MPB-036 from near the Pipe deposit) and 200 grains for chromite (sample 05-MPB-009 from the Thompson deposit). As in the ultramafic and marble bedrock samples studied (McClenaghan et al., 2011), all of the olivine grains are forsteritic. However, much of the forsterite is impure, containing microscopic magnetite or Cr-magnetite inclusions, suggesting that it is metamorphic in origin and not primary igneous olivine. The serpentinization of primary igneous olivine leads to the formation of fibrous serpentine and extremely fine-grained magnetite, which accumulate in the serpentinized cracks in the olivine. When the serpentine is dehydrated to metamorphic olivine during prograde metamorphism, the fine-grained magnetite is incorporated into the metamorphic olivine as ribbons of fine-grained opaque inclusions. Evidence for this occurring in TNB rocks has been provided by Paktunç (1984), who studied olivine from the Thompson Mine. This process is also apparent in olivine grains from till examined in this study.

Olivine compositions that cluster between Fo85 and Fo93, indicate that the the olivine was derived predominantly from ultramafic rocks. The only significant

regional compositional variation for till grains are a higher number of low Fo (50-75) olivine grains in the area south of Pipe, which are probably derived from picritic volcanics from the Bah Lake Formation rather than from ultramafic rocks (Fig. 13c). Ni concentrations in olivine from till are higher (6200 ppm Ni or 0.79% NiO) than olivine from bedrock (up to 4500 ppm or 0.57% NiO) (Fig. 14).

According to a compilation by Deer et al. (1997), the maximum Ni content reported for igneous olivine is 0.55 % NiO (4322 ppm) in Archean komatiitic rocks from Munro Township, Ontario and from the Belingwe Belt in Zimbabwe (Green et al., 1975; Arndt et al., 1977; Renner et al., 1994) and one analysis of olivine from chromitite with 0.67 wt.% NiO (Pavlov and Grigor'eva, 1977). Considering that the parental melts for the ultramafic bodies in the TNB were komatiitic, it is not inconceivable that their olivines had higher than normal primary levels of NiO (i.e. >3000 ppm). However, explaining values of up to 0.79 wt.% NiO by igneous processes alone is difficult. Burnham et al. (2009) proposed a complicated multi-stage process to enrich the most Ni-rich olivines in their study (from Williams Lake) with Ni. These authors made a distinction between magmatic olivine, which are shown as coloured dots, and metamorphic olivine, which are shown as coloured diamonds in Figure 14a. The criteria for this subdivision were not exclusively textural but mainly based on the Fo content of the olivines compared to the Mg-# of the whole rock, classifying those that had Fo contents similar to their whole rock Mg-# as magmatic. According to this classification, magmatic olivine from the TNB has Fo ranges of 88 to 90 for dunitic, 86 for peridotitic and 81 to 84 for pyroxenitic assemblages. Metamorphic olivine, in contrast, shows widely varying Fo and Ni contents irrespective of whole rock composition.

Paktunç (1984) describes olivine "megacryst" grains in the ultramafic body of the Thompson Mine as having fine-grained opaque (magnetite) inclusions concentrated in vein-like arrays similar to magnetite crystallizing in cracks and veins in serpentinized olivine. He argues, based on these textural features, that this type of olivine must have crystallized prograde from formerly serpentinized olivine. Smaller neoblastic (metamorphic) olivine grains in his study have distinctly lower Ni and slightly lower Fo content then the immediately adjacent “megacrystic” olivines (Fig. 14b), explaining the vertical arrays in Ni at almost constant Fo (Fig. 14a and b). The observation of abundant fine-grained magnetite inclusions in olivine in till samples from this study and the large range in Ni values for similar Fo strongly suggests that these are mostly metamorphic olivines formed by dehydration of Ni-enriched serpentine. Most TNB ultramafic rocks have been thoroughly serpentinized and unpublished data from the Minago deposit in the southern TNB (Zellerer, 2008) indicate that some of the serpentine is highly enriched in Ni, which was released through the alteration of olivine and primary FeNi-sulphides (pentlandite). Some of the analyzed serpentine samples contain domains with highly variable Ni contents of up to 12.9 wt.% NiO (Zellerer, 2008). Although these Ni contents are extreme, it is conceivable that if Ni-rich serpentine underwent prograde metamorphism to the degree the TNB rocks experienced (upper amphibolite facies: Bleeker, 1990), the resulting metamorphic olivines could have been enriched in Ni far above their normal magmatic range.

The most Ni-rich olivines in till are in the southern TNB (i.e. the Pipe deposit area, south of Ospwagan Lake, and around Soab), as well as along the forest access roads east of Thompson. Samples from these same areas were found to contain high Cr- and Na-rich diopside grains. This distribution pattern suggests that both olivine and Cr-diopside in these till samples were derived from high-grade metamorphosed ultramafic rocks found immediately east of, and possibly within, the TNB. It should be mentioned that the conversion of serpentine to metamorphic olivine requires considerably lower temperatures than the formation of metamorphic diopside from an ultramafic assemblage.

Olivine from TNB mineralized bedrock samples, as reported by L. Hulbert (GSC unpublished data), does not exceed a restricted compositional array of Fo 78 to 91 and 0 to 3000 ppm Ni (Fig. 14), whereas olivine from non-mineralized ultramafic and mafic rocks has a much wider compositional range both in Fo and Ni (McClenaghan et al. 2012). Till samples with this same restricted compositional range of Fo 78 to 91 and 0 to 3000 ppm Ni are predominantly proximal to the Thompson, Pipe, and Soab deposits and on the shore of Ospawagan Lake.

Chromite

Chromite distribution in till at a regional scale displays some similarities to olivine and Cr-diopside distributions, with an additional occurrence west of the TNB that does not contain olivine. The two clusters of chromite-rich till in the TNB coincide with elevated olivine and Cr-diopside-rich till around the Pipe Mine and the Thompson deposits. Similar to olivine and Cr-diopside, chromite abundances in till are elevated along the forest access roads southeast of the Thompson deposit, further evidence to suggest that debris has been eroded from ultramafic rocks east of the TNB. Till samples along the forest access road south of Paint Lake that are enriched in olivine and Cr-diopside do not contain abundant chromite grains. This absence of chromite could be simply a grain-size effect

— chromite in the source rocks might be too small to be recovered in the >0.25 mm heavy mineral fraction. Elevated chromite abundances are found in till along the highway west of the TNB, within and near the Osik Lake ultramafic dispersal train (Appendix A2, Appendix E1-chromite map) that was identified by DiLabio and Kasycki (1988). The train is related to unmapped ultramafic rocks underlying Osik Lake and the authors postulated that other ultramafic bodies likely occur in the area. Elevated chromite counts in till samples in this area support their conclusion.

The study of TNB bedrock samples (McClenaghan et al., 2012) revealed that chromite and chromian magnetite from mineralized samples from the Pipe and Thompson mines (independent of host-rock lithology) are consistently MgO-poor (<2 wt.% MgO) but vary widely in Cr content (50 to 25 wt.% Cr_2O_3) and form a continuous trend from ferro-ferrichromite to chromian magnetite. Unmineralized ultramafic rocks, in contrast, contain ferri-chromite with comparatively little variation in Cr_2O_3 (40-52 wt.%) and higher MgO (1.5-4.5 wt.%). Chromian spinel from picrite of the Bah Lake Formation is Cr-poor and MgO-rich due to a high spinel component. The bulk of the chromite compositions in till falls within 44 to 53 wt.% Cr_2O_3 and 3 to 10 wt.% MgO, which is more magnesian than the chromites from meta-peridotitie at Thompson. From this cluster extends a small number of grains towards the spinel $(Mg,Fe)Al_2O_4$ corner of the diagram (Fig. 16b, lower right). The more MgO- and Cr-rich chromite compositions that are abundant in the till as well as those lying on the spinel trend have also been reported from ultramafic rocks along the north part of the TNB (Burnham et al., 2009), including those from the Thompson Mine (Paktunç, 1983). In addition, there is a population of Cr-rich (> 60 wt.% Cr_2O_3) chromite that occurs predominantly in till outside the TNB. The shift from "normal" ultramafic chromite compositions with 5 to 10 wt.% MgO and 40 to 60 wt. % Cr_2O_3 to MgO-poor ferro-chromite is considered to be due to serpentinization of surrounding silicate minerals (olivine, orthopryoxene), that depletes the chromite of Mg, while retaining original Cr-levels (Groves et al., 1977).

A striking feature of the chromites that plot along the chromite-magnetite trend is their high Zn content (2-8 wt.% ZnO in three mineralized bedrock samples from Thompson, Pipe, and Birchtree), whereas chromite from non-mineralized ultramafic rocks and picrite contain <2 wt.% ZnO (Fig. 15). The range in Zn content is even broader in chromite from till samples from the Thompson mines, with up to 18 wt.% ZnO trending towards gahnite (Fig. 15a). Curiously, only a few chromite grains in till from the Pipe Mine and to the south have elevated ZnO contents, although the bedrock samples from the Pipe Mine yielded predominantly zincian chromite. The low number of Zn-rich chormite in till from around the Pipe deposit, could be related to the small size (<0.25 mm) of Zn-rich chromite in the bedrock.

The elevated Zn contents of chromite associated with Ni-mineralization in the TNB are not unexpected. Groves et al. (1983) reported elevated ZnO (4.29 wt.%) contents in chromites from serpentinite from the Pipe 2 deposit. Also, Paktunç and Cabri (1995) reported elevated Zn contents in chromites from the TNB, as well as for chromites from the Cuthbert Lake dyke to the east. Chen et al. (1997) and Chen and Zang(2004) reported ZnO contents of up to 7.2 wt.% in spinel from mineralized peridotite and up to 14.6 wt.% in spinel from metapelite-hosted Ni mineralization at the Thompson Mine. Zn-rich chromite in peridotite and overlying till have also been reported in association with magmatic Ni-Cu deposits of the Vammala nickel belt in southwest Finland, where it was suggested as an indicator mineral for Ni mineralization (Peltonen and Lamberg, 1991; Huhta and Peltonen, 1994). They identified a threshold of 0.8 wt.% ZnO, which is likely lower than in the TNB region.

The cause of Zn enrichment in chromite in the TNB ores is likely related to the high grade of metamorphism that has affected the belt. The Thompson deposit is at the highest metamorphic grade (upper amphibolite facies: Bleeker, 1990) of all the deposits in the TNB. Although Zn content is low in the massive Ni-Cu ore (<500 ppm: Burnham et al., 2009), Zn may have been derived from the sulphide-bearing sedimentary host rocks (Pipe Formation), from the desulphurization of sphalerite (as suggested by Chen et al., 1997), or from trace amounts of Zn in pyroxenes during metamorphism (Barnes, 2000). Sphalerite found in mineralized pegmatite breccia from Thompson D1 (sample 05MPB-R36) and in hanging-wall biotite schist at Birchtree (sample 05MPB-R42), is an indication of the presence of Zn minerals in the vicinity of Ni-Cu ore in the TNB.

Spinel and Gahnite

Zn-rich spinel and gahnite abundance in till are low to none. Distribution patterns do not appear to be related to Ni-Cu mineralization, with the highest counts in background samples west of the TNB. Neither mineral is considered to be an indicator of magmatic Ni-Cu mineralization in the TNB.

Both spinel and gahnite form in Si-poor and/or Al-rich environments in high-grade metamorphic rocks. Although gahnite can be used as an indicator mineral for sulphide mineralization in high-grade metamorphic terranes (Heiman et al., 2005), its application is mainly for Zn-rich deposits such as VMS or SEDEX and less

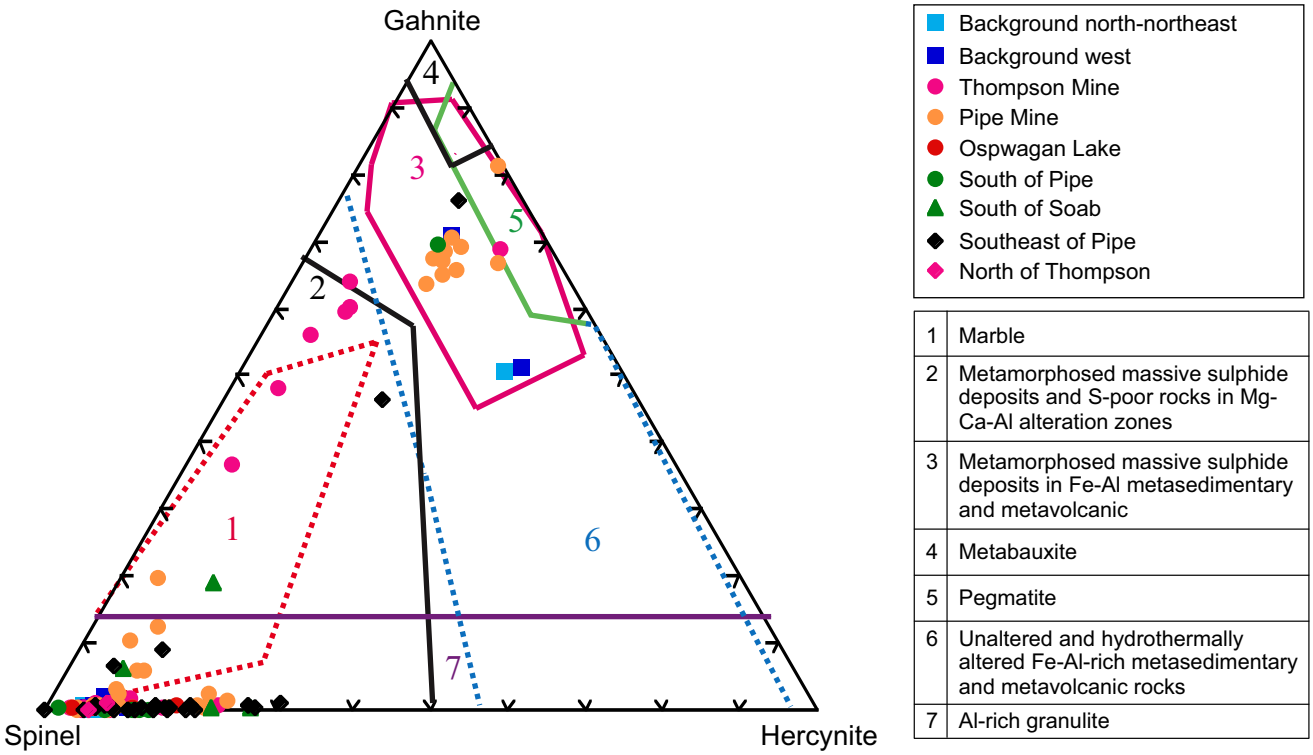

Figure 23. Spinel-gahnite-hercynite ternary plot for spinel and gahnite grains from till.

for magmatic Ni-Cu mineralization, which contains much lower concentrations of Zn. Plotted in a ternary spinel-gahnite-hercynite diagram (Fig. 23) following Heimann et al. (2005), Zn-rich spinels and gahnite from till around the Pipe deposit plot into the field of metamorphic massive sulphide deposits (MMS) close to the Zn apex, while those from Thompson plot along the spinel-gahnite join in an area with for which there is no published data but close to compositions reported by Heiman et al. (2005) in Mg-Ca-rich and S-poor alteration zones in MMS. The Thompson Zn-spinels are less Fe-rich than most MMS spinels reported in the literature compiled by Heimann et al. (2005).

Rutile

Red rutile is moderately abundant in till just southeast of the TNB, and both north of Thompson and in the southern part of the TNB, but is rare at the Thompson and Pipe deposits. In areas where rutile is most abundant in till, the rutile compositions are Cr-rich and Fe-poor. Zack et al. (2004) found that Cr and Nb in rutile from mafic rocks increase concomitantly up to approximately 3000 ppm Cr (0.44 wt.% Cr_2O_3) and 1500 ppm Nb (0.21 wt.% Nb_2O_5) and that rutile with higher Nb but low Cr is characteristic of metapelitic rocks. The compositions of most of the rutile found in this study coincides with the rutile compositions from metamafic rocks outlined by Zack et al. (2004), but also exceed them considerably in Cr, as shown in Figure 19. The rutile found in this study is interpreted to be dominantly from high-grade mafic to ultramafic rocks, whereas rutile with compositions reflecting metapelitic origins are extremely rare. Rutile in background till from north and west of the TNB is considerably less Cr-rich and appears to come from metamafic source rocks.

The highest abundances of red rutile in till occur east of the TNB, overlying Superior Craton rocks. This distribution suggests that most grains are likely derived from rocks east of the TNB and are not an indicator of Ni-Cu mineralization in the TNB.

Corundum and Sapphirine

Both pink corundum and sapphirine, which are rare in till, are distributed over both background areas and the TNB. Pink corundum is most abundant in till southeast of the Pipe deposit, just east of the TNB, as well as within 10 km radius of the Pipe deposit and at the Thompson deposit, suggesting its distribution may be related to TNB ultramafic rocks. Averill (2006) suggested that these grains may be derived from contact zones between peridotite and aluminous metasedimentary rocks and, as such, corundum may be a useful indicator mineral of fertile ultramafic melt in the TNB region.

Similar to spinel and corundum, sapphirine is a mineral characteristic of highly metamorphosed Si-poor and/or Al-rich rocks. Arima and Barnett (1984) analyzed sapphirine in orthopyroxene-cordierite granulite and feldspar-sillimanite granulite from Sisiwek Lake,

highly metamorphic Pikwitonei domain southeast of the TNB, and found that a coupled subsititution of $(Mg,Fe,Mn)^{2+}+Si^{4+} \leftrightarrow 2Al^{3+}$ is responsible for variations in Fe/Mg and Al/Si concentrations and that the most Fe-poor sapphirines are derived from the most magnesian host rocks. Sapphirine, while present in a few till samples, displays what appears to be a random distribution pattern in till that is unrelated to bedrock geology or structure. Its presence likely reflects the high metamorphic grade and comparatively mafic host-rocks. However, it is a not useful indicator for magmatic Ni-Cu mineralization in the TNB.

Ultramafic Bedrock Sources

Distribution patterns for forsteritic olivine, Cr-diopside, orthopyroxne, and, to a lesser extent, chromite in till, from across the study area, are strikingly similar at a regional scale. These minerals have high concentrations within the north-central TNB, including and south of the Thompson and Pipe deposits, but equally high or even higher concentrations occur along forest access roads trending east-southeast of Thompson and south of Paint Lake across the Superior boundary zone. These high concentrations in till east of the TNB suggest that ultramafic rocks containing fresh olivine, Cr-diopside, and orthopyroxne exist up-ice (either northeast or east) of the TNB. Possible candidates are ultramafic bodies embedded in amphibolite and gneiss of the Pikwitonei domain, just east of the Cuthbert Lake dyke and the Cuthbert Lake dyke (Appendix A2). The Cuthbert Lake dyke is a major member of the Molson dyke swarm, which trends parallel to the TNB in the Pikwitonei region and is coeval with the ultramafic rocks of the TNB (1.88 Ga, Heaman et al., 1986). The Cuthbert Lake dyke is exposed intermittently over a length of 100 km or more and is at least 60 m wide (Paktunç, 1987). Similar to other major dykes of the Molson swarm, it is ultramafic rather than mafic in composition, and consists of several bands of more or less plagioclase-bearing olivine-hornblende-pyroxenite to olivine-hornblende-gabbronorite. Cr-diopside, olivine, and hornblende are the most abundant minerals, each ranging between 20 and 40 vol.% each (Paktunç, 1987). Analyses of Cr-diopside from the Cuthbert Lake dyke plot within the compositional range of Cr-diopside analyses from till, but at the lower end of the Mg-# spectrum (≤ Mg-# 86) and medium-high Cr_2O_3 of up to 1.3 wt.% (Fig. 12). Potential bedrock sources for the Cr-rich Cr-diopside have not been found yet.

Olivines from the Cuthbert Lake dyke (Paktunç, 1983) have compositions slightly lower in Fo and Ni than the bulk of olivine compositions found in till (Fig. 14), suggesting that the Cuthbert Lake dyke is not the only or even the predominant source of olivine or Cr-diopside in the study area. Unfortunately, no detailed information on the mineralogy of the other ultramafic bodies in the Pikwitonei is available, but given the high metamorphic grade in the area it is likely that these bodies may be sources for the abundant Cr-diopside and olivine in till along the forest access roads east-southeast of Thompson as well as into the TNB.

Glacial Transport

Due to mine tailings, mine waste, and a thick cover of glaciolacustrine clay, only limited sampling was possible 0 to 1 km down-ice of the Thompson and Pipe deposits. As a result, sample distribution proximal to the deposits is sporadic and biased to sites south of the deposits. Metal-rich till was encountered at most sites 750 m down-ice of mineralization. Inco's 1973 study (Webster, 1973) documented metal-rich till on the west side of the Birchtree deposit. The presence of highly metaliferrous till west of these deposits indicates that mineralized bedrock was eroded by the younger, westward-flowing ice (Webster, 1973; McClenaghan et al. 2009). Clasts of Paleozoic carbonate eroded from Hudson Bay platform rocks to the east, provides further evidence of the westward glacial dispersion across the TNB. The nature and extent of the glacial dispersal of metal-rich till by the younger, westward ice-flow could not be assessed in this study due to sampling limitations of proximal till west of the deposits.

Useful Indicator Minerals for Magmatic Ni-Cu Exploration in the Thompson Nickel Belt

Indicator minerals in till can be a useful tool for magmatic Ni-Cu exploration in the TNB and surrounding region. Matile and Thorliefson (1997) suggested that the large fan of Cr-diopside in till in northern Manitoba reflected the presence of the TNB. Averill (2001, 2009) suggested a broader suite of minerals as potentially useful for detecting the presence of magmatic Ni-Cu mineralization. This study evaluated the suggested suite of indicator minerals and offers the following conclusions.

Sulphides

Pyrrhotite and pentlandite are the main Ni-Cu ore minerals for the TNB deposits. They are most abundant in the 0.25-0.5 mm fraction of the heavy mineral concentrate and occur only in unweathered till proximal (<750 m) to the deposits. Till contains 100 to 10,000s of sulphide grains per 10 kg. In the absence of pentlandite, elevated Ni values in pyrrhotite (>0.25 wt.% Ni) can be used to distinguish pyrrhotite derived from Ni ore from pyrrhotite derived from volcanogenic as as well as other types of massive sulphide deposits, which typically contain lower Ni. Chalcopyrite, also an ore mineral in the TNB deposits, is much less abundant (100 to

1000s grains/10 kg) in till proximal to deposits but is found in fresh and weathered till. It also occurs in other mineralized rocks but its presence together with other indicator minerals (e.g. pyrrhotite and pentlandite) in till suggests Ni-Cu ore in the up-ice region.

Silicates and Oxides

Cr-diopside, enstatite, chromite, and forsteritic olivine are usefull indicators for the presence of ultramafic rocks, which have the potential to host magmatic Ni-Cu deposits and were foundas surprisingly fresh grains in the glacial sediments. Of these minerals, enstatite was not examined in detail in this study because another orthopyroxene variety (hypersthene) is very abundant in background till from the region and it is difficult to differentiate visually between the two minerals. Cr-diopside was not recovered from TNB bedrock in sufficient amounts to establish a compositional link between Cr-diopside in till and mineralized host rocks. Very Cr-rich diopside in till within and especially east of the TNB, which is most likely of high-grade metamorphic origin, suggests that Cr-diopside is not very useful as an indicator mineral for kimberlite or magmatic Ni-Cu deposits in high metamorphic terrains such as the Pikwitonei. It is, however, a useful vector to ultramafic rocks.

Olivine compositions in till from the TNB and east of the TNB show an anomalously wide variation in Ni contents (from a few hundred ppm to >6000 ppm) irrespective of Fo content. This in itself is probably a good indication of Ni ore in the area, since olivine from unmineralized rocks shows Ni values that are strongly linked to and decrease exponentially with Fo content from ~3000-4000 ppm at Fo90 to near 0 at Fo50 (Deer et al., 1997). The erratic Ni values in olivine from the TNB till are probably due to a large proportion of these olivine grains having formed by prograde metamorphism from variably Ni-enriched serpentine, which in turn was an alteration product of the ultramafic igneous rocks that host the Ni-mineralization. The Ni in serpentine is derived partly from the original igneous olivine and partly from Ni released through the alteration of Ni-bearing sulphides in the ore. In addition, olivine from drillcore of ultramafic bedrocks from the Thompson mine site analyzed by L. Hulbert (GSC) indicates abnormally low Ni values (<3000 ppm) in Fo-rich olivine.

The most significant finding of this study is Zn-rich (>2 to 18 wt.% ZnO) chromite and Cr-spinel that is restricted to mineralized bedrock at the Thompson, Birchtree, and Pipe mines and proximal till samples. Although unmineralized ultramafics in the TNB have been metamorphosed to the same degree as those at the mine sites, they lack the Zn-rich chromite found in the mineralized bodies. A threshold value of 2 wt.% ZnO is estimated as the divide between the Zn-rich and Zn-poor chromite.

Other oxides, such as gahnite, spinel, corundum, sapphirine, and rutile, do occur in minor amounts in the till samples from within as well as outside of the TNB. However, they are absent from the crushed bedrock samples or are too small to show up in the heavy mineral fractions used for this study. Therefore, a compositional link between these minerals and Ni-Cu mineralization could not be established. However, all are indicative of a high metamorphic grade and sapphirine, as well as Cr-bearing corundum and rutile, indicate the presence of ultramafic rocks.

Comparison to Till Geochemical Anomalies

Till geochemical data for the <0.063 mm fraction of the TNB till samples have been reported by McClenaghan et al. (2009a, 2011). Elevated geochemical values in 6 till samples from outside of the TNB may indicate Ni-Cu mineralization and warrant further investigation (see Fig. 20 in McClenaghan et al., 2009a). Five of these sample sites/areas have indicator mineral abundances that confirm these sample sites as anomalous:

1. A sample from west of the TNB and south of Osik Lake has elevated Cr and Pd values. This area hosts the Osik Lake ultramafic dispersal train and has been suggested to contain unmapped ultramafic intrusive rocks by DiLabio and Kaszycki (1988). Elevated abundances of indicator minerals chromite, forsterite, orthopyroxene, chalcopyrite, and loellingite in till are worth noting as they comprise a multi-mineral signature similar to that of the deposits in the TNB.
2. Till sample 96-TCA-035 has elevated Pd and Cd values and contains one forsterite grain, though nearby samples contain none.
3. Till sample 96-TCA-037 has elevated Pt, Pd, Mo, Sb, Bi, Hg, and Se values and contains one Cr-diopside grain and two chromite grains, whereas nearby samples contain none.
4. Till sample 96-TCA-044 has elevated Pd and Cu values and contains one grain of chromite; nearby samples contain none.
5. Till sample 05-MPB-005 has elevated Au values and contains elevated chalcopyrite and pyrite counts compared to nearby samples.

Re-picking Archived Heavy Mineral Concentrates

The TCA-series reconnaissance-scale till samples were collected in 1996 primarily in support of kimberlite exploration (Matile and Thorliefson, 1997). Heavy mineral concentrates for these samples were archived at the GSC. Selected samples were re-examined as part

Table 7. Comparison of indicator mineral signatures of Ni-Cu-PGE deposits in the glaciated terrain of Canada.

Deposit	Location	Indicator Minerals in Surficial Sediments	Source of Information
Thompson and Pipe Ni-Cu deposits	Thompson Ni Belt, MB	pentlandite, pyrrhotite, chalcopyrite, sperrylite forsterite, chromite, Cr-diopside	this study
Broken Hammer occurrence	Sudbury, ON	chalcopyrite, sperrylite, gold	Ames et al., 2007
Sudbury-type deposits	Sudbury, ON	gold, PGM	Bajc and Hall, 2000
Shebandowan Ni-Cu-PGE deposit	Shebandowan Greenstone Belt, ON	Cr-diopside	Bajc, 2000
Lac des Iles PGE deposits	Lac des Ilses Complex, ON	chromite, Cr-andradite, sperrylite, stillwaterite, pyrite	Searcy, 2001; Averill, 2007; Barnett and Averil, 2010
Tulameen Ultramafic Complex	southern BC	chromite, tulameenite, isoferroplatinum, magnetite	Cook and Fletcher, 1992

of this study and indicator minerals recounted and additional grains picked. Comparison between indicator mineral abundances of the original picking data and the new re-picking data in this study (Appendix C7) confirmed the original results and/or identified additional grains. Most additional grains recovered were pyrite, chromite, or Cr-diopside. This re-picking and merging of old and new counts into one data set allowed the original data from 1996 samples to be incorporated into this study and provided the regional context for interpreting the data from the 2005 and 2006 samples. Additional grains of chromite and Cr-diospide picked in this study providednew material for mineral grain chemical analysis by EMP. This re-picking demonstrates the value of archiving till heavy mineral concentrates for future studies as indicator mineral picking methods improve over time, commodities of interest change/expand, and new indicator minerals for these commodities are discovered with continued research. Access to archived samples saved the time and the expense of collecting new till samples in remote areas when this current project was undertaken.

Comparison of Indicator Mineral Signatures to Other Magmatic Ni-Cu-PGE Deposits

Averill (2001, 2011) compiled a list of Ni-Cu-PGE indicator minerals (Table 1) that includes oxide, silicate, sulphide, PGE minerals, and native gold. Some of these minerals were comfirmed by this study to be useful indicators of the TNB magmatic Ni-Cu deposits. In addition to the minerals listed in Averill's table, this study also identified pyrrhotite and pentlandite as useful indicators if unweathered till was sampled. Pyrite may also be a useful indicator of magmatic Ni-Cu deposits when it is accompanied by some or all of the other indicator minerals.

Table 7 lists indicator minerals that have been reported in till down-ice from some of the other magmatic Ni-Cu-PGE deposits in Canada for comparison with those from the TNB deposits. Four of the five deposits listed in Table 7 display sulphide and/or PGM indicator mineral signatures in till. The TNB, the Lac des Isles, and the Tulameen deposits all display chromite signatures that can be traced down ice. However, in contrast, the TNB deposits display the most extensive and varied list of indicator minerals, which includes oxides, silicates, sulphides, and PGM, which is due to a combination of factors: the TNB deposits have been sampled and studied in greater detail; the host rocks of the TNB contain the most varied and detectable suite of indicator minerals; and the TNB has been the subject of the most recent case studies and as such has benefitted from the application of the most up-to-date techniques. the TNB host rocks .

CONCLUSIONS

In this study, the collection of surface till samples both around the deposits and regionally throughout the TNB was limited by access, the presence of mine workings, and the thickness of glacial Lake Agassiz sediments overlying till. In spite of these limitations, till sample distribution was sufficient to identify indicator mineral signals in unweathered till up to 750 m down-ice on the west side of the Thompson and Ni-Cu Pipe deposits. Sperrylite is most abundant in the silt-sized (<100 μm) fraction but surprisingly was recovered even in the >0.25 mm size fraction.

The most significant finding of this study, however, is the identification of Zn-rich ferrochromite and chromian magnetite with >2 wt.% ZnO as a usefull and resistant indicator mineral for mineralized rocks in the TNB. It was also recovered from the till samples at the mine sites, but was not found in samples from unmineralized areas. Extremely variable Ni content (from low values of <2000 ppm to e high values of >6000 ppm) in forsteritic olivine (>Fo80) can also be used as an indication of metamorphosed magmatic Ni-deposits. The abundance of fresh olivine in till over and

east of the TNB suggests that it is derived from unweathered rocks within and east of the TNB.

Substantial amounts of metamorphic forsteritic olivine, Cr-diopside, and chromite found in till east of the TNB and in the central and southern TNB are most likely derived from highly metamorphosed ultramafic rocks located east of the TNB in the granulite-facies Pikwitonei domain just westW of the Cuthbert Lake dyke. Chromium-bearing corundum and rutile found together with sapphirine in the same samples confirms derivation from high-grade metamorphic mafic to ultramafic rocks, and suggests that till was transported from the Pikwitonei into the TNB.

The identification of very Cr-rich Cr-diopside (>1.4 wt.% Cr_2O_3) in till as being derived from granulite-facies metamorphosed crustal ultramafics rather than kimberlite-derived mantle xenoliths raises the question of the usefulness of Cr-diopside as a kimberlite indicator mineral in highly metamorphosed terranes.

The area west of the TNB and south of Osik Lake displays a multi-mineral Ni-Cu indicator mineral signature similar to the deposits in the TNB and indicates that this area warrant further investigation.

The re-examination in this study of archived heavy mineral concentrates, originally collected in support of kimberlite exploration, demonstrates the value of archiving heavy mineral concentrates for further study as commodity priorities shift (in this case to magmatic Ni-Cu), and indicator mineral picking methods and expertise evolve to include other deposit types. Archived samples offer a low-cost means to evaluate the exploration potential of exploration targets. However, for archived samples to be of value, metadata about the samples must also be archived.

The GSC's consistent use of the same commercial heavy mineral processing lab offered the significant advantage of being able to merge and directly compare indicator mineral data sets from Matile and Thorleifson (1997), McMartin et al. (2012), and this study.

ACKNOWLEDGEMENTS

Regional till sampling across the TNB in 2005 and 2006 was a collaborative effort between the GSC and the MGS. GSC funding was provided under the Targeted Geoscience Initiative 3 (2005-2010). Funding for the 2005 field season was provided by CAMIRO Project 04E01 and MGS. J. Macek, MGS, is thanked for providing a thorough and enthusiastic field trip of the bedrock geology of the TNB and assisting with bedrock sampling. N. Branson, MGS, provided field logistical support. M. Doherty (ALS Chemex) and T. Lane (CAMIRO) assisted with the planning and sampling in 2005. G. Budulan, U. of Ottawa, provided able field assistance in 2005 and 2006. Vale (Inco at the time of sampling) is thanked for providing access, confidential information, and samples from the Thompson, Pipe, and Birchtree deposits and regional ultramafic rocks, as well as field personnel to assist with the sampling. In particular we thank the following Inco staff for their assistance: S. Mooney, R. Stewart, C. Pike, H. Mahoney, D. Hanson, and D. Sorensen. W. Coker and C. Benn (BHP Billiton) are thanked for providing advice on sampling and mineral picking strategies as CAMIRO project sponsor input. Page layout for this publication was completed by E. Ambrose. A. Plouffe (GSC) provided comments that have improved the manuscript.

REFERENCES

Ames, D.E., McClenaghan, M.B., and Averill, S., 2007. Footwall-hosted Cu-PGE (Au, Ag), Sudbury Canada: towards a new exploration vector, *In* Exploration 07, Exploration in the New Millennium, Proceedings of the Fifth Decennial International Conference on Mineral Exploration, p. 1013-1017.

Arima, M. and Barnett, R.L., 1984. Sapphirine-bearing granulites from the Sipiwesk Lake area of the late Archean Pikwitonei granulite terrain, Manitoba, Canada; Contributions to Mineralogy and Petrology, v. 88, p. 102-112.

Arndt, N.T., Naldrett, A., and Pyke, D.R., 1977. Komatiitic and iron-rich tholeiitic lavas of Munro Township, northeast Ontario; Journal of Petrology, v. 18, p. 319-369.

Arnold, R.G. and Malik, O.P., 1974. Violarite in some nickel ores from Lynn Lake and Thompson, Manitoba and Sudbury, Ontario, Canada; Canadian Mineralogist, v. 12, p. 320-326.

Averill, S.A. 2001. The application of heavy indicator mineralogy in mineral exploration with emphasis on base metal indicators in glaciated metamorphic and plutonic terrains, *In* Drift Exploration in Glaciated Terrain, (eds.) M.B. McClenaghan, P.T. Bobrowsky, G.E.M. Hall, and S.J. Cook; Geological Society of London, Special Publication 185, p. 69-81.

Averill, S.A., 2006. Ni-Cu-PGE and other indicator minerals in CAMIRO bedrock and till samples, Thompson Ni Belt, Manitoba, Appendix 5 *In* CAMIRO Report 1, March 2006.

Averill, S.A., 2007. Recent advances in base metal Indicator mineralogy: an update from Overburden Drilling Management Limited; EXPLORE, Newsletter of the Association of Applied Geochemists, No. 134, p. 2-6.

Averill, S.A., 2009. Useful Ni-Cu-PGE versus kimberlite indicator minerals in surficial sediments: similarities and differences, *In* Application of Till and Stream Sediment Heavy Mineral and Geochemical Methods to Mineral Exploration in Western and Northern Canada, (eds.) R.C. Paulen and I. McMartin; Geological Association of Canada, Short Course Notes 18, p. 125-139.

Averill, S.A., 2011. Viable indicators in surficial sediments for two major base metal deposit types: Ni-Cu-PGE and porphyry Cu; Geochemistry: Exploration, Environment, Analysis, v. 11, p. 279-291.

Bajc, A.F., 2000. Results of regional till sampling in the western part of the Shebandowan greenstone Belt, northwestern Ontario; Ontario Geological Survey, Open File Report 6012.

Bajc, A.F. and Hall, G.E.M., 2000. Geochemical responses of surficial media, north and East Ranges, Sudbury Basin; Ontario Geological Survey, Open File Report 6033, 265 p.

Barnes, S., 2000. Chromite in komatiites, II: modification during green schist to mid-amphibolite facies metamorphism; Journal of Petrology, v. 41, no. 3, p. 387-409.

Barnett, P.J., 2007 Overburden geochemical signature of the Lac des Iles platinum group element deposit, northwestern Ontario, Canada; Canadian Journal of Earth Sciences, v. 44, p. 1151-1168.

Barnett, P.J. and Averill, S.A., 2010. Heavy mineral dispersal trains in till in the area of the Lac des Iles deposit, northwestern Ontario, Canada; Geochemistry: Exploration, Environment, Analysis, v. 10, p. 391-399.

Bleeker, W., 1990. New structural-metamorphic constraints on Early Proterozoic oblique collision along the Thompson nickel belt, Manitoba, Canada, *In* The Early Proterozoic Trans-Hudson Orogen of North America, (eds.) J.F. Lewry and M.R. Stauffer; Geological Association of Canada, Special Paper 37, p. 57-73.

Bleeker, W. and Macek, J. ,1988 Thompson Nickel Belt Project: Pipe Pit Mine, In Report of Activities 1988; Manitoba Energy and Mines, p. 111-115.

Bleeker, W. and Macek, J., 1996. Evolution of the Thompson nickel belt, Manitoba: setting of Ni-Cu deposits in the western part of the Circum Superior Boundary zone; Geological Association of Canada/Mineralogical Association of Canada, Field Trip Guidebook A1, 44 p.

Burnham, O.M, Halden, N., Layton-Matthews, D., Lesher, M., Liwanag, J., Heaman, L., Hulbert, L., Machado, N., Michalak, D., Pacey, M., Peck, D.C., Potrel, A., Theyer, P., Toope, K., and Zwanzig, H., 2009. CAMIRO Project 97E-02, Thompson Nickel Belt: Final report March 2002, revised and updated June 2003. Manitoba Geological Survey, Open File 2008-11.

Cabri, L.J., 1981. The platinum group minerals, *In* Platinum-Group Elements: Mineralogy,Geology, Recovery, (ed.) L.J. Cabri; Canadian Institute of Mining and Metallury, Special Volume 23, p. 83-150.

Cabri, L.J. and Laflamme, J.H.G., 1981. Analyses of mineral containing platinum group elements, *In* Platinum-Group Elements: Mineralogy, Geology, Recovery, (ed.) L.J. Cabri; Canadian Institute of Mining and Metallurgy, Special Publication 23, p. 151-173.

Chen, Y., Fleet, M.E., and Pan, Y., 1993. Platinum-group minerals and gold in arsenic-rich ore at the Thompson Mine, Thompson Nickel Belt, Manitoba, Canada; Mineralogy and Petrology, v. 49, p. 127-146.

Chen, Y., Fleet, M.E., and Zang, W., 1997. Mineral chemistry of spinel from the Thompson nickel deposit, Thompson, Manitoba, In Program with Abstracts; Geological Association of Canada, Mineralogical Association of Canada, Canadian Geophyiscal Union, Joint Annual Meeting, p. 25-26.

Chen, Y. and Zang, W., 2004. The Thompson nickel deposit of Canada: zinc-rich spinels from ultramafic rocks and the nickel sulphide ores, *In* Mineralogy and Geochemistry: Resources, Environment and Life, (eds.) S. Li, J. Shen, and H. Xu; Geological Publishing House, p. 201-212.

Coker, W.B. and DiLabio, R.N.W., 1989. Geochemical exploration in glaciated terrain: geochemical responses, *In* Proceedings of Exploration '87, (ed.) G.D. Garland; Ontario Geological Survey, Special Volume 3, p. 336-383.

Coker, W.B., Dunn, C.E., Hall, G.E.M., Rencz, A.N., DiLabio, R.N.W., Spirito, W.A., and Campbell, J.E., 1991. The behavior of platinum group elements in the surficial environment at Ferguson Lake, N.W.T., Rottenstone Lake, Sask., and Sudbury, Ont., Canada; Journal of Geochemical Exploration, v. 40, p. 165-192.

Cook, S.J. and Fletcher, W.K., 1992. Distribution and behaviour of platinum in soils of the Tulameen ultramafic complex, southern British Columbia, Canada; British Columbia Geological Survey Branch, Paper 1992-6.

Deer, W.A., Howie, R.A., and Zussman, J., 1978. Rock-Forming Minerals, Volume 2A, Single-Chain Silicates, 2nd edition; Longman Group Ltd., London, 668 p.

Deer, W.A., Howie, R.A., and Zussman, J., 1997. Rock-Forming Minerals, Volume 1A Orthosilicates, 2nd edition; The Geological Society, London, 919 p.

de Saboia, L.A., 1978. The West Manasan and the Pipe Mine 2 ultramafic bodies of the Thompson Nickel Belt; M.Sc. thesis, University of Western Ontario.

DiLabio R.N.W. and Kaszycki, C.A., 1988. An ultramafic dispersal train and associated gold anomaly in till near Osik Lake, Manitoba, *In* Current Research, Part C; Geological Survey of Canada, Paper 88-1C, p. 67-71.

Dredge, L.A. and Nixon, F.M. 1992. Glacial and environmental geology of northeastern Manitoba; Geological Survey of Canada, Memoir 432.

Dredge, L A, Nixon, F M., and Richardson, R J., 1986. Quaternary geology and geomorphology of northwestern Manitoba; Geological Survey of Canada, Memoir 418, 38 p.

Dyke, A.S., 2004. An outline of North American deglaciation with emphasis on central and northern Canada, *In* Quaternary Glaciations - Extent and Chronology, Part II: North America, (eds.) J. Ehlers and P.L. Gibbard; Development in Quaternary Science Series, Elsevier B.V., p. 373-424.

Dyke, A.S., Moore, A., and Robertson, L., 2003. Deglaciation of North America; Geological Survey of Canada, Open File 1574, 1 CD-ROM.

Fipke, C.E., Gurney, J.J., and Moore, R.O., 1995. Diamond exploration techniques emphasizing indicator mineral geochemistry and Canadian examples; Geological Survey of Canada, Bulletin 423.

Fraser, H.S., 1985. A journey north: the great Thompson nickel discovery; Inco Ltd., 338 p.

Green, D.H., Nicholls, I.A., Viljoen, M., and Viljoen, R., 1975. Experimental demonstration of the existence of peridotite liquids in earliest Archaean magmatism; Geology, v. 3, p. 11-14.

Groves, D.I., Barrett, F.M., Binns, R.A., and McQueen, K.G., 1977. Spinel phases associated with metamorphosed volcanic-type iron-nickel sulfide ores from Western Australia; Economic Geology, v. 72, p. 1224-1244.

Groves, D.I., Barrett, F.M., and Brotherton, R.H., 1983. Exploration significance of chrome-spinels in mineralized ultramafic rocks and nickel-copper ores; Geological Society of South Africa, Special Publication 7, p. 1224-1244.

Heaman, L.M., Machado, N., Krogh, T.E., and Weber, W., 1986. Precise U–Pb zircon ages for the Molson dyke swarm and the Fox River sill: Constraints for Early Proterozoic crustal evolution in northeastern Manitoba, Canada; Contributions to Mineralogy and Petrology, v. 4, p. 82-89.

Heiman, A., Spry, P.G., and Teale, G.S., 2005. Zincian spinel associated with metamorphosed Proterozoic base-metal sulphide occurrence, Colorado: a re-evaluation of gahnite composition as a guide in exploration; The Canadian Mineralogist, v. 43, p. 601-622.

Hood, C., and McCandless, T.E., 2004. Systematic variations in xenocryst mineral compositions at the province scale, Buffalo Hills kimberlites, Alberta, Canada; Lithos, v. 77, p. 733-748.

Huhta, P. and Peltonen P., 1994. Occurrence and mineral chemistry of chrome spinels in till - implications for prospecting magmatic Ni-Cu-ores in the Vammala Ni-Belt, SW Finland; Tenth Prospecting in Areas of Glaciated Terrain, Abstract Volume, p. 27-29.

Hutchinson, M.T., Nixon, P.H., and Harley, S.L., 2004. Corundum inclusions in diamonds - discriminatory criteria and corundum compositional dataset; Lithos, v. 77, p. 273-286.

Kaszycki, C.A., 1989. Surficial geology and till composition, northwestern Manitoba; Geological Survey of Canada, Open File 2118.

Klassen, R.W., 1986. Surficial geology of north-central Manitoba; Geological Survey of Canada, Memoir 419.

Layton-Matthews, D., Lesher, C. M., Burnham, O. M., Liwanag, J., Halden, N.M., Hulbert, L., and Peck, D.C.; 2007. Magmatic Ni-Cu-platinum group element deposits of the Thompson Nickel Belt, *In* Mineral Deposits of Canada: A Synthesis of Major Deposit Types, District Metallogeny, the Evolution of Geological Provinces, and Exploration Methods, (ed.) W.D. Goodfellow; Geological Association of Canada, Special Publication 5, p. 409-432.

Layton-Matthews, D., Lesher, C.M., Burnham, O.M., Hulbert, L., Peck, D.C., Golightly, J.P., and Keays, R.R., 2010. Exploration for komatiite-associated Ni-Cu-(PGE) mineralization in the Thompson Nickel Belt, Manitoba, Chapter 27 *In* Zinc-Lead, Nickel-Copper-PGE, and Uranium, (eds.) R.J. Goldfarb, E.E. Marsh, and T. Monecke; Society of Economic Geology, Special Publication 15, v. II, p. 513-538.

Liu, X, Zhou, H., Ma, Z., and Chang, L., 1998. Chrome-rich clinopyroxene from orthopyroxenite from Maowu, Dabie mountains, central China: a second record and its implications for petrogenesis; The Island Arc, v. 7, p. 135.

Liwanag, J., 2001. Post-magmatic modification of the sulphide deposits from the Thompson nickel belt, Manitoba, Canada; M.Sc. thesis, University of Manitoba, 207 p.

Macek, J.J., Zwanzig, H.V., and Pacey, M., 2006. Thompson Nickel Belt geological compilation map, Manitoba (parts of NTS 63G, J, O, P and 64A and B); Manitoba Geological Survey, Open File 2006-33, 1 CD-ROM.

Matile, G.L.D. and Thorleifson, L.H., 1997. Till geochemical and indicator mineral reconnaissance of northeastern Manitoba; Manitoba Energy and Mines, Open File 97-3.

McClenaghan, M.B., 2005. Indicator mineral methods in mineral exploration; Geochemistry: Exploration, Environment, Analysis, v. 5, p. 233-245.

McClenaghan, M.B. and Kjarsgaard, B.A., 2007. Indicator mineral and surficial geochemical exploration methods for kimberlite in glaciated terrain, examples from Canada, *In* Mineral Resources of Canada: A Synthesis of Major Deposit Types, District Metallogeny, the Evolution of Geological Provinces and Exploration Methods, (ed.) W.D. Goodfellow; Geological Association of Canada, Special Publication No. 5, p. 983-1006.

McClenaghan, M.B., Matile, G., Layton-Matthews, D., and Pyne, M., 2009a. Till geochemical signatures of magmatic Ni-Cu deposits and regional till geochemistry, Thompson Nickel Belt, Manitoba; Geological Survey of Canada, Open File 6005, CD-ROM.

McClenaghan, M.B., Averill, S.A., Kjarsgaard, I.M., Layton-Matthews, D., and Matile, G. 2009b. Till indicator mineral and geochemical signatures of magmatic Ni-Cu deposits, Thompson Nickel Belt, central Canada, in Proceedings of the 24th IAGS; Association of Applied Geochemists, p. 75-78.

McClenaghan, M.B., Thorleifson, L.H., and DiLabio, R.N.W., 2000. Till geochemical and indicator mineral methods in mineral exploration; Ore Geology Reviews, v. 16, p. 145-166.

McClenaghan, M.B., Kjarsgaard, I.M., Averill, S.A., Layton-Matthews, D., Crabtree, D., and Matile, G., 2012. Indicator mineral signatures of magmatic Ni-Cu deposits, Thompson Nickel Belt, Manitoba: Part 1-bedrock data; Geological Survey of Canada, Open File 6766, CD-ROM.

McClenaghan, M.B., Layton-Matthews, D., and Matile, G., 2011. Till geochemical signatures of magmatic Ni-Cu deposits, Thompson Nickel Belt, Manitoba, Canada; Geochemistry: Exploration, Environment, Analysis, v. 11, p. 145-159.

McMartin, I., Henderson, P.J., Nielsen, E., and Campbell, J.E., 1996. Surficial geology, till and humus composition across the Shield margin, north-central Manitoba and Saskatchewan: geospatial analysis of a glaciated environment; Geological Survey of Canada, Open File 3277.

McMartin, I., Campbell, J.E., and Dredge, L.A., 2012. A trans-jurisdictional database of till composition across theCircum-Kissynew area, Manitoba and Saskatchewan; Geological Survey of Canada, Open File 7064.

McMartin, I., Campbell, J.E., Dredge, L.A., and Robertson, L., 2010a. Digital compilation of ice-flow indicators for central Manitoba and Saskatchewan: datasets, digital scalable maps and 1:500 000 scale generalized map; Geological Survey of Canada, Open File 6405.

McMartin, I., Dredge, L.A., and Robertson, L., 2010b. Ice flow record and carbonate dispersal at the confluence of Hudsonian and Keewatin ice, north-central Manitoba: new results from the Quaternary; Manitoba Mining & Minerals Convention, Abstracts: Manitoba Innovation, Energy and Mines, Mineral Resources Division, p. 52-53.

Nimis, P. and Taylor, W.R., 2000. Single clinopyroxene thermobarometry for garnet peridotites. Part I. Calibration and testing of a Cr-in-Cpx barometer and an enstatite-in-Cpx thermometer; Contributions to Mineralogy and Petrology, v. 139, p. 541-554.

Paktunc, A.D., 1983. Petrology and geochemistry of some ultramafic rocks of the Thompson Nickel Belt and the Cuthbert Lake dykes of the Pikwitonei region, northern Manitoba; Ph.D. thesis, University of Ottawa.

Paktunç, A.D. ,1984. Metamorphism of the ultramafic rocks of the Thompson Mine, Thompson Nickel Belt, northern Manitoba; Canadian Mineralogist, v. 22, p. 77-91.

Paktunç, A.D. ,1987. Differentiation of the Cuthbert ultramafic dikes and related mafic dikes; Contributions to Mineralogy and Petrology, v. 97, p. 405-416.

Paktunç, A.D. and Baer, A.J., 1986. Geothermobarometry of the northwestern margin of the Superior Province; Journal of Geology, v. 94, p. 381-394.

Paktunç, A.D. and Cabri, L.J., 1995. A proton- and electron-microprobe study of gallium, nickel and zinc distribution in chromian spinel; Lithos, v. 35, p. 261-282.

Pavlov, N.V. and Grigor'eva, I.I., 1977. Deposits of chromium, *In* Ore Deposits in the USSR, (ed.) V.E. Smirnov; Pitman Publications, London, v. 1, p. 179-236.

Peltonen, P. and Lamberg, P., 1991. Chromian spinel in Svecofennian ultramafic intrusions: compositional evolution during fractional crystallization, cooling, regional metamorphism and alteration; Geological Survey of Finland, Special Paper 12, p. 23-31.

Peredery, W.V. and Geological Staff, 1982. Geology and nickel sulphide deposits of the Thompson Nickel Belt, Manitoba, *In* Precambrian Sulphide Deposits, (ed.) R.W. Hutchinson; H.S. Robinson Memorial Volume; Geological Association of Canada, Special Paper 25, p. 165-209.

Prest, V.K., Donaldson, J.A., and Mooers, H.D., 2000. The omar story: the role of omars in assessing glacial history of west-central North America; Géographie physique et Quaternaire, v. 54, p. 257-270.

Quirt, D.H., 2004. Cr-diopside (clinopyroxene) as a kimberlite indicator mineral for diamond exploration in glaciated terranes, *In* Summary of Investigations 2004, Volume 2; Saskatchewan Geological Survey, Miscellaneous Report 2004-4.2, Paper A-10, 14 p.

Renner, R., Nisbet, E.G., Cheadle, M.J., Arndt, N.T., Bickle, M.J., and Cameron, W.E., 1994. Komatiite flows from the Reliance Formation, Belingwe Belt, Zimbabwe. I. Petrography and Mineralogy; Journal of Petrology, v. 35, p. 361-400.

Sage, R.P., 2000. Kimberlites of the Lake Timiskaming Structural Zone, Supplement; Ontario Geological Survey, Open File Report 5937, 123 p.

Searcy, C.A., 2001. Preliminary data results of drift exploration for platinum group elements, northwestern Ontario; Ontario Geological Survey, Open File Report 6054.

Sobolev, V.S., Sobolev, N.V., and Lavrent'ev, Y.G., 1975. Chrome-rich clinopyroxene from the kimberlites of Yakutia; Neues Jahrbuch für Mineralogie, Abhandlungen, v. 123, p. 213-218.

Thorleifson, L.H., 1996. Review of Lake Agassiz history: sedimentology, geomorphology and history of the central Lake Agassiz basin, *In* Field Trip Guidebook B2; Geological Association of Canada - Mineralogical Association of Canada, Joint Annual Meeting, Winnipeg, Manitoba, May 27–29, 1996, p. 56-79.

Thorleifson, L.H. and Garrett, R.G., 1993. Prairie kimberlite study-till matrix geochemistry and preliminary indicator mineral data; Geological Survey of Canada, Open File 2745.

Tiainen, M., Lahtinen, R., and Salminen, R., 1991. Similarity analysis applied to till geochemical data from southwest Finland - geochemical signatures of Vammala and Kylmäkoski nickel deposits; Transactions of the Institute of Mining and Metallurgy, Section B, Applied Earth Sciences, v. 100, p. B209-B215.

Tsujimori, T. and Liou, J.G., 2004. Coexisting chromian omphacite and diopside in ultramafic schist from the Chugoku Mountains, SW Japan: the Cr effect on the omphacite-diopside immiscibility gap; American Mineralogist v. 89, p. 7-14.

Webster, R.B., 1973. Basal till investigations in the Thompson area; Inco Internal Report.

Zack, T. Van Eynatten, H., and Kronz, A., 2004. Rutile geochemistry and its potential use in quantitative provenance studies; Sedimentary Geology, v. 171, p. 37-58.

Zellerer, S., 2008. Paragenesis of ultramafic-hosted nickel-copper-PGE sulphide mineralization at the Minago Deposit, southern Thompson Nickel Belt, Manitoba; B.Sc. thesis, Carleton University, Ottawa.

Zwanzig, H.V., Macek, J.J., and McGregor, C.R. 2007. Lithostratigraphy and geochemistry of the high-grade metasedimentary rocks in the Thompson Nickel Belt and adjacent Kisseynew Domain, Manitoba: implications for nickel exploration; Economic Geology, v. 102, p. 1197-1216.

Zwanzig, H.V. and McRitchie, W.D., 1997. Revised stratigraphy of the Setting Lake area (parts of NTS 63O/1 and 2, and 63J/15), *In* Report of Activities; Manitoba Energy and Mines, p. 103-108.

APPENDIX A3. Till sample location information for 2005, 2006 samples collected in the Thompson deposit area as part of the case study, 2007 (MOB) samples collected by I. McMartin, and 1996 (TCA) archived samples re-examined in this study.

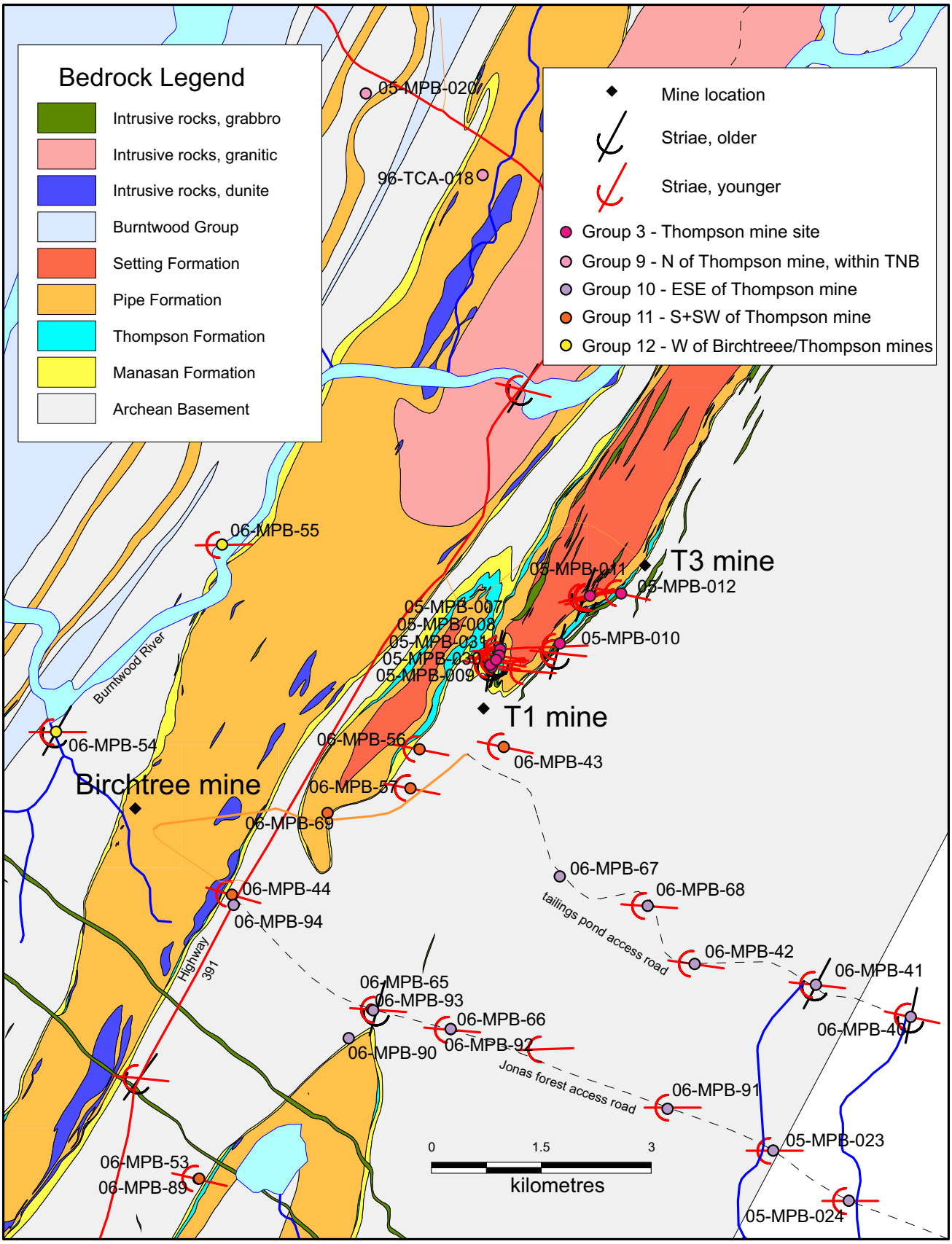

APPENDIX A4. Till sample location information for 2005, 2006 samples collected in the Pipe deposit area as part of the case study, 2007 (MOB) samples collected by I. McMartin, and 1996 (TCA) archived samples re-examined in this study.

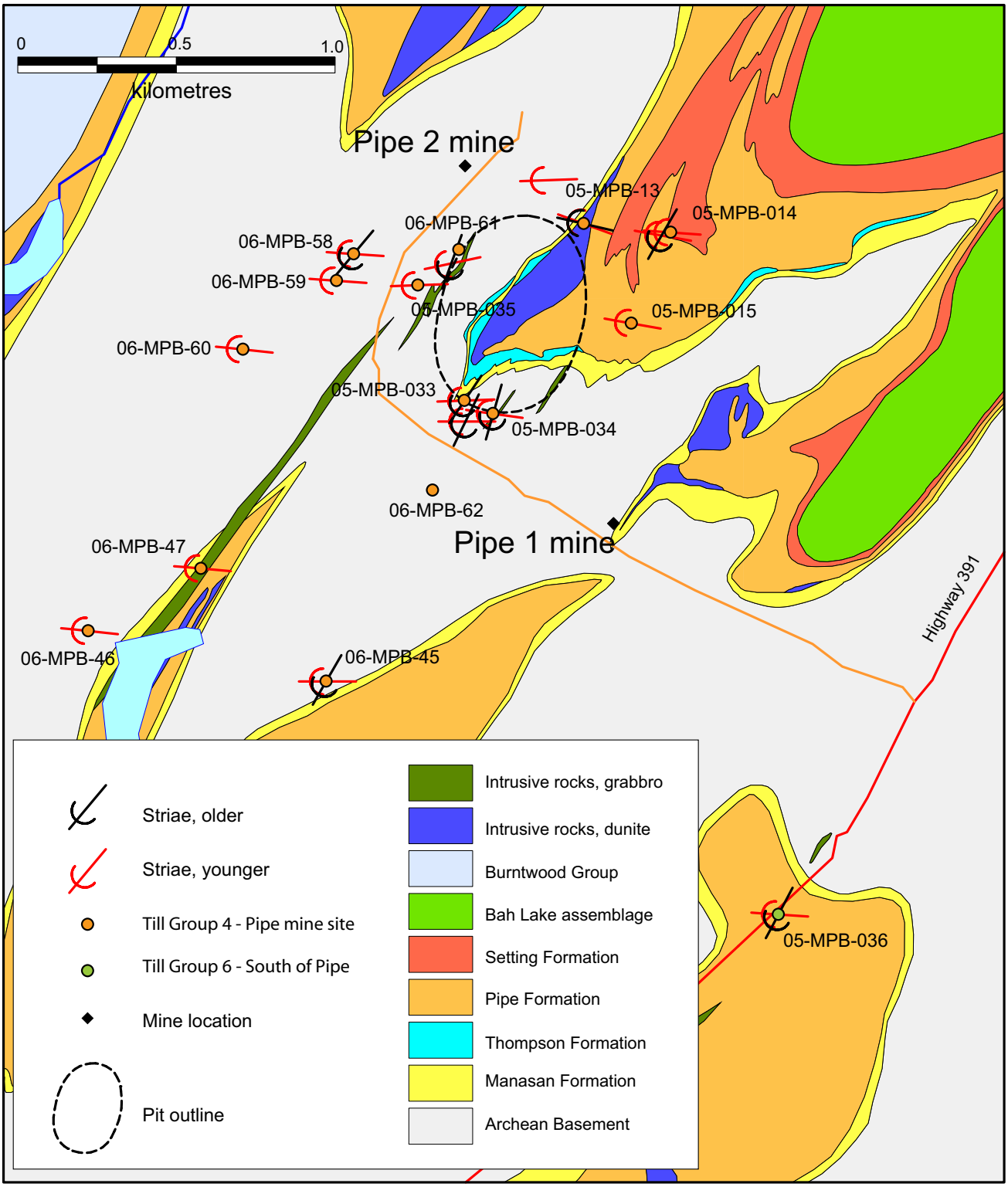

APPENDIX D1. Photographs of classified pebbles in the 0.5 to 5 cm pebble fraction of 2005 and 2006 till samples.

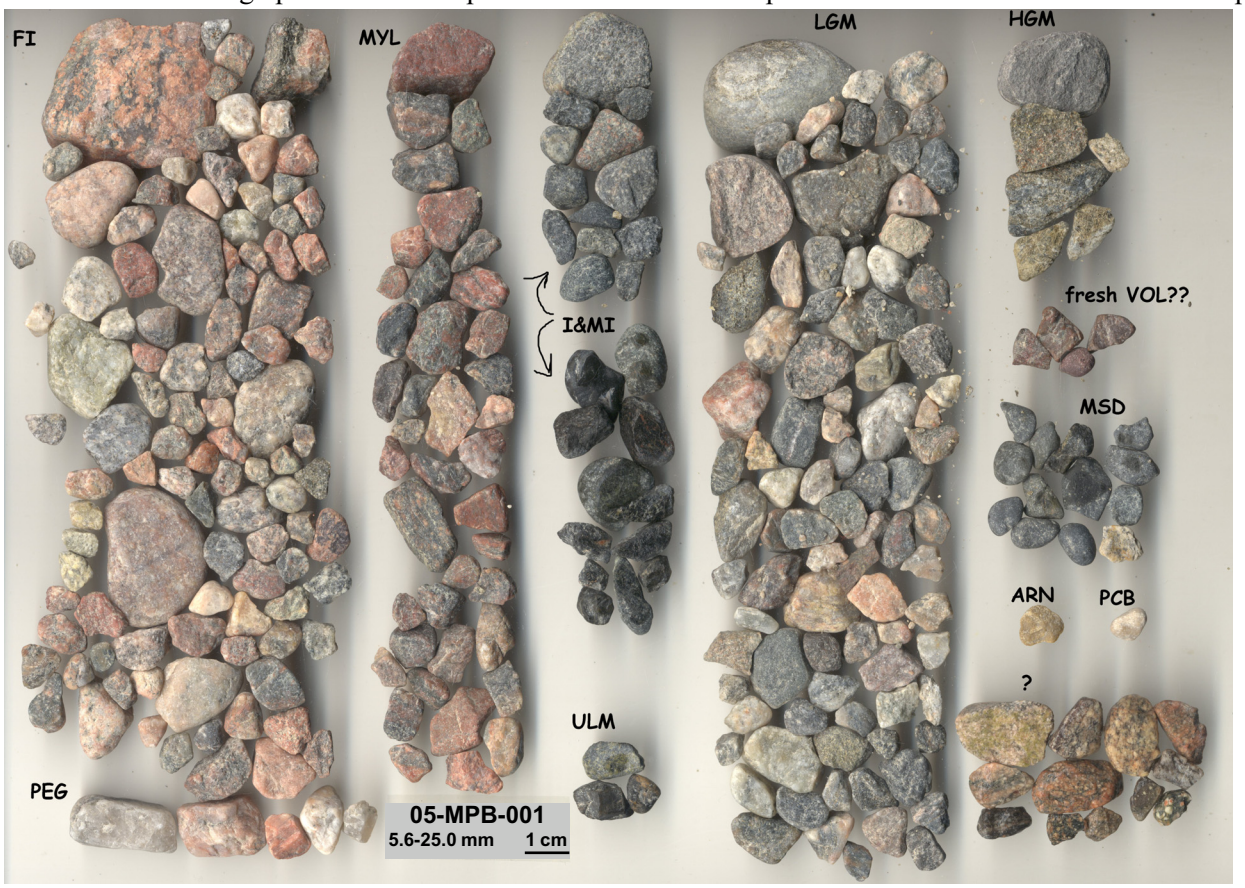

APPENDIX D1 continued.

APPENDIX D1 continued.

APPENDIX D1 continued.

APPENDIX D1 continued.

APPENDIX D1 continued.

APPENDIX D1 continued.

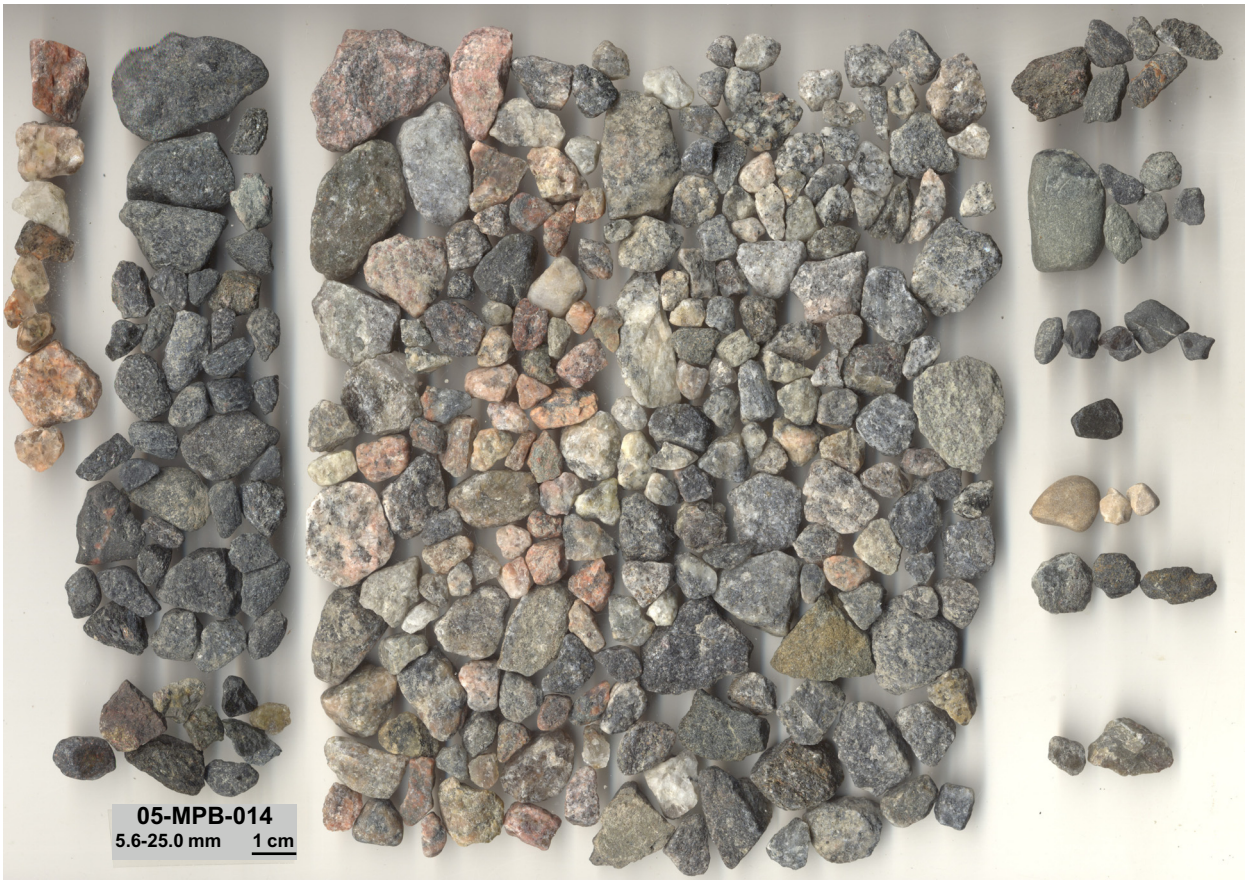

APPENDIX D1 continued.

APPENDIX D1 continued.

APPENDIX D1 continued.

APPENDIX D1 continued.

APPENDIX D1 continued.

APPENDIX D1 continued.

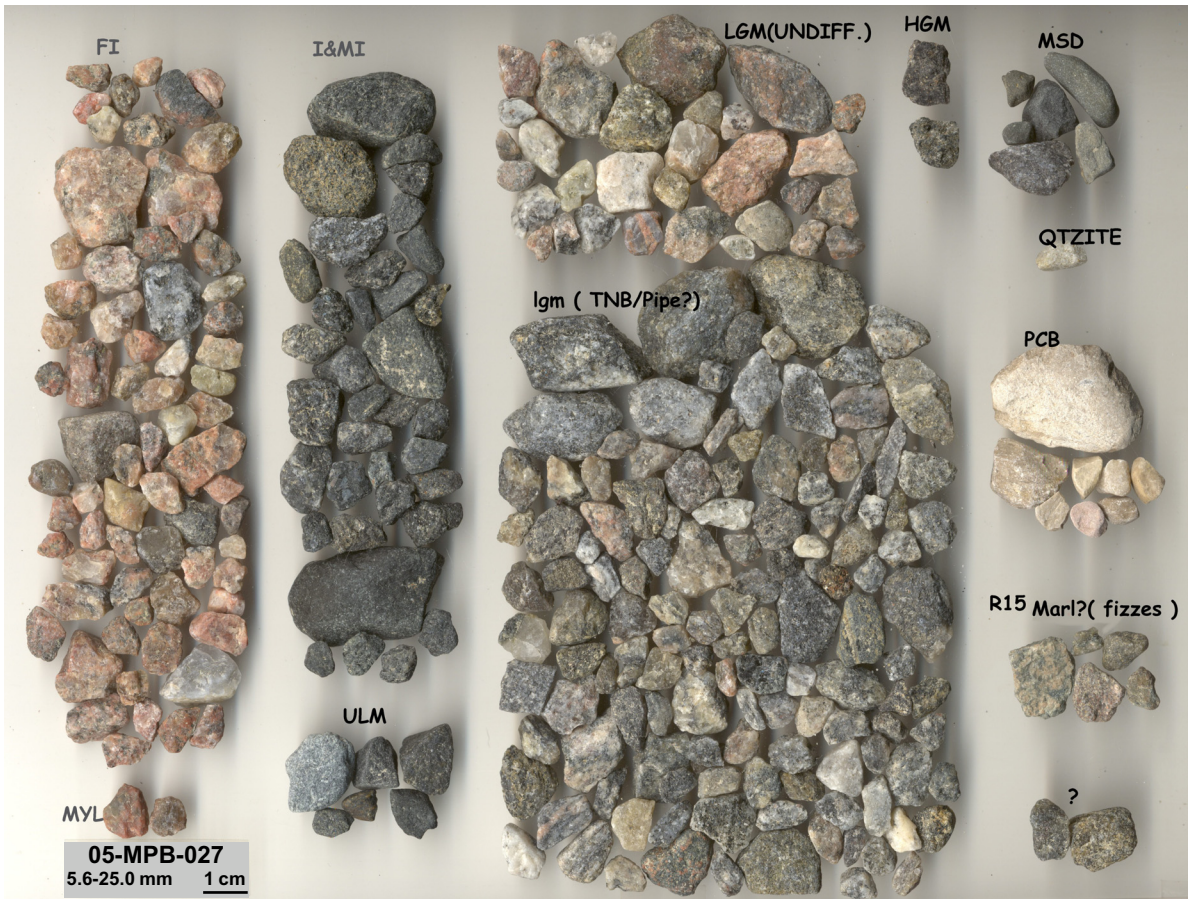

APPENDIX D1 continued.

APPENDIX D1 continued.

APPENDIX D1 continued.

APPENDIX D1 continued.

APPENDIX D1 continued.

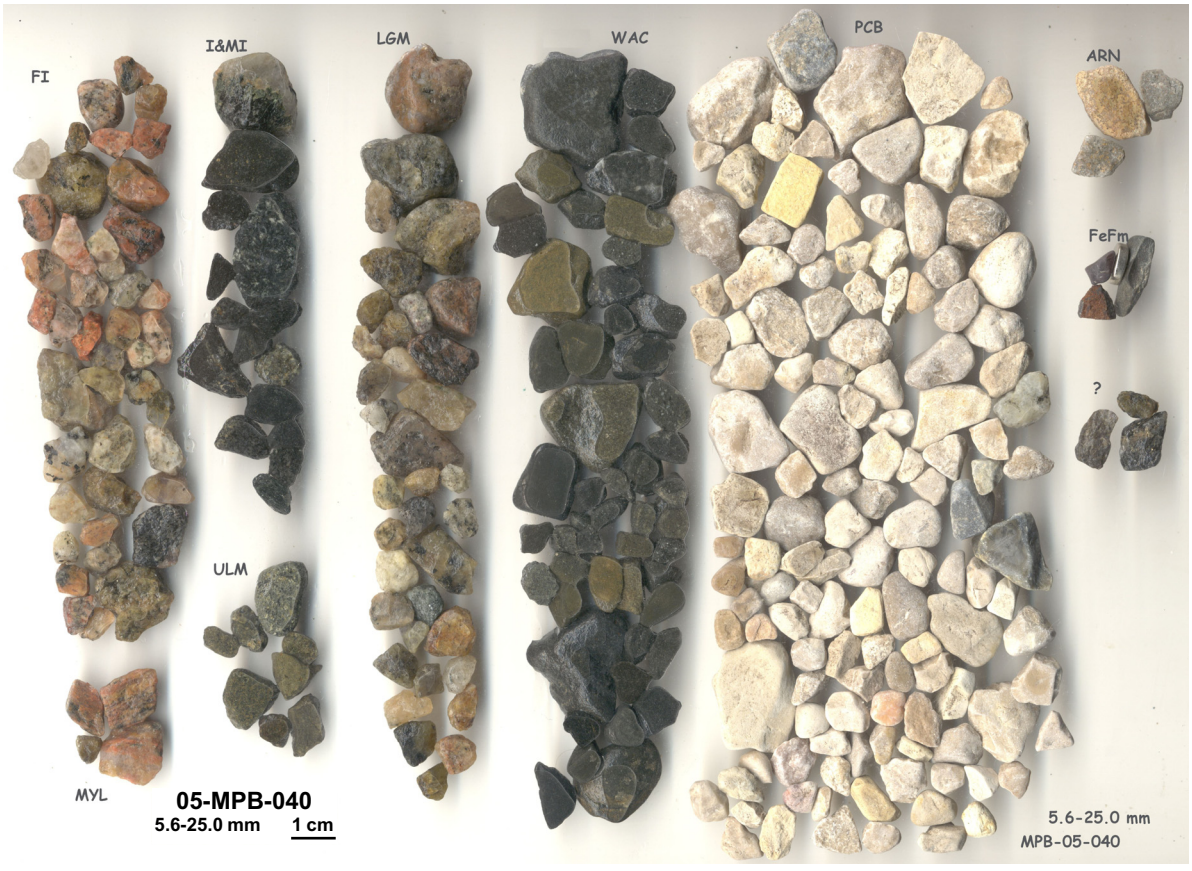

APPENDIX D1 continued.

APPENDIX D1 continued.

APPENDIX D1 continued.

APPENDIX D1 continued.

APPENDIX D1 continued.

APPENDIX D1 continued.

APPENDIX D1 continued.

APPENDIX D1 continued.

APPENDIX D1 continued.

APPENDIX D1 continued.

APPENDIX D1 continued.

APPENDIX D1 continued.

APPENDIX D1 continued.

APPENDIX D1 continued.

APPENDIX D1 continued.

APPENDIX D1 continued.

APPENDIX D1 continued.

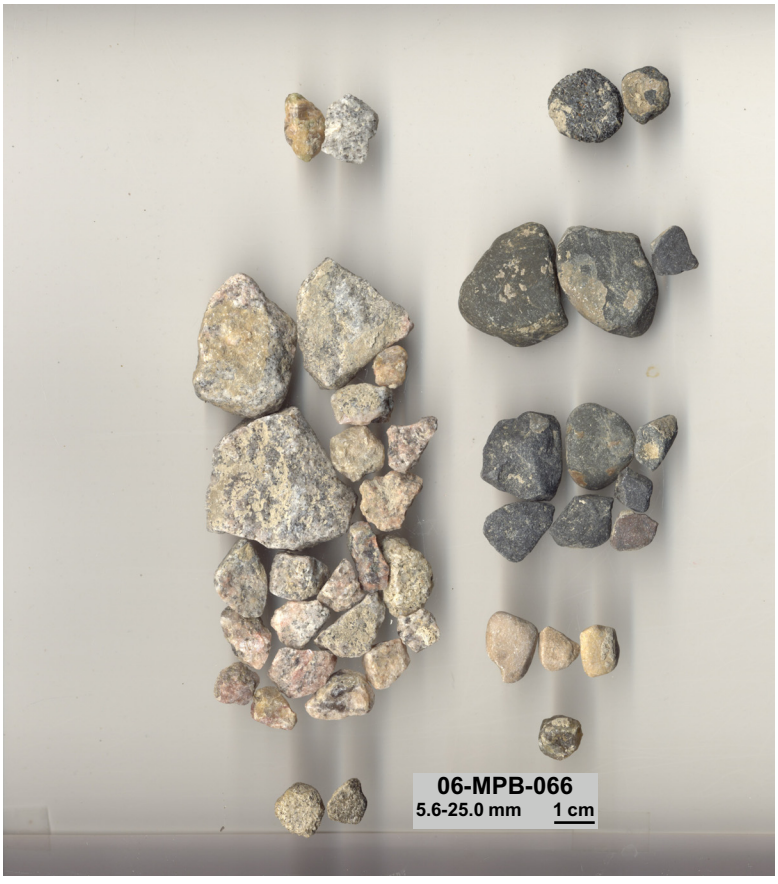

APPENDIX D1 continued.

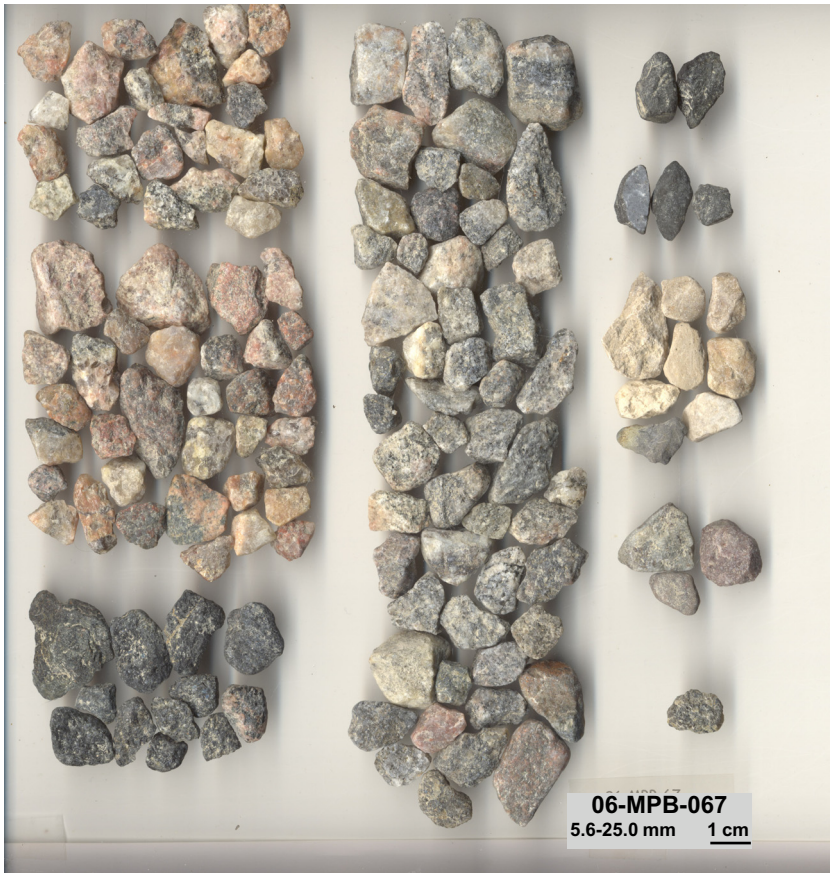

APPENDIX D1 continued.

APPENDIX D1 continued.

APPENDIX E. DISTRIBUTION MAPS FOR SELECTED INDICATOR MINERAL ABUNDANCES IN THE 1996, 2005, 2006, AND 2007 (MOB) TILL SAMPLES

Appendix E1. Regional distribution maps

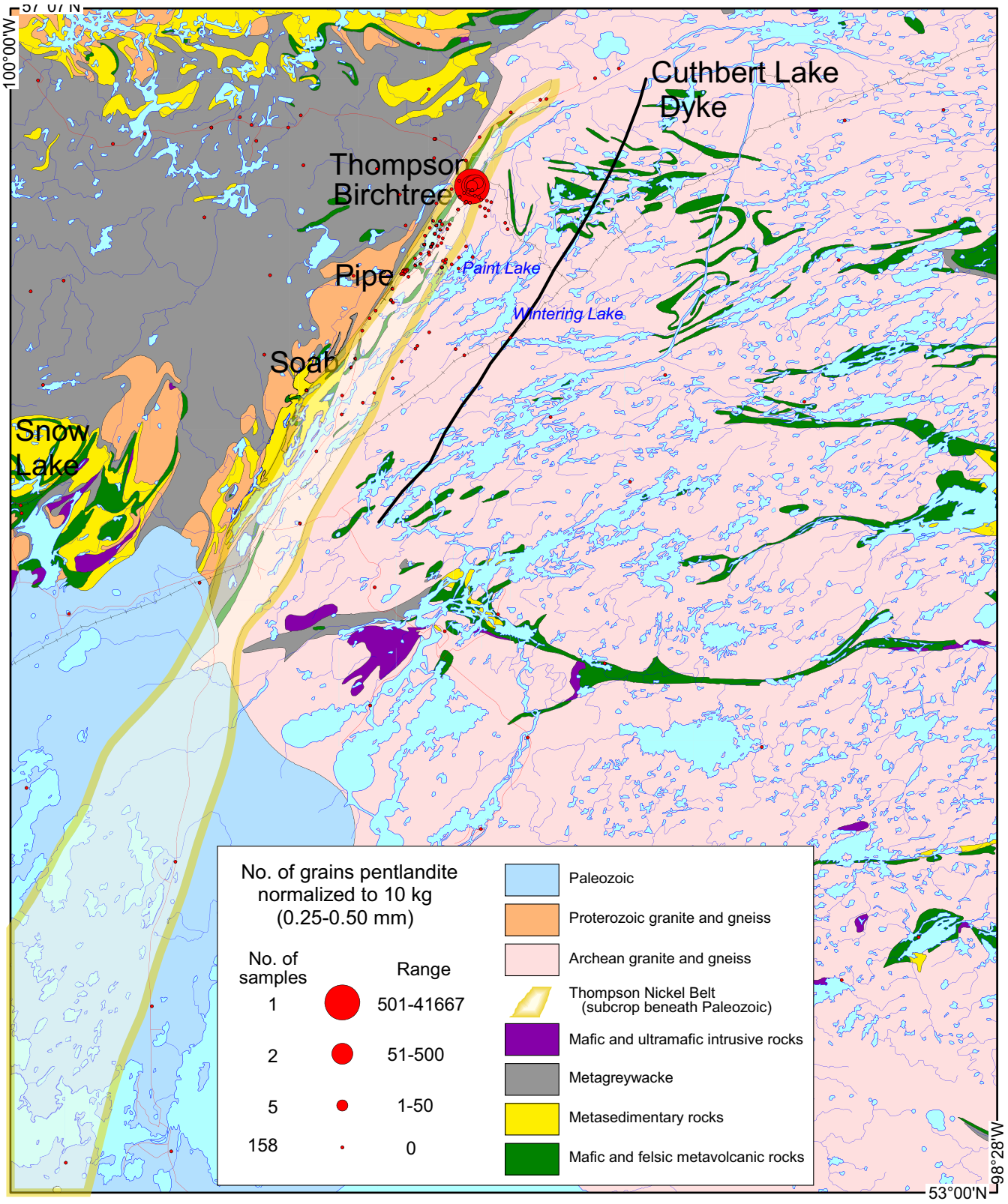

Appendix E1. Map 1, pentlandite.

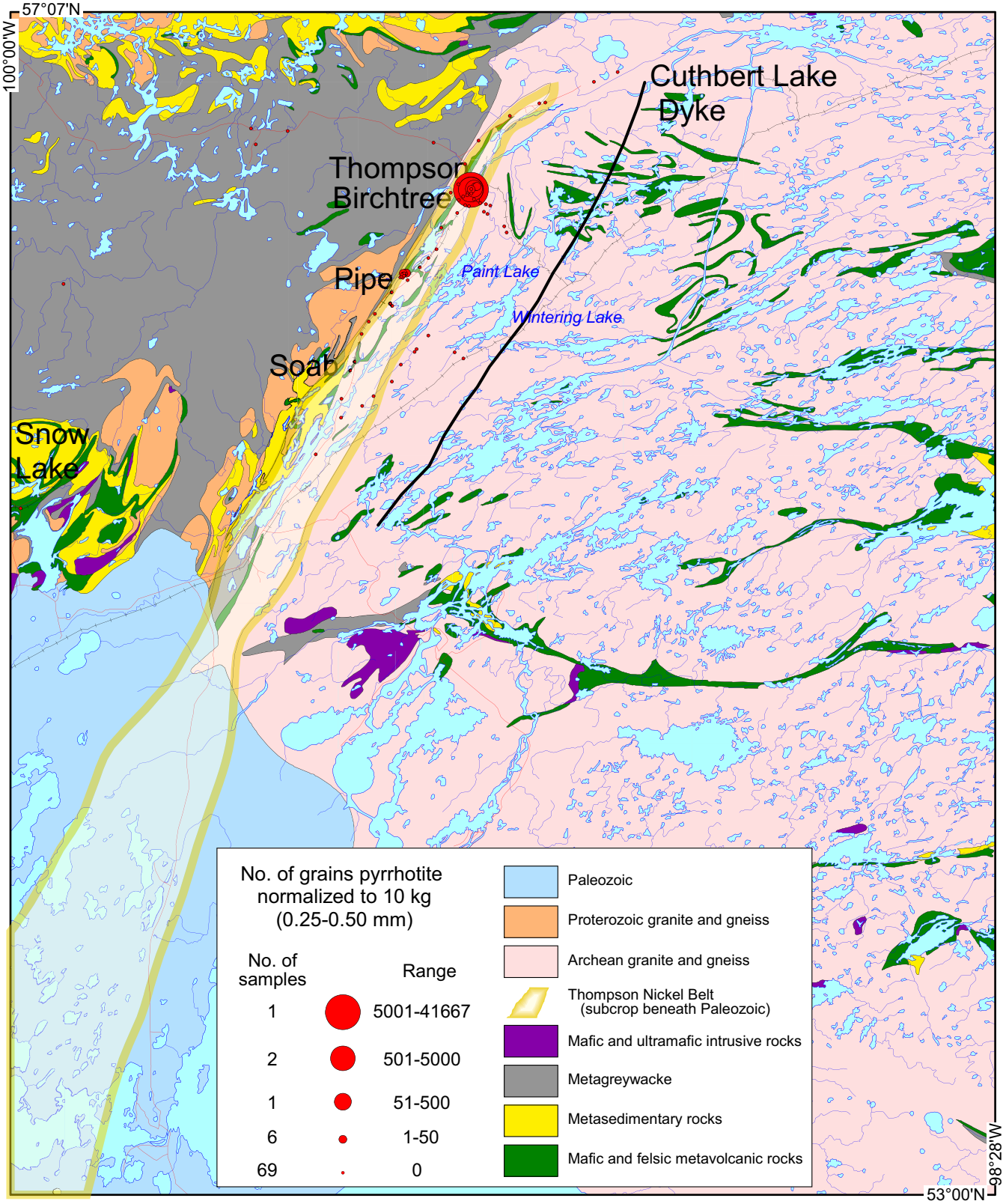

Appendix E1 continued. Map 2, pyrrhotite.

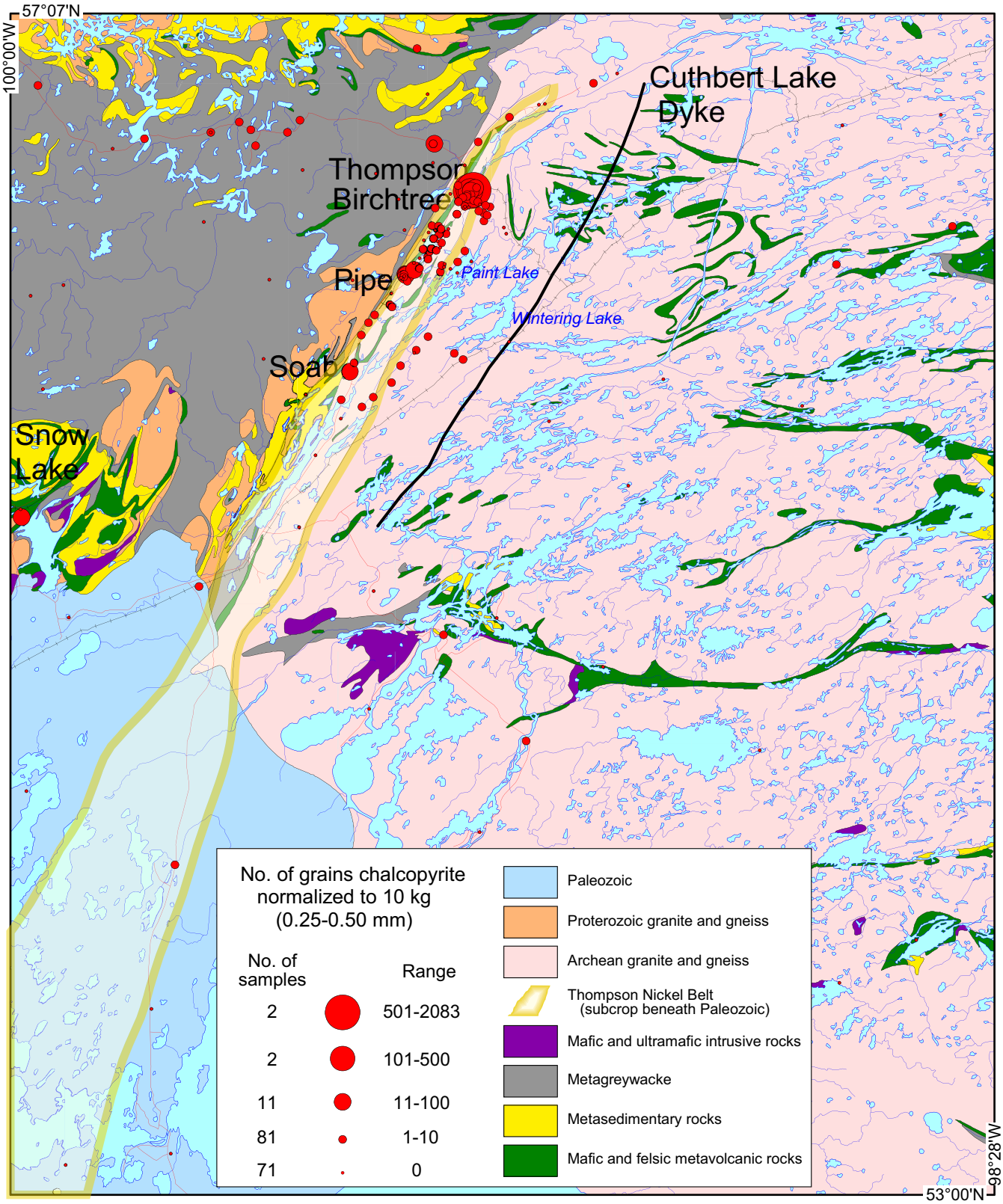

Appendix E1 continued. Map 3, chalcopyrite.

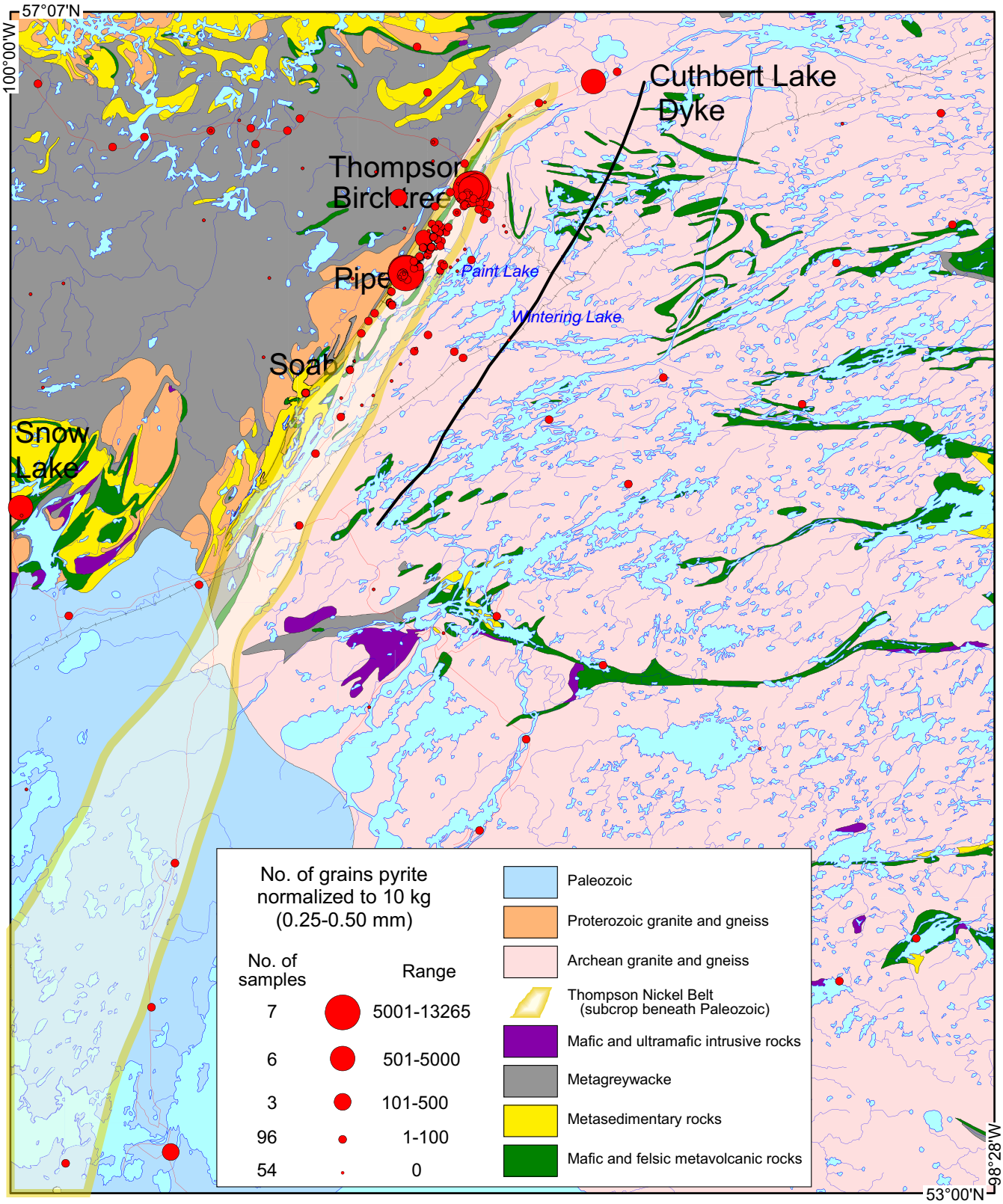

Appendix E1 continued. Map 4, pyrite.

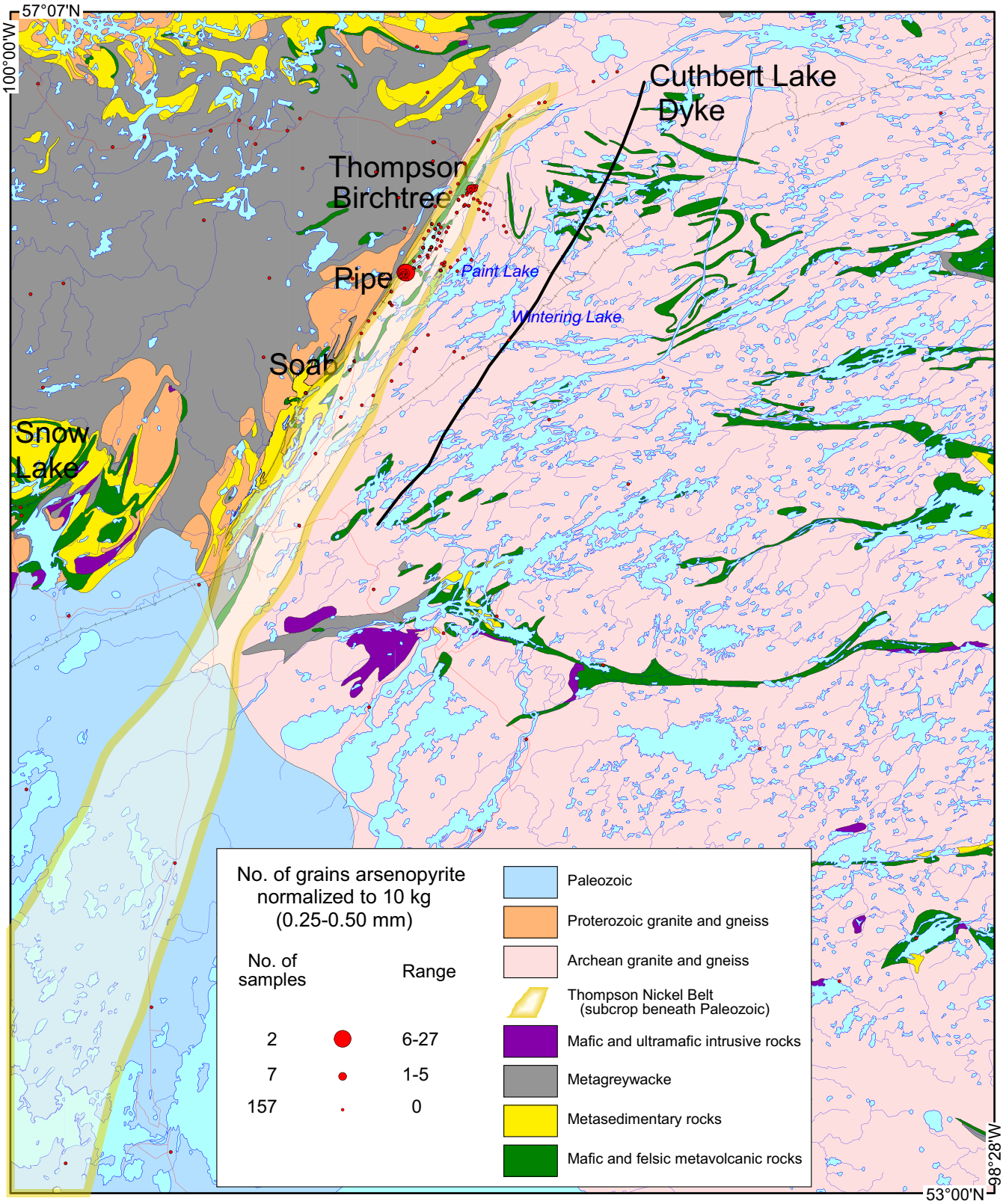

Appendix E1 continued. Map 5, arsenopyrite.

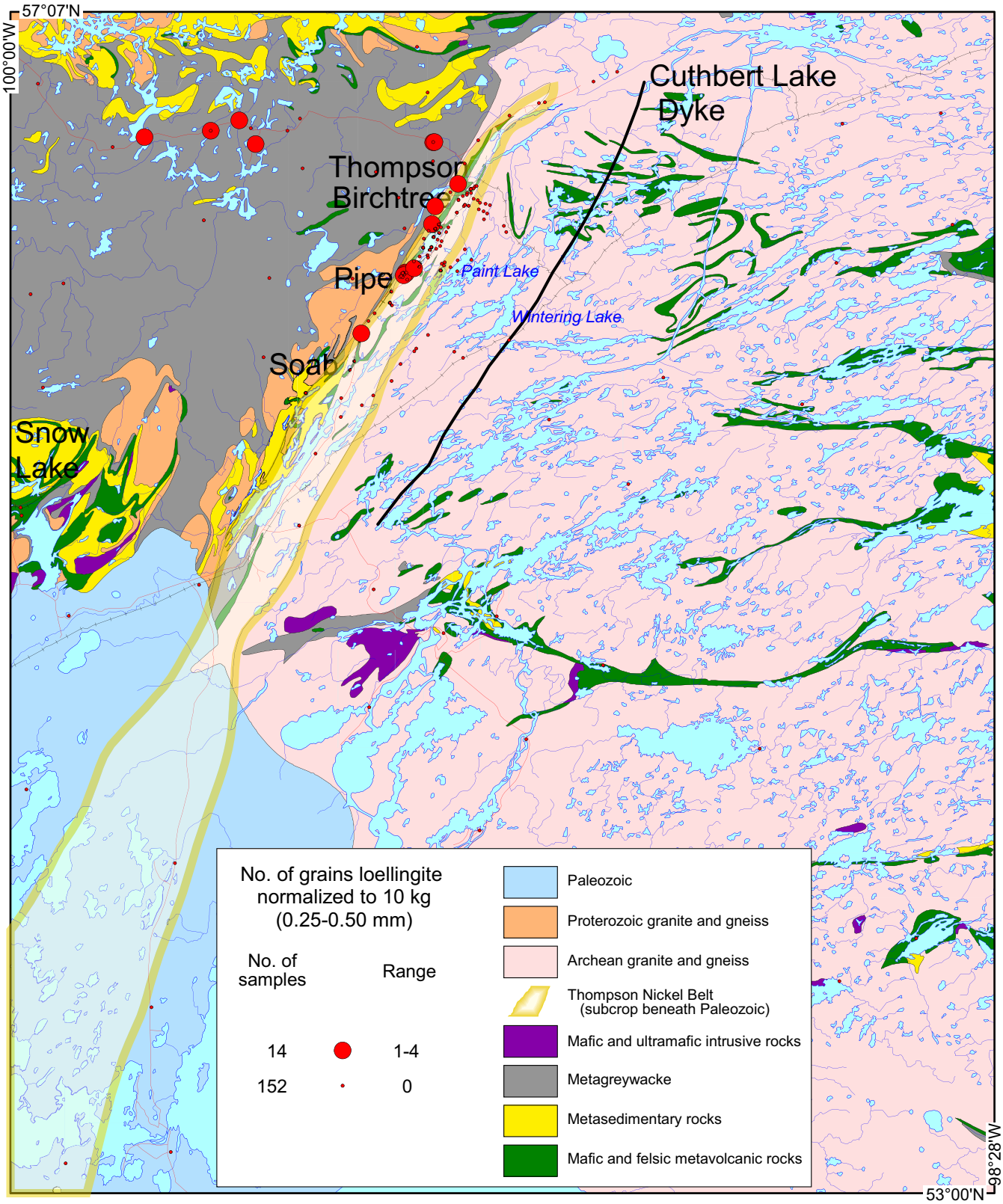

Appendix E1 continued. Map 6, loellingite.

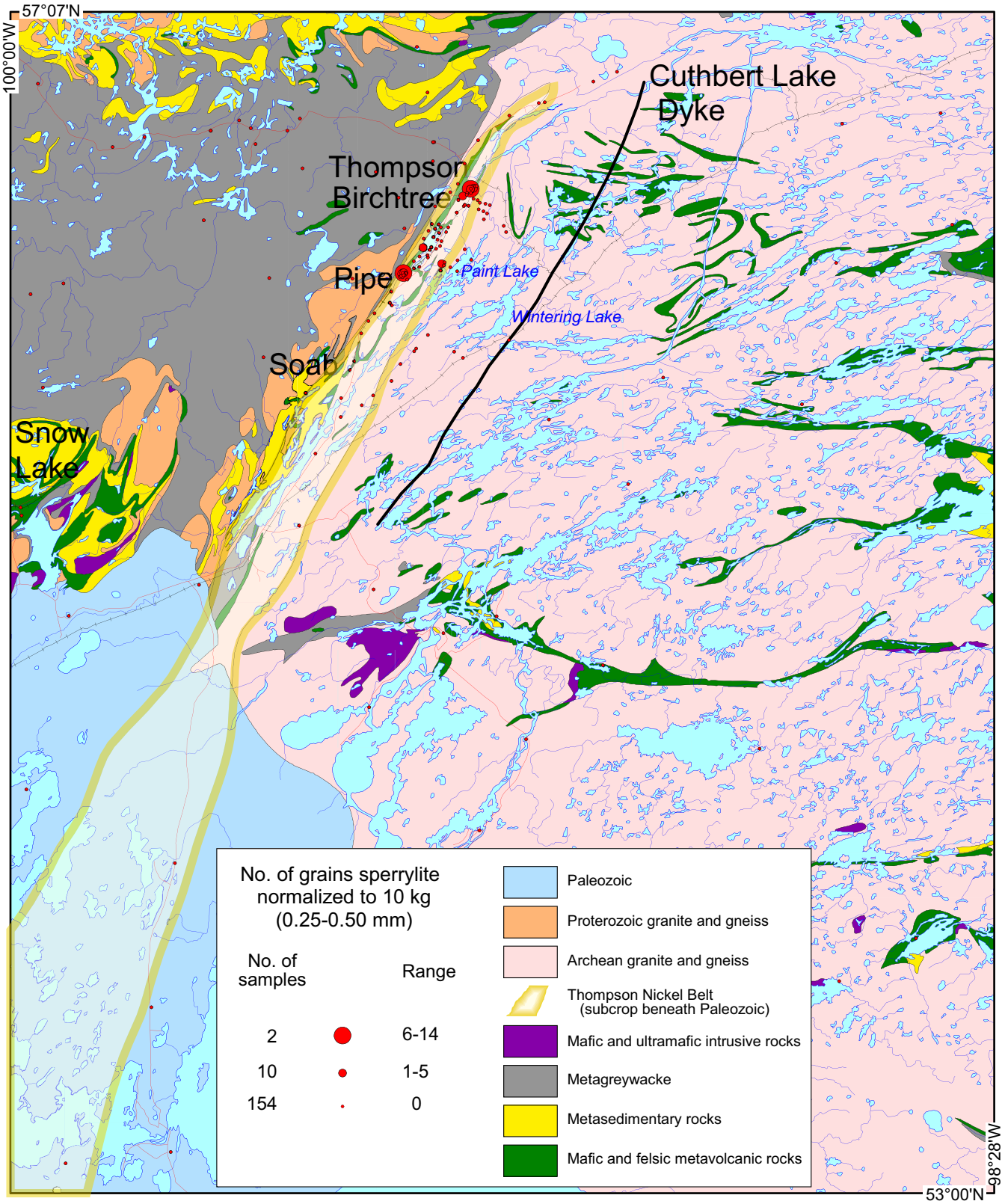

Appendix E1 continued. Map 7, sperrylite.

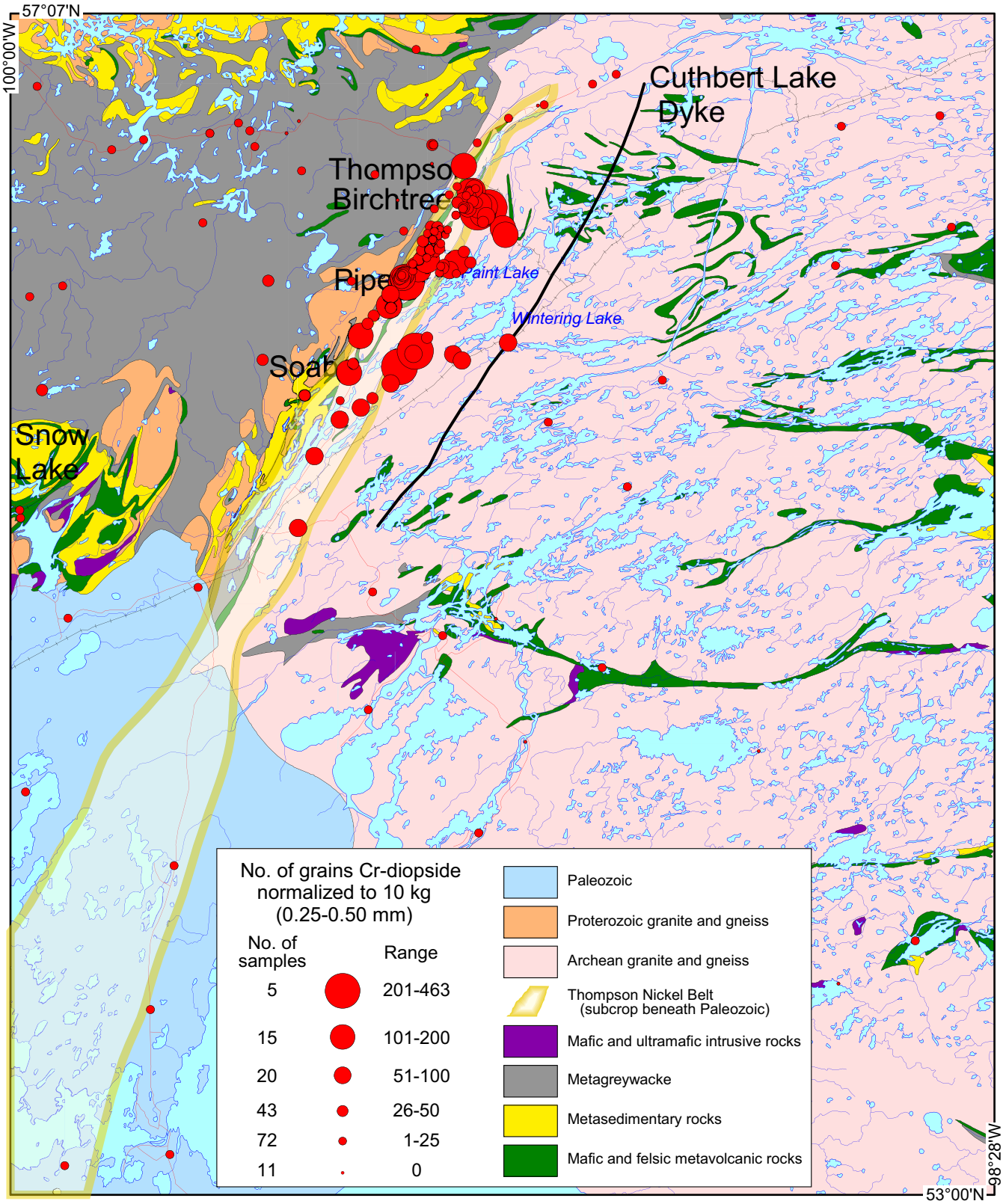

Appendix E1 continued. Map 8, total Cr-diopside.

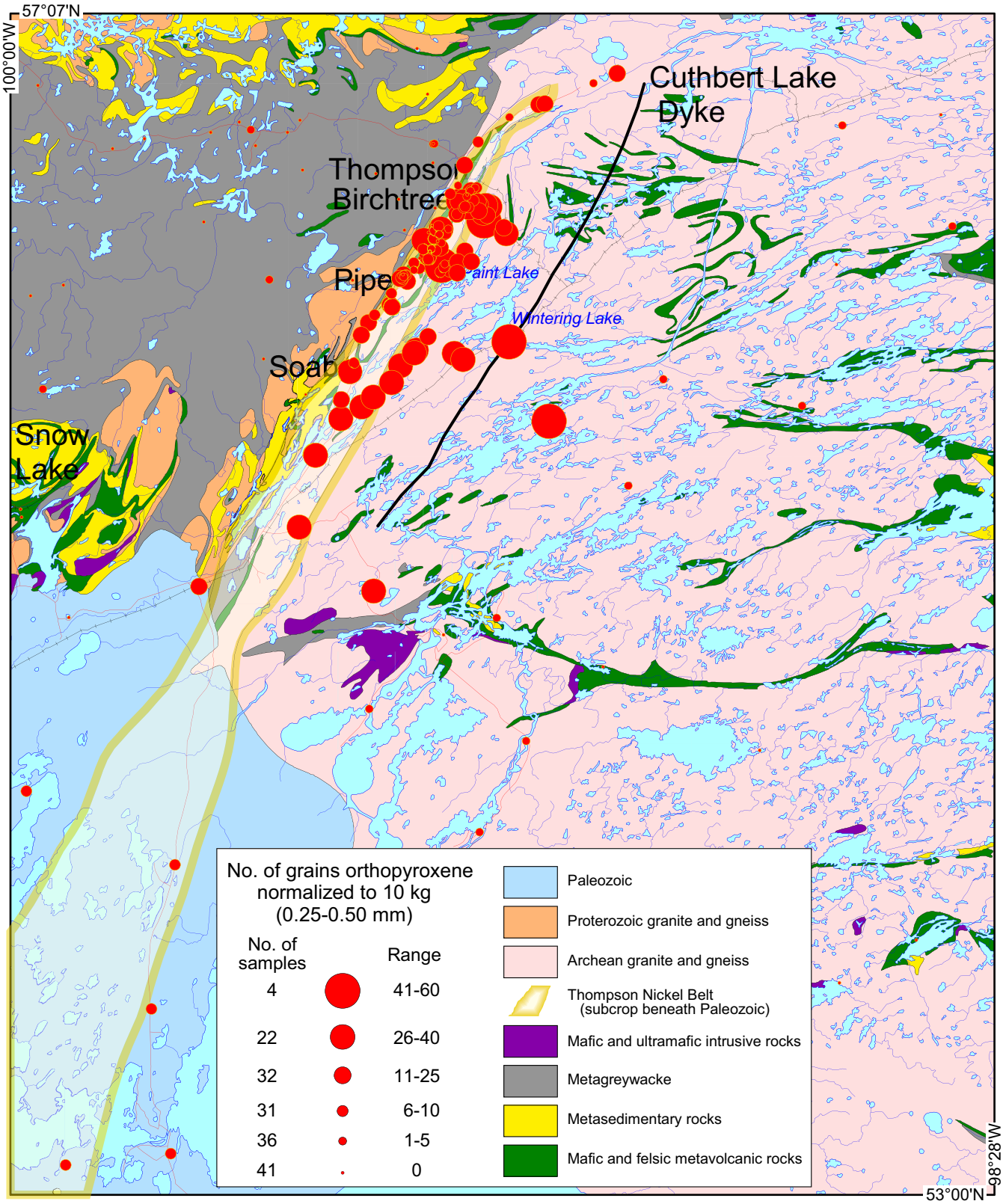

Appendix E1 continued. Map 9, orthopyroxene.

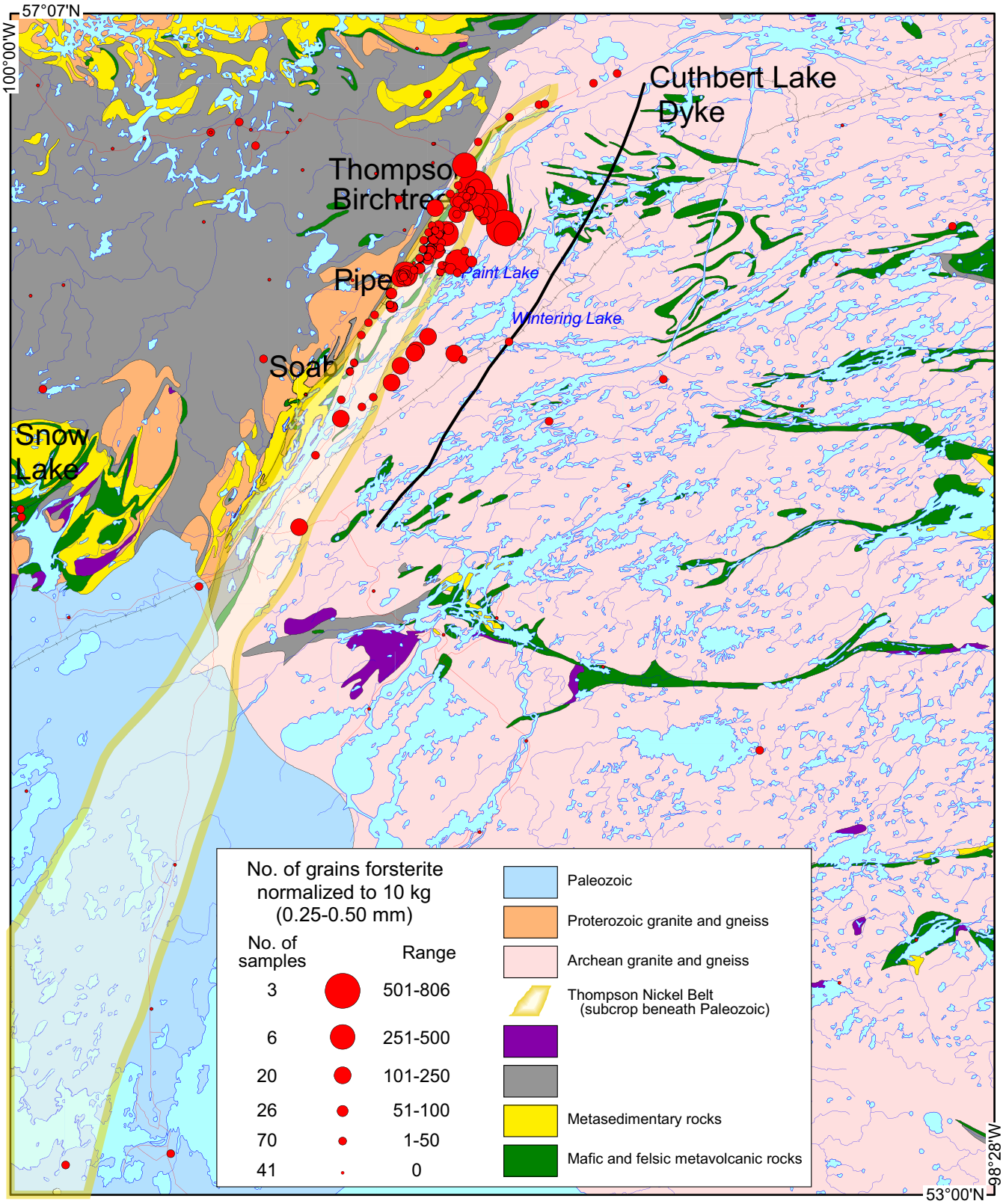

Appendix E1 continued. Map 10, forsterite.

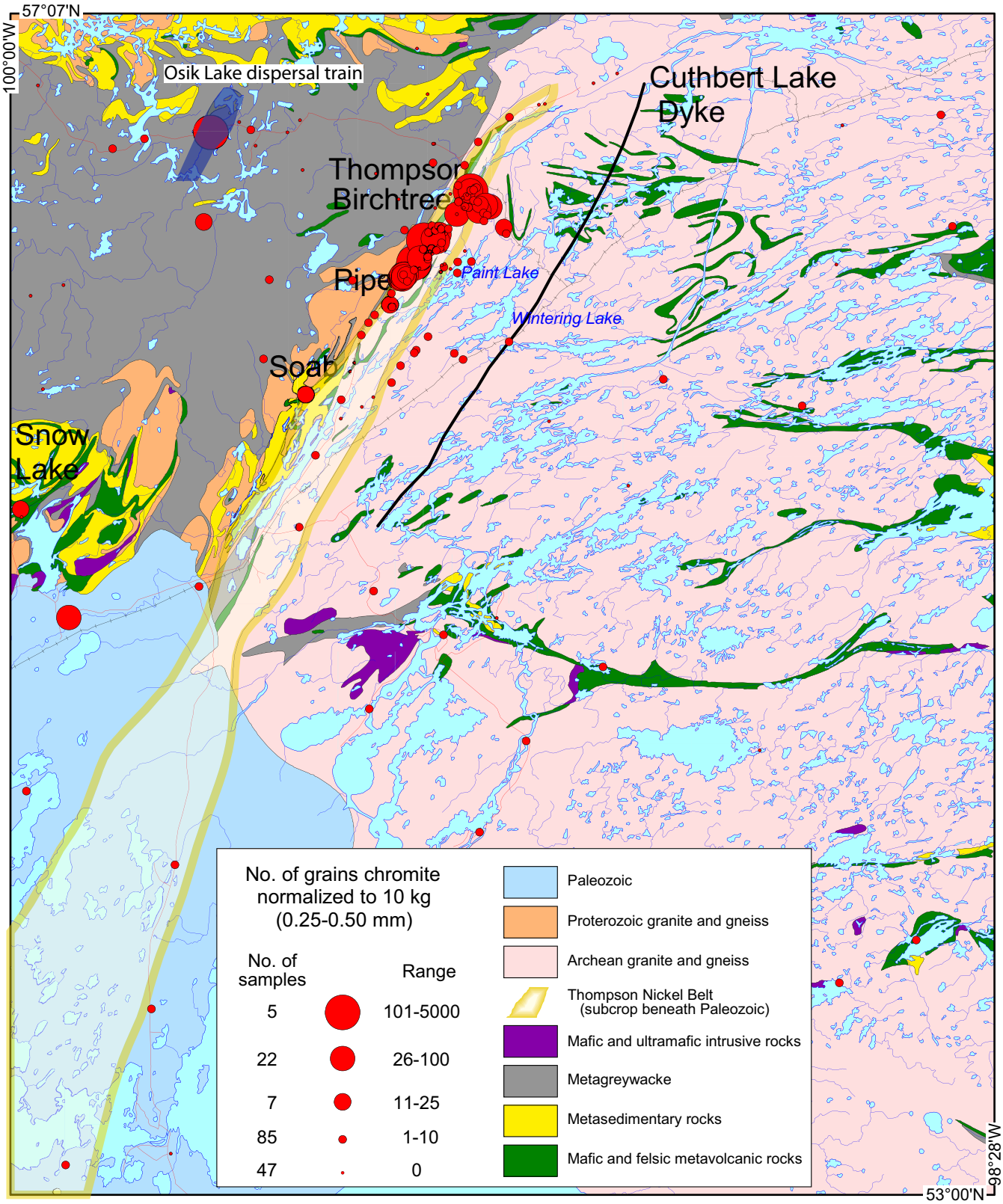

Appendix E1 continued. Map 11, chromite.

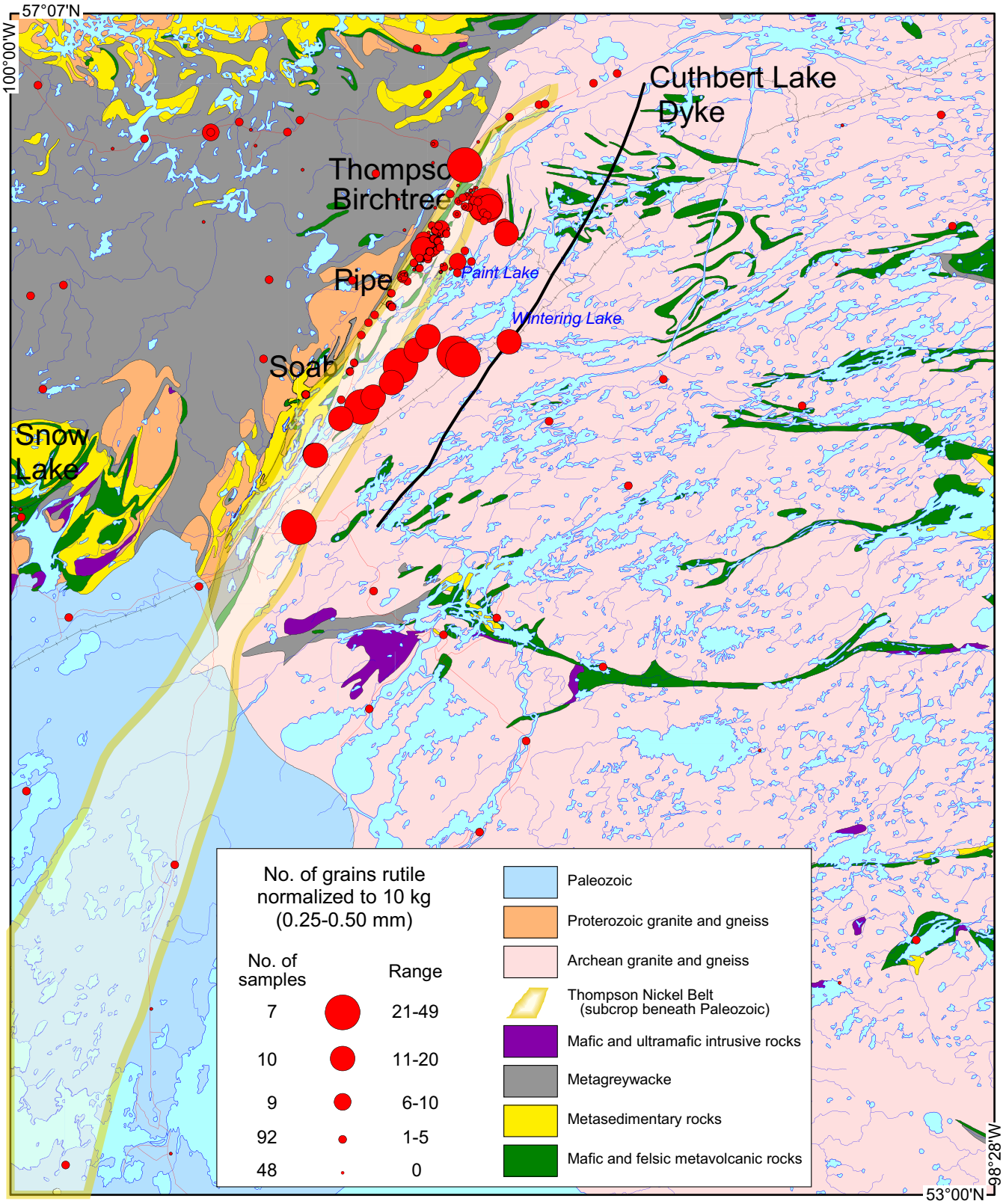

Appendix E1 continued. Map 12, red rutile.

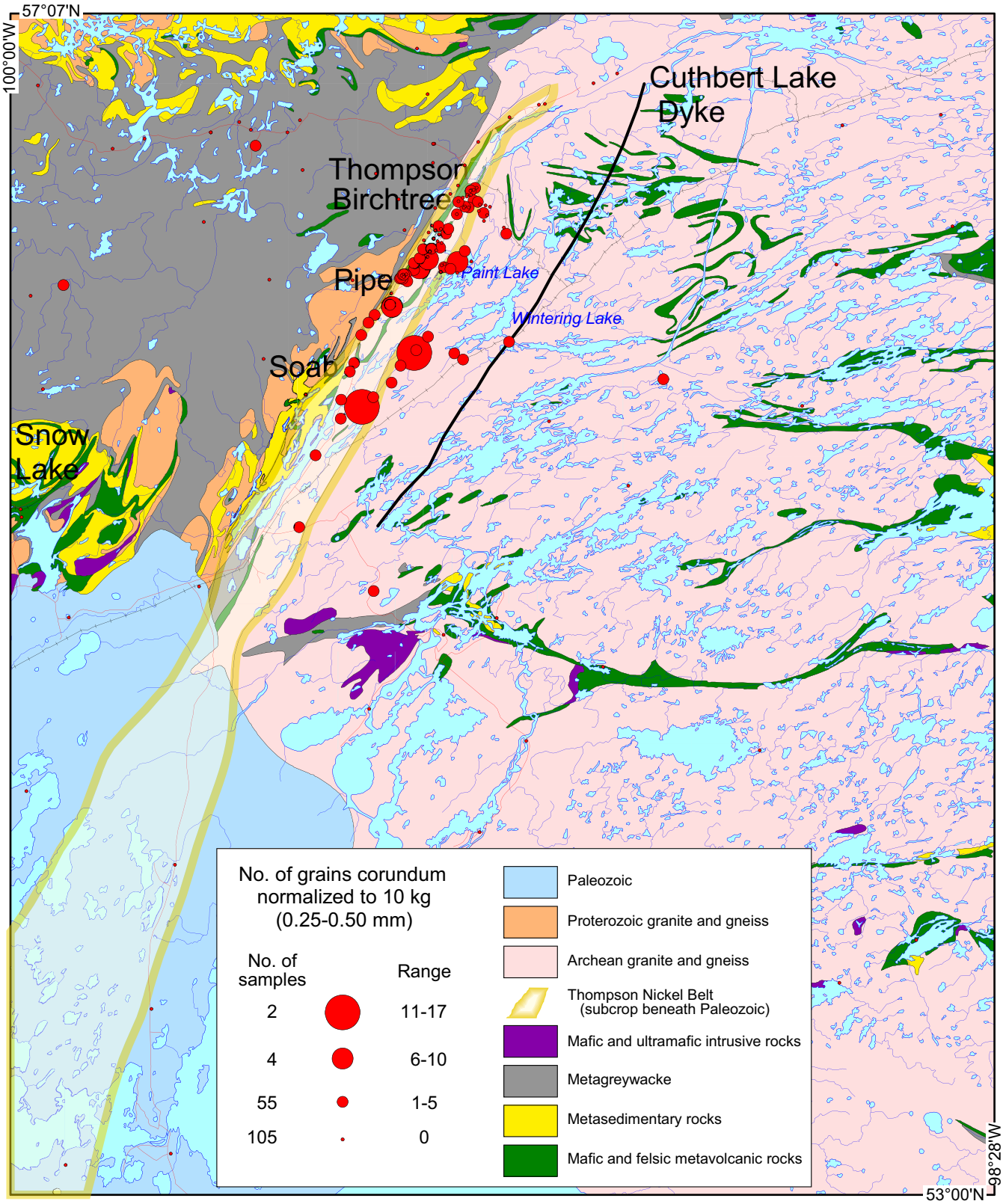

Appendix E1 continued. Map 13, corundum.

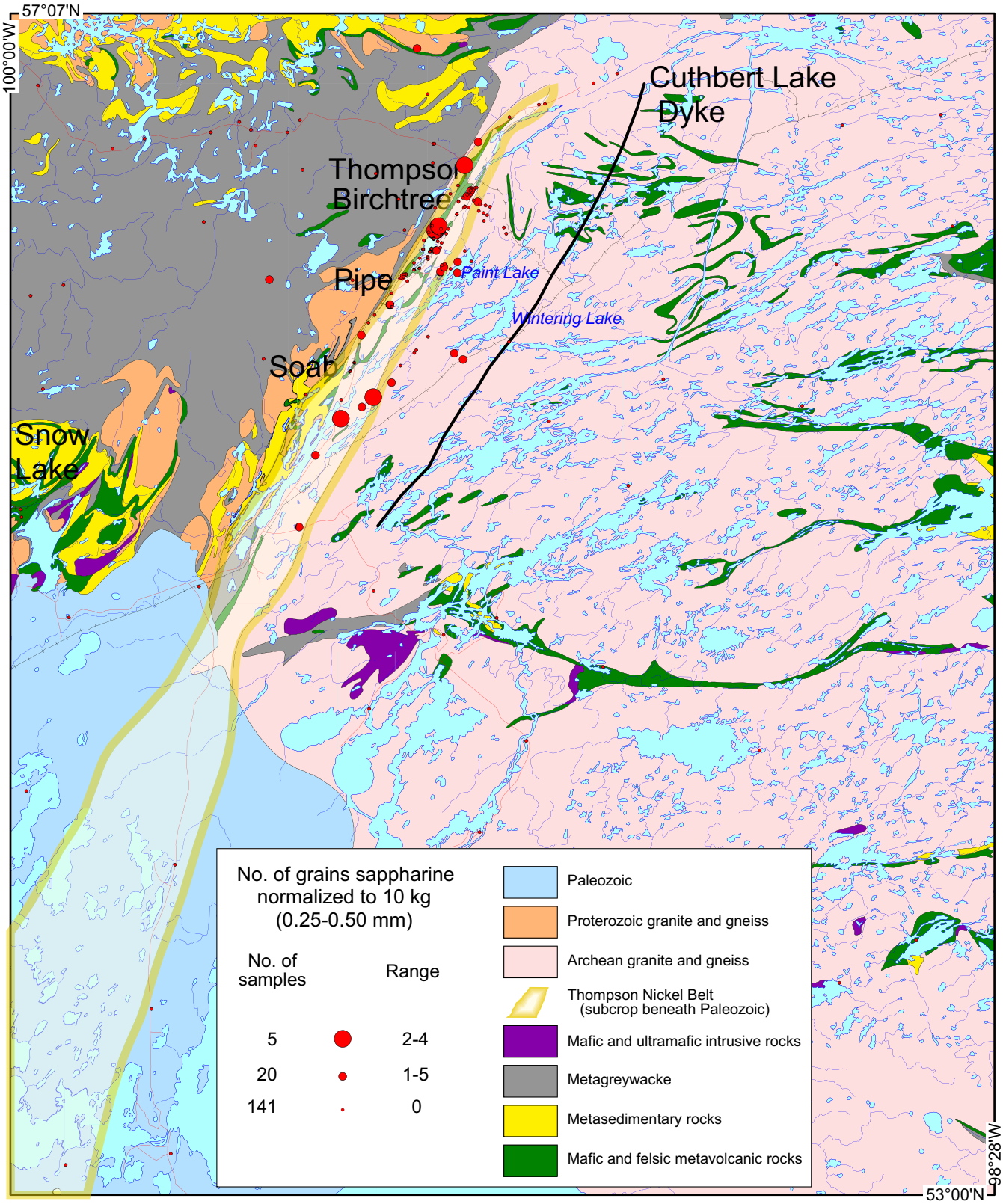

Appendix E1 continued. Map 14, sappharine.

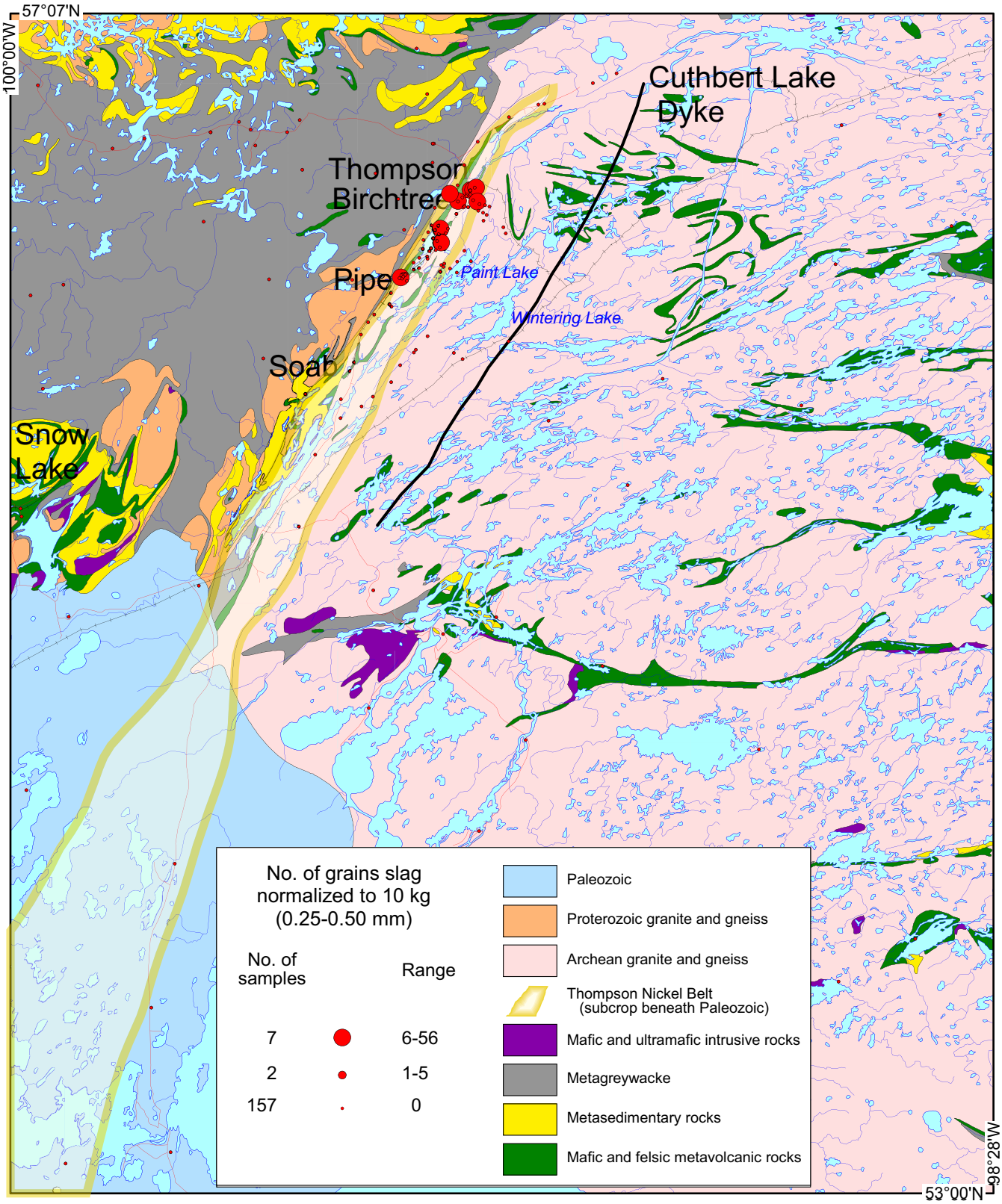

Appendix E1 continued. Map 15, slag.

Appendix E2. Thompson Mine site maps

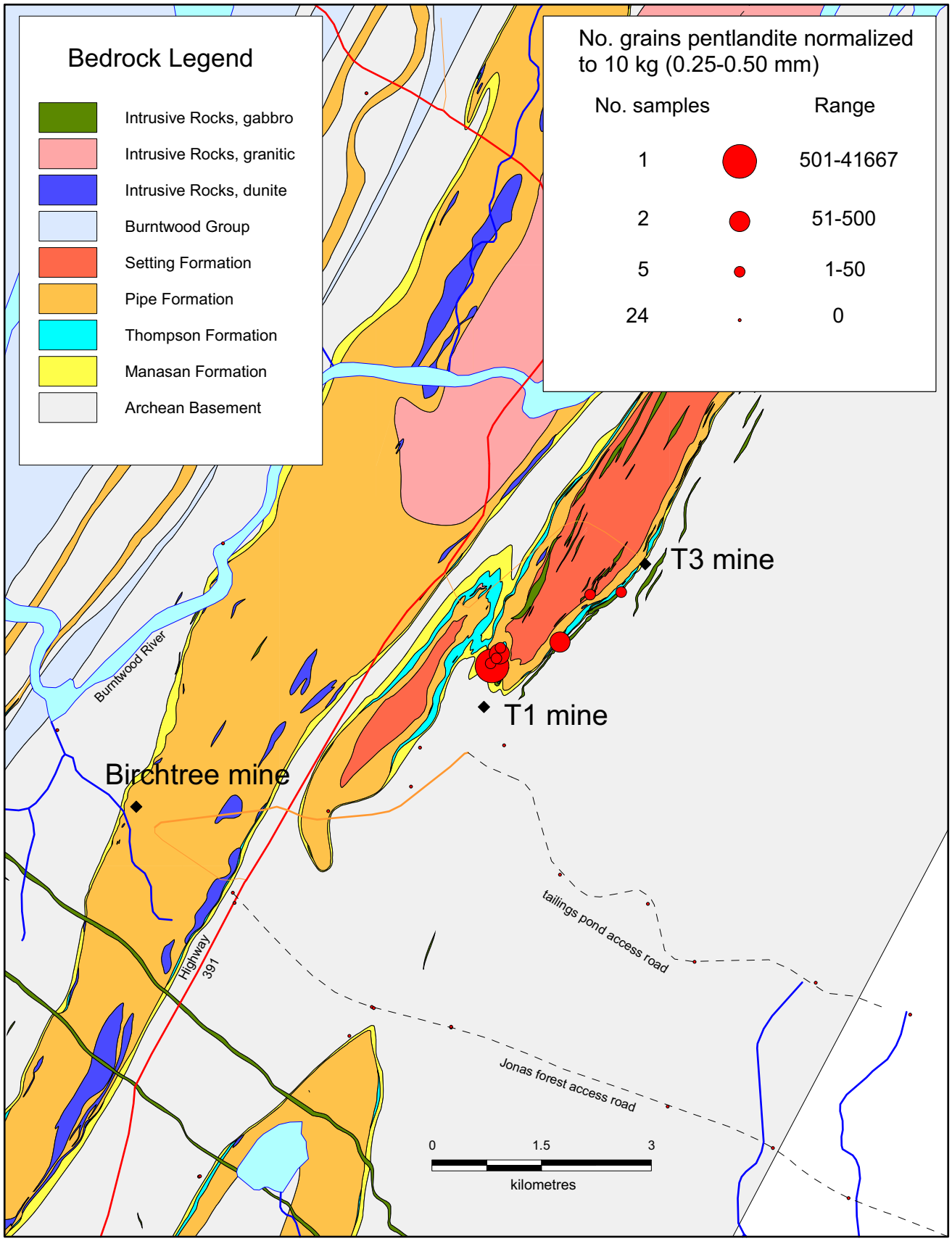

Appendix E2. Map 16, pentlandite.

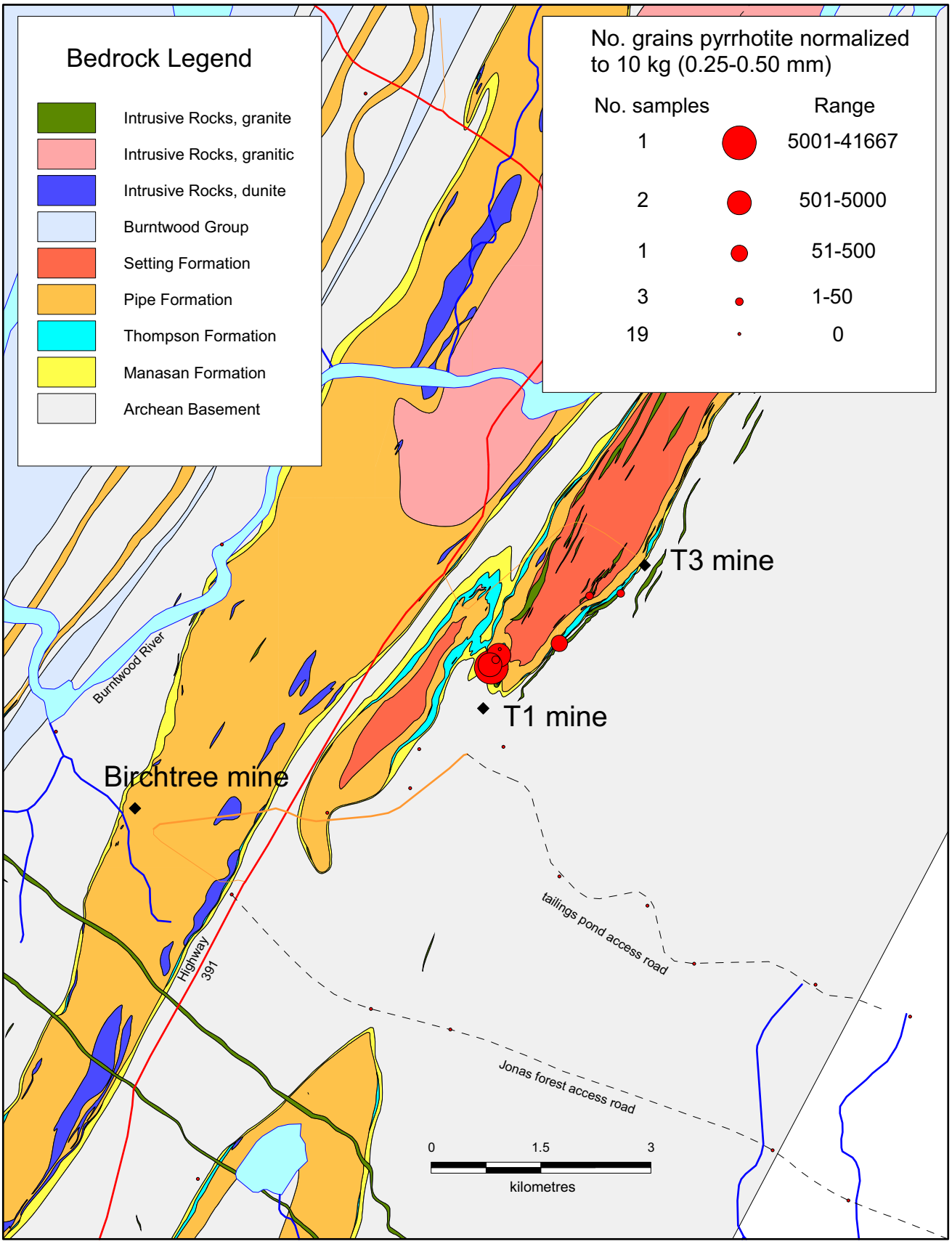

Appendix E2 continued. Map 17, pyrrhotite.

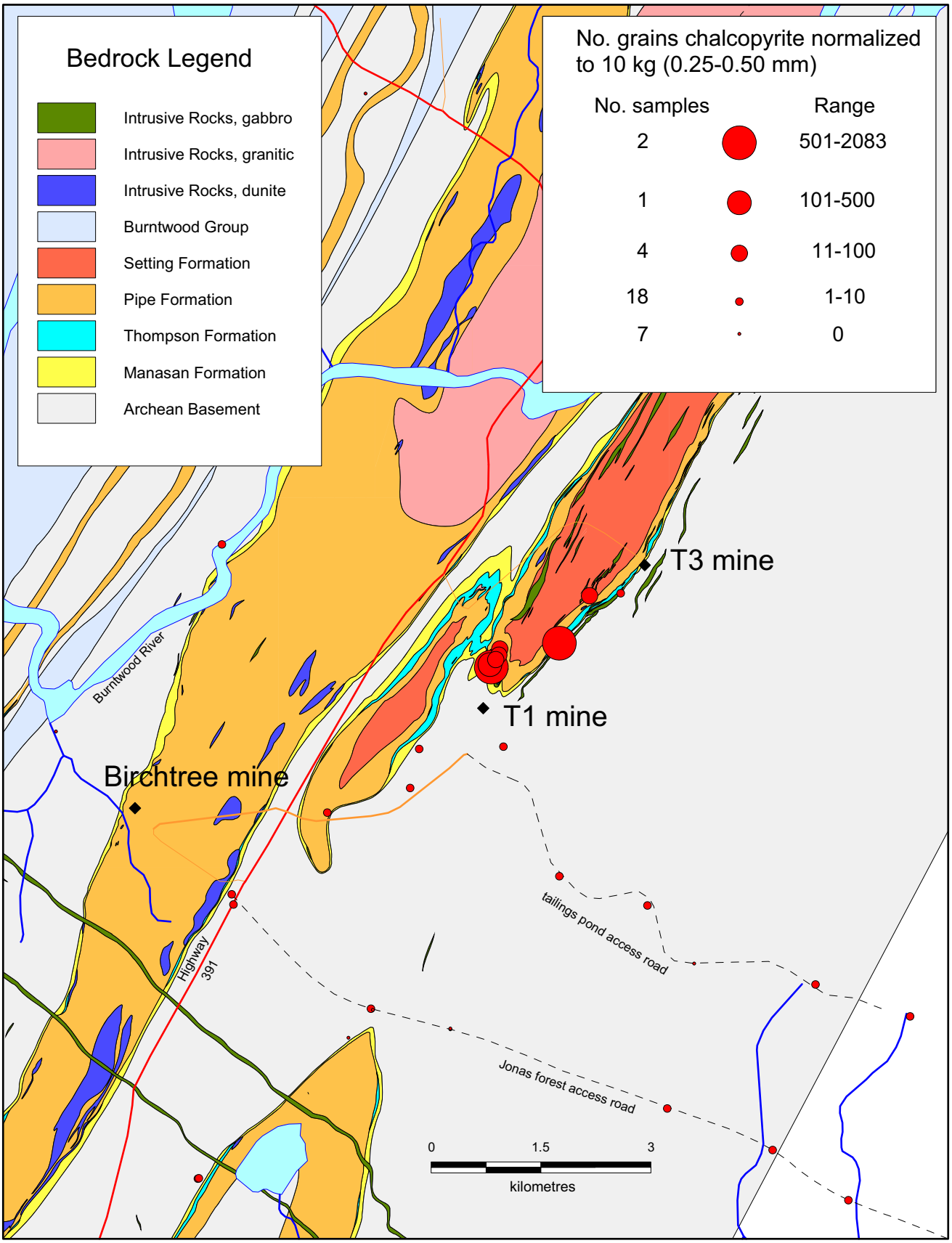

Appendix E2 continued. Map 18, chalcopyrite.

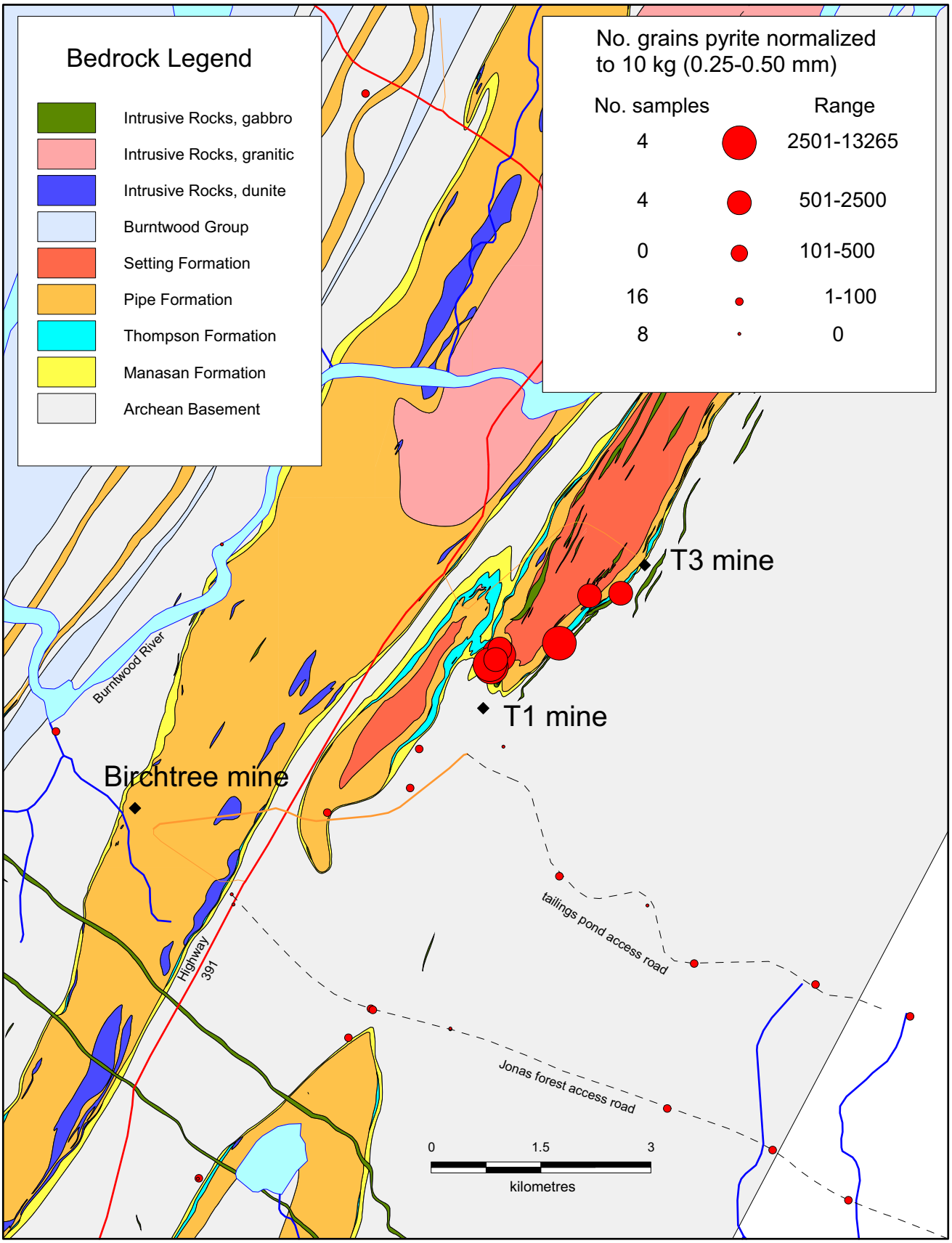

Appendix E2 continued. Map 19, pyrite.

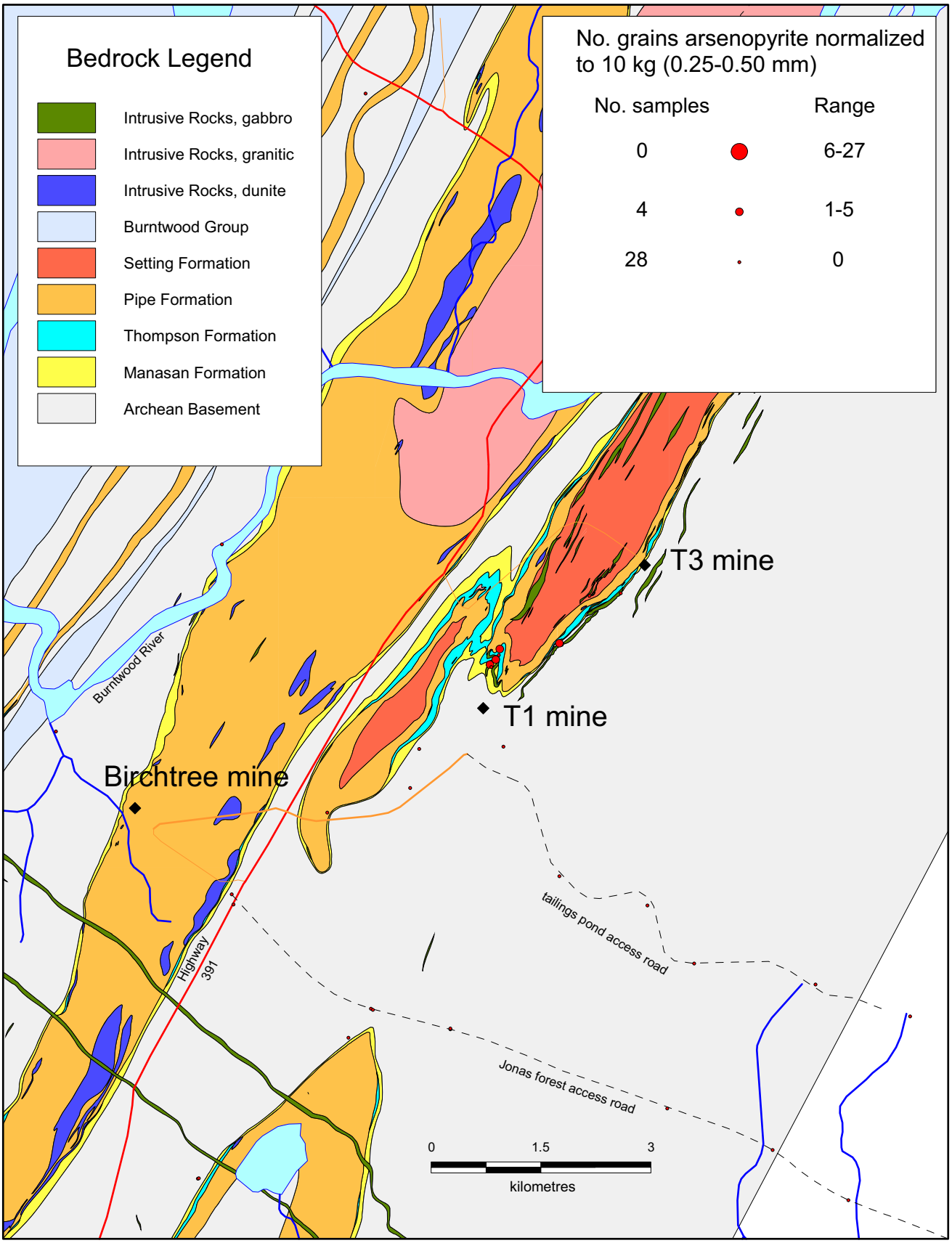

Appendix E2 continued. Map 20, arsenopyrite.

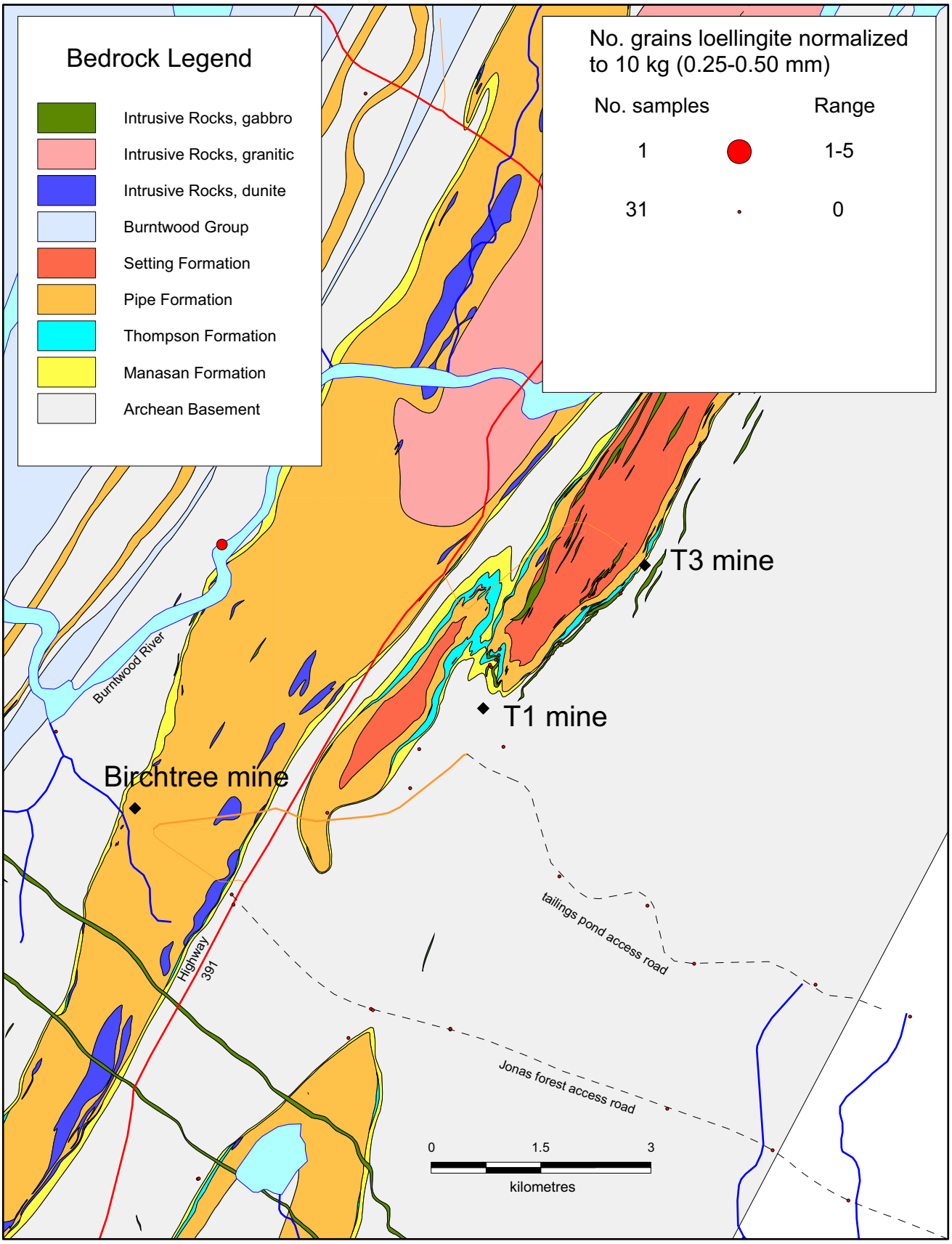

Appendix E2 continued. Map 21, loellingite.

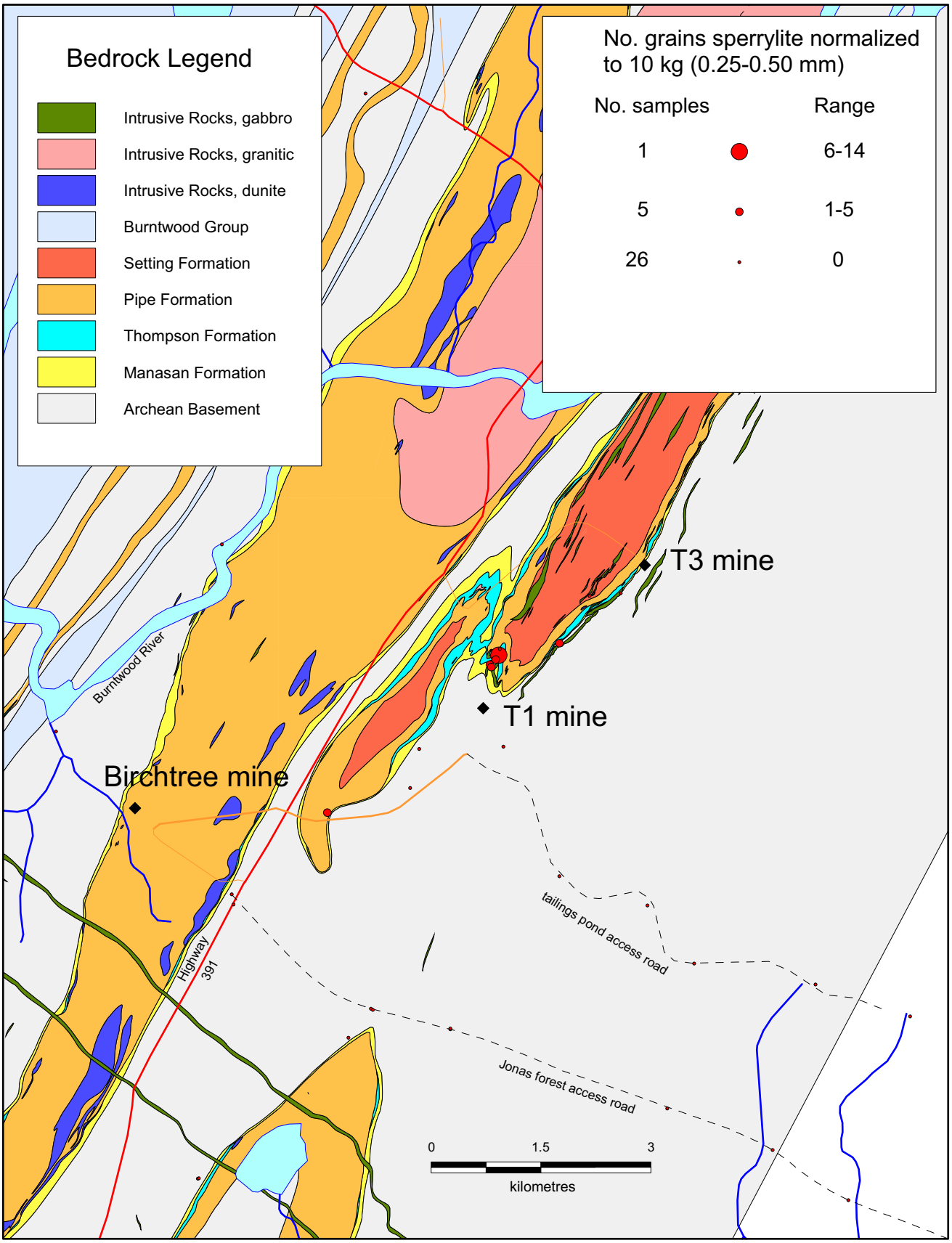

Appendix E2 continued. Map 22, sperrylite.

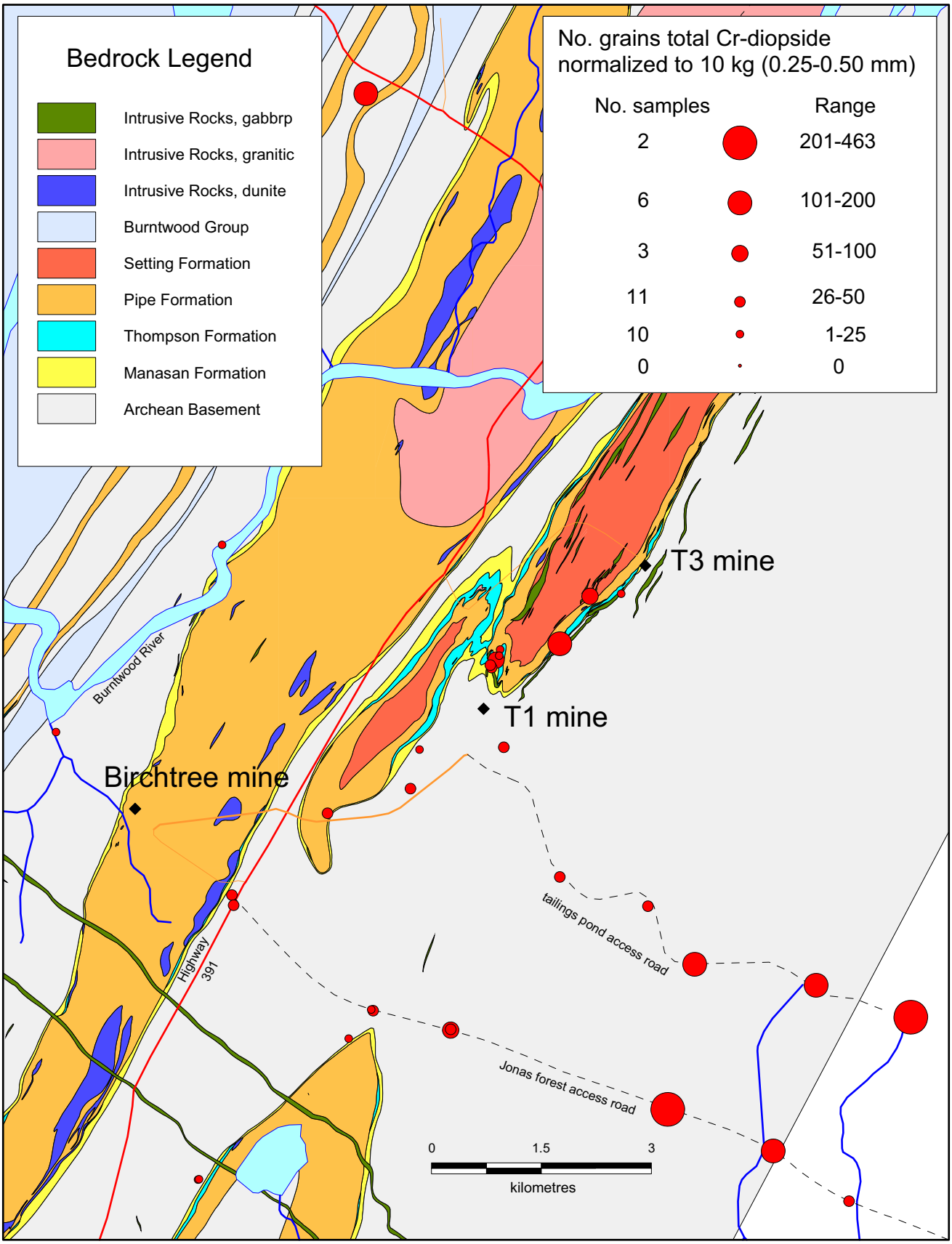

Appendix E2 continued. Map 23, total Cr-diopside.

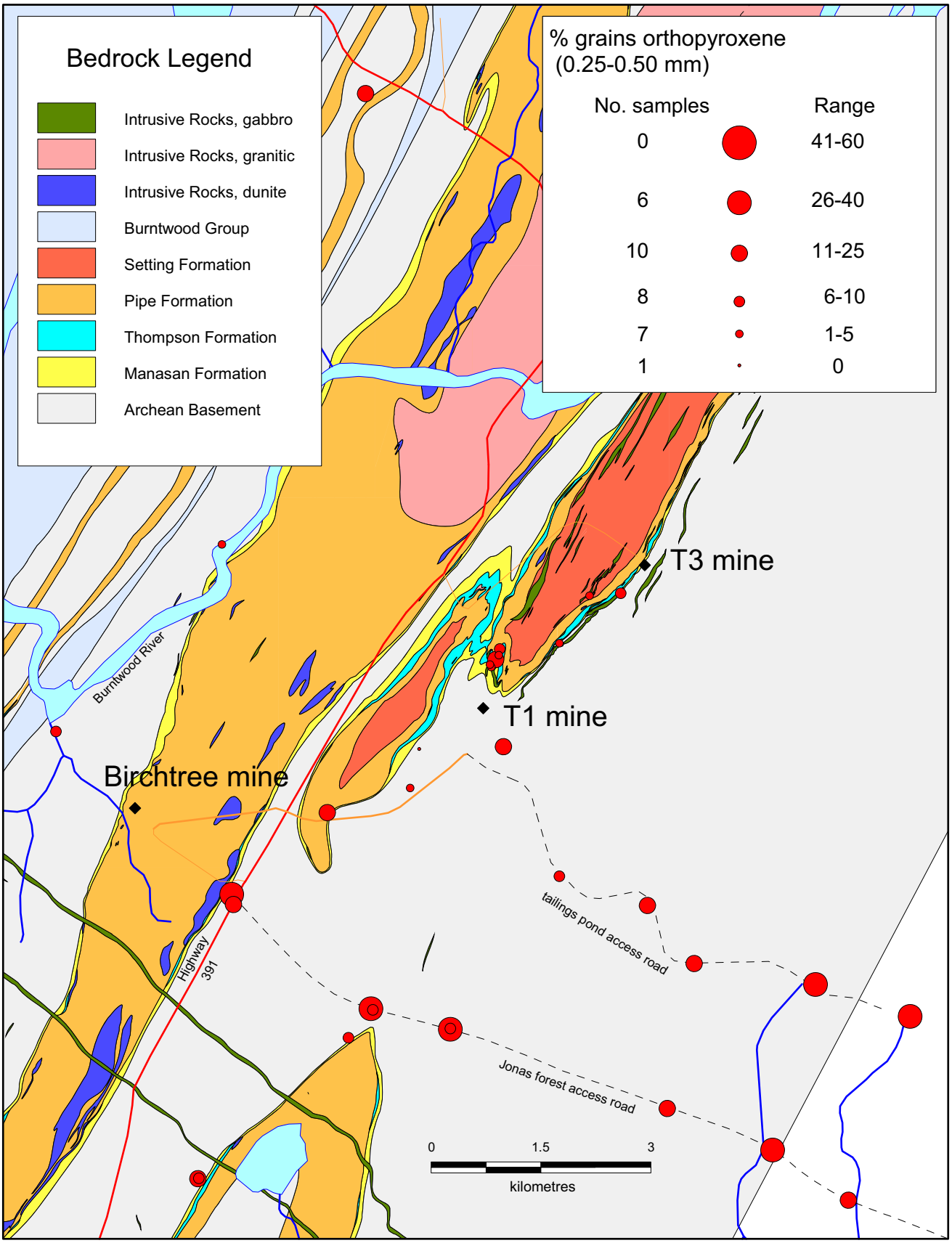

Appendix E2 continued. Map 24, total orthopyroxene.

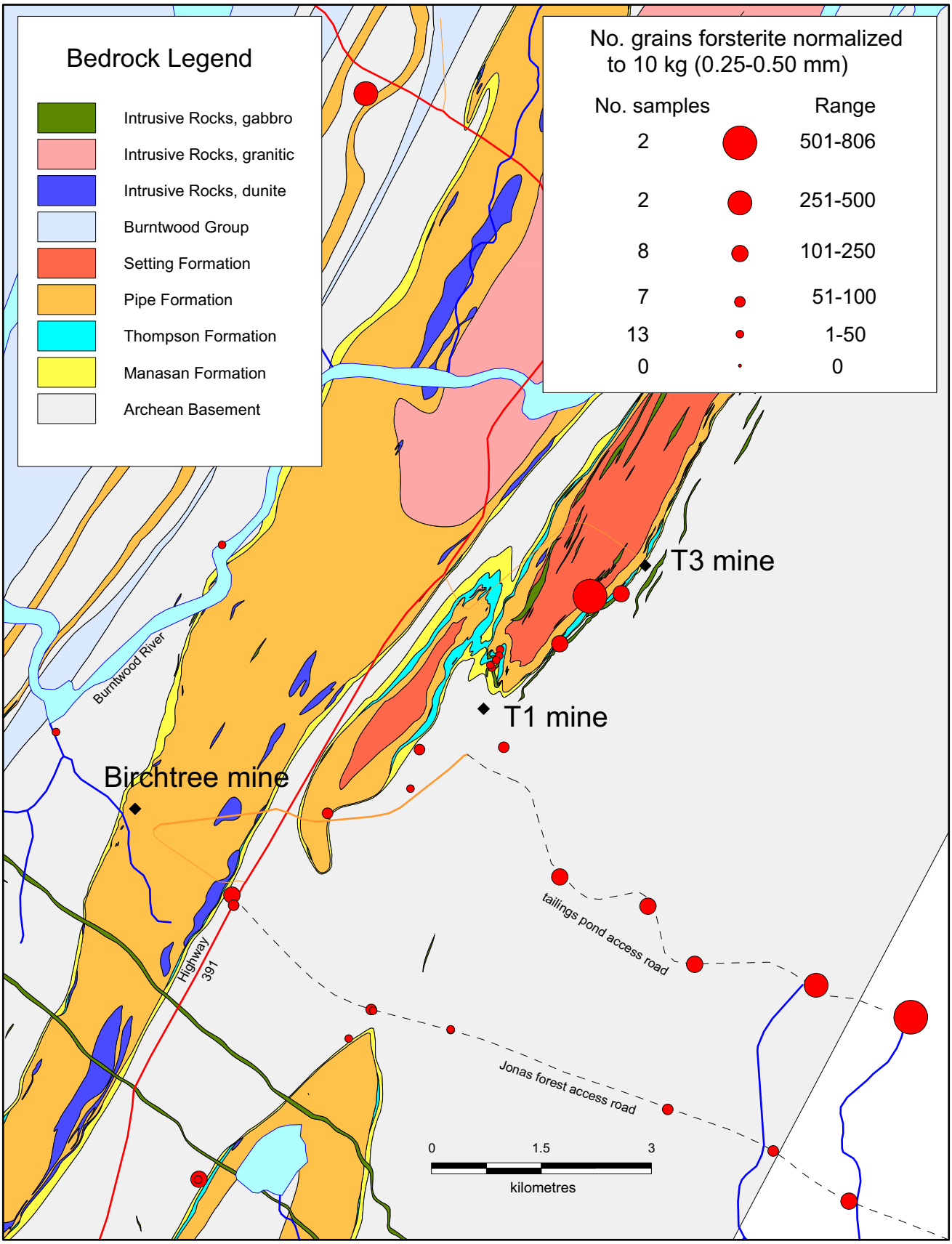

Appendix E2 continued. Map 25, forsterite.

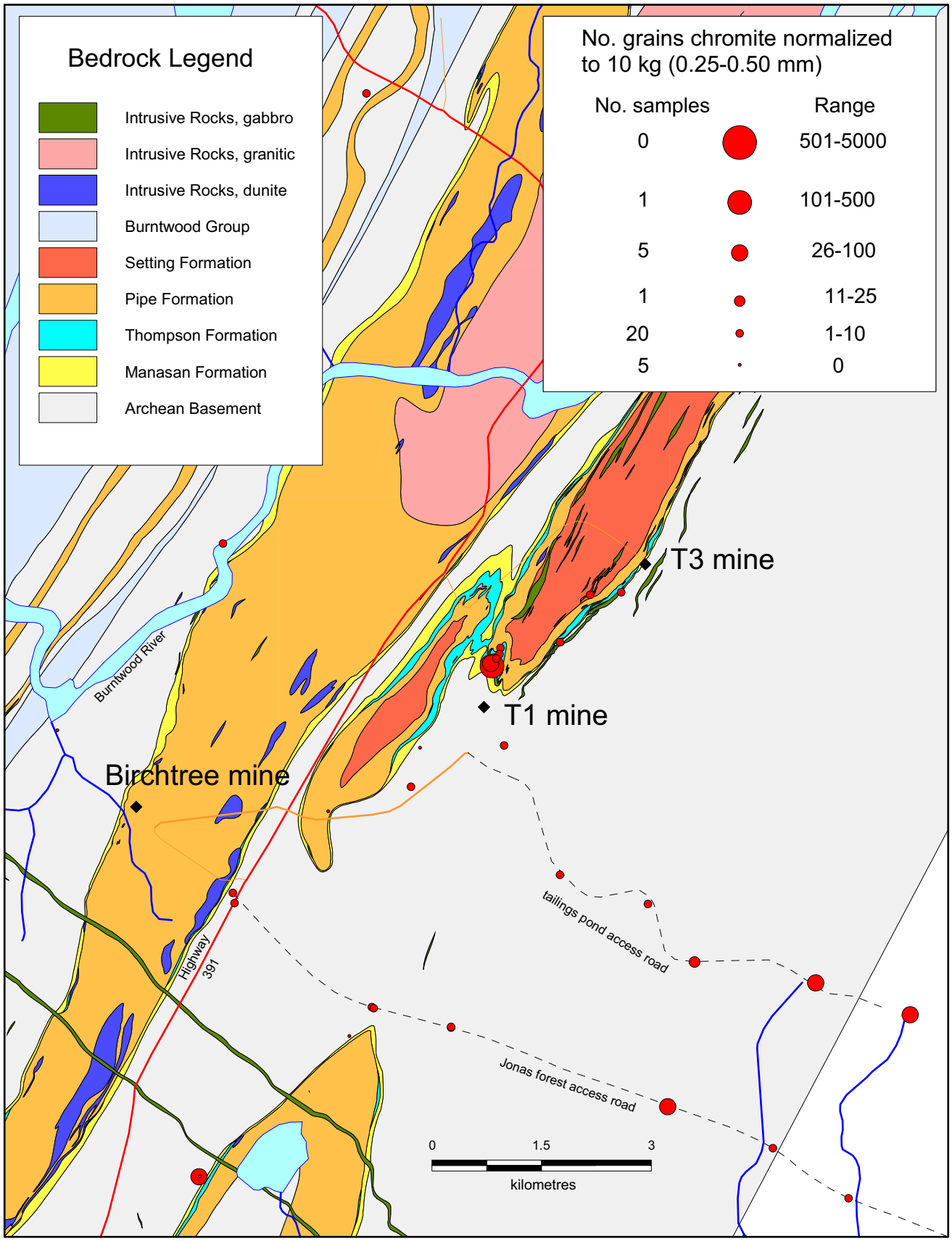

Appendix E2 continued. Map 26, chromite.

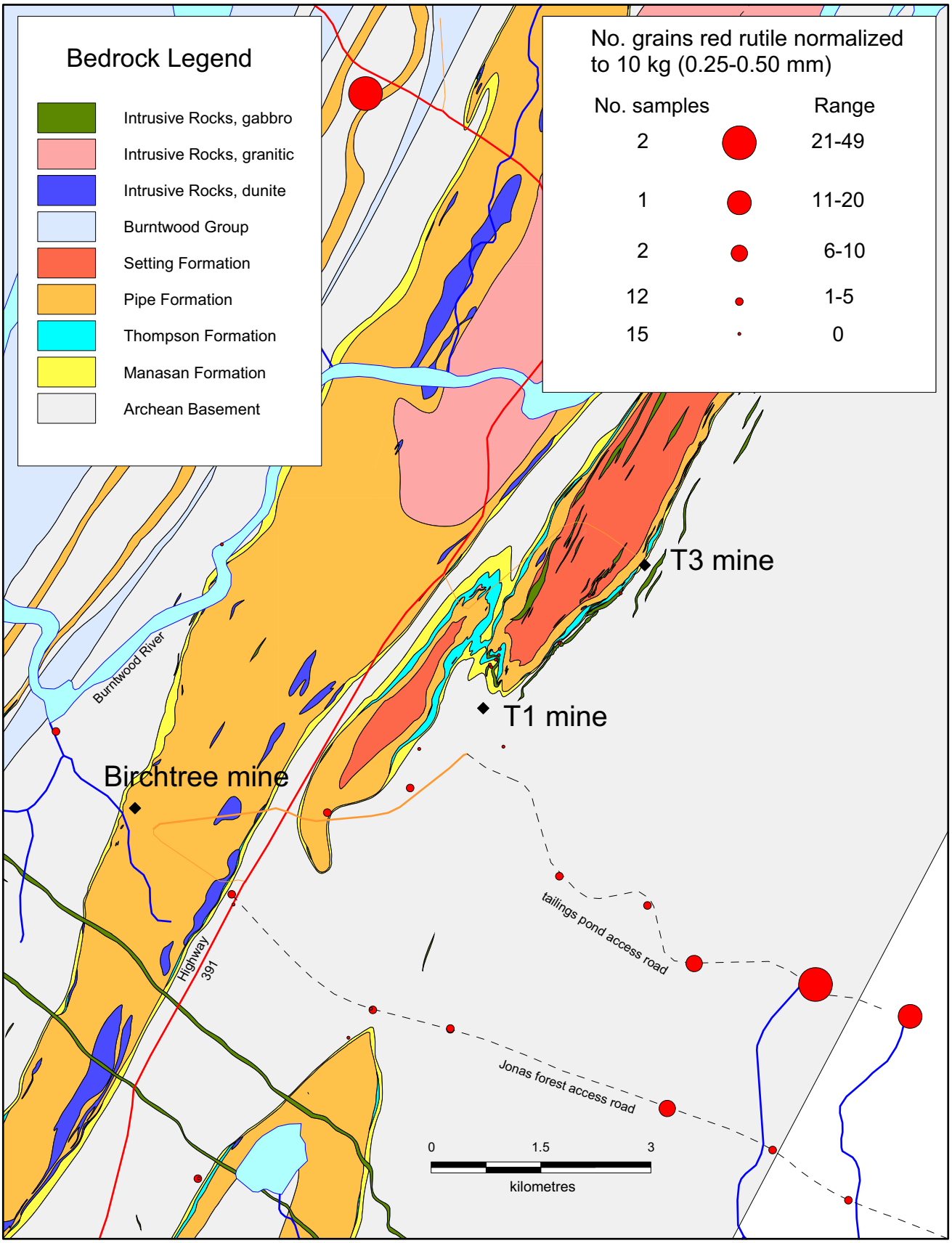

Appendix E2 continued. Map 27, red rutile.

Appendix E3. Pipe Mine site maps

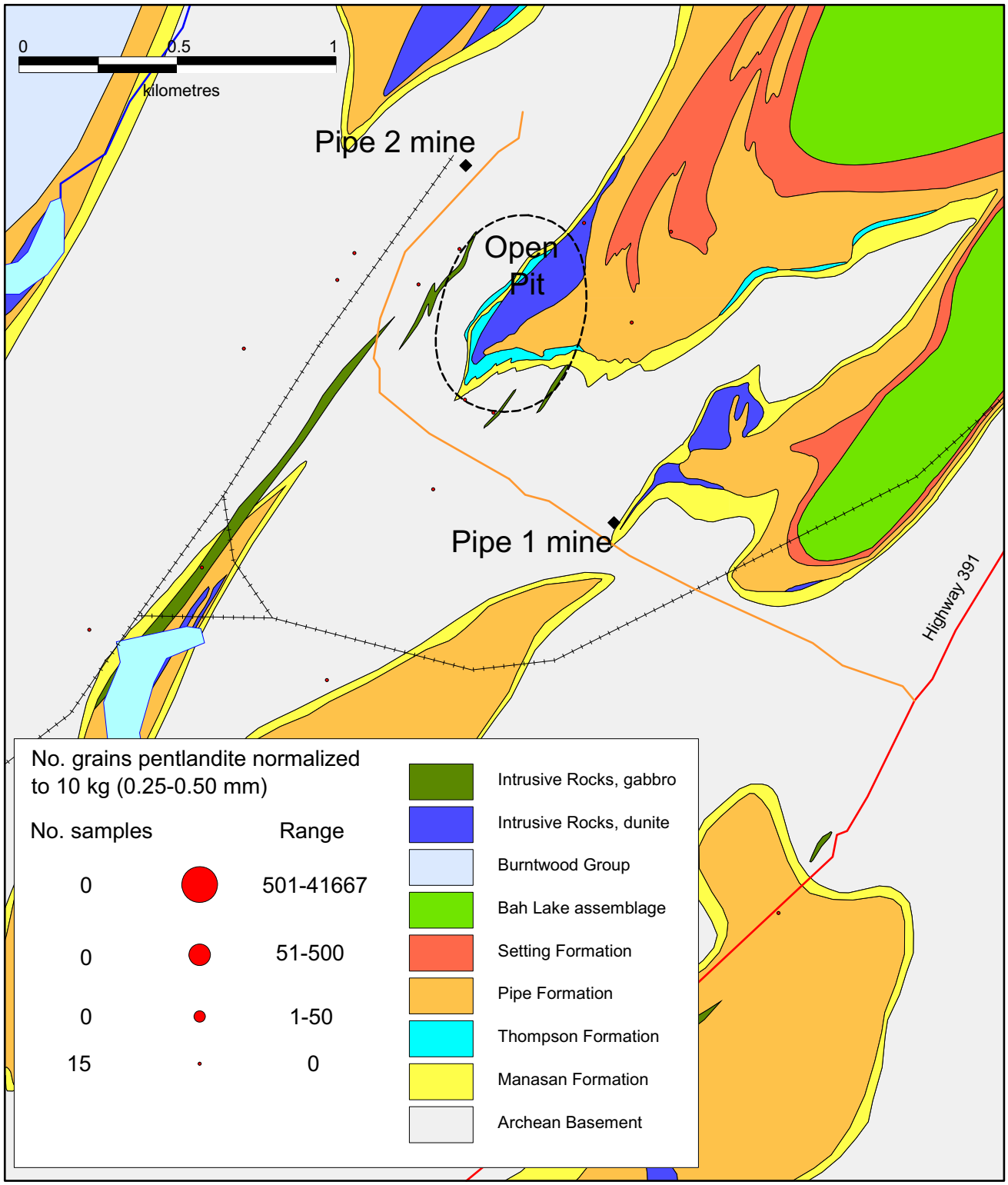

Appendix E3. Map 28, pentlandite.

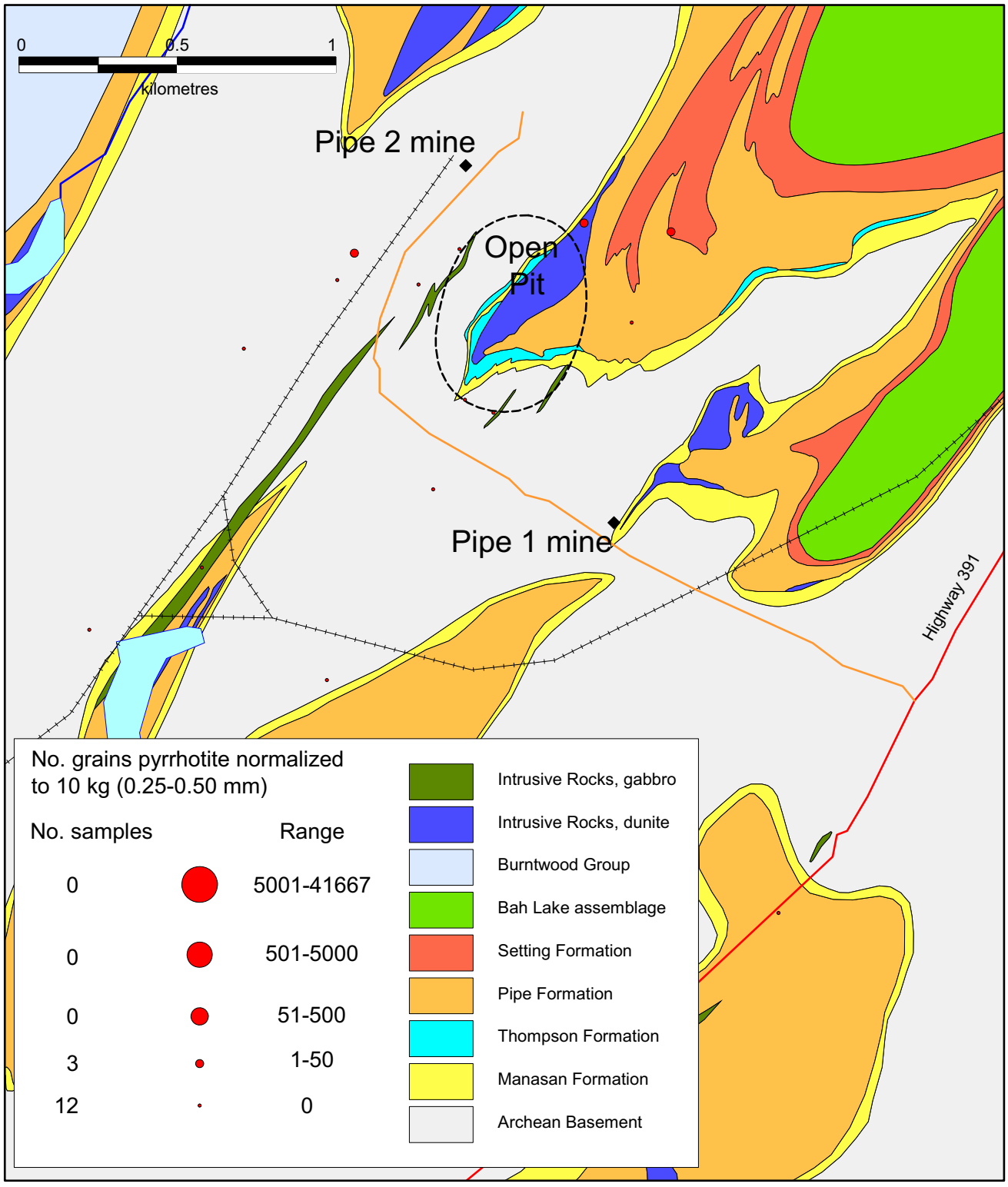

Appendix E3 continued. Map 29, pyrrhotite.

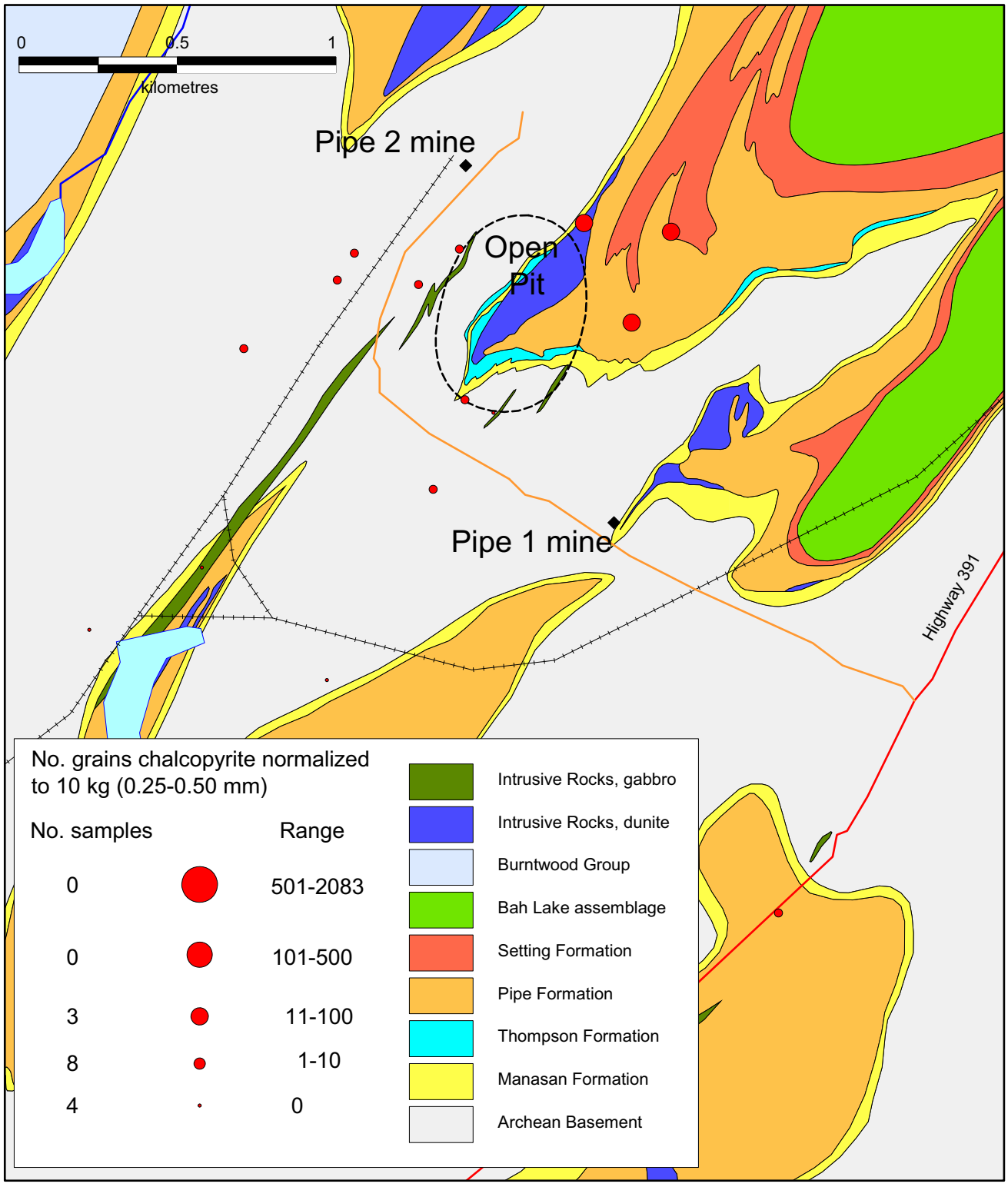

Appendix E3 continued. Map 30, chalcopyrite.

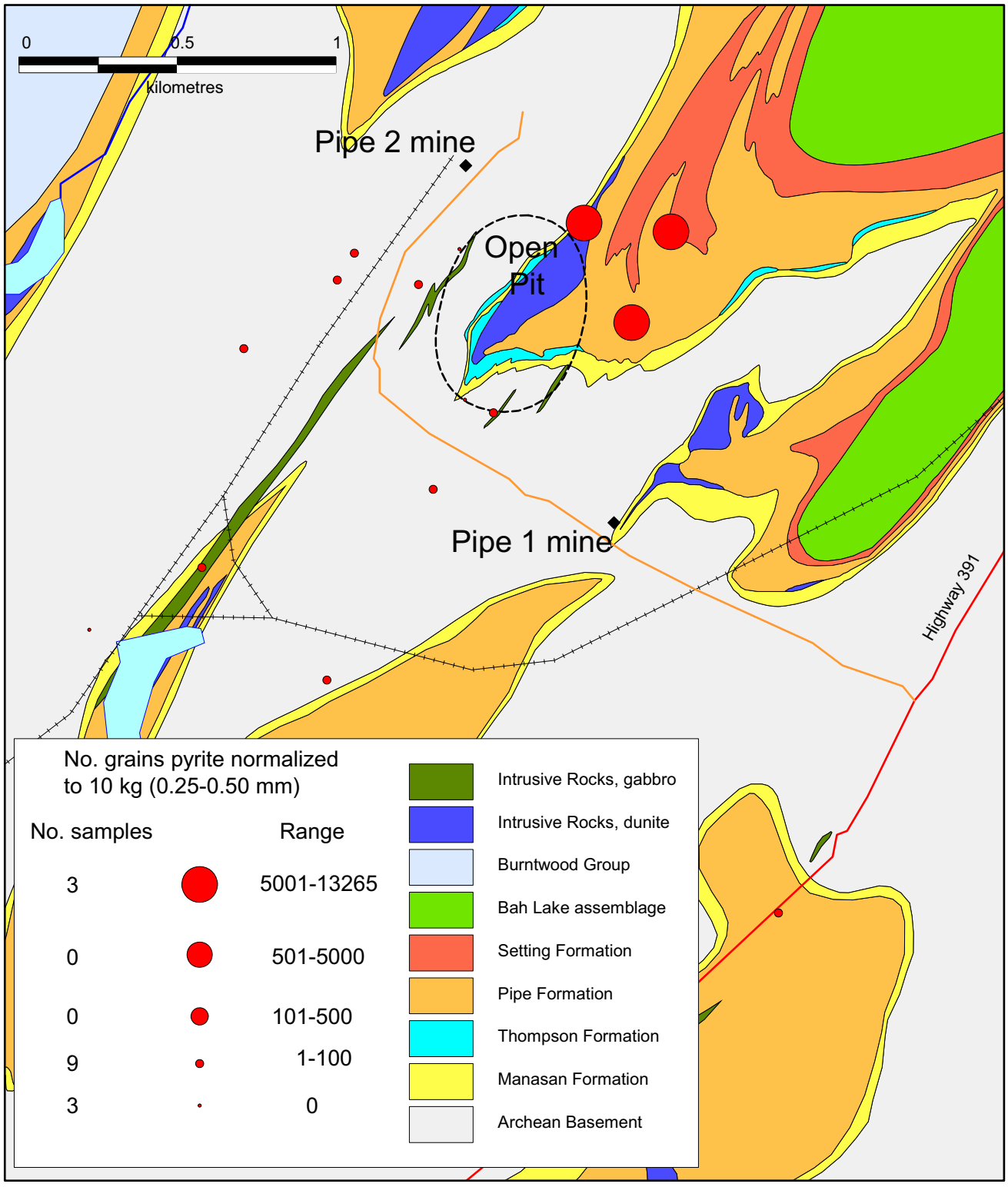

Appendix E3 continued. Map 31, pyrite.

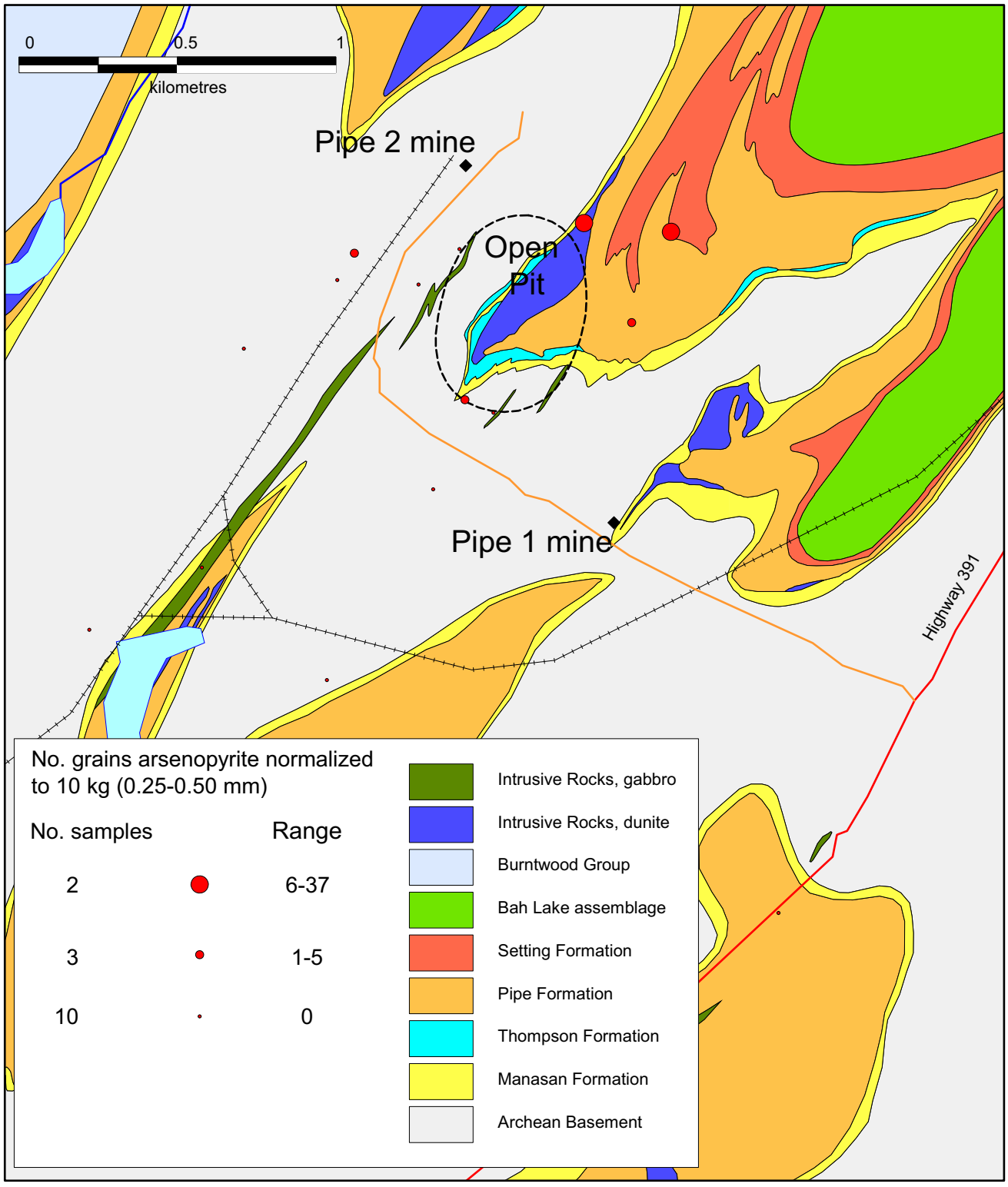

Appendix E3 continued. Map 32, arsenopyrite.

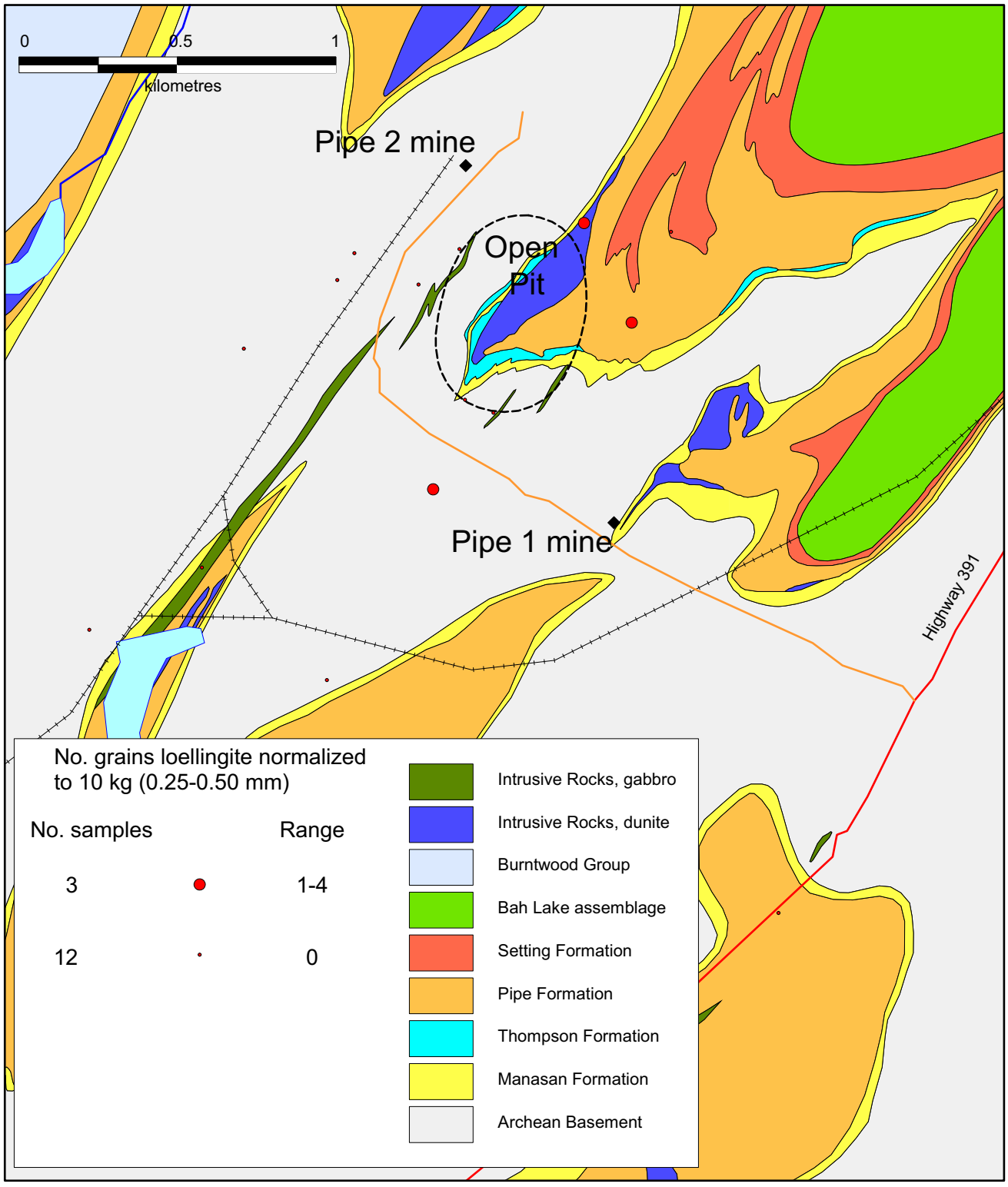

Appendix E3. Map 33, loellingite.

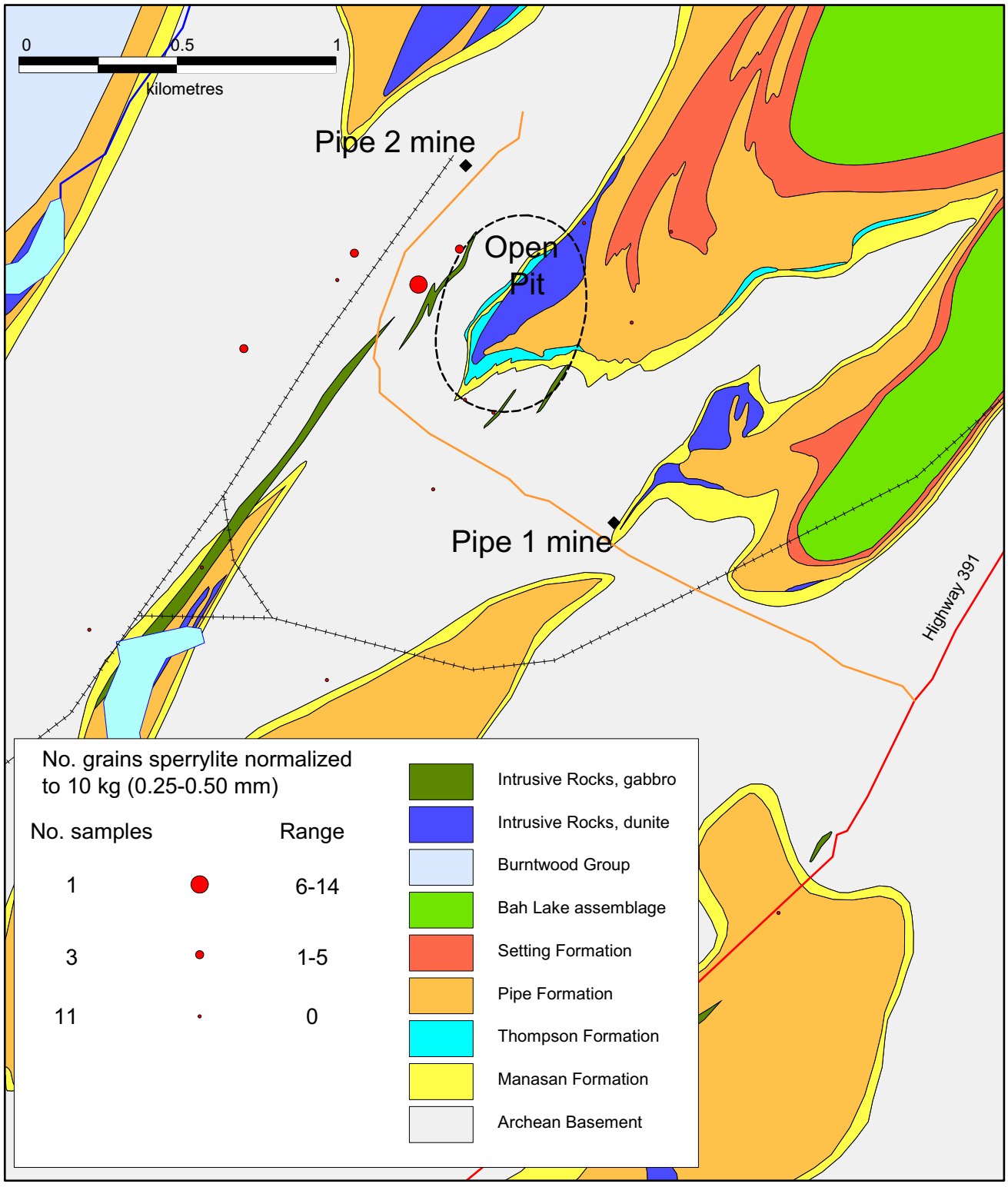

Appendix E3 continued. Map 34, sperrylite

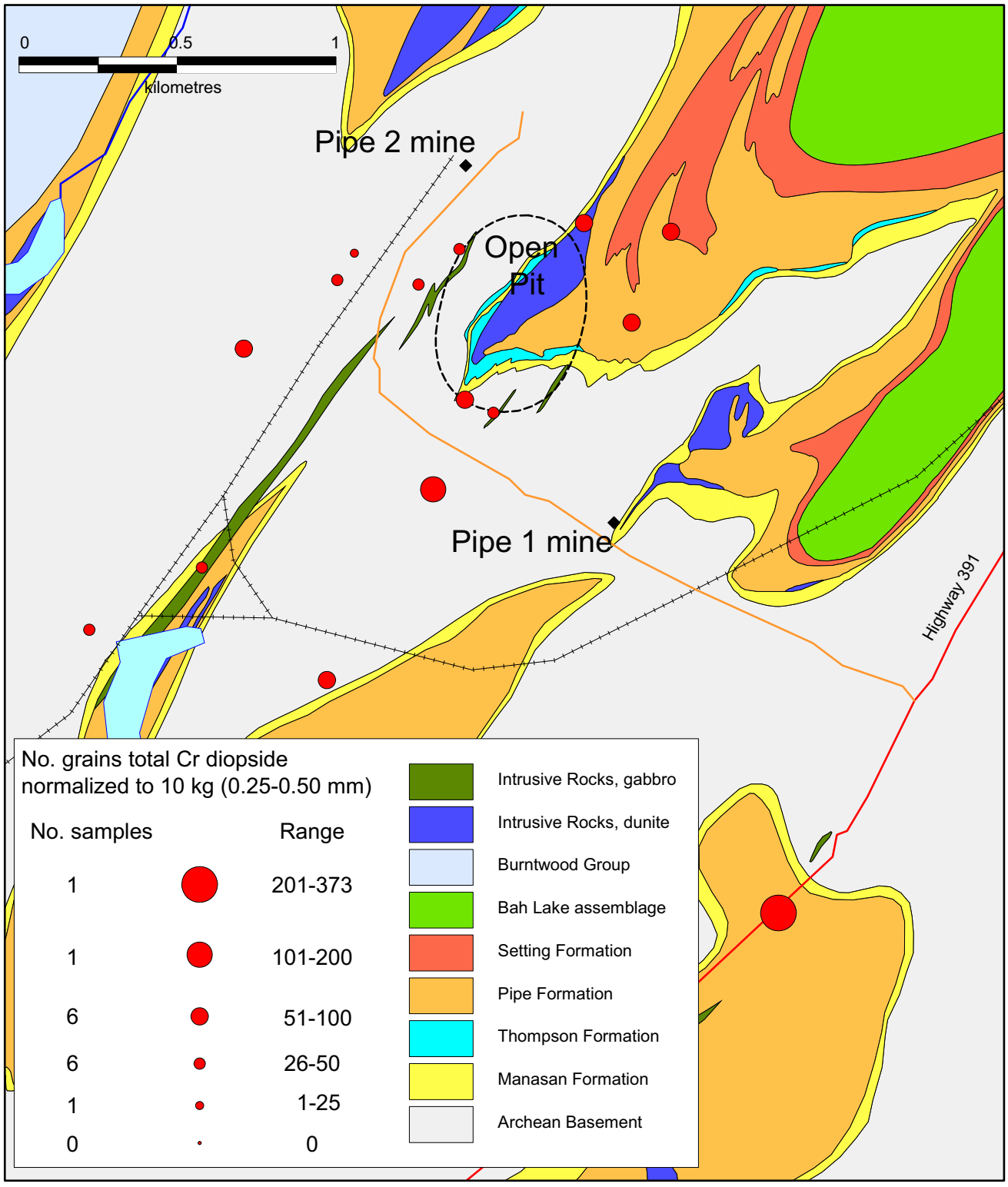

Appendix E3. Map 35, total Cr-diopside.

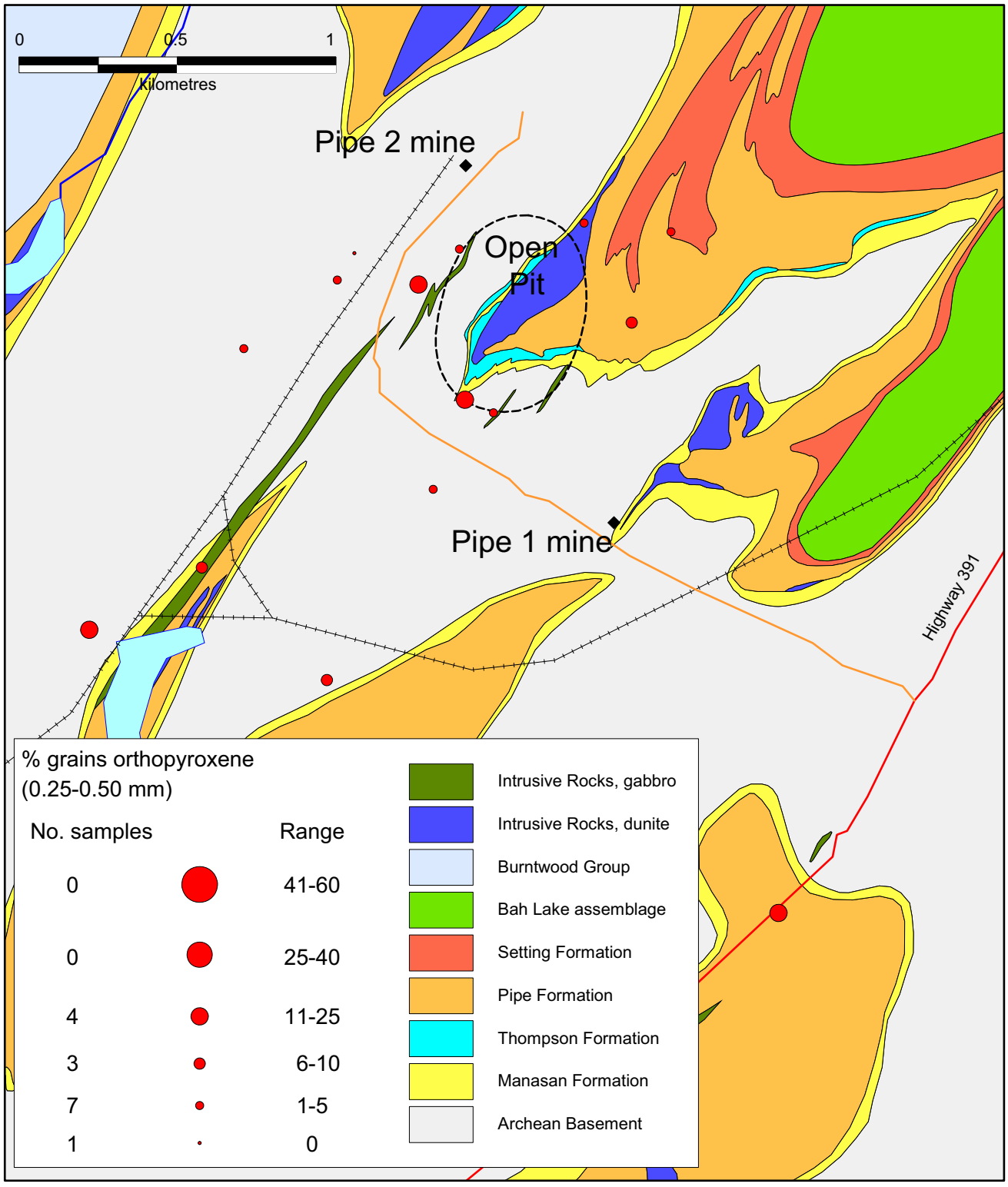

Appendix E3 continued. Map 36, orthopyroxene

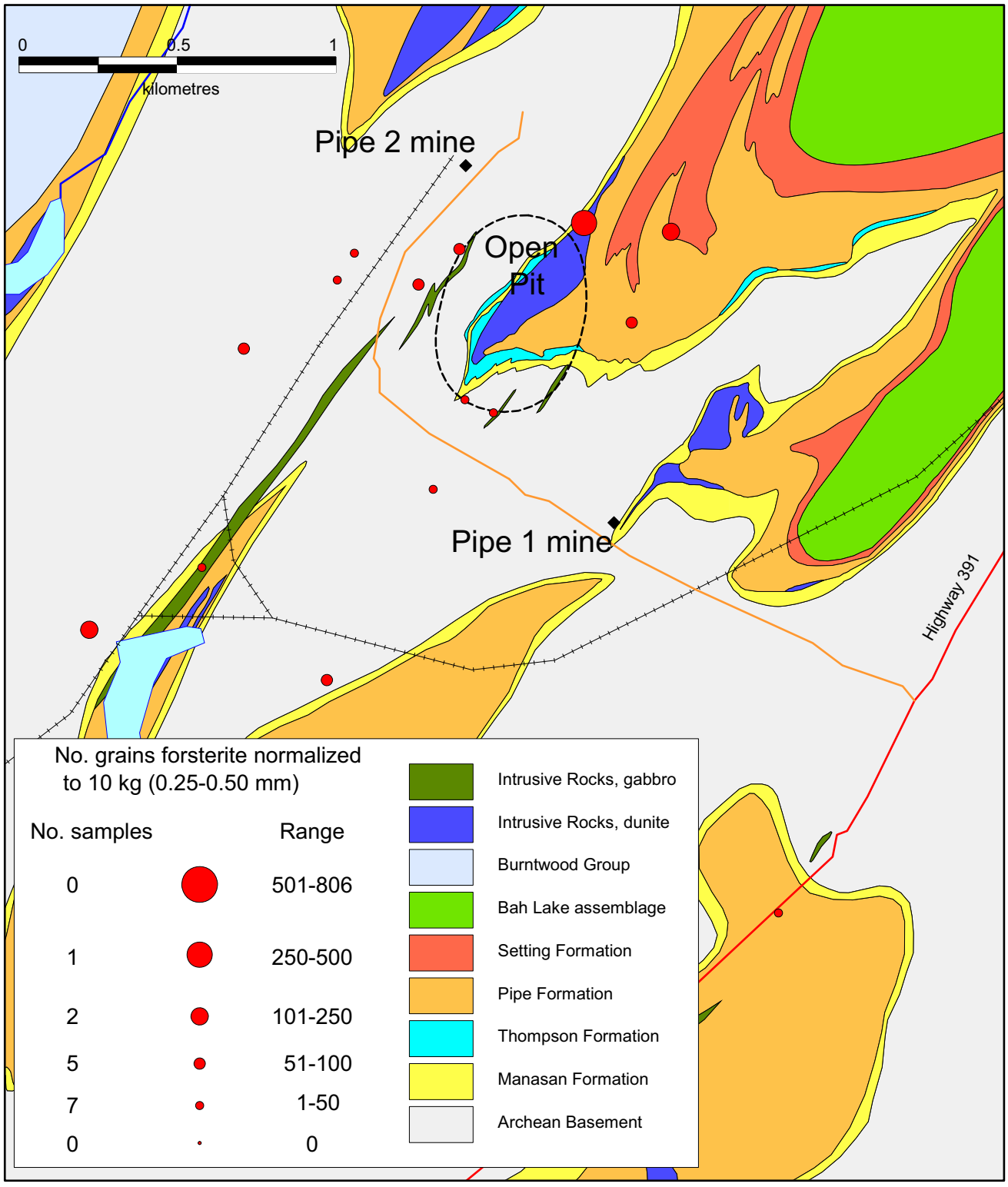

Appendix E3. Map 37, forsterite.

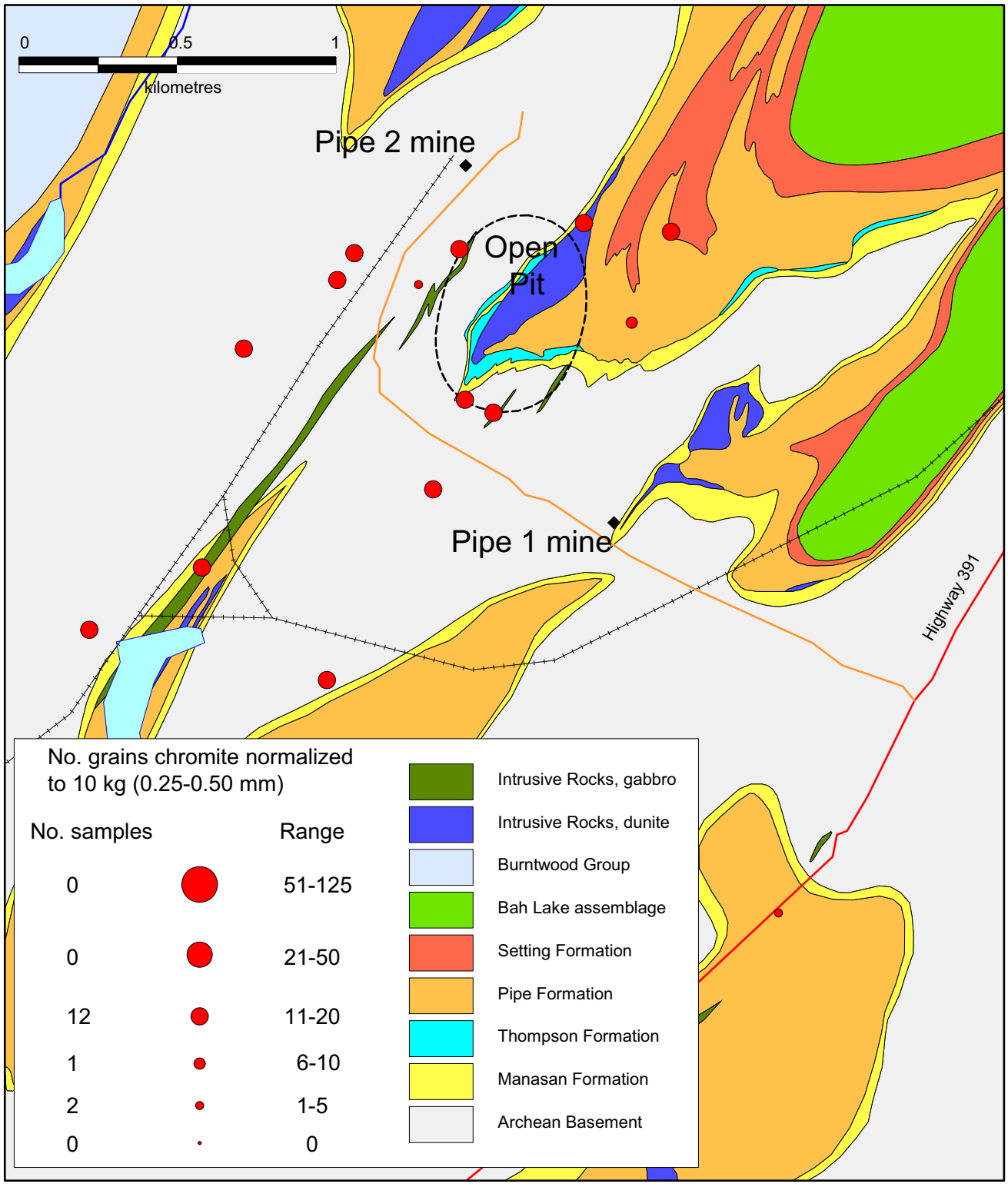

Appendix E3 continued. Map 38, chromite

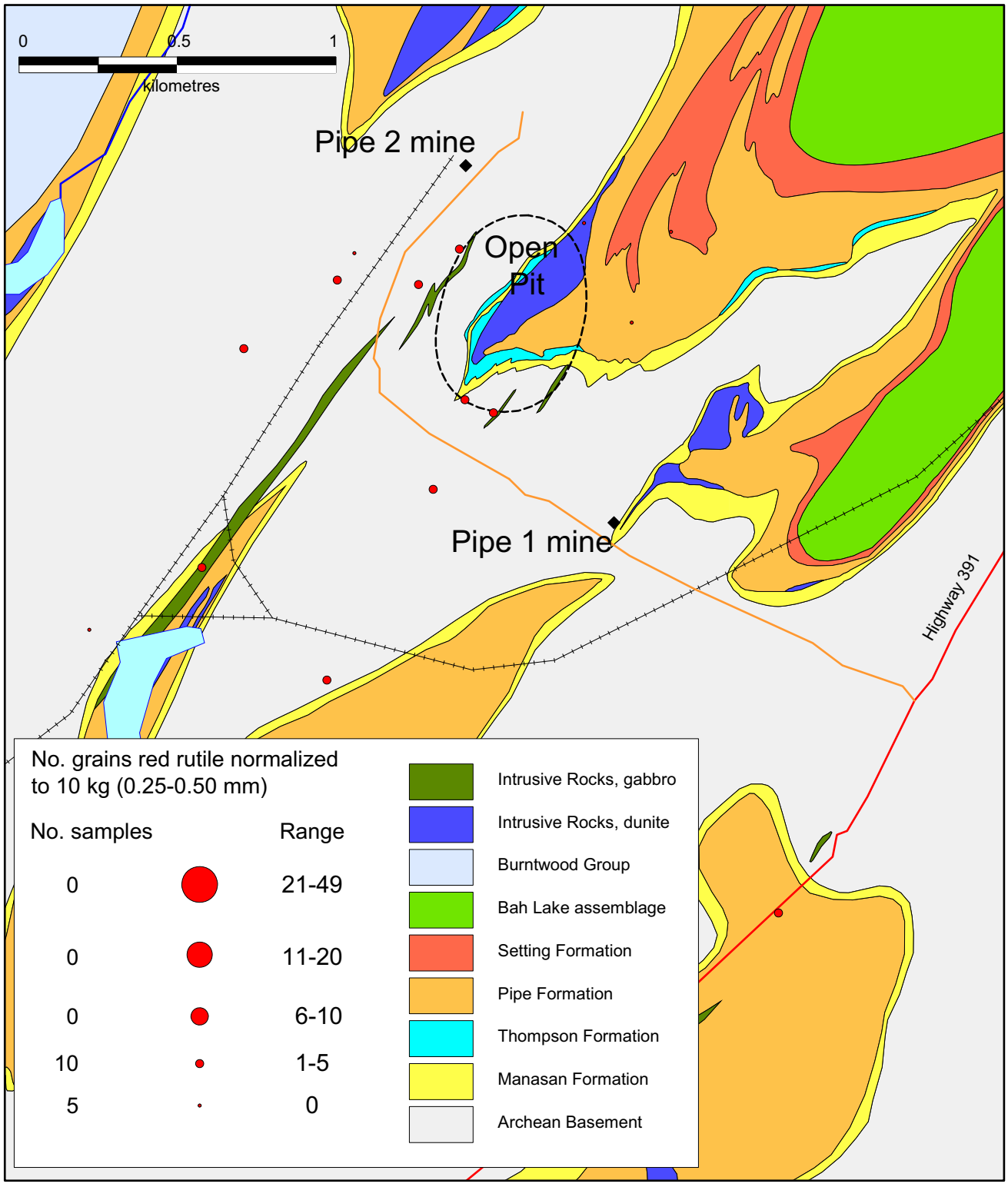

Appendix E3 continued. Map 39, red rutile.

APPENDIX F. ELECTRON MICROPROBE DATA AND METHODS

Appendix F2. Electron microprobe grain mount maps

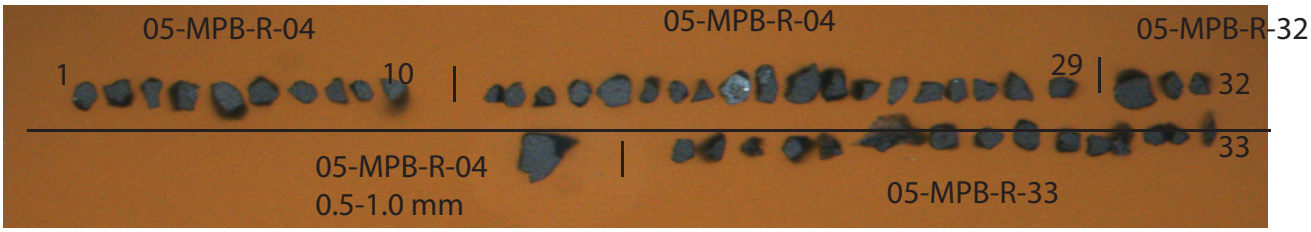

Mineral mount: 05-0616 P01. Thompson Nickel Belt; mineral: chromite, size: 0.25-0.5 mm.

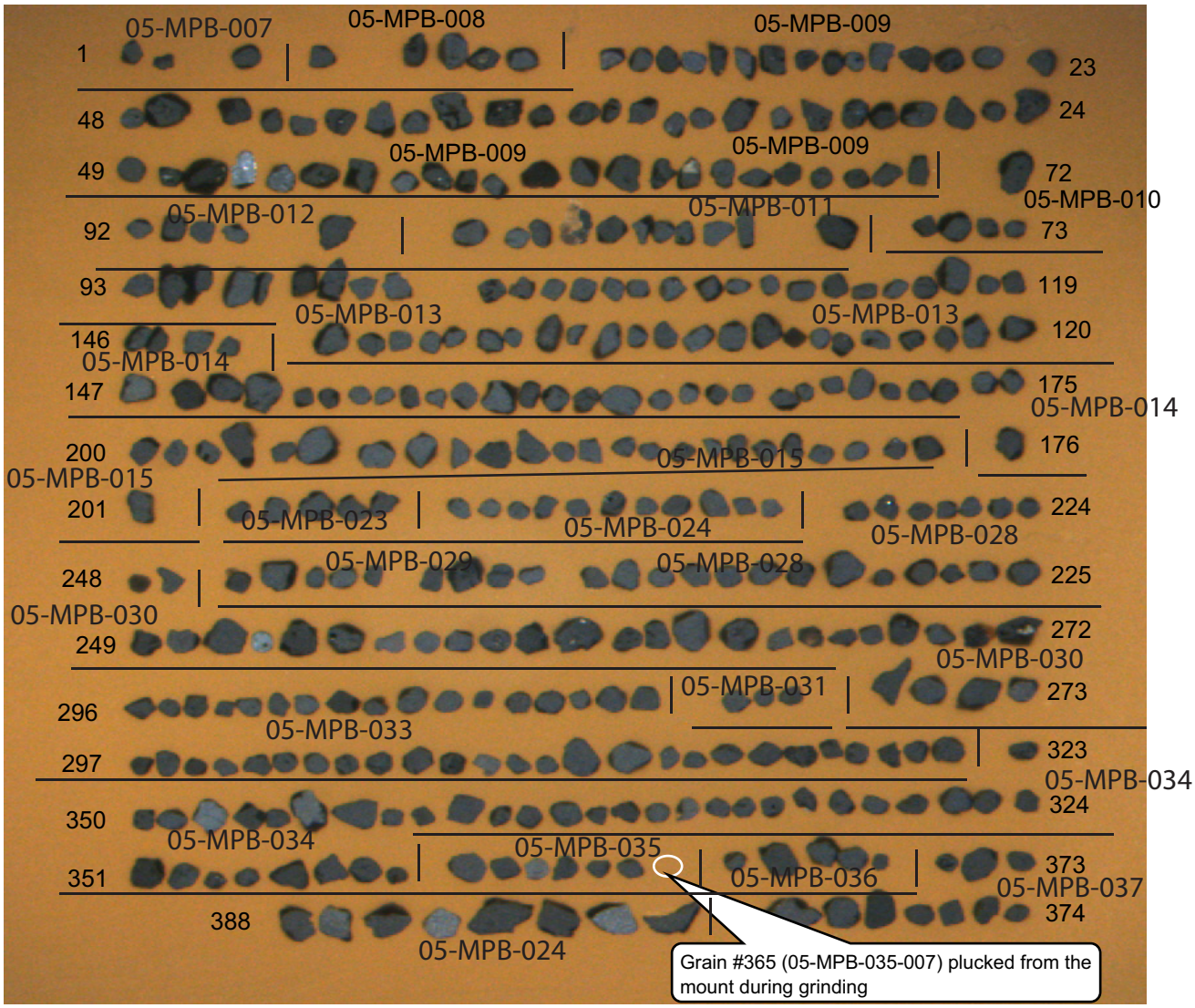

Mineral mount: 05-0616 P02. Thompson Nickel Belt; minerals: oxide, size: 0.25-0.5 mm.

Appendix F2 continued.

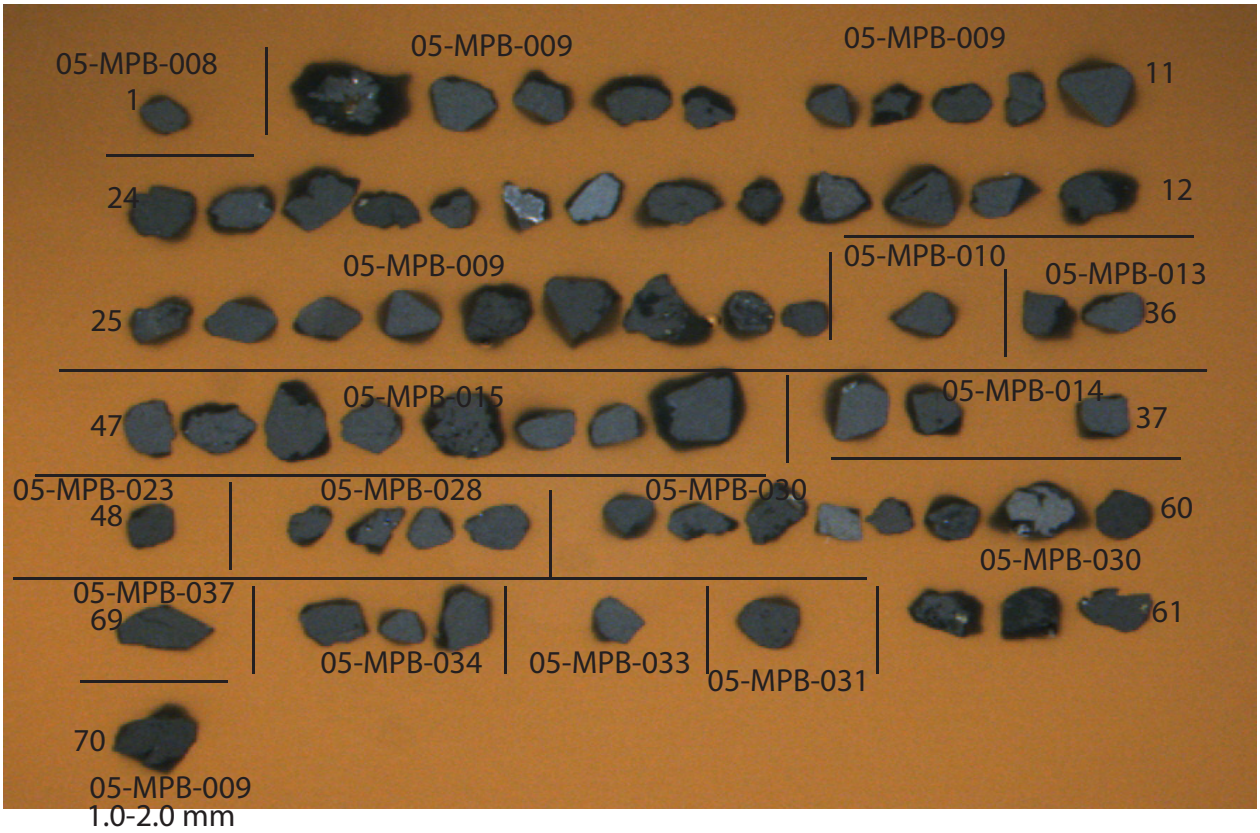

Mineral mount: 05-0616 P03. Thompson Nickel Belt; minerals: oxide, size: 0.5-1.0 mm.

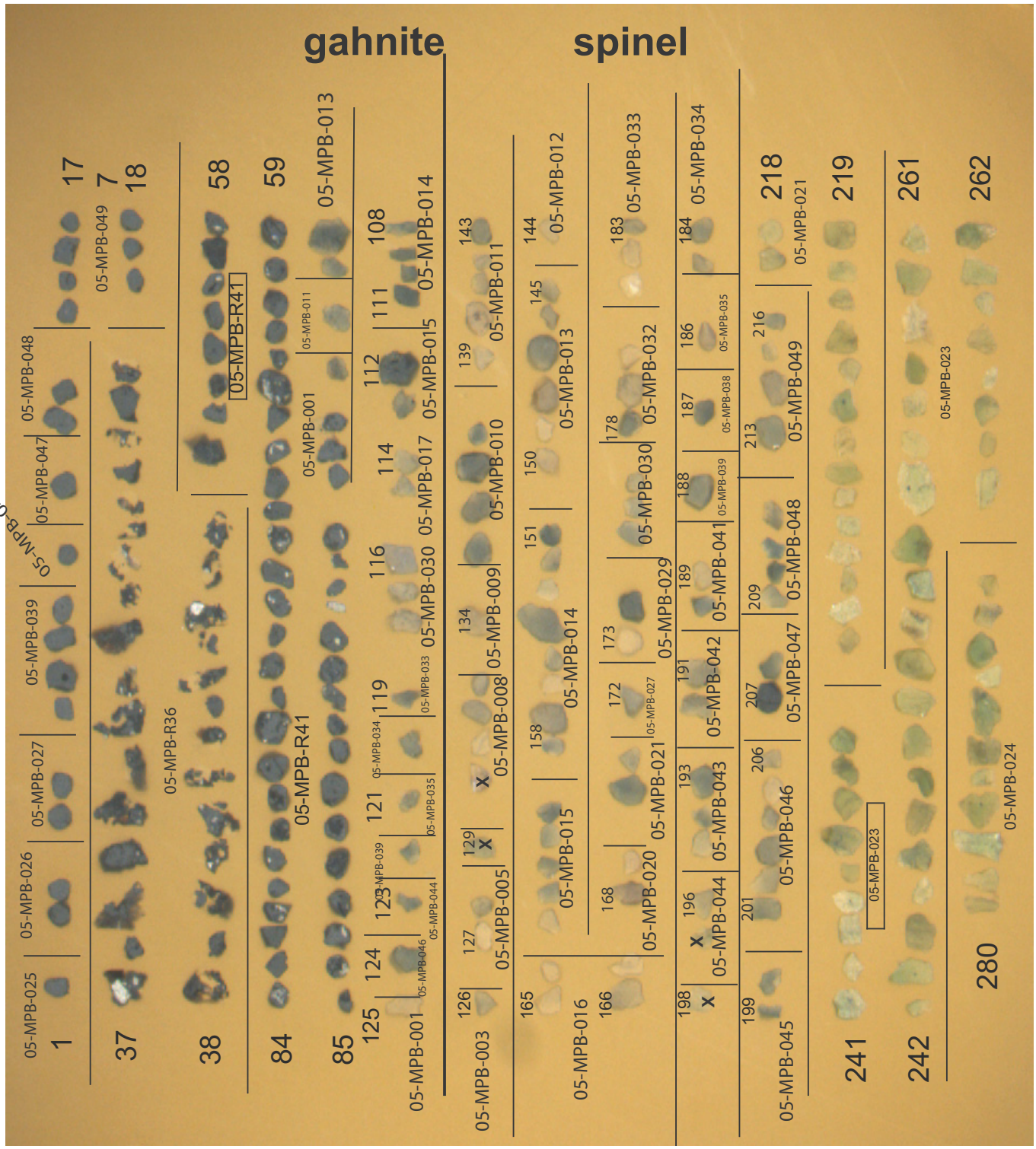

Appendix F2 continued.

Mineral mount:
06-0051-P01.
Thompson Nickel Belt;
size: 0.25-0.5 mm

Appendix F2 continued.

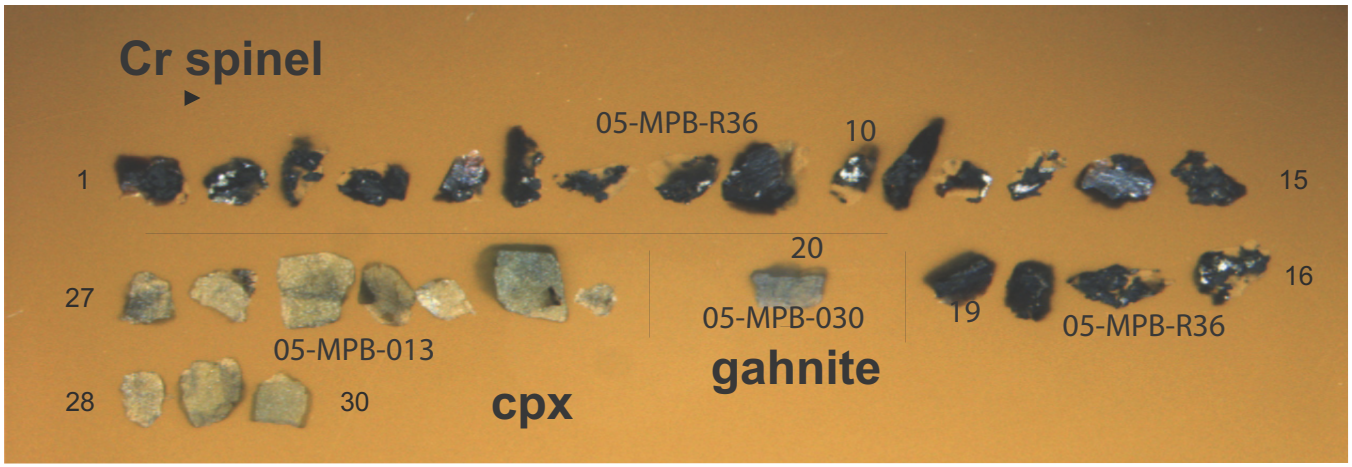

Mineral mount: 06-0051-P02. Thompson Nickel Belt; size: 0.5-1.0 mm; cpx = clinopyroxene.

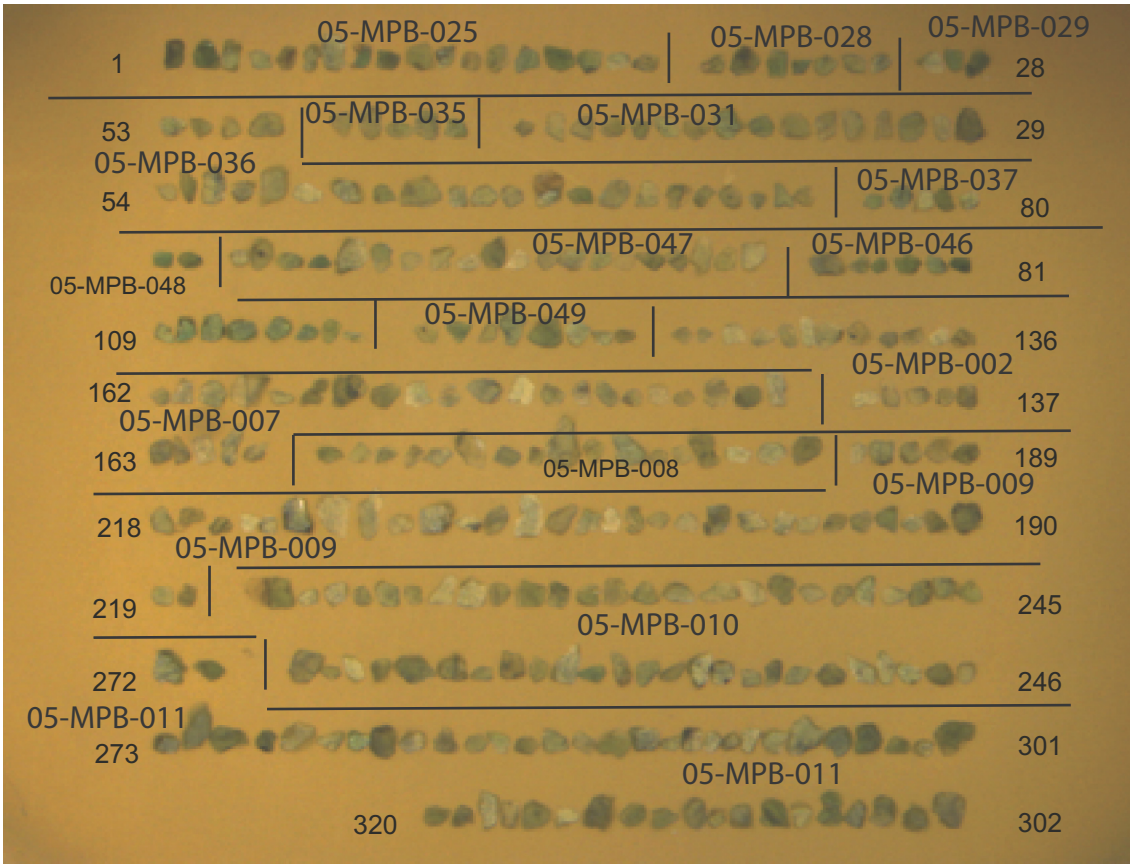

Mineral mount: 06-0051-P03. Thompson Nickel Belt; size: 0.25-0.5 mm.

Appendix F2 continued.

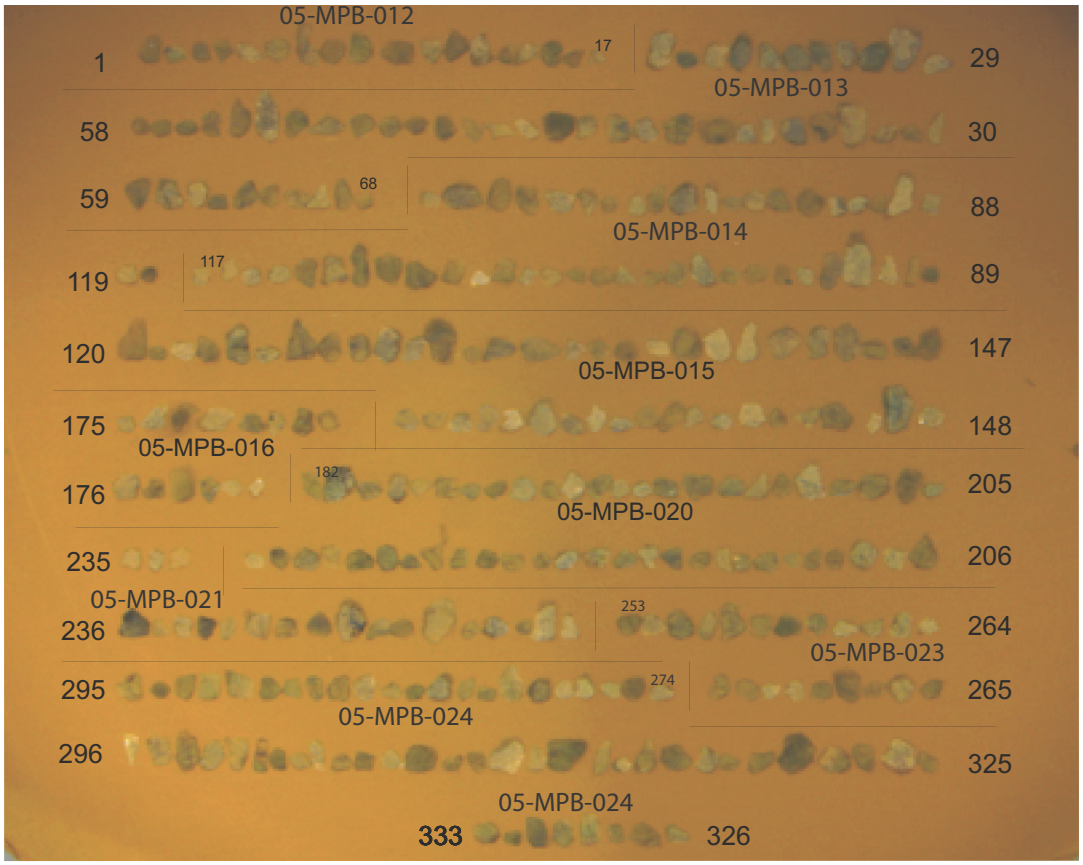

Mineral mount: 06-0051-P04. Thompson Nickel Belt; mineral: Cr-diopside, size: 0.25-0.5 mm.

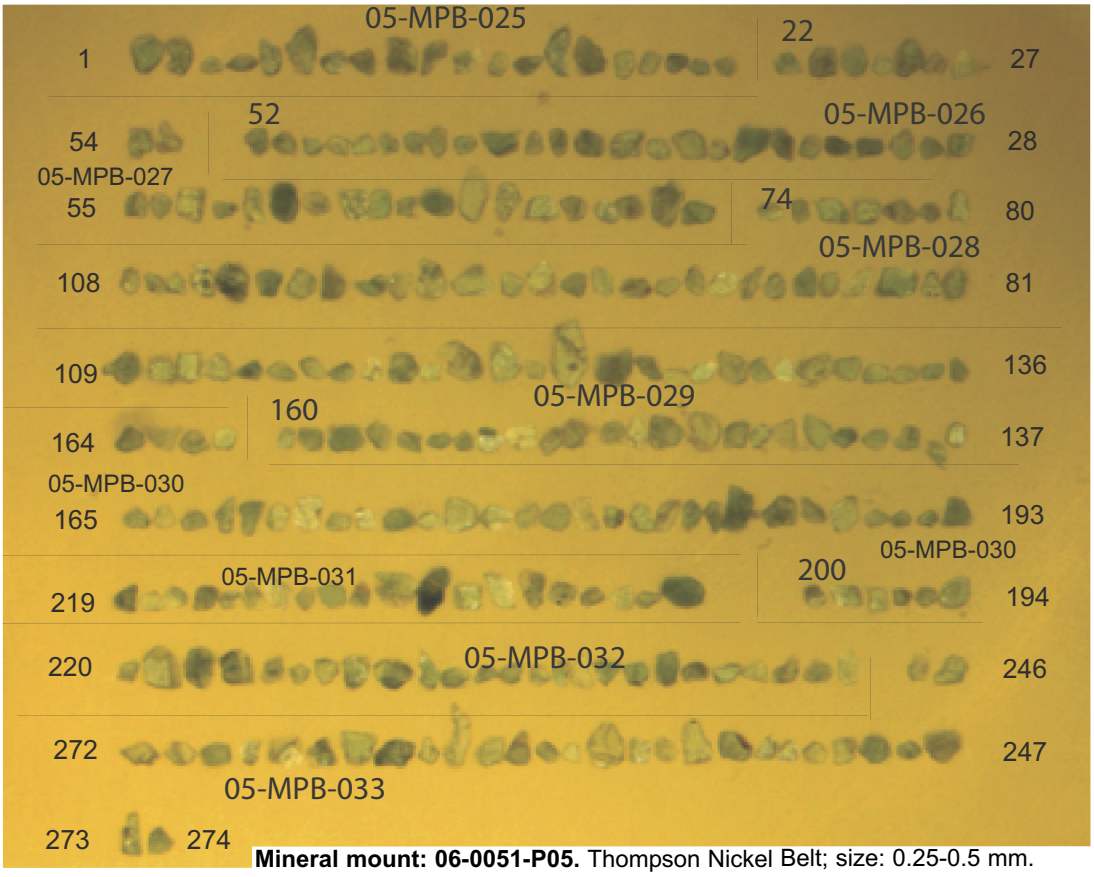

Mineral mount: 06-0051-P05. Thompson Nickel Belt; size: 0.25-0.5 mm.

Appendix F2 continued.

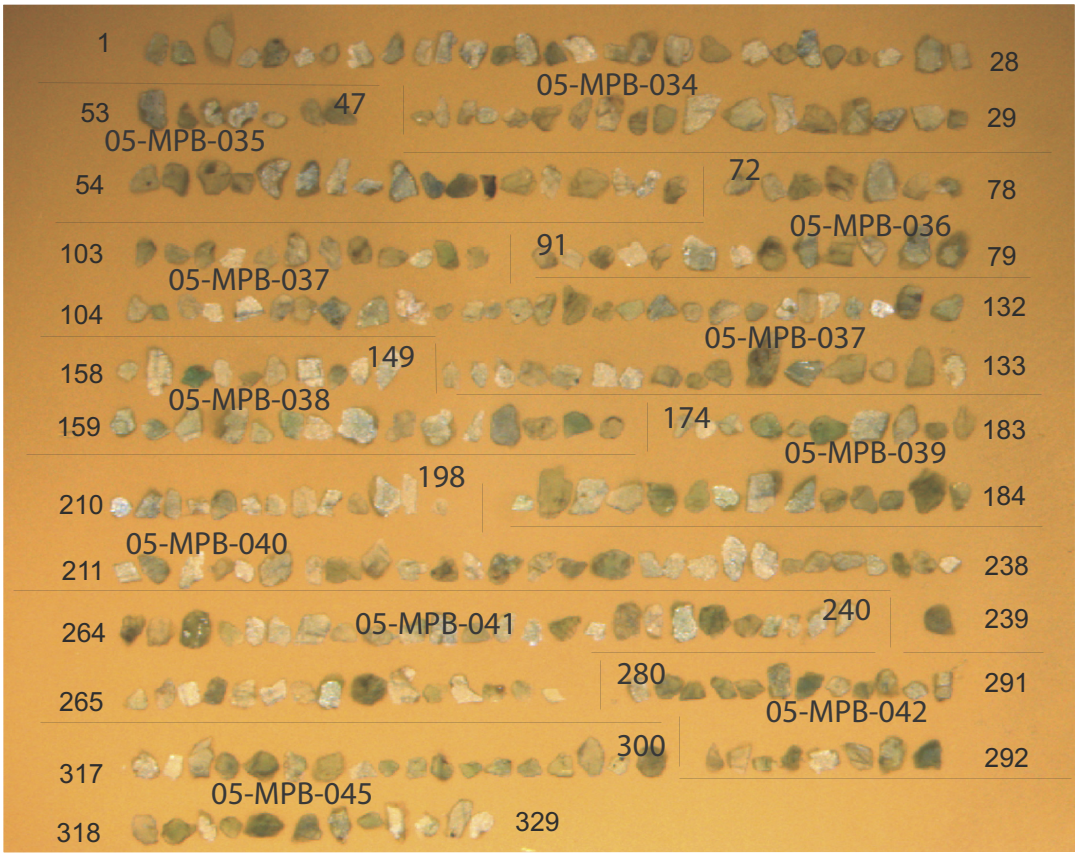

Mineral mount: 06-0051-P06. Thompson Nickel Belt; size: 0.25-0.5 mm.

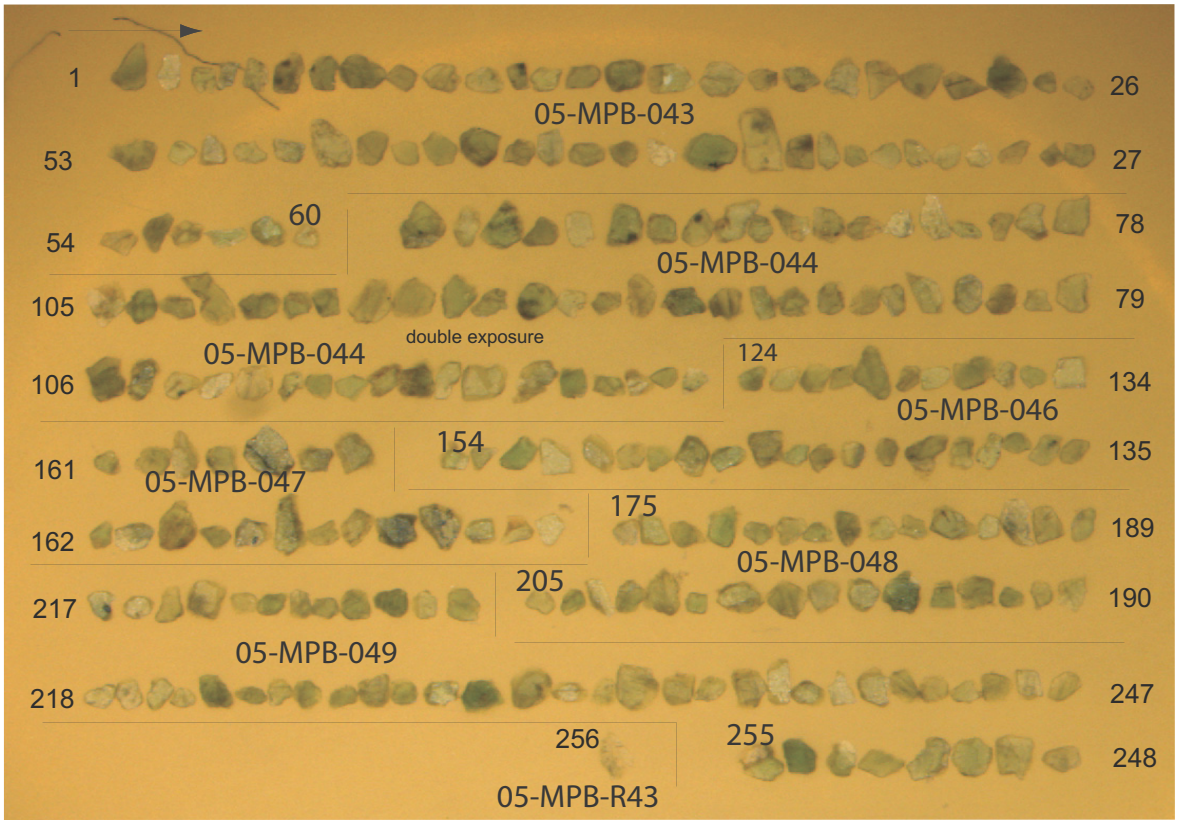

Mineral mount: 06-0051-P07. Thompson Nickel Belt; size: 0.25-0.5 mm.

Appendix F2 continued.

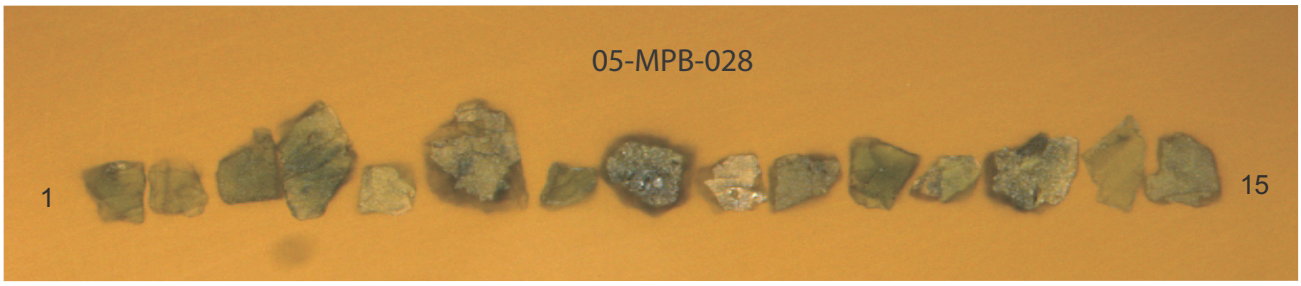

Mineral mount: 06-0051-P08. Thompson Nickel Belt; size: 0.5-1.0 mm.

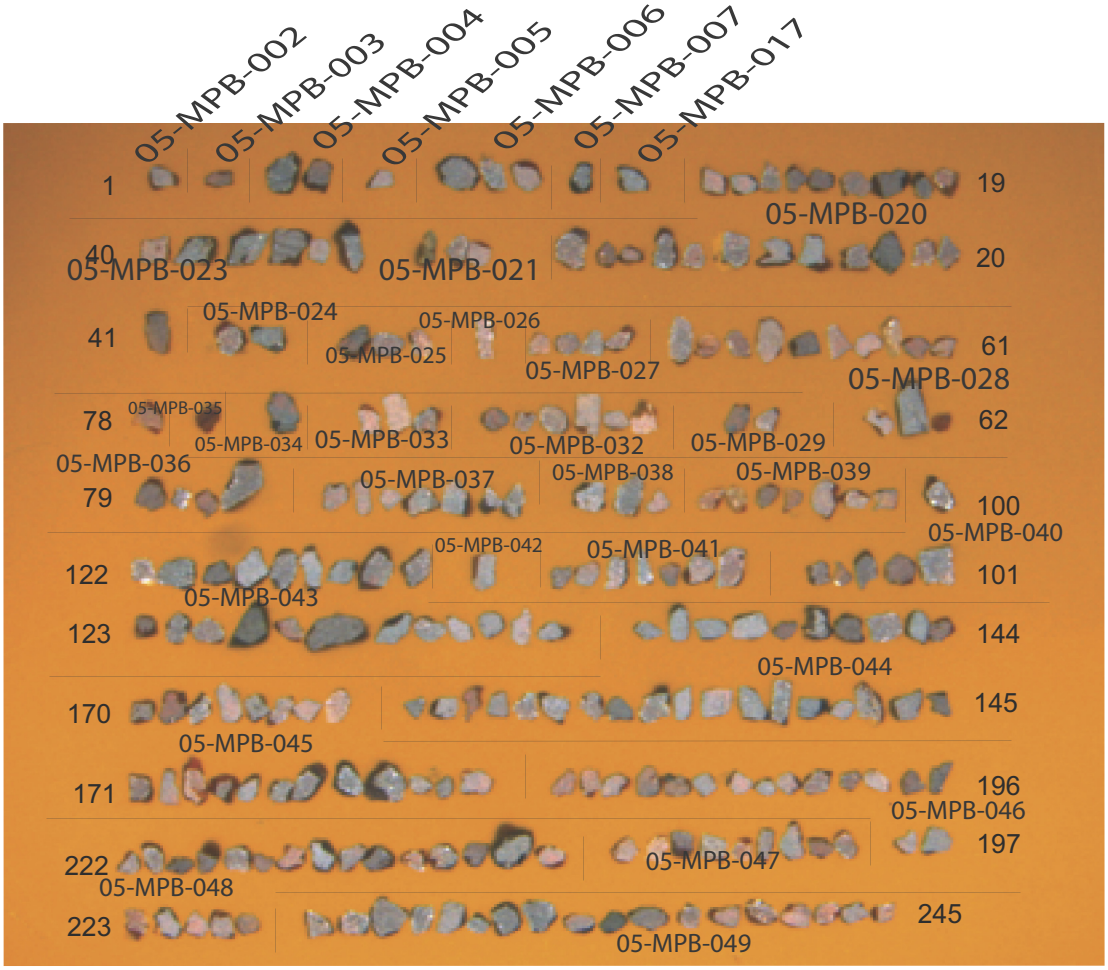

Mineral mount: 06-0051-P09. Thompson Nickel Belt; size: 0.25-0.5 mm.

Appendix F2 continued.

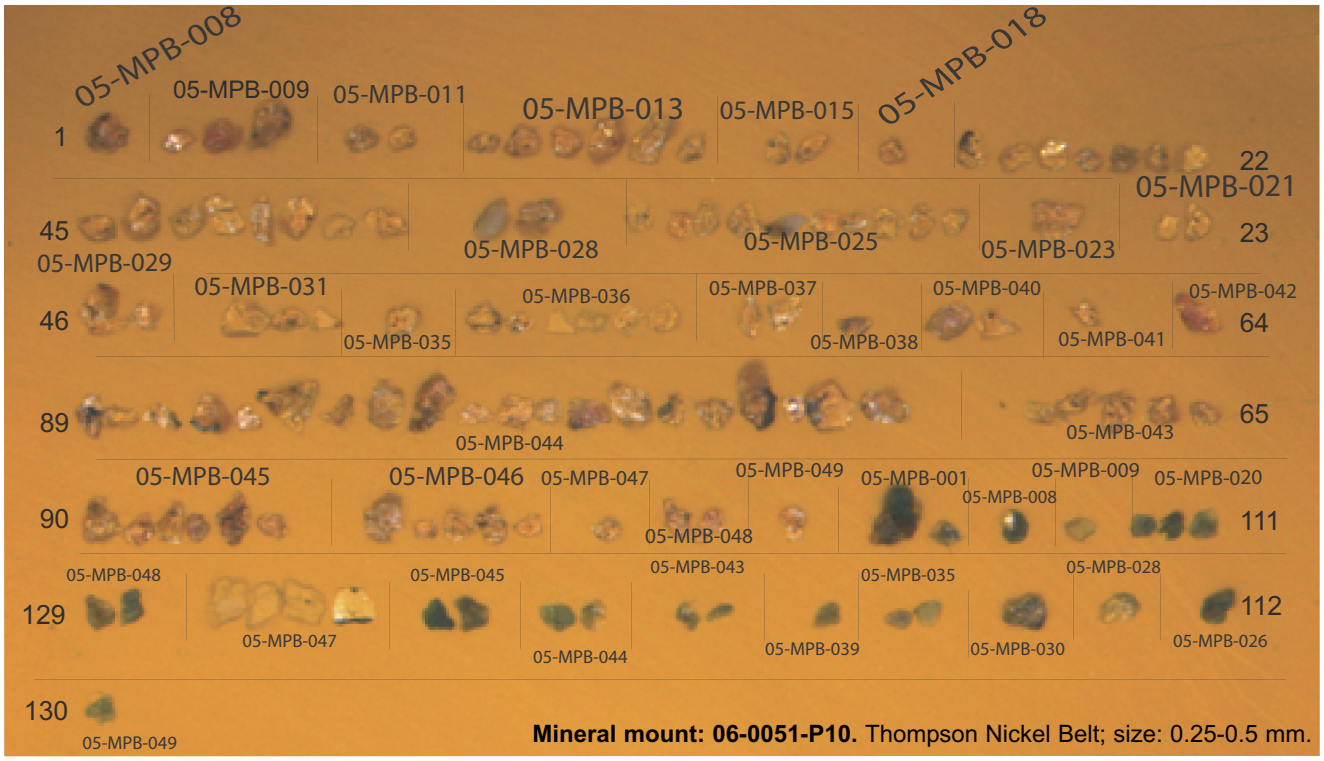

Mineral mount: 06-0051-P10. Thompson Nickel Belt; size: 0.25-0.5 mm.

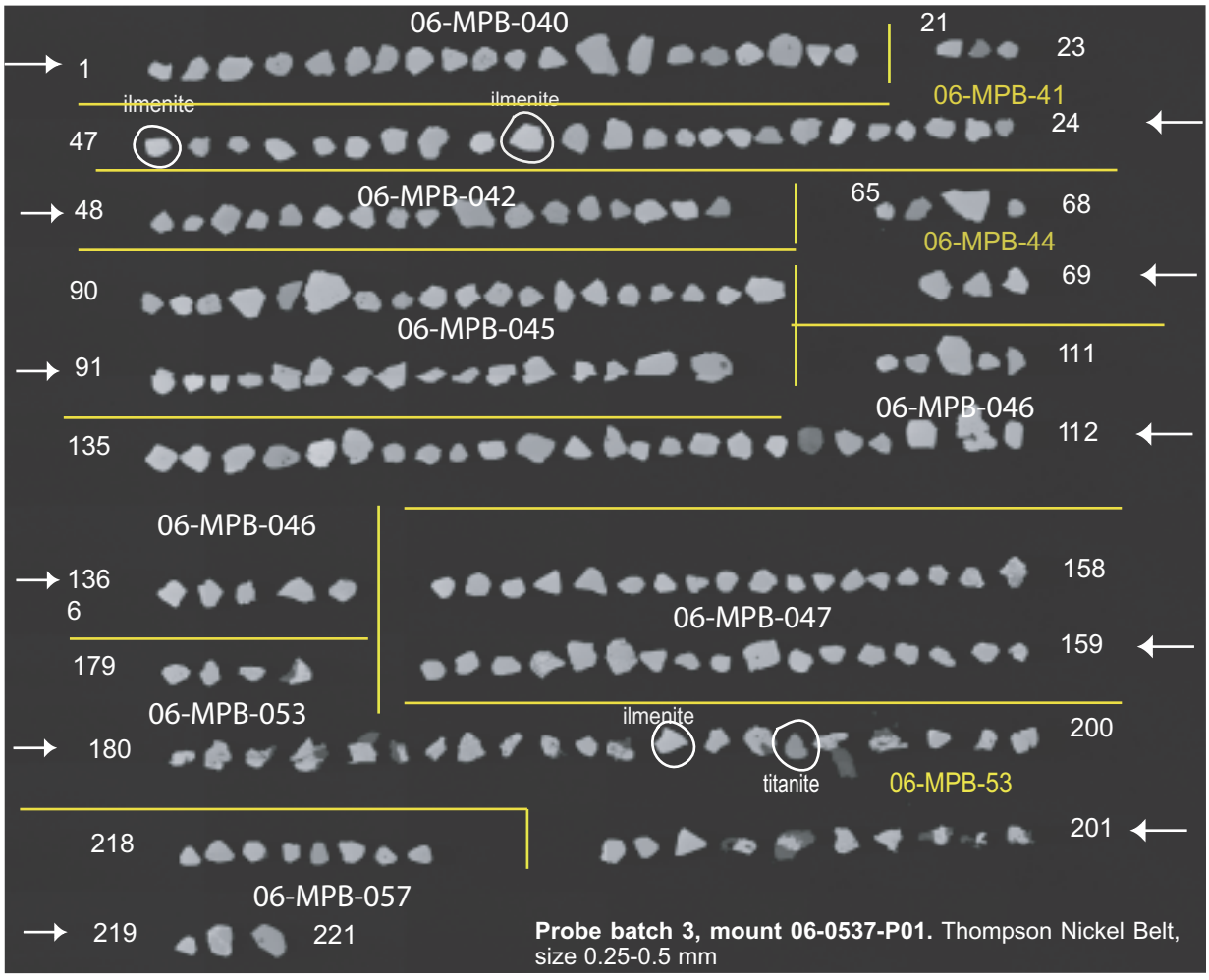

Probe batch 3, mount 06-0537-P01. Thompson Nickel Belt, size 0.25-0.5 mm

Appendix F2 continued.

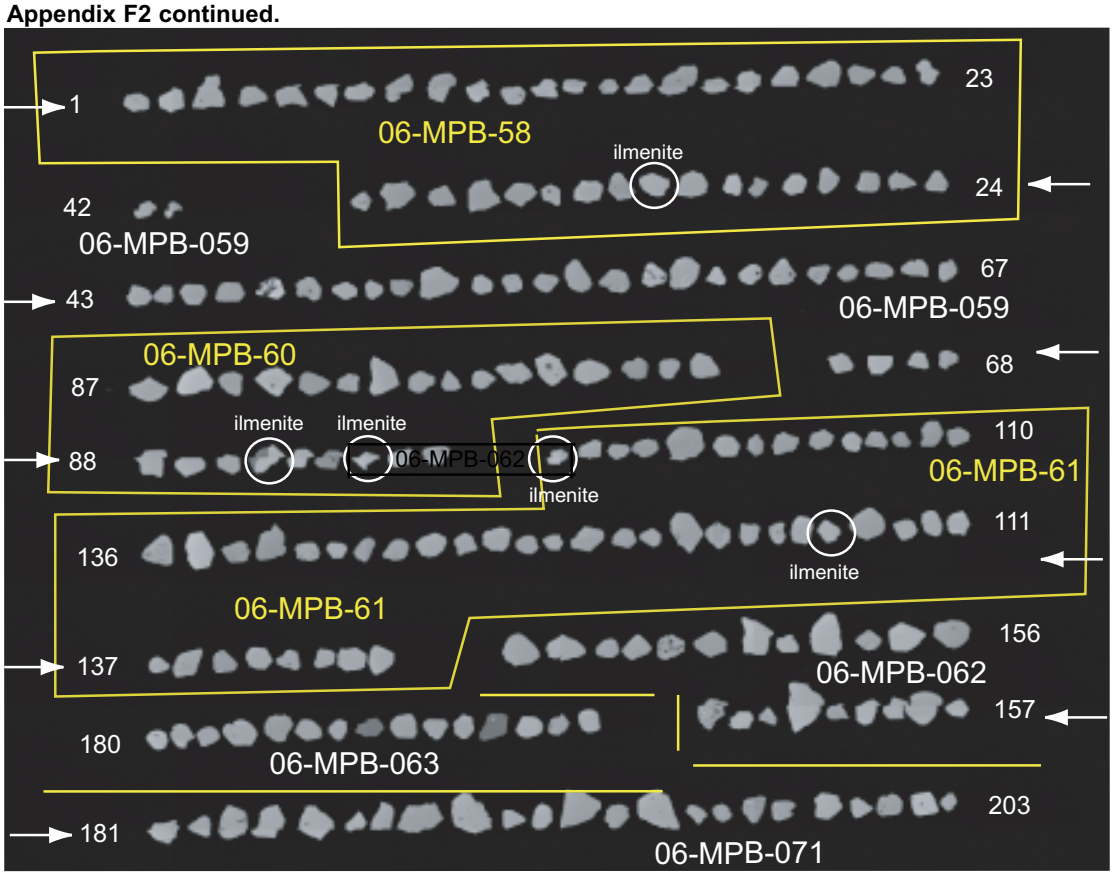

Probe batch 3, mount 06-0537-P02. Thompson Nickel Belt,

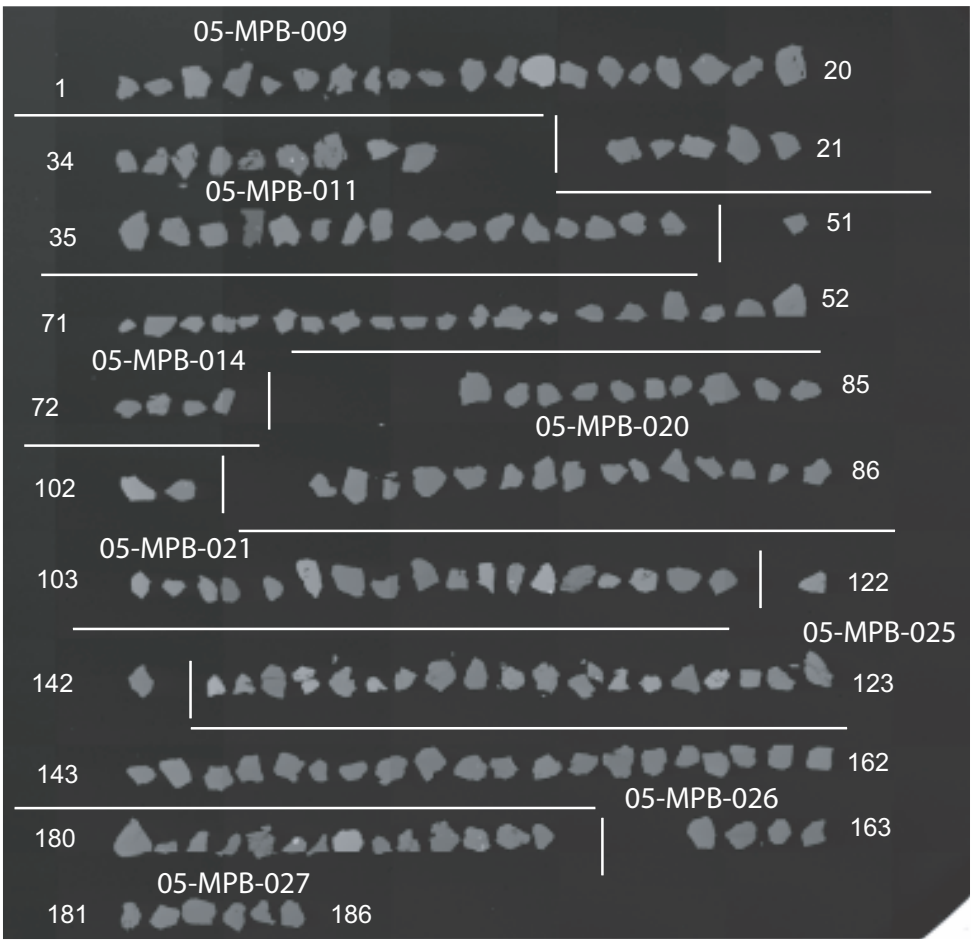

Probe batch 3, mount 06-0537-P03. Thompson Nickel Belt, Size: 0.25-0.5mm, mineral: olivine, size: 0.25-0.5 mm.

Appendix F2 continued.

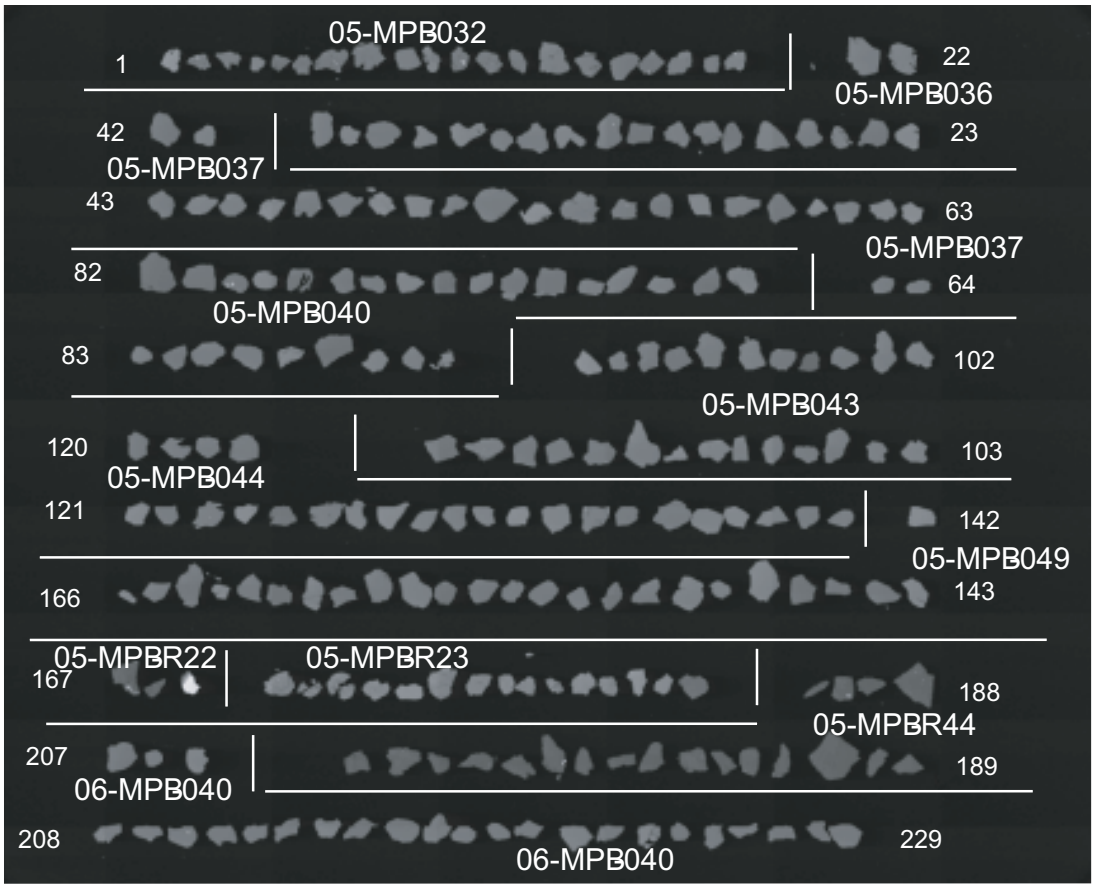

Probe batch 3, mount 06-0537-P04. Thompson Nickel Belt, samples: 05-MPB-32, 35, 37, 40, 43, 44, 49, R-22, R23, R-44; 06-MPB-40; mineral: olivine, size: 0.25-0.5 mm.

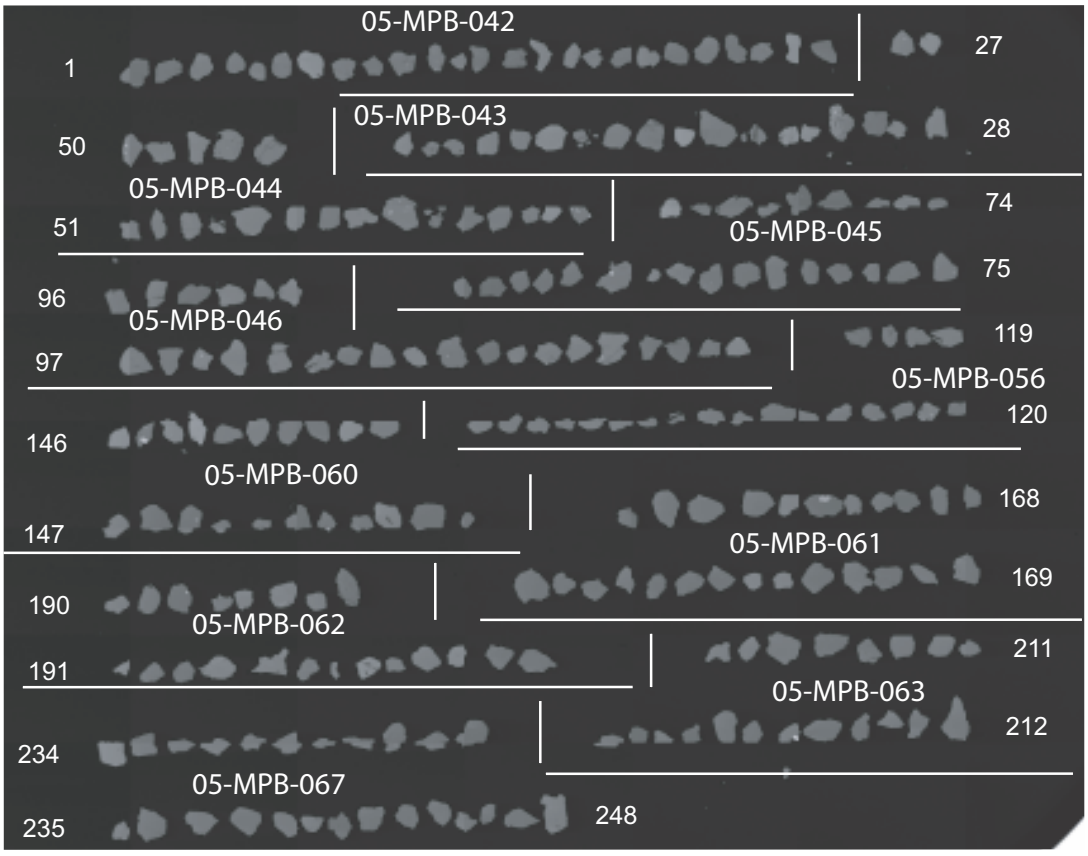

Probe batch 3, mount 06-0537-P05. Thompson Nickel Belt, samples: 06-MPB-42, -43, -44, -45, -46, -56, -60, -61, -62, -63, -67; mineral: olivine, size: 0.25-0.5 mm.

Appendix F2 continued.

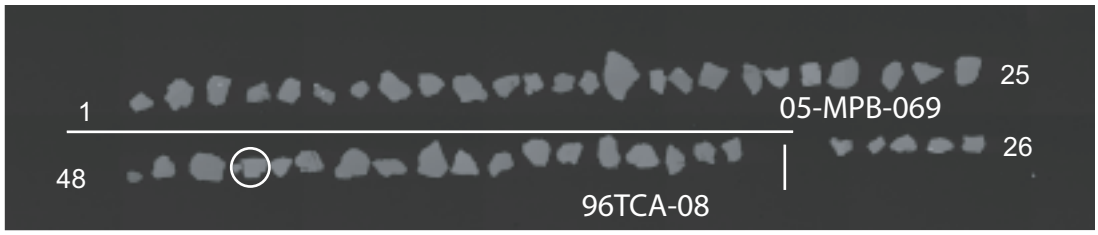

Probe batch 3, mount 06-0537-P06. Thompson Nickel Belt, mineral: olivine, size: 0.25-0.5 mm.

Probe batch 3, mount 06-0537-P07. Thompson Nickel Belt, mineral: slag, size: 0.25-0.5 mm.

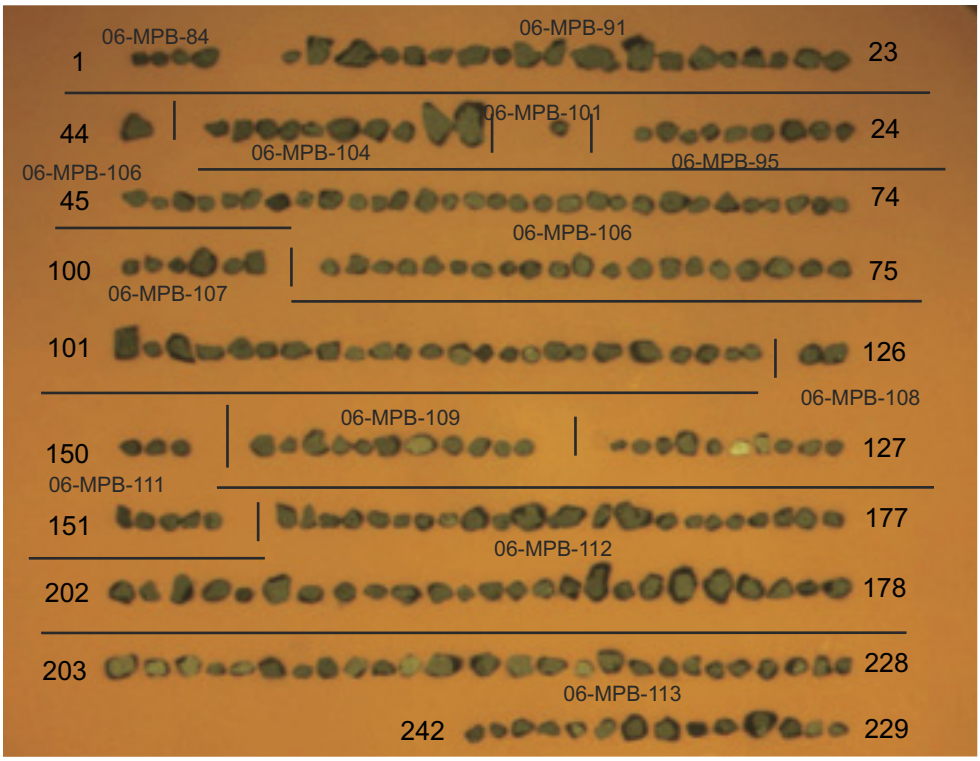

Mineral mount: 07-0410-P02. Thompson Nickel Belt; mineral: chromite, size: 0.25-0.5 mm.

Appendix F2 continued.

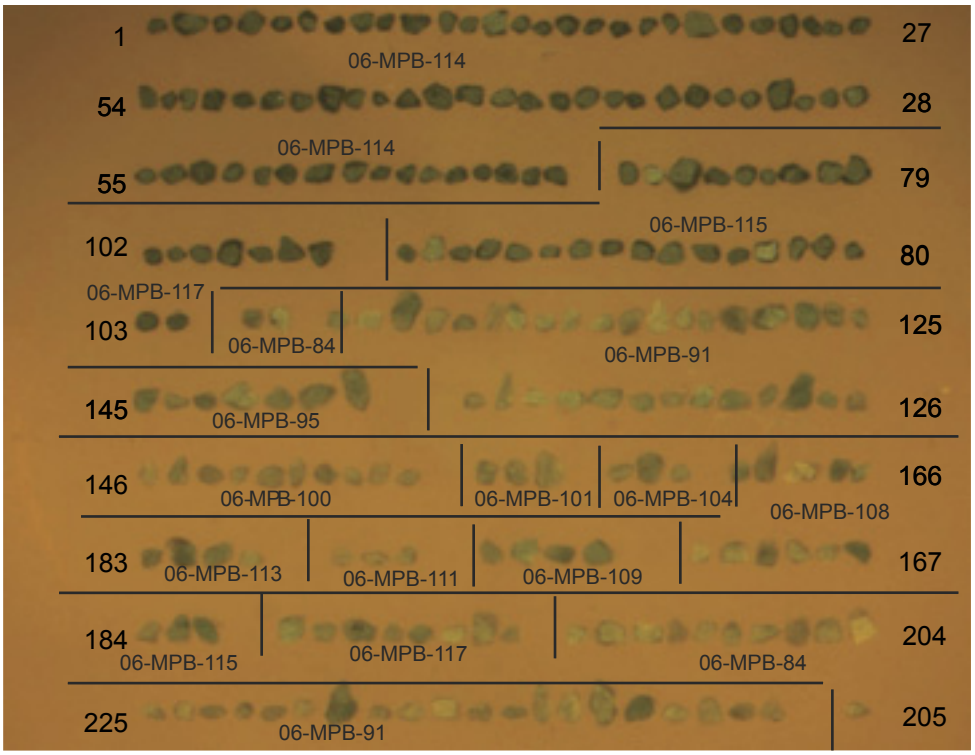

Mineral mount 07-0410-P03. Thompson Nickel Belt; mineral: Cr-diopside, size: 0.25-0.5 mm.

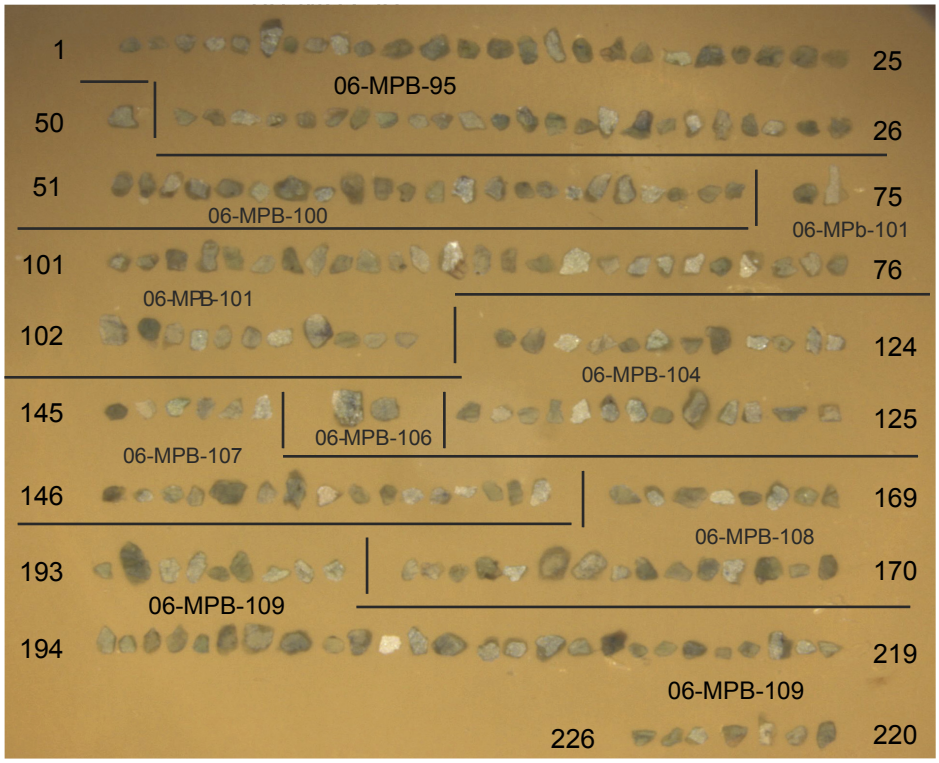

Mineral mount 07-0410-P04. Thompson Nickel Belt; mineral: pyroxene, size: 0.25-0.5 mm.

Appendix F2 continued.

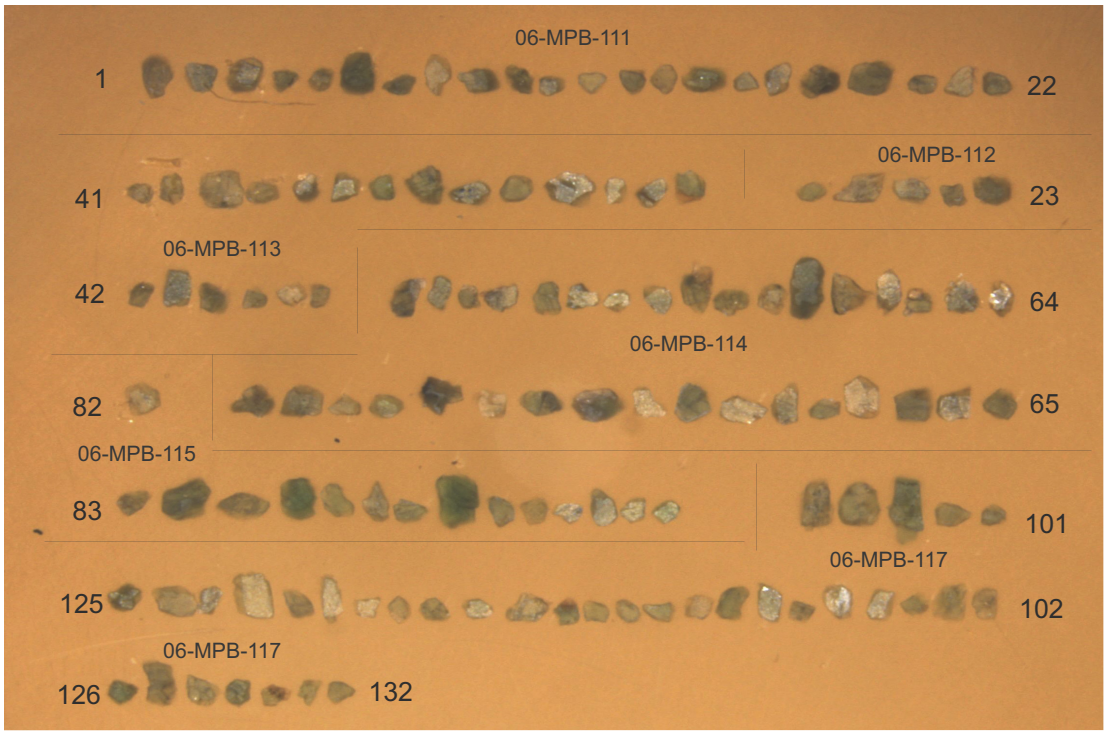

Mineral mount 07-0410-P05. Thompson Nickel Belt; mineral: pyroxene, size: 0.25-0.5 mm.

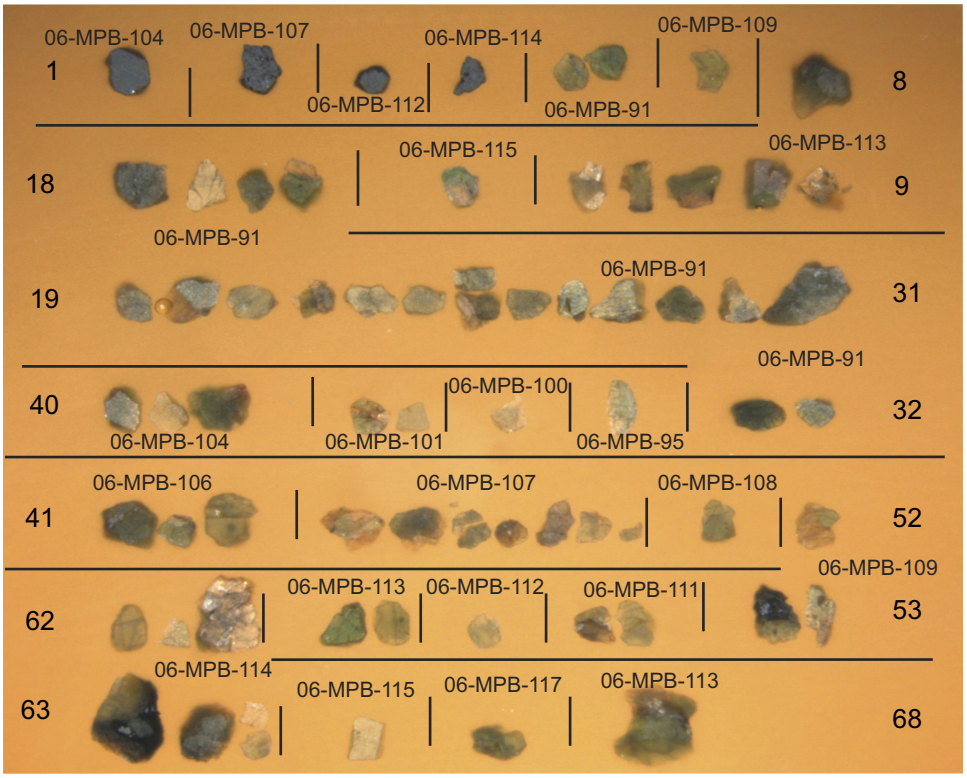

Mineral mount 07-0401-P06. Thompson Nickel Belt; minerals: chromite + pyroxene, size: 0.5-1.0 mm.

Appendix F2 continued.

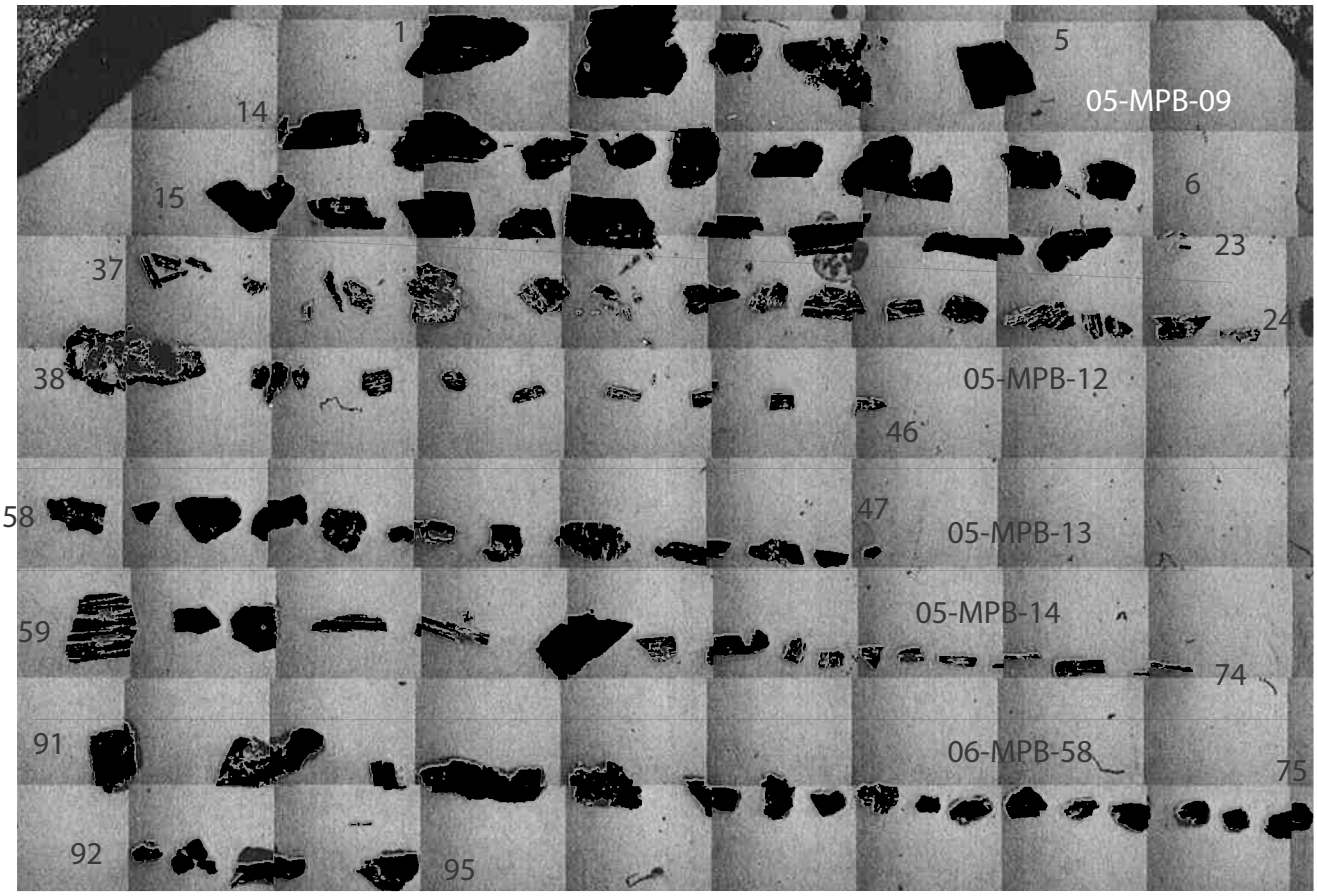

Mineral mount PS22710. Thompson Nickel Belt; mineral: pyrrhotite, size: 0.25-0.5 mm.

Appendix F3. Electron microprobe operating conditions

A. Analytical Conditions for Carleton University, Ottawa

Quantitative sulphide analyses were carried out with an automated 4 spectrometer Cameca MBX electron microprobe by wavelength dispersive x-ray analysis method (WDX) at the Earth Sciences department, Carleton University, Ottawa. Raw data were processed using the PAP overlap correction procedure.

Operating conditions were 20kV accelerating voltage, 30 nA beam current, focused beam (2-3 micron diameter). Counting times were 10-20 seconds or 40,000 accumulated counts.

Element	Line	Standard
S	Kα	synth. $Fe_{1-x}S$
Fe	Kα	synth. $Fe_{1-x}S$
Co	Kα	Co
Ni	Kα	synthetic NiAs
Cu	Kα	synthetic $CuFeS_2$
Zn	Kα	synthetic ZnS

Element	Line	Standard
As	Lα	synthetic NiAs
Se	Lα	Bi_2Se_3
Ag	Lα	Ag
Te	Lα	Te
Au	Mα	Au
Bi	Mα	Bi_2Se_3

B. Analytical Conditions for Geoscience Laboratories, Sudbury

Mineral analysis was carried out using a Cameca SX-100 Electron Probe Micro Analyzer (EPMA) at the Geoscience Laboratories (Ontario Geological Survey) in Sudbury, Ontario.

Specific routines were employed for each mineral group in order to produce ideal conditions for minor/trace element analysis. The routines, which are shown in the tables, below illustrate the the choice of standards together with the analyzing crystals (XTAL's), counting times, operating voltage, beam current, limits of detection (L.O.D.'s using the 3 sigma definition) and limits of quantification (L.O.Q.'s using the 10 sigma definition).

Chromite

Oxide	Standard	Mode	XTAL	L.O.D. wt%	L.O.Q. wt%	Count time (seconds)	Gun (kV)	Beam (nA)
SiO_2	Diopside	WDS	TAP	0.004	0.015	40	20	200
TiO_2	$SrTiO_3$	WDS	PET	0.022	0.075	30	20	20
Al_2O_3	Gahnite	WDS	TAP	0.023	0.076	15	20	20
V_2O_3	V_2O_5	WDS	LLIF	0.005	0.017	40	20	200
Cr_2O_3	Cr_2O_3	WDS	LLIF	0.021	0.071	30	20	20
Nb_2O_3	$FeNb_2O_5$	WDS	PET	0.019	0.063	20	20	200
MgO	Diopside	WDS	TAP	0.017	0.057	15	20	20
CaO	Diopside	WDS	PET	0.006	0.022	20	20	200
MnO	$MnTiO_3$	WDS	LLIF	0.031	0.104	15	20	20
FeO	Fe_2O_3	WDS	LLIF	0.028	0.095	15	20	20
NiO	NiO	WDS	LLIF	0.008	0.026	20	20	200
ZnO	Gahnite	WDS	LLIF	0.012	0.041	20	20	200

Olivine

Oxide	Standard	Mode	XTAL	L.O.D. wt%	L.O.Q. wt%	Count time (seconds)	Gun (kV)	Bea (nA
SiO_2	Olivine	WDS	TAP	0.026	0.087	15	20	20
TiO_2	$SrTiO_3$	WDS	PET	0.006	0.020	30	20	200
Al_2O_3	Kyanite	WDS	TAP	0.003	0.011	60	20	200
Cr_2O_3	Cr_2O_3	WDS	LLiF	0.004	0.015	30	20	200
MgO	Olivine	WDS	TAP	0.018	0.061	15	20	20
CaO	Diopside	WDS	PET	0.004	0.014	30	20	200
MnO	$MnTiO_3$	WDS	LLiF	0.013	0.043	30	20	20
FeO*	Fe_2O_3	WDS	LiF	0.022	0.072	30	20	20
CoO	Co metal	WDS	LiF	0.005	0.017	60	20	200
NiO	NiO	WDS	LLiF	0.004	0.013	20	20	200
ZnO	Gahnite	WDS	LLiF	0.006	0.021	30	20	200

Gahnite

Oxide	Standard	Mode	XTAL	L.O.D. wt%	L.O.Q. wt%	Count time (seconds)	Gun (kV)	Beam (nA)
SiO_2	Diopside	WDS	TAP	0.003	0.012	40	20	200
TiO_2	$SrTiO_3$	WDS	PET	0.02	0.068	30	20	20
Al_2O_3	Gahnite	WDS	TAP	0.03	0.1	15	20	20
V_2O_3	V_2O_5	WDS	LLIF	0.005	0.015	40	20	200
Cr_2O_3	Cr_2O_3	WDS	LLIF	0.015	0.051	30	20	20
Nb_2O_3	$FeNb_2O_5$	WDS	PET	0.016	0.053	20	20	200
MgO	Diopside	WDS	TAP	0.017	0.058	15	20	20
CaO	Diopside	WDS	PET	0.006	0.019	20	20	200
MnO	$MnTiO_3$	WDS	LLIF	0.006	0.019	20	20	200
FeO	Fe_2O_3	WDS	LLIF	0.024	0.082	15	20	20
NiO	NiO	WDS	LLIF	0.007	0.024	20	20	200
ZnO	Gahnite	WDS	LLIF	0.041	0.138	15	20	20

Corundum

Oxide	Standard	Mode	XTAL	L.O.D. wt%	L.O.Q. wt%	Count time (seconds)	Gun (kV)	Bea (nA
SiO_2	Diopside	WDS	TAP	0.004	0.013	20	20	200
TiO_2	$SrTiO_3$	WDS	LPET	0.002	0.006	40	20	200
Al_2O_3	Al_2O_3	WDS	TAP	0.018	0.059	15	20	20
Cr_2O_3	Cr_2O_3	WDS	PET	0.004	0.013	40	20	200
MgO	Diopside	WDS	TAP	0.003	0.01	20	20	200
MnO	$MnTiO_3$	WDS	LiF	0.004	0.014	30	20	200
FeO*	Fe_2O_3	WDS	LiF	0.005	0.016	20	20	200
NiO	NiO	WDS	LLIF	0.003	0.011	20	20	200
ZnO	Gahnite	WDS	LLiF	0.005	0.016	20	20	200

Appendix F3 continued.

Clinopyroxene

Oxide	Standard	Mode	XTAL	L.O.D. wt%	L.O.Q. wt%	Count time (seconds)	Gun (kV)	Beam (nA)
SiO_2	Diopside	WDS	TAP	0.029	0.098	10	20	20
TiO_2	$SrTiO_3$	WDS	LPET	0.008	0.028	40	20	20
Al_2O_3	Anorthite	WDS	TAP	0.017	0.056	15	20	20
Cr_2O_3	Cr_2O_3	WDS	LPET	0.008	0.027	20	20	200
MgO	Diopside	WDS	TAP	0.021	0.069	15	20	20
CaO	Diopside	WDS	LPET	0.012	0.041	40	20	20
MnO	$MnTiO_3$	WDS	LLiF	0.011	0.036	40	20	20
FeO*	Fe_2O_3	WDS	LiF	0.017	0.056	40	20	20
CoO	Co metal	WDS	LiF	0.005	0.017	40	20	200
NiO	NiO	WDS	LLiF	0.005	0.017	20	20	200
ZnO	Gahnite	WDS	LLiF	0.007	0.024	20	20	200
Na_2O	Albite	WDS	TAP	0.006	0.019	20	20	200
K_2O	Orthoclase	WDS	LPET	0.002	0.007	40	20	200

Saphirrine

Oxide	Standard	Mode	XTAL	L.O.D. wt%	L.O.Q. wt%	Count time (seconds)	Gun (kV)	Beam (nA)
SiO_2	Al_2SiO_5	WDS	TAP	0.023	0.076	15	20	20
TiO_2	$SrTiO_3$	WDS	LPET	0.008	0.026	45	20	20
Al_2O_3	Al_2SiO_5	WDS	TAP	0.026	0.087	15	20	20
Cr_2O_3	Cr_2O_3	WDS	PET	0.005	0.018	40	20	200
MgO	Diopside	WDS	TAP	0.019	0.062	15	20	20
CaO	Diopside	WDS	PET	0.010	0.033	45	20	20
MnO	$MnTiO_3$	WDS	LLiF	0.010	0.033	45	20	20
FeO*	Fe_2O_3	WDS	LPET	0.002	0.007	45	20	20
CoO	Co metal	WDS	LiF	0.005	0.016	40	20	200
NiO	NiO	WDS	LLiF	0.005	0.016	20	20	200
ZnO	Gahnite	WDS	LLiF	0.007	0.022	20	20	200
Na_2O	Albite	WDS	TAP	0.004	0.012	40	20	200
K_2O	Orthoclase	WDS	LPET	0.002	0.006	40	20	200

Rutile

Oxide	Standard	Mode	XTAL	L.O.D. wt%	L.O.Q. wt%	Count time (seconds)	Gun (kV)	Beam (nA)
SiO_2	Diopside	WDS	TAP	0.006	0.019	40	20	200
TiO_2	$SrTiO_3$	WDS	PET	0.026	0.087	30	20	20
Al_2O_3	Gahnite	WDS	TAP	0.021	0.070	15	20	20
V_2O_3	V_2O_5	WDS	LiF	0.013	0.042	20	20	200
Cr_2O_3	Cr_2O_3	WDS	PET	0.006	0.021	40	20	200
Nb_2O_3	$FeNb_2O_5$	WDS	LPET	0.012	0.040	20	20	200
MgO	Diopside	WDS	LiF	0.022	0.074	20	20	200
CaO	Diopside	WDS	TAP	0.015	0.049	15	20	20
MnO	$MnTiO_3$	WDS	LPET	0.01	0.032	30	20	20
FeO	Fe_2O_3	WDS	LLiF	0.014	0.048	30	20	20
NiO	NiO	WDS	LiF	0.023	0.075	30	20	20
ZnO	Gahnite	WDS	LLIF	0.006	0.020	20	20	200
ZnO	Gahnite	WDS	LLiF	0.006	0.020	40	20	200
SnO	Sn metal	WDS	LPET	0.007	0.025	20	20	200